

Mónica Blasco Castellón

Geochemical characterisation of  
low temperature carbonate  
geothermal systems. Problematic  
and applications

Departamento  
Ciencias de la Tierra

Director/es  
Gimeno Serrano, María José

<http://zaguan.unizar.es/collection/Tesis>

© Universidad de Zaragoza  
Servicio de Publicaciones

ISSN 2254-7606

Tesis Doctoral

GEOCHEMICAL CHARACTERISATION OF LOW  
TEMPERATURE CARBONATE GEOTHERMAL  
SYSTEMS. PROBLEMATIC AND APPLICATIONS

Autor

Mónica Blasco Castellón

Director/es

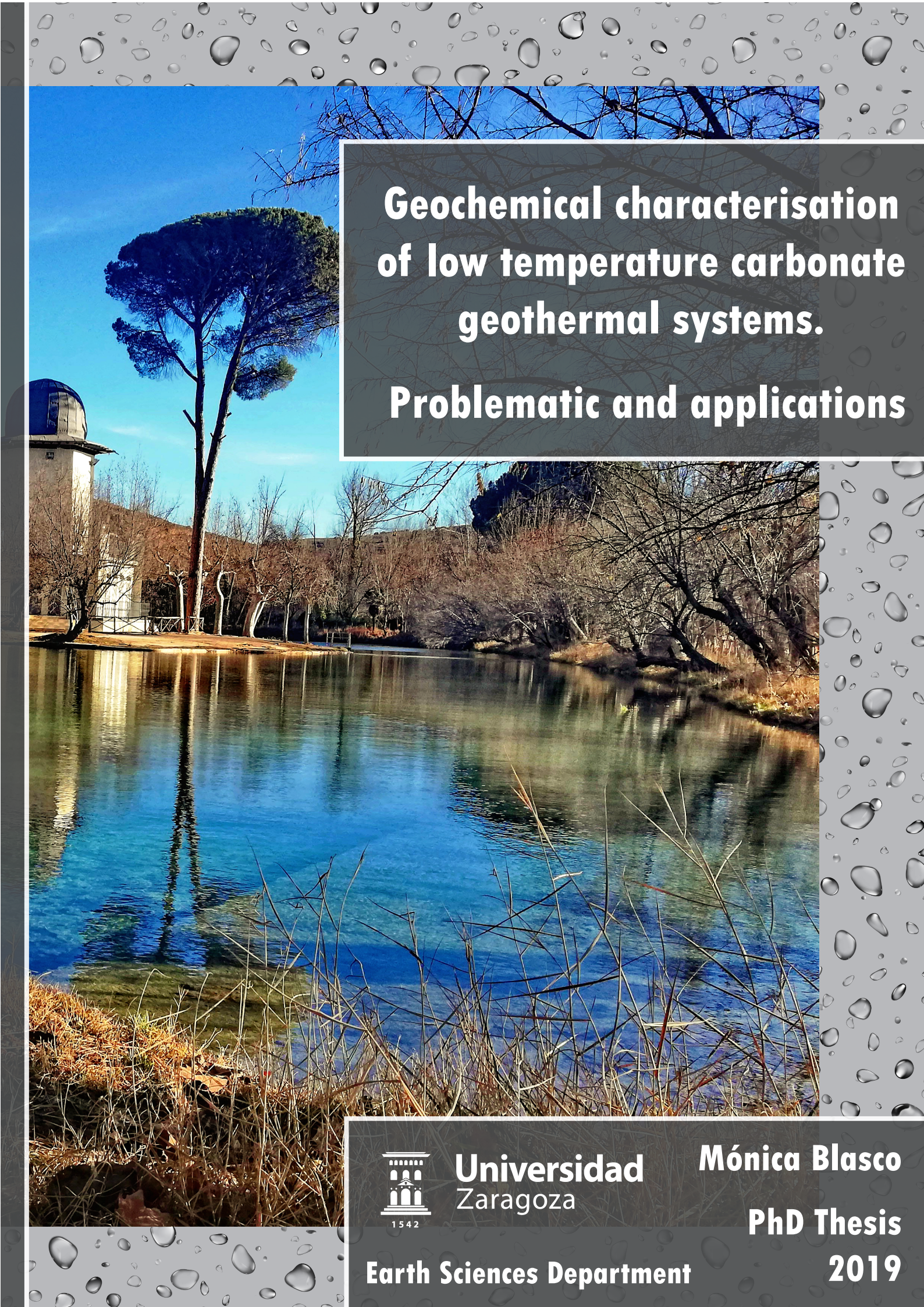
Gimeno Serrano, María José

**UNIVERSIDAD DE ZARAGOZA**

Ciencias de la Tierra

2019





# **Geochemical characterisation of low temperature carbonate geothermal systems.**

## **Problematic and applications**



**Universidad  
Zaragoza**

**Mónica Blasco**

**PhD Thesis**

**Earth Sciences Department**

**2019**











Departamento de  
Ciencias de la Tierra  
**Universidad Zaragoza**

# **Geochemical characterisation of low temperature carbonate geothermal systems. Problematic and applications.**

Tesis doctoral presentada por  
MÓNICA BLASCO CASTELLÓN  
cumpliendo todos los requisitos para obtener el título  
*de Doctor por la Universidad de Zaragoza*

Directora de tesis:  
Dra. María José Gimeno Serrano  
Profesor Titular de la Universidad de Zaragoza

Zaragoza, 2019



Esta Tesis Doctoral ha sido elaborada en la modalidad de compendio de publicaciones, y consta de los siguientes trabajos publicados para su publicación en revistas incluidas en el Journal of Citations Reports:

*This PhD dissertation has been developed in the modality of scientific papers compilation and it consists of the following published paper in journals indexed in the Journal of Citations Reports:*

1. Blasco, M., Auqué, L. F., Gimeno, M. J., Acero, P., Asta, M. P. (2017). Geochemistry, geothermometry and influence of the concentration of mobile elements in the chemical characteristics of carbonate-evaporitic thermal systems. The case of the Tiermas geothermal system (Spain). *Chemical Geology*, 466, 696–709. DOI: 10.1016/j.chemgeo.2017.07.013
2. Blasco, M., Gimeno, M. J., Auqué, L. F. (2018). Low temperature geothermal systems in carbonate-evaporitic rocks: Mineral equilibria assumptions and geothermometrical calculations. Insights from the Arnedillo thermal waters (Spain). *Science of The Total Environment*, 615, 526–539. DOI: 10.1016/j.scitotenv.2017.09.269
3. Blasco, M., Auqué, L. F., Gimeno, M. J. (2019). Geochemical evolution of thermal waters in carbonate – evaporitic systems: the triggering effect of halite dissolution in the dedolomitisation and albitisation processes. *Journal of Hydrology*, 570, 623-636. DOI: 10.1016/j.jhydrol.2019.01.013
4. Blasco, M., Auqué, L. F., Gimeno, M. J., Acero, P., Gómez J., Asta, M. P. (2019). Mineral equilibria and thermodynamic uncertainties in the geothermometrical characterisation of carbonate geothermal systems of low temperature. The case of the Alhama-Jaraba system (Spain). *Geothermics*, 78, 170-182. DOI: 10.1016/j.geothermics.2018.11.004

An additional paper, entitled “Characterisation of recent aragonite travertine deposits associated to the Fitero thermal waters (Spain) I: stable isotopes equilibrium evaluation”, which is in this moment under review in the *Sedimentary Geology Journal*, has been included.



*“¡Qué extraña cosa el conocimiento! Una vez que ha penetrado  
en la mente, se aferra a ella como la hiedra a la roca”*

*- Mary W. Shelley, en Frankenstein -*

*A mi familia*



Esta tesis doctoral se ha realizado en el marco de una ayuda para contratos predoctorales de Formación del Profesorado Universitario (FPU) con referencia FPU14/01523, del Ministerio de Educación, Cultura y Deporte de España. El Grupo de Modelización Geoquímica, de la Universidad de Zaragoza, reconocido como Grupo de Referencia por el Gobierno de Aragón, ha aportado los fondos necesarios para el desarrollo del trabajo.





# Agradecimientos

La ayuda, dedicación y apoyo de un gran número de personas ha conseguido que esta tesis doctoral llegue a buen fin y estoy sumamente agradecida a todas ellas.

A mi directora, María José Gimeno Serrano, por tu apoyo constante, ayuda desinteresada tanto en temas académicos como personales a lo largo de muchos años y no solo durante estos últimos cuatro y la infinidad de horas dedicadas a este estudio. A Luis Auqué, porque has guiado todo este trabajo y no cabe ninguna duda de que sin ti no hubiese sido posible, porque me has hecho aprender todo lo que sé, por tu meticulosidad e implicación y por las horas de conversaciones sobre cualquier tema.

A Quique Oliver, por tu ayuda en los análisis y preparación de las muestras. A Juan Mandado, por tu paciencia en el microscopio y la ayuda con todas las fotos. A María Pilar Asta y Patricia Acero por vuestras opiniones y consejos. A Javier Gómez, por estar ahí y echar una mano siempre que podías.

A los trabajadores de los Balnearios en que se tomaron las muestras, por su disposición y ayuda. Igualmente, a las personas anónimas que nos ofrecían su ayuda.

A Niklaus Waber y Christoph Wanner, por recibirme en la Universidad de Berna durante mi estancia en Suiza.

Gracias también a Christoph Wanner, de la Universidad de Berna, y a Carmine Apollaro, de la Universidad de Calabria, que han actuado como revisores externos de esta tesis.

Quiero también extender mi agradecimiento fuera del ámbito académico ya que el apoyo y comprensión de mi familia, pareja y amigos ha sido decisivo para que esta tesis saliera adelante. Gracias por estar ahí, apoyarme, aconsejarme y animarme en los malos ratos. Gracias especialmente a mis padres que siempre han confiado en mí, me han apoyado, respaldado y han hecho todo lo posible para que yo llegue donde me proponga. También a Manuel Martínez, que es quien ha estado más cerca de mí en todo momento y ha sido mi apoyo incondicional y me daba un poquito más de fuerzas cada día. Gracias también por tu ayuda con las figuras de todos los trabajos y con el diseño y maquetación de esta tesis.

Finalmente, agradezco también a todas las personas que de una forma u otra han intervenido en el desarrollo de esta tesis y han hecho este camino un poquito más fácil.



# General overview of the thesis dissertation

This thesis dissertation is structured in the following six chapters.

Chapter 1 consists of a general introduction to the studied topic, the characterisation of low temperature geothermal systems hosted in carbonate rocks, explaining the problems and difficulties in this type of studies and their importance. It also includes a statement of the main objectives of the research and the explanation of the main contributions of the PhD candidate in the different stages of the investigation. In Chapter 2 the location and the main geological and hydrogeological features of the studied areas are presented. Chapter 3 contains a detailed explanation of the methodology followed to develop this thesis (this chapter is completed with a conference paper presented as supplementary material, S.1, where the possible uncertainties when working with geochemical codes and different databases are evaluated).

Chapter 4 presents the Results of the study and it is the main body of this thesis since it presents the five papers that form this dissertation. Although these papers are independent and each one presents a different study, all of them deal with different low temperature and carbonate geothermal systems with the objective of 1) evaluating the best methodologies for their characterisation, 2) identifying the main secondary processes and the evolution of the waters and 3) discussing the interest of this type of systems. The last paper, under review at the moment, shows a more specific study on the aragonite precipitates associated to one of the thermal systems. Broadly, these papers present the following studies:

## Paper 1:

This paper presents the characterisation of the low temperature geothermal system of Tiermas, hosted in carbonates from the Paleocene-Eocene. The reservoir temperature has been established by the combination of classical chemical geothermometers (SiO<sub>2</sub>-quartz, Na-K, K-Mg and Na-K-Ca), specific geothermometers for carbonate systems (Ca-Mg), isotopic geothermometers and geothermometrical modelling. Additionally, the influence that mobile elements (i.e. not controlled by mineral equilibrium) have in the chemical characteristics and mineral equilibria in the reservoir has also been evaluated. Since a favourable tectonic structure for CO<sub>2</sub> storage has been recognised in the Paleocene-Eocene carbonates of this area, the chemical characterisation of these waters is going to be useful to better understand the potential geochemical processes in a CO<sub>2</sub> deep geological storage.

### Paper 2:

The geochemical and geothermometrical characterisation of the low temperature geothermal system of Arnedillo, hosted in Jurassic carbonate rocks, is presented in this. The reservoir temperature has been estimated, as in paper 1, by the combination of chemical geothermometers (classical and specific), isotopic geothermometers and geothermometrical modelling. One of the most relevant results from this work was the calculation of the order degree of the dolomite present in this aquifer. Since dolomite is a mineral phase with important thermodynamic uncertainties associated with its order degree, this calculation has been very useful in this and in further studies (see below).

### Paper 3:

In this paper the study initiated in paper 2 with the Arnedillo thermal system is completed with the study of the Fitero geothermal waters since both systems belong to the same aquifer at depth. However, although the waters emerging in both sites are from the same reservoir some differences regarding the composition, mineral equilibria and temperatures at depth are evident. Therefore, after the geothermometrical characterisation of the Fitero waters (chemical and isotopic geothermometers and geothermometrical modelling) the study has focused on the identification and evaluation of the main processes responsible for these differences and for the geochemical evolution of the waters in the aquifer. The main processes identified are the albitisation and dedolomitisation processes triggered by halite dissolution. This study was performed by using direct and inverse modelling methodologies and the results have been generalised to be applicable to other types of environments.

### Paper 4:

The Alhama – Jaraba geothermal system hosted in carbonates from Jurassic and Upper Cretaceous is characterised in this paper. This is also a low temperature system, but the reservoir temperature is even lower than in the previous thermal systems, which increases the complications in the temperature estimation due to the lack of some mineral equilibria (present in the previous cases), and/or to the thermodynamic uncertainties affecting some of the most probable mineral equilibria in low temperature conditions (carbonates and clays). The reservoir characterisation of these waters is additionally complicated because they are affected by secondary processes such CO<sub>2</sub> loss and mixing (in the case of Jaraba). Nevertheless, chemical geothermometers and geothermometrical modelling have been used trying to deal with the above mentioned problems and we finally state a proposal of a suitable procedure to be used in these cases.

### Paper 5:

The study of the Fitero travertines is initiated in this paper. These precipitates are constituted mainly by aragonite and, therefore, provide an excellent opportunity to study this calcium carbonate mineralogical phase, considerably less studied than calcite. Moreover, other travertines with high calcite proportions are also precipitated from the same water and can be used for comparison and result discussion. In this paper two common concerns in the study of calcium carbonate deposits are addressed. First, the possible factors controlling the precipitation of calcite and/or aragonite are discussed and evaluated in this system. Then, the stable isotope signature is evaluated since stable isotope signatures in travertines and tufas are used in paleoclimatic and paleoenvironmental reconstructions and the study of an active precipitating system at present can help to shed light on the interpretation and understanding of past deposits. Several  $\delta^{18}\text{O}$  fractionation equations are applied and the results suggest an apparent equilibrium situation. However, this situation does not seem coherent with the high  $\text{CO}_2$  loss deduced from the geochemistry of waters and the  $\delta^{13}\text{C}$  values measured in the travertines and the waters. This interesting result has also been investigated and discussed.

In Chapter 5 a joint discussion is presented integrating the results of the various papers and highlighting the most important findings. Moreover in this chapter some future research lines to complete this study are proposed and, finally the main conclusions are shown. Finally, the bibliographic references of the dissertation are listed.



# Abstract

The study and characterisation of high temperature geothermal systems has focused the interest of researchers since long ago given their high possibilities of exploitation (energy production). However, the interest on low temperature systems has become relevant only recently. One of the reasons is that the technological advances allow nowadays using the heat of these systems for different uses. The other is that they present similar characteristics to the ones expected in CO<sub>2</sub> geological storages. Therefore, the methodology used for their characterisation is directly applicable in the studies of characterisation of future storage sites and they can be used as analogues for the deduction and evaluation of possible processes taking place in these storages.

There are several issues with the low temperature geothermal systems that make their study more complicated than those with high temperature. The first problem is that waters at depth do not always attain the mineral equilibria on which the geothermometrical techniques are based, because at low temperature the reactions are slower. The difficulties increase in the case of carbonate aquifers with a more restricted number of mineral phases that make unsuitable the use of the traditional geothermometrical techniques (cation geothermometers or albite-K-feldspar equilibrium).

In this thesis various low temperature geothermal systems hosted in carbonate rocks have been characterised. In some of these systems the presence of detrital material in the aquifer has allowed the successful application of the traditional techniques. However, in other cases, the geothermometrical characterisation had to rely mainly on carbonates (calcite and dolomite) and aluminosilicate phases, which in some cases present important thermodynamic uncertainties (order degree in dolomite, and crystallinity and composition in the case of the aluminosilicates). Considering all these difficulties, one of the main results of the thesis is the proposal of a methodology to deal with them by evaluating the order degree of the dolomite present in the aquifer and performing sensitivity analyses of the thermodynamic data of aluminosilicates.

Another important issue treated in this thesis is the evaluation of the influence of halite dissolution in the aquifer. The study performed in paper 3 has demonstrated that this process is a decisive factor in the control of the chemical evolution of the waters triggering the anhydrite dissolution and the dedolomitisation and albitisation processes. Due to this interesting finding, an important part of the study focused on the analyses of these processes under different conditions by means of geochemical simulations.

The interest of the study of these special geothermal systems is not limited to the water characterisation. Another very interesting subject is the study and characterisation of the carbonate precipitates, travertines, which generate from the waters. The isotopic information of these deposits is used in paleoclimatic and paleoenvironmental reconstructions and, therefore, the study of recent travertines can provide very valuable information. Two samples of travertines precipitated in two pipes in the Fitero spa have been studied in this thesis. They precipitated from very similar waters but one is almost pure aragonite and the other has higher calcite proportions. This fact has provided an excellent opportunity to study and compare both mineral phases with respect to their precipitation and to the isotopic fractionation. The use of several aragonite stable isotope fractionation equations suggest that the precipitation of the Fitero travertines took place close to an apparent equilibrium situation despite the high CO<sub>2</sub> outgassing identified, which has also been discussed in detail. Finally, using several natural aragonites, a  $\delta^{18}\text{O}$  fractionation equation has been proposed which is very close to one of the most used experimental equations for aragonites.



# Resumen

El estudio y caracterización de sistemas geotermales de alta temperatura ha atraído siempre el interés de los investigadores debido a sus grandes posibilidades de aprovechamiento (producción de energía). Sin embargo, el interés en sistemas de baja temperatura ha sido menor y sólo recientemente ha comenzado a crecer. La razón de este creciente interés es que los avances tecnológicos permiten actualmente el uso del calor contenido en estos sistemas para diferentes usos, algo que en el pasado era inviable. Otro motivo de interés es que estos sistemas presentan características similares a las esperables en los almacenamientos geológicos de CO<sub>2</sub>. Esto hace que la metodología utilizada para su caracterización pueda ser directamente aplicable en los estudios previos de los futuros almacenamientos y, además, hace que los propios sistemas geotermales puedan ser utilizados como análogos para la deducción y evaluación de los procesos que podrían tener lugar en dichos almacenes.

El principal problema en el estudio de los sistemas de baja temperatura es que las aguas en profundidad no siempre alcanzan el equilibrio mineral en el que se basan las diferentes técnicas geotermométricas, ya que a bajas temperaturas las reacciones son más lentas. En el caso de tratarse de acuíferos carbonatos las dificultades son incluso mayores, ya que las fases mineralógicas presentes en el reservorio son más restringidas que en otro tipo de acuíferos y las técnicas geotermométricas tradicionales (geotermómetros catiónicos o el equilibrio albita-feldespató potásico) no siempre son aplicables. En algunos de los sistemas carbonatados estudiados hay también algo de material detrítico en el acuífero y se han podido usar las técnicas tradicionales con buenos resultados. Sin embargo, en otros casos, la caracterización geotermométrica ha tenido que basarse en los carbonatos (calcita y dolomita) y en algunas fases aluminosilicatadas con los consiguientes problemas de incertidumbres termodinámicas (el grado de orden en la dolomita, o la cristalinidad y composición para los aluminosilicatos).

En esta tesis, a través del estudio de varios sistemas geotermales de baja temperatura alojados en rocas carbonatadas, se propone una metodología para hacer frente a estos problemas y limitaciones. Esta consiste en realizar una evaluación del grado de orden de la dolomita presente en el acuífero y un análisis de sensibilidad de los datos termodinámicos de aluminosilicatos.

Otro tema de gran interés estudiado en la tesis es la evaluación de la importancia de la disolución de halita en el acuífero. Este estudio ha demostrado que es un factor muy importante en el control de la evolución química de las aguas puesto que desencadena la disolución de

anhidrita y da lugar a la generación de procesos de dedolomitización y albitización. Dada la importancia del tema y el hecho de que estos procesos son comunes en diferentes ambientes, se decidió realizar varias simulaciones geoquímicas para evaluar el comportamiento de estos procesos en diferentes condiciones.

El interés de los sistemas geotermales de baja temperatura no se limita solo a la caracterización de sus aguas. Otro aspecto importante es la presencia de sólidos carbonatados (travertinos) generados por precipitación a partir de dichas aguas. El estudio isotópico de este tipo de depósitos en sistemas geológicos pretéritos se utiliza para las reconstrucciones paleoclimáticas y paleoambientales y, por tanto, el estudio de travertinos recientes puede proporcionar importante información para mejorar la comprensión e interpretación de los depósitos antiguos. En esta tesis se han caracterizado dos muestras de travertinos de Fitero precipitados a partir de aguas muy similares pero con composiciones finales muy diferentes: uno es casi aragonito puro (lo cual en sí es de gran interés por ser mucho más raros) mientras que el otro tiene mayores proporciones de calcita. Esta particularidad ha permitido estudiar y comparar las dos mineralogías y evaluar las posibles diferencias en la precipitación y en el fraccionamiento isotópico de una y otra. El estudio del fraccionamiento isotópico ha indicado que la precipitación se ha producido, aparentemente, cerca del equilibrio isotópico a pesar de la alta tasa de pérdida de CO<sub>2</sub> identificada, situación que también ha sido discutida. Finalmente, usando datos de varios aragonitos naturales precipitados en muy diferentes condiciones, se ha podido proponer una ecuación para el fraccionamiento del  $\delta^{18}\text{O}$  que ha resultado ser similar a una de las ecuaciones experimentales más usadas en aragonitos.

# Index

---

<b>1. INTRODUCTION.....</b>	<b>1</b>
1.1 Objectives of the research.....	3
1.2 PhD candidate contributions.....	4
<b>2. STUDY AREAS .....</b>	<b>5</b>
2.1 Tiermas geothermal system.....	6
2.1.1 Geology.....	7
2.1.2 Hydrogeology .....	9
2.2 Alhama-Jaraba geothermal system .....	9
2.2.1 Geology.....	10
2.2.2 Hydrogeology .....	13
2.3 Fitero-Arnedillo geothermal system.....	13
2.3.1 Geology.....	15
2.3.2 Hydrogeology .....	17
<b>3. METHODOLOGY.....</b>	<b>19</b>
3.1 Bibliographic review .....	19
3.2 Sampling.....	19
3.2.1 Water sampling .....	10
3.3 Analytical techniques .....	21
3.3.1 Water samples.....	21
3.3.1.1 Alkalinity determination .....	21
3.3.1.2 Anion analyses .....	21
3.3.1.3 Cation analyses.....	22
3.3.1.4 Stable isotope analyses.....	22
3.3.2 Solid samples .....	23

3.3.2.1	Petrographical and textural study.....	23
3.3.2.2	Mineralogical analyses.....	23
3.3.2.3	Carbon and oxygen isotope analyses .....	23
<b>3.4</b>	<b>Data analysis and calculations .....</b>	<b>24</b>
3.4.1	Water data treatment.....	24
3.4.1.1	Chemical geothermometers.....	24
3.4.1.2	Isotopic geothermometers.....	29
3.4.1.3	Geochemical modelling .....	31
3.4.2	Solid data treatment .....	35
3.4.2.1	Stable isotope fractionation.....	35
<b>4.</b>	<b>RESULTS.....</b>	<b>39</b>
4.1	<b>Paper 1. Geochemistry, geothermometry and influence of the concentration of mobile elements in the chemical characteristics of carbonate-evaporitic thermal systems. The case of the Tiermas geothermal system (Spain).....</b>	<b>39</b>
4.2	<b>Paper 2. Low temperature geothermal systems in carbonate-evaporitic rocks: Mineral equilibria assumptions and geothermometrical calculations. Insights from the Arnedillo thermal waters (Spain) .....</b>	<b>55</b>
4.3	<b>Paper 3. Geochemical evolution of thermal waters in carbonate – evaporitic systems: the triggering effect of halite dissolution in the dedolomitisation and albitisation processes .....</b>	<b>71</b>
4.4	<b>Paper 4. Mineral equilibria and thermodynamic uncertainties in the geothermometrical characterisation of carbonate geothermal systems of low temperature. The case of the Alhama-Jaraba system (Spain) .....</b>	<b>87</b>
4.5	<b>Paper 5. Characterisation of recent aragonite travertine deposits associated to the Fitero thermal waters (Spain) I: stable isotopes equilibrium evaluation .....</b>	<b>103</b>
<b>5.</b>	<b>JOINT DISCUSSION AND CONCLUSIONS.....</b>	<b>139</b>
5.1	<b>Geothermometrical approach .....</b>	<b>139</b>
5.2	<b>The influence of halite in the reservoir.....</b>	<b>143</b>
5.3	<b>Fitero travertines.....</b>	<b>144</b>
5.3.1	Mineralogy.....	144
5.3.2	Isotope signature .....	145
5.4	<b>Applications to CO<sub>2</sub> geological storages.....</b>	<b>148</b>
5.5	<b>Future research lines.....</b>	<b>149</b>

<b>5.6</b>	<b>Final conclusions.....</b>	<b>150</b>
<b>5.7</b>	<b>Conclusiones finales .....</b>	<b>151</b>
	<b>REFERENCES .....</b>	<b>153</b>
	<b>SUPPLEMENTARY MATERIAL .....</b>	<b>171</b>
	<b>APPENDICES .....</b>	<b>177</b>
	<b>APPENDIX 1. Impact factor, subject category and contributions.....</b>	<b>179</b>
	<b>APPENDIX 2. Resignation of the co-authors to use the papers in other PhD dissertations.....</b>	<b>185</b>



# 1. INTRODUCTION

---

Geothermal systems appear in a wide range of different geological environments where a heat source and a fluid to transfer the heat exist (Nicholson, 1993). The classification of geothermal systems can be done taking into account different features (Nicholson, 1993): reservoir equilibrium state, fluid type, reservoir temperature, host rock and heat source.

- ✓ Reservoir equilibrium state. According to this there are two types: systems in dynamic equilibrium and systems in static equilibrium. The first ones are those in which water is continuously entering the system through the recharge areas, the water is heated and then it goes out of the reservoir. The heat in these systems is transferred by convection and by the fluid circulation. In the systems under static equilibrium the recharge does not exist or it is minimal and the heat transfers by conduction.
- ✓ Fluid type. There are also two types in this group: liquid-dominated systems and vapour-dominated systems. Liquid-dominated systems are those containing mainly liquid water and are the most common, along with those with different liquid and vapour proportions. In the vapour-dominated systems the discharge is mostly steam, and they are quite scarce. In some cases the liquid-dominated systems are called water-dominated systems, but this term is incorrect since both liquid and vapour are water but in different states.
- ✓ Reservoir temperature. This is probably the most relevant way of classification of thermal systems since it is also determinant of their possible use as energetic resource. There are different classifications under this category (see Lee, 1996 or Williams et al., 2011). The classification presented here is the one explained by Sánchez et al. (2011) who divide the geothermal systems as follows: high-temperature systems ( $> 150$  °C), medium-temperature systems (100 – 150 °C), low-temperature systems (30 – 100 °C) and very low-temperature systems ( $< 30$  °C). Systems of high- and medium-temperature are mainly used for

electricity production while in low- and very-low temperature systems the heat is directly used, for example, in heating and refrigeration systems, agriculture applications (e.g. greenhouses, aquaculture (e.g. fish farms), industrial processes or balneotherapy (Sánchez et al., 2011).

- ✓ Host rock. Broadly, geothermal systems can be divided into volcanic (including volcanic and plutonic rocks), clastic-sedimentary and carbonate-sedimentary (and their metamorphosed rocks). The importance of taking into account this classification is that the rocks interacting with the fluid will determine its geochemistry.
- ✓ Heat source. Under this category geothermal systems are divided in volcanogenic and non-volcanogenic. Volcanogenic systems are those where the heat source is magma and they are always high-temperature systems. In non-volcanogenic systems the fluid is heated by deep circulation as a result of the regional geothermal gradient or due to tectonic activity and they can result in both, high and low temperature systems.

The systems studied in this thesis can be classified as non-volcanogenic, liquid-dominated, low-temperature systems in dynamic equilibrium and hosted in carbonate sedimentary rocks.

There are many studies focused on systems of high- or medium-temperature because they can be easily used for energy production. The number of studies about low-temperature systems is much less, although they are increasing because the technological advances provide new techniques which allow using these low temperature resources on a larger scale (Sánchez et al., 2011). Chemical characterisation of thermal waters along with the identification of the main water-rock interaction process responsible for that and the reservoir temperature estimation, should be the first steps when evaluating the geothermal potential of a geothermal area (D'Amore and Arnórsson, 2000) and this type of characterisation is the one pursued in this research.

There is a second reason why the interest on this type of systems is increasing and it is related to the social concern about the global warming and the need of reducing the atmospheric carbon dioxide emissions (e.g. Echevarria and Xiu, 2014; Metz et al., 2005). One of the ways of reducing the carbon dioxide emitted to the atmosphere is its capture in the emission's plants and its storage in oceans, in geological formations, in inorganic carbonates or through industrial fixation (e.g. Metz et al., 2005). From all these storage options, probably the most viable is the geological storage in deep formations, specifically in the deep saline aquifers (e.g. Bachu, 2000; Choi et al., 2014; Elío et al., 2015; Herzog et al., 1997). In this context, low-temperature geothermal systems provide an excellent analogy of the storage sites since they have many similarities in terms of temperature, salinity, depth and geological context. The characterisation



of these geothermal systems can be used to obtain a better understanding of the possible processes expected in this type of storages as it has been done by different authors such as Auqué et al. (2009), Choi et al. (2012), Flaathen et al. (2009) Gal et al. (2012), Güleç and Hilton (2016) or Lu et al. (2011).

The studied systems are hosted in carbonate formations in contact with evaporites and in some cases with some disperse detrital material. These hosting rocks, in contrast with the volcanic or clastic cases, have some particularities that make their study very interesting and necessary. The interaction of the waters with those rocks will determine the geochemistry of the waters and the mineral equilibria in the deep reservoir which, in turn, will condition the applicability of the geothermometrical techniques, one of the most relevant aspects in the characterisation of a thermal area.

When the hosting rocks are volcanic or clastic the mineral assemblage at depth is quite large and their thermodynamic data are well known (e.g. albite or K-feldspar). However, in carbonate systems the mineral set is limited to carbonates and some aluminosilicates, some of which are affected by thermodynamic uncertainties that make the geothermometrical characterisation of the system more difficult. That is why it becomes necessary to address this issue and to identify the best approach to the problem.

Finally, the growing interest on these thermal systems has not only to do with the waters but also with the carbonate solids (travertines) that can precipitate in the springs. Apart from helping to fully characterise the geothermal system, the study of these solids and their stable isotope signatures, can be very useful to better understand the isotopic fractionation in ancient travertines improving their use for paleoclimatic and paleoenvironmental reconstructions (e.g. Andrews, 2006; Capezzuoli et al., 2014; Ford and Pedley, 1996; Fouke et al., 2000; Garnett et al., 2004; Jones and Renaut, 2010; Kele et al., 2011, 2008; Lachniet, 2015; Liu et al., 2006, 2010; Osácar et al., 2016, 2013; Pedley, 2009; Pentecost, 2005).

## 1.1 Objectives of the research

The general objective of this research is to increase the knowledge on low temperature geothermal systems associated to carbonate rocks. In this general context the following specific objectives are addressed:

- To obtain a complete geochemical and geothermometrical characterisation of the low temperature and carbonate geothermal systems of Tiermas, Arnedillo-Fitero and Alhama-Jaraba.

- To test and evaluate the applicability, in low temperature systems hosted in carbonate rocks, of different geothermometrical techniques proven to be very useful in other systems (i.e. high temperature with granitic or basaltic rocks).
- To establish the most suitable approaches to the various problems and limitations found and propose an adequate methodology for these systems.
- To evaluate the possible applications of the obtained results for the study and understanding of CO<sub>2</sub> storage sites.

A final objective is the characterisation of the travertines deposited from the Fitero thermal waters. The two main issues are: 1) to identify the main mineral phases presents in the travertines (calcite and/or aragonite) and discuss the main factors responsible for it; and 2) to evaluate the stable isotope signature of the travertines and its fractionation to help with the interpretation of ancient travertines when they are used in paleoclimatic and paleoenvironmental reconstructions.

## **1.2 PhD candidate contributions**

Although the publication of the different papers that conform this thesis dissertation would not have been possible without the collaboration of the co-authors, my contribution to them is present in every single step given.

The main tasks during the development of this doctoral thesis can be summarised as follows:

- Bibliographic revision of the literature related to carbonate systems of low temperature and carbonate precipitates, among other issues of interests.
- Planning and performance of the water sampling campaigns carried out and the preparation of the samples for analyses.
- Study of the solid samples with field emission scanning electron microscope (FESEM) and the petrographic microscope with the help and guidance of the co-authors.
- Preparation of the solid samples for the X-Ray Diffraction analyses.
- Treatment of the analytical data and, along with the co-authors, interpretation of the results.
- Writing of the manuscripts with the guidance and assistance of the co-authors.
- Synthesis of the results and conclusions for preparing this thesis dissertation with the guidance and assistance of my thesis supervisor.
- Apart from this, I have prepared and presented many of the obtained results in different International and National Congresses.

## 2. STUDY AREAS

---

Although the papers presented in the Results section contain a complete description of the geology of the areas around the selected geothermal systems, a summary of the geological and hydrogeological information is included in this section.

The three studied systems have some important characteristics in common that have been the reason to select them for this study: they have low temperature waters and their aquifers are, mainly, in carbonate rocks. All of them are located in Spain, the Tiermas and the Alhama-Jaraba systems in the Aragon region, and the Arnedillo-Fitero system between Navarra and La Rioja regions, as shown in Figure 1.



**Figure 1.** Spain map showing the general location of the three studied geothermal systems: Tiermas and Alhama-Jaraba systems in Aragon Region, and the Fitero-Arnedillo system in Navarra and La Rioja Regions.

## 2.1 Tiermas geothermal system

The Tiermas springs are in the northwest of the Zaragoza province close to the border with Navarra at an altitude of about 580 m a.s.l. The waters emerge in the north shore of the Yesa reservoir, which covers the springs during most of the year. Only during a few months after summer, when the irrigation campaign empties the reservoir, the level of the reservoir descends enough to leave the springs under exposure (Figure 2).

The medicinal and therapeutic properties of these waters are known since long ago, at least since Roman times, who gave it the name of “Tiermas” due to the existence of thermal waters (González, 1867). There was a village associated to the springs and with the same name but it was flooded in 1959 to fill in the reservoir (Armijo, 2006). Nowadays the closest village is Sigües, about 10 Km to the east.



**Figure 2.** Tiermas photographs. Panel a: Yesa Dam when the level goes down and the Tiermas springs are exposed. Thermal waters can be seen in the shore next to the ruins of the old village. Panel b: One of the points where thermal waters emerge.

### 2.1.1 Geology

The system is located in the the Aragonian pre-Pyrenees, in the Jaca-Pamplona Basin, bounded by the Boltaña anticline and the Pamplona fault, on the east and west, respectively, by the Axial Zone and the Inner Ranges on the north and by the Outer Ranges on the south.

The Jaca-Pamplona Basin comprises materials from Triassic to Miocene with a Paleozoic basement of sedimentary and metasedimentary rocks (Saura and Teixell, 2006; Figure 3) but only the rocks from the Cretaceous and more modern, outcrop (IGME, 1973; Larrasoña et al., 1996). This basin is of great structural complexity with two structural trends giving place to two fault systems of NNE-SSW and E-W direction (IGME, 1973; Figure 3).

The Triassic rocks are represented by the Buntsandstein (conglomerates, sandstones, lutites) and Keuper (evaporites, lutites, limestones) facies (Pueyo et al., 2012). Over them, (as there are not Jurassic rocks in the area) the marine deposits from the Upper Cretaceous appear, constituted by limestones, dolostones, marls and, on the top, the sandstones and conglomerates of the Marbore Sandstones (Faci, 1997; IGME, 1973).

The Upper Cretaceous is overlaid by the Paleogene materials: Paleocene Alveoline Limestones, Lower-Middle Eocene Guara Limestones and Turbidites of the Hecho Group (Faci, 1997; IGME, 1973). The Alveoline Limestones are mainly carbonates and calcarenites with abundant bioclasts (Faci, 1997; IGME, 1973). The Guara Limestones consist of bioclastic limestones with bioclasts in the bottom and marls in the top (Faci, 1997; IGME, 1973; Puigdefàbregas, 1975).

The Hecho Group is constituted by siliciclastic turbidites and marls with important carbonate mega-layers (up to 200 m thickness) intercalations (Bauluz et al., 2008; Faci, 1997; IGME, 1973).

Then, a regressive series was deposited in the Middle to Upper Eocene constituted by the Sabiñánigo Sandstones, the Arguís-Pamplona Marls and the Belsué-Atarés Marls and Sandstones, overlaid by evaporitic materials (anhydrite, halite and potassium salts) indicative of the transition to a paralic environment (Ayora et al., 1995; Faci, 1997; IGME, 1973). Finally, the basin was filled by the alluvial continental sediments during the Oligocene and Miocene (Faci, 1997; IGME, 1973).

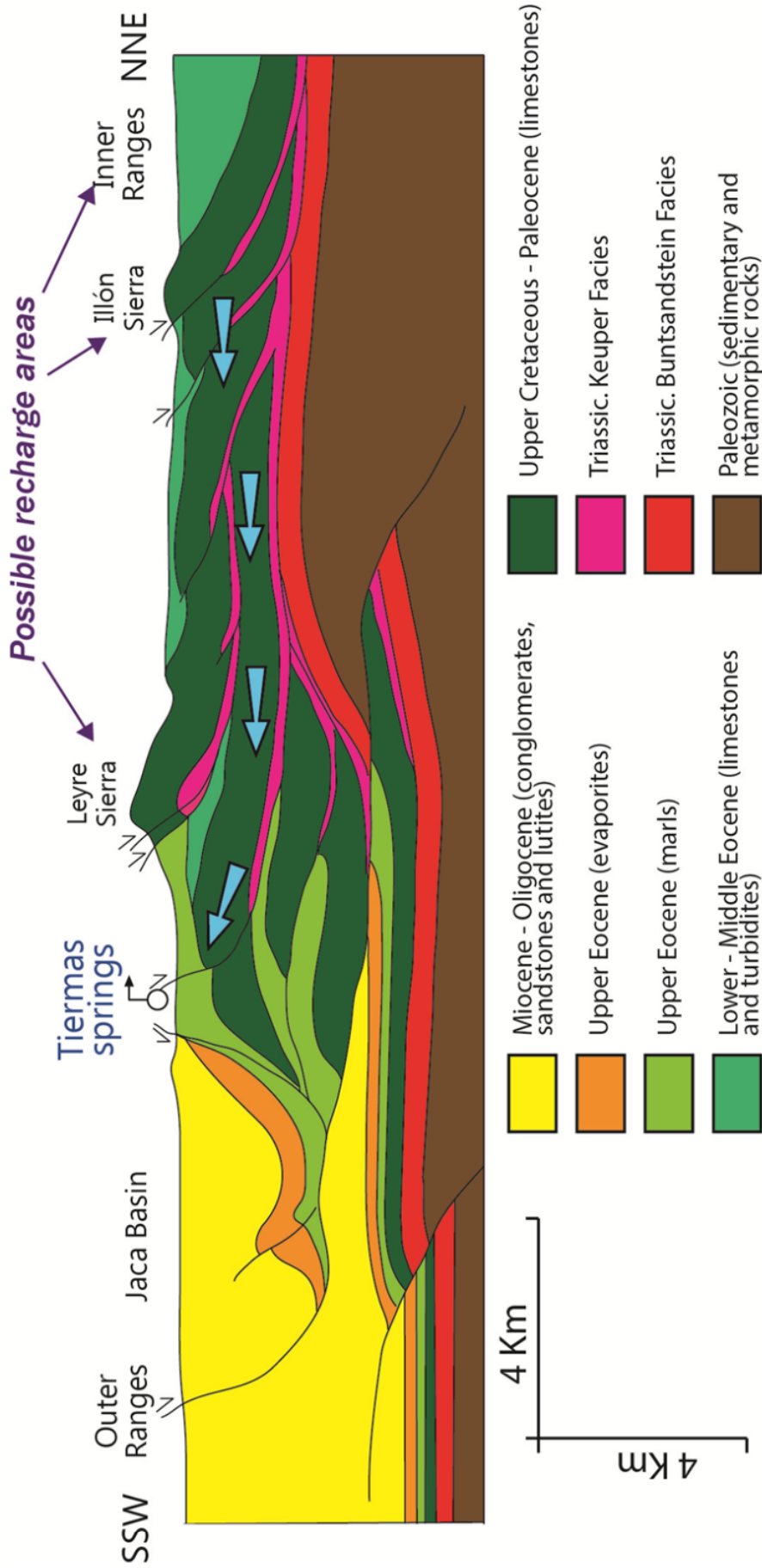


**Figure 3.** Cross section showing the general structure and geology of the Tierras geothermal system (modified from ALGECO2 project; IGME, 2010). The structural complexity of the area can be appreciated. The aquifer is hosted in the Upper Cretaceous-Paleocene limestones (dark green). The approximate location of Tiermas springs and the possible recharge is shown. Blue arrows represent the flow direction. A geological map can be found in the results section, paper 1.

### 2.1.2 Hydrogeology

The potential aquifer of the Tiermas thermal waters is considered to be hosted in the Paleocene – Eocene marine rocks: the Alveoline Limestones, Guara Limestones and the turbidites from the Hecho Group (Faci, 1997; ITGE-DGA, 1994; Sánchez, 2000; Sánchez et al., 2004, 2000).

The recharge areas are not precisely defined by they are thought to be in the Paleocene and Eocene outcrops located to the north of the springs in the Leyre, Illón and Orba Sierras or in the Inner Ranges (ITGE-DGA, 1994; Figure 3).

The flow of the waters from the recharge areas to the springs in the N-S direction is interrupted by the NNE-SSW fractures which make the flow vertical and produce the ascent of the waters to surface and their emergence with flow rates of about 200 L/s and temperatures close to 40 °C (ITGE-DGA, 1994).

## 2.2 Alhama-Jaraba geothermal system

Continuing in the Aragón region, this system is one of the main thermal systems in Spain with several springs in the surroundings of the Alhama de Aragón and Jaraba villages, separated about 12 km from each other.

In Jaraba, the waters spring close to the Mesa river at an elevation of 737 m a.s.l.. There are 14 catalogued springs but there are many others without an official classification, some of them visible and others beneath the waters of the river (Figure 4; Auqué et al., 2009; ITGE-DGA, 1994). These waters were also known since roman times when they were named “aguas de las ninfas” but it was in 1120 when the first pool was built in the location where La Virgen spa is placed nowadays (ITGE-DGA, 1994; Martín, 2016). Since then the use of the thermal waters has increased and the facilities related to them also. There are 5 exploitations in Jaraba at present: three spas (La Virgen, Serón and Sicilia) and two bottling plants (Fontecabras and Lunares).

There are twelve catalogued springs in Alhama emerging at an elevation of 660 m a.s.l.. Although the roman remains are scarce in this place, these waters were mentioned by latin historians such as Ptolomeo or Plinio. The first facility dates from 1122 and it was named “La Casita” or “Baños Viejos de San Roque” (ITGE-DGA, 1994; Martín, 2016). There are several springs exploited at present in the two spas of the village (Termas Pallares and Alhama de Aragón) and also additional fountains in the municipality (Figure 5).

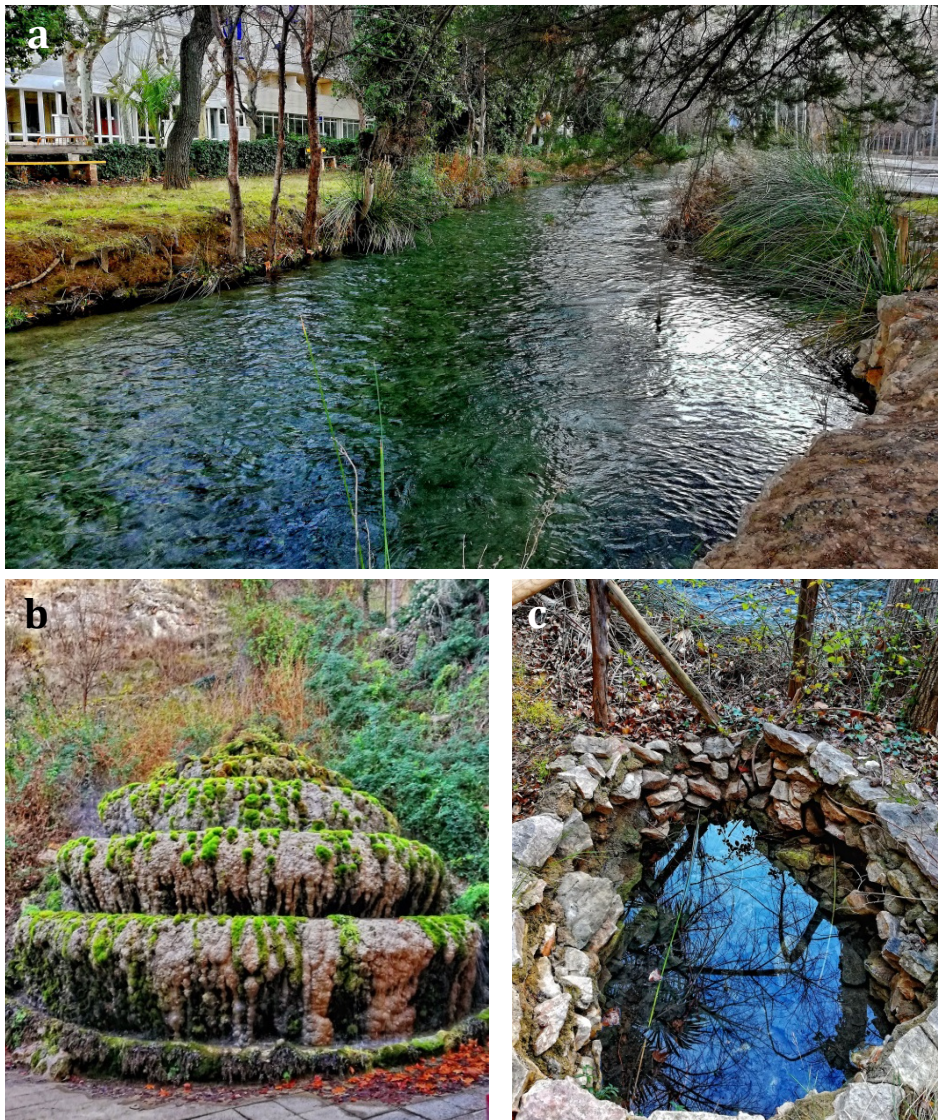


**Figure 4.** Jaraba photographs. Panel a: Mesa River, in which numerous emergences of waters appear. Panel b: fountain of thermal water in the Serón Spa. Panel c: Small pond next to the Mesa River where thermal waters emerge.

### 2.2.1 Geology

The system is located in the Iberian Chain, between its west limit and the tertiary Almazán Basin. The materials in this area range from Paleozoic to Quaternary (IGME, 1991; Figure 6).

The basement of the area consists of Paleozoic rocks constituted, mainly, by quartzites, schists and phyllites. These are followed by the common Triassic facies: Bundsandstein (conglomerates, sandstones and clays), Muschelkalk (limestones, dolostones and marls) and Keuper (marls, clays and evaporites). The Jurassic in the area is scarce and it is only represented by a marine carbonate formation from the transit Triassic-Jurassic, similar to the Cortes de Tajuña Formation, and constituted by dolomitic breccias and massive dolostones.



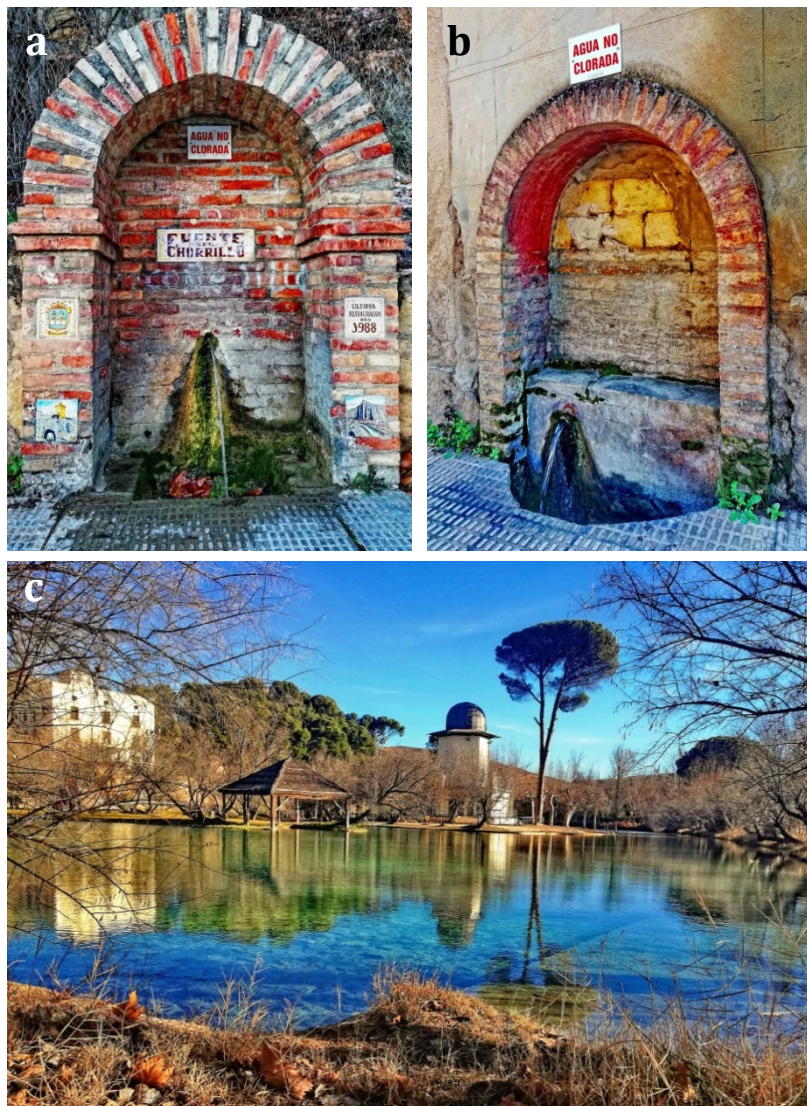


**Figure 5.** Alhama de Aragón photographs. Panels a and b: two fountains of thermal waters in the village. Panel c: thermal lake inside the Termas Pallarés Spa, where there are several thermal waters springs.

The Lower Cretaceous overlies the Jurassic and it consists of the Utrillas Sandstones (Albian) and the marine carbonate formations from the Upper Cretaceous: Santa María de las Hoyas (limestones, marls, sandstones and clays), Nuevalos (limestones, dolomitic limestones and dolostones with fossils), Monterde (nodulitic limestones), Jaraba (massive dolostones and limestones with bioclasts), Pantano de la Tranquera (dolomitic breccias and dolostones with marls intercalations at bottom), Hontoria del Pinar (bioclastic limestones) and Burgo de Osma (limestones).

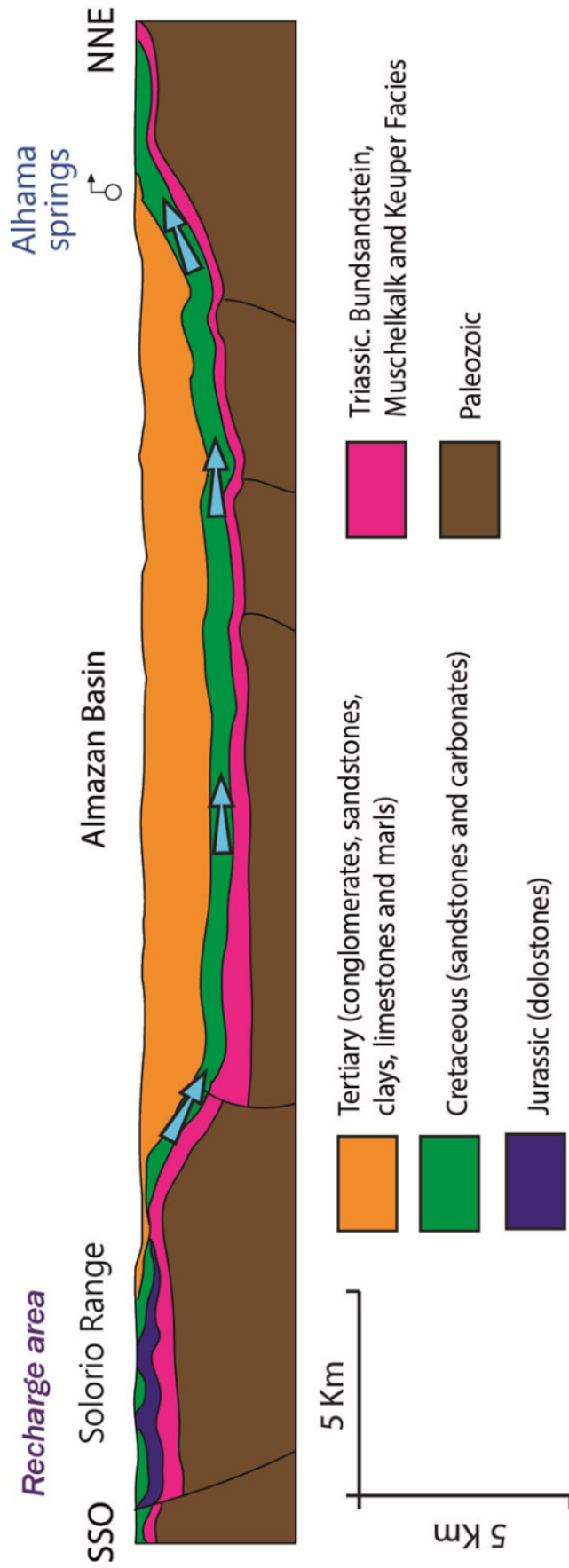


**Figure 6.** Cross section showing the general structure and geology of the Alhama-Jaraba system (modified from ALGECO2 project; IGME, 2010). The main aquifer is hosted in the cretaceous carbonates (green). The approximate location of Alhama springs and the recharge area is shown. The Blue arrows represent the flow direction. A geological map can be found in the results section, paper 4.

A tectonic inversion took place at the end of the Cretaceous that created the tertiary Almazan Basin which was filled in by detrital deposits from Paleogene and Neogene. The Paleogene sediments consist of conglomerates, sandstones, clays, limestones and marls, and the Neogene materials are conglomerates, sandstones and clays. Finally, the quaternary deposits consist of glacial, terraces or alluvial deposits.

The structure of the area was defined by the superposition of the Hercinian and Alpine orogenies. The general structure of the area consists of anticlinals and synclinals in the NW-SE direction and hercinian faults of the same direction lately reactivated during the alpine tectonics, changing to W-E direction (Auqué et al., 2009).

### **2.2.2 Hydrogeology**

There are two carbonate aquifers in this area: the Solorio aquifer, in the Jurassic materials, and the Alhama aquifer in the Upper Cretaceous rocks. Although the hydrological model of this system is not clearly defined, it is accepted that both aquifers are interconnected although the water flow occurs mainly through the Cretaceous carbonates (Sánchez et al., 2004).

There are two possible recharge areas: 1) one through the Jurassic rocks in the Solorio range with a SW-NE water flow direction (Figure 6); and 2) a recharge through the cretaceous formations in the area of Deza with a NW-SE flow direction.

The discharge is always associated to the Cretaceous carbonates and the flow rates are around 600 L/s in Jaraba and 550 L/s in Alhama (De Toledo and Arqued, 1990; IGME, 1980; Sánchez et al., 2004), making this system one of the largest naturally flowing systems in Europe (similar to the one in Budapest with 580 L/s which is considered the Europe's largest naturally flowing thermal system; Goldscheider et al., 2010 and references therein). The spring temperatures in Alhama are always about 30 °C but in Jaraba they range from 22 to 32 °C due to a mixing process with shallow and cooler waters (Blasco et al., 2016; Tena et al., 1995).

## **2.3 Fitero-Arnedillo geothermal system**

The waters of this system emerge in the Fitero and Arnedillo villages separated about 35 km from each other and located in Navarra and La Rioja regions, respectively. Fitero springs emerge at an altitude of about 420 m a.s.l. inside the two spas of the village, the Virrey Palafox spa (or “Baños Viejos”) and the Becquer Spa (or “Baños Nuevos”; Figure 7). The two main thermal springs in Arnedillo emerge at an altitude of about 655 m a.s.l. one inside the Arnedillo

spa, and the other in the Cidacos river, in a kind of natural pools where the waters can suffer mixing with the river waters (Figure 7).



**Figure 7.** Arnedillo and Fitero photographs. Panel a: Arnedillo thermal water inside the spa. Panel b: pools built next to the Cidacos River where thermal waters emerge. Panel c: Fitero thermal waters in the Becquer spa.

Although the first documented references of the use of these waters for balneotherapy are from the Middle Ages (XI century in the case of Arnedillo), the roman remains indicate the previous knowledge of the medicinal and therapeutic properties of the waters ( Lopez de Azcona, 1988; even in prehistoric times; Olcoz, 2017).

### 2.3.1 Geology

This system is located in the NW part of the Iberian Chain and the springs emerge through the Cameros thrust, which put into the contact between the Cameros Range and the tertiary Ebro Basin, (Coloma et al., 1997; Sánchez and Coloma, 1998; Figure 8).

The Cameros Range consists of different Mesozoic materials, from Triassic to Upper Cretaceous (Figure 8). The Triassic is constituted by Buntsandstein (sandstones, siltstones and breccias), Muschelkalk (dolostones) and Keuper (anhydrite, marls and clays) facies (Coloma, 1998; Gil et al., 2002). The Jurassic is represented by the typical marine formations of the Iberian Chain (Coloma, 1998; Gil et al., 2002; Gómez and Goy, 1979; Goy et al., 1976): Imón (well stratified dolostones), Cortes de Tajuña (massive dolostones and limestones, and dolomitic breccias with anhydrite), Cuevas Labradas (limestones and dolostones well stratified with some marls intercalations on the top), Cerro del Pez (marls with some disperse limestone intercalation), Barahona (nodular bioclastic limestones with thin marls intercalation in the bottom), Turmiel (marls and limestones alternation with abundant fossil content), Chelva (limestones), Aldealpozo (black limestones) and Torrecilla (limestones with corals).

After the marine Jurassic sedimentation the Cameros Basin was created due to the rifting that started at the end of the Jurassic and lasted during the Cretaceous, and continental sediments were deposited (Coloma, 1998; Gil et al., 2002; Mas et al., 1993). These continental sediments are divided into five groups (Tischer, 1965), three of them consisting of lutites and sandstones deposited in a fluvial environment (Tera, Oncala and Urbión Groups) and the other two constituted by limestones, marls and limolites representative of a lacustrine sedimentation (Enciso and Oliván Groups). The post-rift sedimentation is represented by the Urgon Facies (carbonates), the Utrillas Formation (sandstones) and carbonates from the Upper Cretaceous (Gil et al., 2002).

After the tertiary inversion, which produced the elevation of the Cameros Range, during Paleogene and Neogene the Ebro Basin was filled with detrital material and compressive structures were generated, being the most important the Cameros Thrust (Coloma, 1998; Gil et al., 2002).

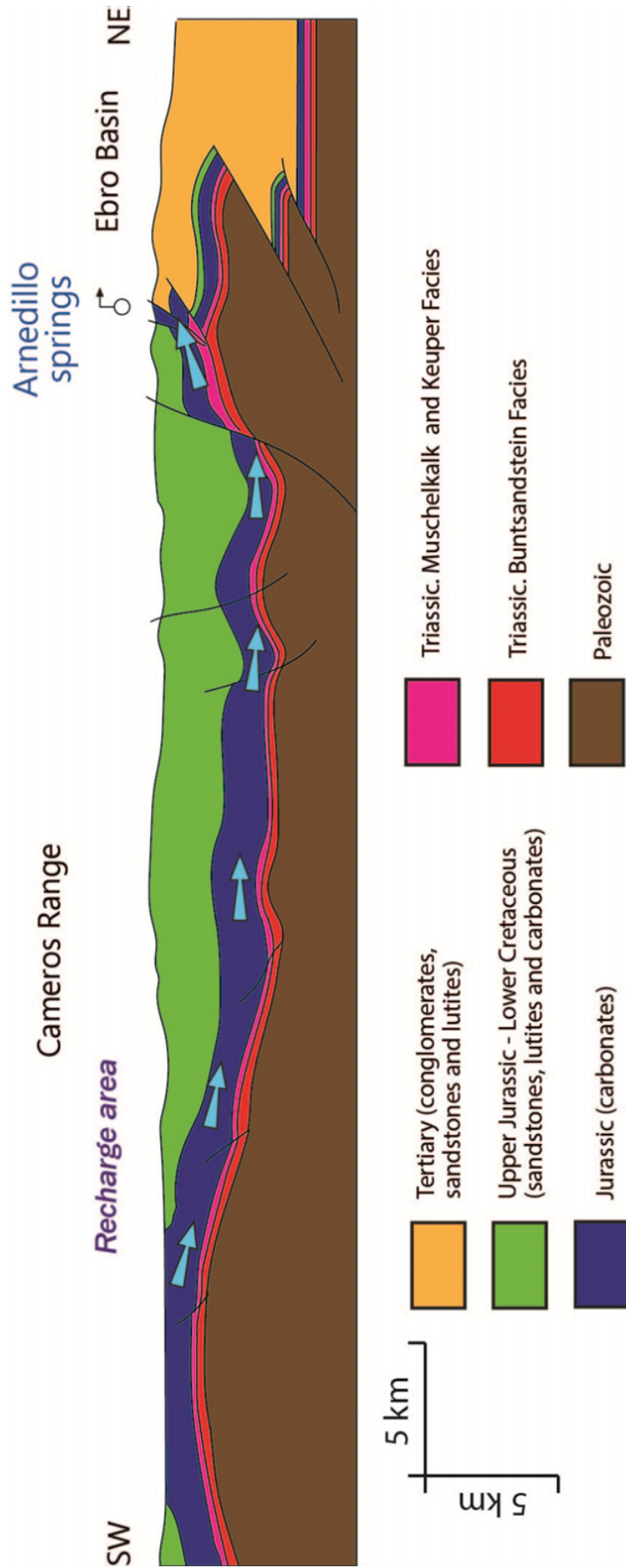


**Figure 8.** Cross section showing the general structure and geology of the Fitero-Arnedillo system (modified from ALGECO2 project; IGME, 2010). The aquifer is hosted in the Upper Jurassic carbonates (included in the blue colour). The approximate location of Arnedillo springs and the recharge area is shown. Blue arrows represent the flow direction. A geological map can be found in the results section, papers 2, 3 and 5.

### 2.3.2 Hydrogeology

The aquifer of the Fitero-Arnedillo thermal waters is hosted in the marine formations deposited during the Jurassic. These formations are divided into three groups, two permeable groups separated by other less permeable one. Imón, Cortes de Tajuña and Cuevas Labradas constitute the first permeable group; and Chelva, Aldealpozo and Torrecilla Formations the second one. The intermediate less permeable group is formed by Cerro del Pez, Barahona and Turmiel Formations. Since an important fracture system affect these rocks all these formations are interconnected but the main flow is hosted in the first permeable group (Coloma et al., 1995; Sánchez et al., 1999; Sánchez and Coloma, 1998).

The recharge of the waters takes place by direct infiltration through the Jurassic outcrops, from permeable stretches of rivers, and through the outcrops of the continental sediments deposited in the syn-rift period (Coloma et al., 1997, 1995; Figure 8). The discharge is favoured by the Cameros Thrust which makes the waters ascent rapidly to surface and spring with temperatures about 50 °C and flow rates close to 50 L/s in Fitero and 20 L/s in Arnedillo.





# 3. METHODOLOGY

---

A description of the methodologies used in this PhD thesis is presented in this section. Each paper contains its specific Methodology section and therefore, only a general overview of the main techniques of analysis and data treatment is described here.

## 3.1 Bibliographic review

The first necessary step was to perform an in-depth bibliographical compilation:

- To understand the state of the art in the knowledge of low-temperature geothermal systems hosted in carbonate rocks, and of the aragonite travertines, and the main problems associated to their study.
- To learn about the various methodologies and techniques to, finally, be able to select the most adequate ones to each specific case.
- To obtain the necessary information about the three studied geothermal systems regarding the geological context and the previous geochemical and/or hydrological studies.

## 3.2 Sampling

A sampling campaign was carried out in October 2015 when several water samples were taken in Arnedillo and Fitero springs (Figure 9) following the procedure described below. In the case of Tiermas and Alhama-Jaraba systems the study was performed using the analytical data obtained in previous sampling campaigns performed by the Geochemical Modelling Group of the University of Zaragoza following the same methodology. The Fitero travertines samples were also taken previously by the members of the Geochemical Modelling Group in two

different points: in an old pipe that no longer exists and which discharged water from the cooling pool in the Becquer spa, and the other in a currently active pipe that discharges the water from the same spa to the river.



**Figure 9.** Photographs taken during the sampling campaign. In panel a some of the material used in the sampling is shown. In panel b the thermal water is being filtered in the field by using a kitasato. In panel c the pH is measured in situ. Finally, in panel d the bottles in which water samples have been taken are labelled.

### 3.2.1 Water sampling

As it is known, a water sample is a system in constant evolution since taken until it is analysed. Even being isolated from the environment, it will evolve depending on the initial conditions in the system and the environmental conditions. This will lead to a change in the physico-chemical characteristics of the water, which, in turn, will make the obtained analytical data not representative of the real conditions in the springs. The parameters which suffer the fastest variation are pH and temperature and therefore, they must be determined *in situ*. It is also important to determine the alkalinity and the anion as soon as possible. Finally, the cations and isotopes can be analysed later on as long as the water sample has been treated and stabilised correctly (filtered and acidified). Taking these precautions into consideration a specific protocol was followed for the water sampling and it is described next.

pH and temperature were determined in each sampling point by a Thermo Orion 250A pH-meter with combined pH electrode ORION 815600 Ross with temperature compensation. The pH-meter was calibrated with the standard buffer solutions of pH 7.0 and 10.00. The electrical conductivity was measured with a conductivimeter Jenway 4200 with a K=1 probe and automatic correction of temperature.

Samples for cation, anion and isotope analyses were taken separately in polyethylene bottles previously washed with ultrapure HNO<sub>3</sub>, rinsed with distilled water and air-dried. Samples for anions and <sup>34</sup>S were taken in 500 ml bottles and samples for cations and oxygen and deuterium isotopes in 100 ml bottles. Samples for cation and oxygen and deuterium isotope analyses were filtered through 0.1 µm, by using a KITASATO and, in the case of cations, the samples were also acidified to pH less than 1 with ultrapure HNO<sub>3</sub>. Samples for <sup>13</sup>C determination were taken in small crystal vials containing mercury chloride to avoid the microbial activity.

### **3.3 Analytical techniques**

#### **3.3.1 Water samples**

The detailed description below corresponds to the analytical procedure followed for the Fitero and Arnedillo water samples taken during the development of this doctoral thesis. For the other systems the analytical techniques were similar and the details are included in the corresponding papers in the results section.

##### ***3.3.1.1 Alkalinity determination***

As explained above, alkalinity should be determined without delay, so it was measured in the Geochemistry Laboratory of the Earth Science Department at the University of Zaragoza, only a few hours after the sampling (Figure 10). It was measured with a Mettler titrator using H<sub>2</sub>SO<sub>4</sub> 0.02N and determination of the final point at pH = 4.5 with a pH-meter Thermo Orion 250A.

##### ***3.3.1.2 Anion analyses***

Chloride, sulphate and fluoride were also analysed in the Geochemistry Laboratory of the Earth Science Department at the University of Zaragoza with the assistance of Enrique Oliver, laboratory technician, in 24 hours after collection.

Chloride and fluoride were determined by a selective ion analyser equipment, with the specific chloride electrode ORION 94-17B and fluoride electrode ORION 94-09. The determination was done by direct measurement using CISA and Tisab II as interference suppressor for chloride and

fluoride, respectively. Sulphates were determined by colorimetry using a modification of the Nemeth method (Nemeth, 1963).

### **3.3.1.3 Cation analyses**

Cations were analysed in the Scientific and Technological Centre at the University of Barcelona. Ca, Na, K, Mg, Sr and Si were determined by Inductively Coupled Plasma Emission Spectrometry (ICP-OES) with a Perkin Elmer Optima 3200rl equipment in standard conditions. The rest of the minor cations were analysed by Inductively Coupled Plasma Mass Spectrometry (ICP-MS) with an Agilent 7500ce equipment in standard conditions.

### **3.3.1.4 Stable isotope analyses**

Stable isotopes were also analysed in the Scientific and Technological Centre at the University of Barcelona.  $\delta^{18}\text{O}$  and  $\delta^2\text{H}$  in water,  $\delta^{13}\text{C}$  in the dissolved inorganic carbon, and  $\delta^{34}\text{S}$  and  $\delta^{18}\text{O}$  in dissolved sulphates, were analysed by Continuous Flow Isotope-Ratio Mass Spectrometry (CF-IRMS) with a Delta plus xp Thermofisher equipment.  $\delta^{18}\text{O}$ ,  $\delta^2\text{H}$  and  $\delta^{13}\text{C}$  were directly analysed using the secondary standards traceable to certified standards: NBS18, NBS19, SMOW and SLAP.  $\delta^{34}\text{S}$  and  $\delta^{18}\text{O}$  in dissolved sulphate were measured after precipitating it as  $\text{BaSO}_4$  (0.2 mg in silver capsule for oxygen and 0.3 mg in tin capsule for sulphur) and using the NBS-127, SO-5 and SO-6 secondary standards.

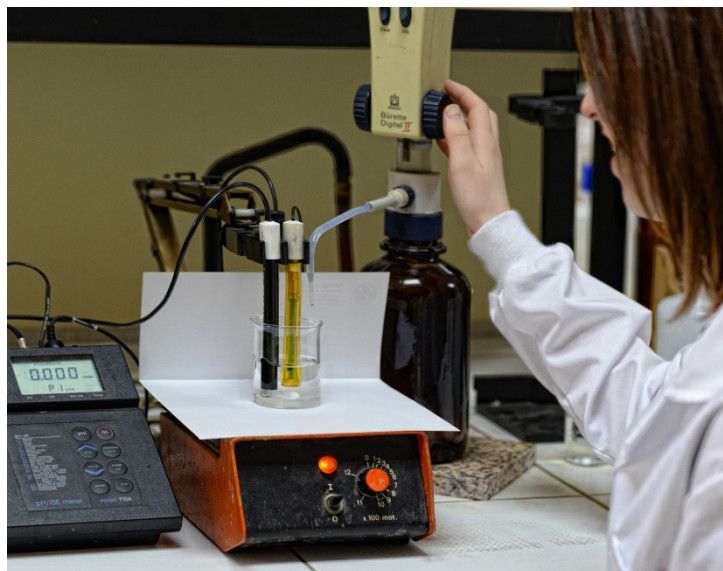


**Figure 10.** Alkalinity measurement in the Geochemistry Laboratory of the Earth Sciences Department of the University of Zaragoza.

### 3.3.2 Solid samples

#### 3.3.2.1 Petrographical and textural study

The samples were first described after observation at hand-size scale. A more detailed study of their characteristics and textures was done through their study by conventional optical petrographical microscope on polished thin sections and field emission scanning electron microscope (FESEM).

Thin sections were done by the Service of preparation of rocks and hard materials at the University of Zaragoza. And they were studied by petrographic microscope in the Earth Science Department of the University of Zaragoza. The FESEM observation was carried out in the Service of optical microscopy at the University of Zaragoza and it was performed on carbon-coated samples using a field emission scanning electron microscope Carl Zeiss MERLIN™ (Carl Zeiss Group, Jena, Germany).

#### 3.3.2.2 Mineralogical analyses

The samples were separated in several subsamples, corresponding to different bands, using a micro-drill and then they were crushed with a steel jaw crusher and ground to a size fraction below 60  $\mu\text{m}$ . The bulk mineralogical composition was determined by X-ray diffractometry (XRD) using a PANalytical X'Pert PRO MPD powder diffractometer in Bragg-Brentano  $\theta/2\theta$  geometry of 240 millimetres of radius with a focalizing Ge (111) primary monochromator, a X'Celerator detector and using  $\text{CuK}\alpha 1$  radiation:  $\lambda = 1.5406 \text{ \AA}$  at the X-Ray Diffraction Unit in the Scientific and Technical Centers of the University of Barcelona (Spain). Semi-quantitative phase analysis of the identified crystalline phases was done by means of the Rietveld method (Rietveld, 1969).

#### 3.3.2.3 Carbon and oxygen isotope analyses

$\delta^{13}\text{C}$  and  $\delta^{18}\text{O}$  analyses were performed at the Stable Isotope Analysis Service of the University of Salamanca. The  $\text{CO}_2$  extraction for the analyses was done following standard techniques (McCrea, 1950) with an ISOCARB device connected to a SIRA series 10 mass spectrometer from VG Isotech.

## **3.4 Data analysis and calculations**

### **3.4.1 Water data treatment**

The first treatment of the data was through their representation in ion-ion plots, and other more specific diagrams like the Piper diagram or binary plots showing the isotopic signatures, the saturation indexes and other evolutionary trends.

Apart from these basic explorative evaluations the principal methodologies used for determining the reservoir temperature of the studied geothermal systems have been the chemical and isotopic geothermometers and the geothermometrical modelling. Other useful geochemical modelling approaches have been used to evaluate the reliability of the analyses or to infer the main processes controlling the chemical evolution of the waters. A short summary is presented next.

#### ***3.4.1.1 Chemical geothermometers***

The use of chemical geothermometers is the methodology traditionally used for the temperature estimation in a deep reservoir. A chemical geothermometer is an empiric or experimental calibration based on the chemical reactions that control the elemental contents of the waters and are dependent on temperature (e.g. Marini, 2004; Truesdell, 1976). In that way, the temperature at depth can be calculated knowing the elemental contents of the waters. Although this technique is widely used it has some important limitations that should be taken into account.

The application of this principle assumes that the elemental contents of the waters have not changed during their ascent from the deep reservoir to the surface and, therefore, the characteristics of the waters in the spring are considered to be representative of the conditions at depth. This assumption is not always true due to the possible modifications caused by secondary processes acting during the ascent to surface such as dissolution/precipitation of mineral phases, CO<sub>2</sub> outgassing or mixing with other waters. Another assumption that has to be accepted is that the waters have attained the equilibrium in the reservoir with the mineral phases considered for the calibration of the geothermometers.

Several chemical geothermometers and calibrations are available in the scientific literature but not all of them can be used in all systems. The classical cationic geothermometers provide very good results in high temperature systems hosted in granitic or basaltic rocks, since the equilibrium with the appropriate mineral phases are easily attained in those system (for example with albite and K-feldspar in the case of the Na-K geothermometer; Arnórsson et al., 1983; Asta et al., 2010; Auqué et al., 1997; Buil et al., 2006; Choi et al., 2005; D'Amore et al., 1987; Fouillac and Michard, 1981; Fournier, 1981, 1977; Giggenbach et al., 1983; Giggenbach, 1988;

Kharaka and Mariner, 1989; Mariner et al., 2006; Mutlu and Güleç, 1998; Pingitore et al., 2002; Sonney and Vuataz, 2010; Stefánsson and Arnórsson, 2000). The application of these cationic geothermometers is much more complicated (and it is usually considered inadequate) in low temperature carbonate systems since those mineral phases are not always present and if they are, the low temperature of the waters makes difficult to attain the equilibrium (Chiodini et al., 1995; D'Amore and Arnórsson, 2000; Karimi and Moore, 2008; Levet et al., 2002; López-Chicano et al., 2001; Sonney and Vuataz, 2010). Interestingly, however, they have been successfully used in some systems in which they were considered inadequate (e.g. Apollaro et al., 2012; Fernández et al., 1988; Gökgöz and Tarkan, 2006; Michard and Bastide, 1988; Mohammadi et al., 2010; Pastorelli et al., 1999; Wang et al., 2015).

Through the different papers presented in the Results section a vast variety of chemical geothermometers are evaluated and their application in carbonate systems of low temperature is discussed, including the classical cationic geothermometers, the silica geothermometers and, moreover other geothermometers specifically calibrated to be applied in systems with these characteristics. All these geothermometers and calibrations are summarised in Table 1 and a brief description of them is presented below.

#### *Silica geothermometers*

The two main silica geothermometers are the SiO<sub>2</sub>-quartz and SiO<sub>2</sub>-chalcedony geothermometers which rely on the quartz or chalcedony equilibrium in the deep reservoir. Various calibrations are available and some of the most common have been used here (Table 1).

All the quartz-silica geothermometers were developed from experimental data on silica solubility. Regarding chalcedony, the calibration by Fournier (1977) and Fournier and Potter (1982) were derived from solubility experiments above 125 °C extrapolated to low temperatures. The calibration from Arnórsson et al. (1983) is based on data from natural samples from Icelandic drill-holes.

Generally speaking, quartz is the silica phase controlling the dissolved silica concentrations at high temperatures while chalcedony controls them at low temperatures. Therefore, it is expected that the SiO<sub>2</sub>-quartz geothermometer would be adequate at temperatures of 150-225°C while the SiO<sub>2</sub>-chalcedony geothermometer would be better at lower temperatures (D'Amore and Arnórsson, 2000; Fournier, 1977; Marini, 2004). However, in some cases it is just the opposite and therefore, the best option is to follow the recommendation by Fournier (1991) and check always both geothermometers to identify the governing silica phase.

**Table 1.** Chemical geothermometers and calibrations considered in the study. Concentration units for the elements involved are all in mg/L except for the SiO<sub>2</sub>-quartz calibration proposed by Michard (1979) and the Na-Li and Li geothermometers in which the concentrations are expressed in mol/L.

Geothermometer	Calibration	Author
SiO <sub>2</sub> -quartz	$T = \frac{1315}{5.205 - \log(\text{SiO}_2)} - 273.15$	Truesdell (1976)
	$T = \frac{1309}{5.19 - \log(\text{SiO}_2)} - 273.15$	Fournier, (1977) and Fournier and Potter (1982)
	$T = \frac{1322}{0.435 - \log(\text{SiO}_2)} - 273.15$	Michard (1979)
SiO <sub>2</sub> -chalcedony	$T = \frac{1032}{4.69 - \log(\text{SiO}_2)} - 273.15$	Fournier, (1977) and Fournier and Potter (1982)
	$T = \frac{1112}{4.91 - \log(\text{SiO}_2)} - 273.15$	Arnórsson et al. (1983)
Na-K	$T = \frac{1390}{1.75 + \log(\text{Na}/\text{K})} - 273.15$	Giggenbach (1988)
	$T = \frac{1217}{1.483 + \log(\text{Na}/\text{K})} - 273.15$	Fournier (1979)
K-Mg	$T = \frac{4410}{13.95 - \log(K^2/\text{Mg})} - 273.15$	Giggenbach et al. (1983)
Na-K-Ca	$T = \frac{1647}{\log(\text{Na}/\text{K}) + \beta \left[ \log\left(\frac{\sqrt{\text{Ca}}}{\text{Na}}\right) + 2.06 \right] + 2.47} - 273.15$	Fournier and Truesdell (1973) <sup>1</sup>
Na-Li	$T = \frac{1000}{0.33 + \log(\text{Na}/\text{Li})} - 273.15$	Fouillac and Michard (1981)
Li	$T = \frac{2258}{1.44 + \log(\text{Li})} - 273.15$	Fouillac and Michard (1981)
Mg-Li	$T = \frac{2200}{5.47 + \log\left(\frac{\sqrt{\text{Mg}}}{\text{Li}}\right)} - 273.15$	Kharaka and Mariner (1989)
Ca-Mg	$T = \frac{979.8}{3.1170 - \log\left(\frac{\text{Ca}}{\text{Mg}}\right) + 0.07003 \log \Sigma eq} - 273.15$	Chiodini et al. (1995) <sup>2</sup>
SO <sub>4</sub> -F	$T = \frac{1797.7}{0.7782 + \log\left(\frac{\text{SO}_4}{\text{F}_2}\right) - 0.08653 \log \Sigma eq} - 273.15$	Chiodini et al. (1995) <sup>2</sup>

<sup>1</sup> $\beta=4/3$  should be used if the temperature obtained is lower than 100 °C; if with that value of  $\beta$  the temperature is higher than 100 °C, the temperature should be recalculated considering  $\beta = 1/3$ .

<sup>2</sup> $\Sigma eq$  is the summation (in eq/L) of the major dissolved species. Chiodini et al. (1995) performed their calibration for the Ca-Mg geothermometer by using a disordered dolomite.



*Na-K geothermometer*

This geothermometer is based on the equilibrium between  $\text{Na}^+$  and  $\text{K}^+$  in the solution and albite and K-feldspar (e.g. D'Amore and Arnórsson, 2000). Several calibrations have been developed and the ones used here are the Fournier, 1979 and the Giggenbach, 1988 calibrations, both of them derived empirically from deep geothermal wells. In some cases the equation proposed by Verma and Santoyo, (1997), which was proposed after improving the Fournier (1979) equation, has also been used.

The applicability of this geothermometer will be conditioned to the existence of the albite – K-feldspar equilibrium at depth, which is not always attainable in low temperature carbonate systems producing incoherently high temperatures (D'Amore et al., 1987).

*K-Mg geothermometer*

This geothermometer is controlled by the equilibrium of K-feldspar and a Mg-bearing phase at depth, such as chlorite, saponite or montmorillonite (e.g. Marini, 2004). Giggenbach et al. (1983) developed the calibration empirically from deep geothermal wells.

This equilibrium is attained more quickly than the albite – K-feldspar and it can be approached at temperatures as low as 25 °C (Marini, 2004). This fact makes this geothermometer more adequate in systems of lower temperature but, on the contrary, it also implies a strong response during the ascent of the waters and cooling due to the fast uptake of Mg (D'Amore and Arnórsson, 2000; Marini, 2004).

*Giggenbach diagram*

This is not strictly a geothermometer but a way to evaluate the water equilibria and the possibilities of using the cation geothermometers. It is the combination of the Na-K and K-Mg geothermometers in a ternary diagram proposed by Giggenbach (1988). Isothermal equilibrium lines are represented in the diagram for the Na/K and K/Mg ratios, and the intersection of both isotherms at different temperatures drawn the full equilibrium line (Figure 11), which indicates that waters have attained the equilibrium with respect to the phases on which Na-K and K-Mg geothermometers are based on. Giggenbach (1988) delimited the fields of partially equilibrated waters (or mature waters) and immature waters (Figure 11) in the diagram, meaning that if a water is in the second field it is unsuitable for the use of these geothermometers (Giggenbach, 1988). If the water is in the partially equilibrated waters field both geothermometers can be evaluated.

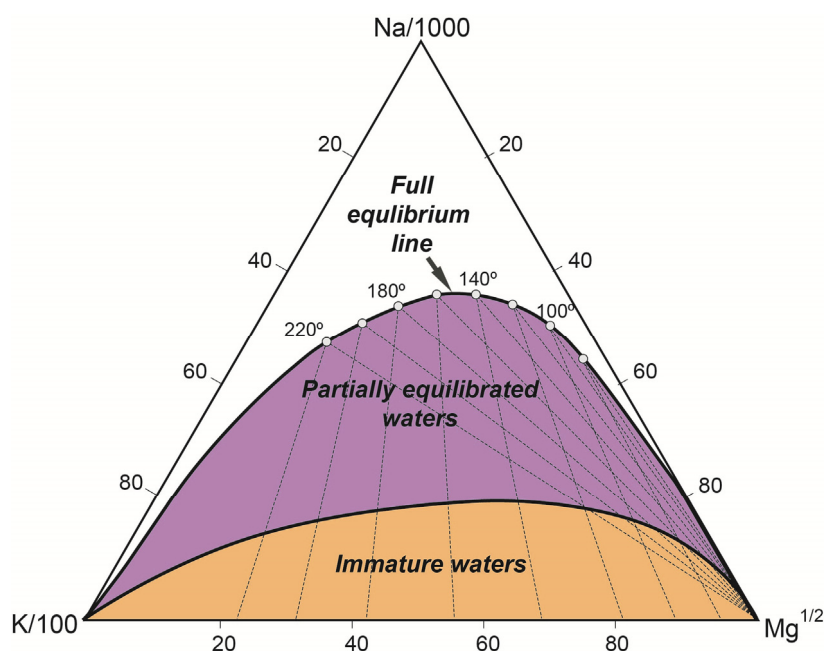


**Figure 11.** Giggenbach triangular diagram where the full equilibrium line and the immature and partially equilibrated waters fields are indicated.

#### *Na-K-Ca geothermometer*

The Na-K-Ca geothermometer was empirically developed by Fournier and Truesdell (1973) from natural waters with temperature ranging from 4 to 340 °C to deal with the problem that the Na-K geothermometer provided too high temperatures in Ca-rich waters (Nicholson, 1993). It is not clear which mineral phases control this geothermometers but it could be feldspar, micas or clays (alkaline feldspar and calcium-bearing silicate; D'Amore and Arnórsson, 2000; D'Amore et al., 1987), since in most cases, although the total Ca content is controlled by carbonates, the Na-K-Ca ratio can be explained only by silicate minerals (Fournier and Truesdell, 1973).

This geothermometer does not lead to unreasonably high temperature in low temperature and non-equilibrated waters (D'Amore and Arnórsson, 2000) but it is very sensitive to differences in CO<sub>2</sub> contents in those waters (Chiodini et al., 1991; Marini, 2004), and therefore, the results obtained in carbonate systems should be treated with caution.

#### *Lithium geothermometers*

There are several lithium geothermometers and the ones that have been used in some of the systems studied here are the Na-Li and the Mg-Li geothermometers. The first one was derived empirically by Fouillac and Michard (1981) in granitic areas, the second was also empirically derived by Kharaka and Mariner (1989) to be used up to 350 °C.

Due to the fact that the Li-bearing minerals are not abundant, the lithium concentration in waters is assumed to be mainly controlled by cation-exchange reactions with clays and zeolites (D'Amore et al., 1987; Nicholson, 1993).

Although the Na-Li geothermometer has been considered in some cases adequate for carbonate systems (Minissale and Duchi, 1988), in general, the lithium geothermometers can be considered inadequate in low temperature systems with lithium concentrations lower than 1ppm (D'Amore et al., 1987). Additionally, the Mg-Li geothermometer can also be affected by the Mg uptake during the ascent of waters to surface as in the case of K-Mg geothermometer.

#### *Other geothermometers specifically developed for low temperature carbonate systems*

Two alternative geothermometers were developed to be applied in this type of systems: the Ca-Mg and the SO<sub>4</sub>-F geothermometers. They were first proposed by Marini et al. (1986) and then revised by Chiodini et al. (1995). The Ca-Mg geothermometer is based on the calcite-dolomite equilibrium in the deep reservoir, which can be easily attained in carbonate rocks. However, this geothermometer is not always free of uncertainties because it is affected by the solubility of these minerals and, although for calcite is quite well defined, in the case of dolomite it will be dependent on its order degree (Chiodini et al., 1995). The SO<sub>4</sub>-F geothermometer requires the anhydrite-fluorite equilibrium to be attained in the reservoir and therefore, it can only be applied in systems where evaporitic rocks are present and even in these cases it is not always applicable as fluorite is not common in these systems (Chiodini et al., 1995).

#### **3.4.1.2 Isotopic geothermometers**

The isotopic geothermometers are based on similar assumptions than the chemical geothermometers, that the isotope fractionation between two species in equilibrium is a function of the temperature of the waters, calculating the isotope fractionation as expressed in eq. (1):

$$1000\ln\alpha_{A-B} = 1000\ln\left(\frac{1000 + \delta_A}{1000 + \delta_B}\right) \approx \delta_A - \delta_B \quad (1)$$

where  $\delta_A$  and  $\delta_B$  are the isotopic signature of the species

The most used isotopic geothermometers are those based on the  $\delta^{18}\text{O}$  exchange between water and the sulphate species. Some others used in this thesis have been the ones based on the  $\delta^{13}\text{C}$  exchange between CO<sub>2</sub> and HCO<sub>3</sub>, and on the  $\delta^{18}\text{O}$  exchange between CO<sub>2</sub> and water. The isotopic geothermometers and calibrations used along this thesis are listed in Table 2.

**Table 2.** Isotopic geothermometers and calibrates used in this study.

Geothermometer	Calibration	Author
$\text{CO}_2(\text{gas})\text{-HCO}_3^-$ ( $\delta^{13}\text{C}_{\text{CO}_2\text{-HCO}_3}$ )	$T = \left( \frac{-9.483 \cdot 10^3}{1000 \ln \alpha_{\text{CO}_2\text{-HCO}_3^-} - 23.89} \right) - 273.15$	Mook et al. (1974)
	$T = \left( \sqrt{\frac{1.092 \cdot 10^6}{1000 \ln \alpha_{\text{CO}_2\text{-HCO}_3^-} + 4.54}} \right) - 273.15$	Deines et al. (1974)
$\text{CO}_2(\text{gas})\text{-H}_2\text{O}$ ( $\delta^{18}\text{O}_{\text{CO}_2\text{-H}_2\text{O}}$ )	$T = \left( \frac{16.6 \cdot 10^3}{1000 \ln \alpha_{\text{CO}_2\text{-H}_2\text{O}} + 4.69} \right) - 273.15$	O'Neil and Adami (1969)
	$T = \left( \sqrt{\frac{3.97 \cdot 10^6}{1000 \ln \alpha_{\text{CO}_2\text{-H}_2\text{O}} - 0.31}} \right) - 273.15$	Truesdell (1974)
	$T = \left( \frac{17.6 \cdot 10^3}{1000 \ln \alpha_{\text{CO}_2\text{-H}_2\text{O}} + 17.93} \right) - 273.15$	Brenninkmeijer et al. (1983)
$\text{SO}_4\text{-H}_2\text{O}$ ( $\delta^{18}\text{O}_{\text{HSO}_4\text{-H}_2\text{O}}$ )	$T = \left( \sqrt{\frac{3.26 \cdot 10^6}{1000 \ln \alpha_{\text{HSO}_4^- \text{-H}_2\text{O}} + 5.81}} \right) - 273.15$	Seal et al. (2000) <sup>1</sup>
	$T = \left( \sqrt{\frac{3.251 \cdot 10^6}{1000 \ln \alpha_{\text{HSO}_4^- \text{-H}_2\text{O}} + 5.1}} \right) - 273.15$	Friedman and O'Neil (1977).
$\text{SO}_4\text{-H}_2\text{O}$ ( $\delta^{18}\text{O}_{\text{SO}_4\text{-H}_2\text{O}}$ )	$T = \left( \sqrt{\frac{2.41 \cdot 10^6}{1000 \ln \alpha_{\text{SO}_4^{2-} \text{-H}_2\text{O}} + 5.77}} \right) - 273.15$	Halas and Pluta (2000)
	$T = \left( \sqrt{\frac{2.68 \cdot 10^6}{1000 \ln \alpha_{\text{SO}_4^{2-} \text{-H}_2\text{O}} + 7.45}} \right) - 273.15$	Zeebe (2010)
$\text{SO}_4\text{-H}_2\text{O}$ ( $\delta^{18}\text{O}_{\text{CaSO}_4\text{-H}_2\text{O}}$ )	$T = \left( \sqrt{\frac{3.31 \cdot 10^6}{1000 \ln \alpha_{\text{CaSO}_4 \text{-H}_2\text{O}} + 4.69}} \right) - 273.15$	Boschetti et al. (2011) <sup>2</sup>

<sup>1</sup>This calibration is the combination of those of Lloyd (1968) and Mizutani and Rafter (1969).

<sup>2</sup>This calibration is the combination of those of Chiba et al. (1981) and Zheng (1999).

As already explained for the chemical geothermometers, the application of the isotopic geothermometers also presents problems due to the possible reequilibrium during the ascent of the waters and due to the lack of equilibrium in low temperature systems, where the fractionation process is slower.

In the case of the geothermometers based on the  $\delta^{18}\text{O}$  exchange between the water and the sulphate species, the calibration should be selected according to the dominant sulphate species in the water. The classical and traditionally used calibrations are those based on the  $\delta^{18}\text{O}$  exchange between water and the  $\text{HSO}_4^-$  species (Friedman and O'Neil, 1977; Seal et al., 2000) but this species is only dominant in acidic waters. Other more recent calibrations consider the  $\text{SO}_4^{2-}$  species (Halas and Pluta, 2000; Zeebe, 2010) which will be expected to control the equilibrium exchange in neutral waters. Finally, Boschetti et al. (2011) proposed the use of the

calibration based on the  $\delta^{18}\text{O}$  exchange between water and dissolved anhydrite ( $\text{CaSO}_4^0$ ) in systems where the waters have attained the equilibrium with respect to this mineral phase.

### 3.4.1.3 Geochemical modelling

Geochemical modelling can be defined as the interpretation of hydrogeochemical systems by applying different chemical and physical principles (Gimeno and Peña, 1994). In this way it is possible to define the chemical states of the waters (distribution of species and water saturation states with respect to the mineral phases), understand the interaction processes of water, rock and gases and predict the chemical changes (Bethke, 2008). The geochemical modelling has suffered a great evolution from the early 60s, when the pioneers Garrels and Thompson (1962) applied the first model, by hand calculation, to obtain the species distribution in seawater. Then, Garrels and Mackenzie (1967) developed what today is known as reaction path modelling (which will be explained latter) predicting the reactions in a spring when the water evaporated. The next step was given by Helgeson (1968) introducing the computerised modeling which has exponentially developed since then.

#### *Thermodynamic data*

Many geochemical codes are available with different capacities. The code selected for this study was the PHREEQC code (Parkhurst and Appelo, 2013) and two of the thermodynamic databases provided with it: the LLNL database (derived from the database 'thermo.com.V8.R6.230' by Johnson et al., 2000) and the WATEQ4F database (Ball and Nordstrom, 2001). The first one includes reliable data for a great number of minerals and aqueous species in a temperature range of 0 to 300 °C, including polynomial expression fitted to experimental data for the calculation of the equilibrium constants at different temperatures (Johnson et al., 2000). The second one includes a vast number of major and trace species, mineral and gas phases for natural water systems, and it is applicable with confidence in the temperature range from 0 to 100 °C (Ball and Nordstrom, 2001). This database uses the Van'T Hoff equation<sup>1</sup> for the calculation of the equilibrium constants at different temperatures, except for some minerals such as calcite, anhydrite or quartz, where it uses a polynomial expression as in the LLNL.

---

<sup>1</sup>  $\log K_T = \log K_{T_0} - \frac{\Delta H_R^0}{2.303R} \left( \frac{1}{T} - \frac{1}{T_0} \right)$ , where  $K_T$  is the equilibrium constant at the desired temperature,  $K_{T_0}$  the equilibrium constant at 25 °C,  $\Delta H_R^0$  the standard reaction enthalpy,  $R$  the gases constant,  $T$  the temperature and  $T_0$  the temperature of 25 °C.

The results obtained can be slightly different depending on the selected database and therefore, a sensitivity analysis to the thermodynamic data was performed in Blasco et al. (2017) to evaluate the possible uncertainties. This analysis can be found as supplementary material in this thesis dissertation.

The thermodynamic data for some minerals, such quartz or calcite, are quite well known, but even in those cases some minor differences in the results between databases can be found. The differences are larger for minerals such as dolomite or the aluminosilicates. In the case of dolomite the uncertainties are associated to the order degree (Carpenter, 1980; Chiodini et al., 1995; Helgeson et al., 1978; Hyeong and Capuano, 2001; Reeder, 2000) and in the aluminosilicates to the crystallinity or the variations in the composition (Merino and Ramson, 1982; Nordstrom et al., 1990; Palandri and Reed, 2001). Apart from the evaluation of the uncertainties associated to these two thermodynamic databases, some additional thermodynamic data have been included in the WATEQ4F database for some aluminosilicate phases and dolomite. Everything about the uncertainty analyses has been thoroughly described and evaluated in the papers presented in the Results section.

### *Charge imbalance*

The charge imbalance calculation is one of the first information obtained when a modelling is performed with the assistance of PHREEQC code (and other codes also) and provides valuable information regarding the analytical data. It is an indicator of the accuracy and reliability of the analytical data, at least for the major elements (e.g. Appelo and Postma, 2005). It should be one of the first things to evaluate prior to perform the next modelling calculations. PHREEQC calculates the charge imbalance considering the positive ( $\text{Na}^+$ ,  $\text{Ca}^{2+}$ ,  $\text{Mg}^{2+}$ ,  $\text{K}^+$ ) and negative charges ( $\text{HCO}_3^-$ ,  $\text{Cl}^-$ ,  $\text{SO}_4^{2-}$ ) as indicated in eq. (2):

$$\% \text{ imbalance} = \left[ \frac{\sum_{i=1}^I (m_i \cdot z_i)_{\text{cations}} - \sum_{i=1}^I (m_i \cdot z_i)_{\text{anions}}}{\sum_{i=1}^I (m_i \cdot z_i)_{\text{cations}} + \sum_{i=1}^I (m_i \cdot z_i)_{\text{anions}}} \right] \quad (2)$$

where  $m_i$  is the molal concentration of the dissolved species and  $z_i$  their charge (in absolute value). Imbalance of about 2 % are almost inevitable in the majority of laboratories (Parkhurst and Appelo, 2013), but, in general, analyses are considered acceptable up to charge imbalances of 5 %. Imbalances higher than that indicate that the analyses should be re-examined and considered with caution (Appelo and Postma, 2005; Nordstrom et al., 1989).

### *Speciation-solubility calculations*

The speciation-solubility calculations allow obtaining the distribution, concentration and activity of the dissolved species present in the water and the saturation indices (SI) of the water with respect to the mineral phases. The saturation index is calculated according to eq. (3):

$$SI = \log \left[ \frac{IAP}{K_T} \right] \quad (3)$$

where  $K_T$  is the equilibrium constant of the mineral at the considered temperature and IAP is the ionic activity product calculated as in eq. (4):

$$IAP = \frac{a_B \cdot a_C}{a_A} \quad (4)$$

where,  $a_A$ ,  $a_B$  and  $a_C$  are the activities of the products and reactants in the schematic reaction  $A \rightarrow B + C$ .

A value of  $SI = 0$  ( $IAP = K_T$ ) indicates that the water is in equilibrium with respect to that mineral phase while  $SI > 0$  ( $IAP > K_T$ ) and  $SI < 0$  ( $IAP < K_T$ ) represent over- and undersaturation situations respectively.

### *Geothermometrical modelling*

The geothermometrical modelling, as for the chemical and isotopic geothermometers, allows determining the water temperature in the deep reservoir, and it also needs the same assumptions: the existence of water – minerals equilibria at depth and that the chemical composition has not changed during the ascent of the waters to the surface.

This methodology was initially proposed to be used in alkaline thermal waters by Michard and his co-workers (Michard et al., 1986; Michard and Fouillac, 1980; Michard and Roekens, 1983) but it was soon generalised to other types of thermal systems by Reed and co-workers (Palandri and Reed, 2001; Pang and Reed, 1998; Reed and Spycher, 1984).

Although the assumption made is that the measured elemental concentrations have not changed during the ascent to surface, the waters will undergo a cooling process which will lead to a redistribution of the dissolved species and to changes in the saturation state of the waters with respect to some minerals. In this context, the geothermometrical modelling strength is that it can reconstruct the conditions at depth by simulating a progressive increase of the temperature to a value in which the saturation states of a certain set of minerals is in, or close to, equilibrium, which will be indicative of the reservoir temperature.

The selection of the minerals to consider in the modelling is one of the key points and it has to be done according to the mineralogy present in the aquifer and choosing those minerals that the

waters are expected to be in equilibrium with. The minerals that have been considered in the systems studied in the thesis are calcite, dolomite and anhydrite, since they are hosted in carbonate rocks in contact to evaporitic facies, and some others such as quartz, albite, K-feldspar and other aluminosilicates since the waters are also in contact to some detrital material (see the papers for more information).

Although this technique, like the chemical geothermometers, is also based on the assumption of the mineral equilibria at depth, it presents several advantages over them:

- It allows a better identification of the mineral equilibria in the deep reservoir (Michard et al., 1986; Michard and Fouillac, 1980; Michard and Roekens, 1983).
- The modelling can be performed considering two different approaches: 1) in closed system conditions, assuming the only process affecting waters is cooling during the ascent; or 2) in open system conditions, assuming the waters undergo reequilibration processes during the ascent and allowing precipitation – dissolution of mineral phases.
- Finally, by using different approaches, the action and effects of secondary processes can be identified and corrected as for example CO<sub>2</sub> outgassing (Palandri and Reed, 2001; Pang and Reed, 1998) or mixing with shallower and cooler waters (Pang and Reed, 1998).

#### *Direct and inverse modelling*

The main aim of the geochemical modelling is to find the model that explains the characteristics of the waters and is able to predict how they would evolve under certain conditions. These models can be obtained in a direct or in an inverse way (e.g. Plummer, 1992, 1984).

The inverse modelling is also known as mass balance calculation. It defines the mass transfers taking place between two, or more, connected points in a system from the known chemical characteristics of the waters in those points. The model predicts the minerals that precipitate or dissolve, the ion exchanges, the ingass or outgass process and the quantities of these reactions. This type of calculation provides all the mathematically possible combinations of mass transfer reactions which would explain the observed concentration changes between the two connected points, in the form of several possible models. The limitation is that this calculation only considers the mass balance principle without taking into account the thermodynamic feasibility of the considered reactions (e.g. Zhu and Anderson, 2002).

The direct modelling, also known as reaction path calculations, consists of predicting the evolution of a water under certain established conditions from the known chemical composition of that water. The hypothetical composition of the final water is predicted along with the minerals



that will precipitate or dissolve when certain reactions are assumed to take place in the system. In this case the calculation considers the thermodynamic principles (Zhu and Anderson, 2002).

A good agreement between some of the mass balance models and the reaction path calculations would support the feasibility of those reactions in the system.

### 3.4.2 Solid data treatment

As the study of the travertine samples has been mainly focused on the evaluation of the stable isotope fractionation, only this treatment is summarised next.

#### 3.4.2.1 Stable isotope fractionation

The isotopic signature of carbonate precipitates (travertines or speleothems) is widely used in paleoenvironmental and paleoclimatic reconstructions since the isotopic fractionation between water and the precipitating carbonate, calculated as previously expressed in equation 1, is a function of temperature (e.g. Andrews, 2006; Capezzuoli et al., 2014; Ford and Pedley, 1996; Fouke et al., 2000; Garnett et al., 2004; Jones and Renaut, 2010; Kele et al., 2011, 2008; Lachniet, 2015; Liu et al., 2006, 2010; Osácar et al., 2016, 2013; Pedley, 2009; Pentecost, 2005). However, the interpretation of the isotopic contents is not always easy since the fractionation can be affected by factors such as the CO<sub>2</sub> outgassing or the precipitation rates (e.g. Fouke et al., 2000; Kele et al., 2008; 2011). Another difficulty is that various fractionation equations have been proposed for calcite–water fractionation and aragonite–water fractionation but there is not an agreement about if they are actually representative of the real equilibrium (e.g. Kele et al., 2015; Lachniet, 2015). Therefore, the study of recent precipitates, where the isotopic data of water and solid carbonate are available, provides useful information to obtain a better interpretation of ancient carbonate precipitates.

The  $\delta^{13}\text{C}$  data in this study cannot be used for this purpose because they were measured in the dissolved inorganic carbon (DIC) which could be considered to be as HCO<sub>3</sub><sup>-</sup> and the fractionation between aragonite (or calcite) and HCO<sub>3</sub><sup>-</sup> has been reported to be independent of temperature (Rubinson and Clayton, 1969; Turner, 1982; Romanek et al., 1992). Only the  $\delta^{13}\text{C}$  fractionation between aragonite (or calcite) and the dissolved CO<sub>2</sub> is temperature-dependant (e.g. Chacko et al., 2001; Romanek et al., 1992; Scheele and Hoefs, 1992).

Regarding the  $\delta^{18}\text{O}$ , several  $\delta^{18}\text{O}$  aragonite – water equilibrium equations have been applied (Table 3):

**Table 3.** Different  $\delta^{18}\text{O}$  equilibrium equations considered. Temperature (T) is in Kelvin and  $\delta^{18}\text{O}$  values are vs. V-SMOW.

	Equilibrium equation	Author
$\delta^{18}\text{O}_{\text{aragonite-water}}$	$1000 \ln\alpha = 18.04 \cdot \frac{1000}{T} - 31.12$	Grossman and Ku (1986)
	$1000 \ln\alpha = 18.56 \cdot \frac{1000}{T} - 33.49$	Patterson et al. (1993)
	$1000 \ln\alpha = 18.56 \cdot \frac{1000}{T} - 32.54$	Thorrold et al. (1997)
	$1000 \ln\alpha = 16.74 \cdot \frac{1000}{T} - 26.39$	White et al. (1999)
	$1000 \ln\alpha = 18.45 \cdot \frac{1000}{T} - 32.54$	Böhm et al. (2000)
	$1000 \ln\alpha = 20.44 \cdot \frac{1000}{T} - 41.48$	Zhou and Zheng (2003)
	$1000 \ln\alpha = 17.88 \cdot \frac{1000}{T} - 30.76$	Kim et al. (2007)
	$1000 \ln\alpha = -12.815 + 5.793x - 3.7554 \cdot 10^{-1}x^2 + 3.2966 \cdot 10^{-2}x^3 - 2.2189 \cdot 10^{-3}x^4 + 8.9981 \cdot 10^{-5}x^5 - 1.636 \cdot 10^{-6}x^6$	Chacko and Deines (2008) <sup>1</sup>
	$1000 \ln\alpha = 22.5 \cdot \frac{1000}{T} - 46.1$	Wang et al. (2013)
$\delta^{18}\text{O}_{\text{aragonite/calcite-water}}$	$1000 \ln\alpha = 20 \cdot \frac{1000}{T} - 36$	Kele et al. (2015)
$\delta^{18}\text{O}_{\text{calcite-water}}$	$1000 \ln\alpha = 18.03 \cdot \frac{1000}{T} - 32.17$	Kim and O'Neil (1997)
	$1000 \ln\alpha = 17.4 \cdot \frac{1000}{T} - 28.6$	Coplen (2007)

<sup>1</sup> $x = 10^6/T^2$ , where T is Kelvin

- Grossman and Ku (1986) derived their equation from aragonitic foraminifera, gastropods and scaphods in the temperature range of 2.5 to 26 °C.
- Patterson et al. (1993) deduced the equation from the characterisation of aragonitic fish otoliths in the temperature range of 3.2 to 30.3 °C.
- Thorrold et al. (1997) also deduced an equation from aragonitic fish otoliths in the temperature range of 18 to 25 °C.
- White et al. (1999) studied aragonitic marine molluscs in the range of temperatures from 8 to 24 °C to derive an equation.
- Böhm et al. (2000): proposed an equation from the evaluation of aragonitic sponges in the temperature range of 3 to 28 °C.
- Zhou and Zeng (2003) performed experiments of aragonite precipitation in the temperature range of 10 to 70 °C to obtain the equation

- Kim et al. (2007) carried out experiments with inorganic synthetic aragonites in the temperature range of 10 to 40 °C to propose their equation.
- Chacko and Deines (2008) derived an equation applicable in the temperature range of 0 to 130 °C from the calculation of the partition function ratios (for aragonite and water) from statistical mechanical calculation and a compilation of vibrational frequency data.
- Wang et al. (2013): deduced the equation after aragonite precipitation from seawater experiments in the temperature range of 25 – 55 °C.
- Kele et al. (2015): proposed an equation from a combination of data of natural calcite and aragonite travertines. Therefore, it can be used in travertines composed by a mixture of aragonite and calcite.

As one of the studied samples consists of a calcite – aragonite mixture the two most common  $\delta^{18}\text{O}$  calcite – water fractionation equations have also been used (Table 3):

- Kim and O'Neil (1997): derived from inorganic calcites synthesised in laboratory in the range of 10 to 40 °C.
- Coplen (2007): proposed the equation from vein calcite samples from Devils Hole (Nevada, USA).



# 4. RESULTS

---

## 4.1 Paper 1

**Geochemistry, geothermometry and influence of the concentration of mobile elements in the chemical characteristics of carbonate-evaporitic thermal systems. The case of the Tiermas geothermal system (Spain)**

*Mónica Blasco, Luis F. Auqué, Maria J. Gimeno, Patricia Acero, Maria P. Asta*

Chemical Geology 466, 696-709 (2017)

Impact Factor (2017): 3.57

Quartile and Category (2017): Q1 (19/85), Geochemistry and geophysics

DOI: 10.1016/j.chemgeo.2017.07.013

Sent: 14 October 2016

Accepted: 17 July 2017

Available online: 19 July 2017

Final publication: 5 September 2017





Contents lists available at ScienceDirect

## Chemical Geology

journal homepage: [www.elsevier.com/locate/chemgeo](http://www.elsevier.com/locate/chemgeo)

## Geochemistry, geothermometry and influence of the concentration of mobile elements in the chemical characteristics of carbonate-evaporitic thermal systems. The case of the Tiermas geothermal system (Spain)

Mónica Blasco<sup>a,\*</sup>, Luis F. Auqué<sup>a</sup>, María J. Gimeno<sup>a</sup>, Patricia Acero<sup>a</sup>, María P. Asta<sup>b</sup><sup>a</sup> Geochemical Modelling Group, Petrology and Geochemistry Area, Earth Sciences Department, University of Zaragoza, Spain C/ Pedro Cerbuna 12, 50009 Zaragoza, Spain.<sup>b</sup> Environmental Microbiology Laboratory (EML), École Polytechnique Fédérale de Lausanne (EPFL), EPFL-ENAC-IIE-EML, Station 6, 1015 Lausanne, Switzerland.

## ARTICLE INFO

## Keywords:

Geothermal system  
Geothermometry  
Chemical geothermometers  
Isotopic geothermometers  
Geothermometrical modelling  
Mobile elements

## ABSTRACT

The Tiermas low temperature geothermal system, hosted in the Paleocene-Eocene carbonates of the Jaca-Pamplona basin, has been studied to evaluate the geochemistry and the temperature of the waters in the deep reservoir. These waters are of chloride-sodium type and emerge with a temperature of about 37 °C. Two hydrogeochemical groups of waters have been distinguished: one with lower sulphate concentration and lower TDS (about 7500 ppm) and the other with higher sulphate content and TDS values (close to 11,000 ppm). There are also slight differences in the reservoir temperature estimated for each group. These temperatures have been determined by combining several geothermometrical techniques: (1) classical chemical geothermometers (SiO<sub>2</sub>-quartz, Na-K, K-Mg and Na-K-Ca), (2) specific geothermometers for carbonate systems (Ca-Mg), (3) isotopic geothermometers and, (4) geothermometrical modelling.

The good agreement in the temperature obtained by these techniques, including the cationic geothermometers which are not usually considered suitable for this type of systems, allows establishing a reliable range of temperature of 90 ± 20 °C for the low-sulphate waters and 82 ± 15 °C for the high-sulphate waters.

The mineral assemblage in equilibrium in the reservoir is assumed to be the same for both groups of waters (calcite, dolomite, quartz, anhydrite, albite, K-feldspar and other aluminosilicate phases); therefore, the differences found in the reservoir temperature and, mostly, in the geochemical characteristics of each group of waters must be due to the existence of two flow paths, with slightly different temperatures and intensity of water-rock interaction.

Anhydrite is at equilibrium in the reservoir suggesting that, although this system is hosted in carbonates, evaporites may also be present. The dissolution of halite (and the consequent increase in the chloride concentration) conditions the chemical characteristics of the waters and the equilibrium situations in the reservoir and waters acquire their chloride-sodium affinity at depth and not during their ascent to the surface.

Finally, a favourable tectonic structure for CO<sub>2</sub> storage has been recognised in the Paleocene-Eocene carbonates of this area. Therefore, considering the characteristics of these waters (in equilibrium with calcite, dolomite and anhydrite in the reservoir), the results of this work are useful to understand some of the geochemical processes that might take place during the CO<sub>2</sub> injection: 1) precipitation of carbonates and sulphates in the vicinity of the injection well due to desiccation of the waters and, 2) carbonate dissolution and sulphate precipitation in the long term.

## 1. Introduction

Geothermal systems have always been of interest for industrial or touristic use of their waters (e.g., in greenhouses or balneotherapy). One of the first steps in the evaluation of the geothermal potential of an area is the study of the geochemical and isotopic characteristics of the

thermal springs (e.g. D'Amore and Arnórsson, 2000). These studies provide information about the water evolution along the hydrological circuit and about its temperature in the reservoir. The general geochemical and geothermometric characterisation of the Tiermas geothermal system is presented in this paper.

The Tiermas thermal waters have been used in balneotherapy since

\* Corresponding author at: Geochemical Modelling Group, Petrology and Geochemistry Area, Earth Sciences Department, University of Zaragoza, Spain.  
E-mail address: [monicabc@unizar.es](mailto:monicabc@unizar.es) (M. Blasco).

<http://dx.doi.org/10.1016/j.chemgeo.2017.07.013>

Received 14 October 2016; Received in revised form 19 May 2017; Accepted 17 July 2017

Available online 19 July 2017

0009-2541/ © 2017 Elsevier B.V. All rights reserved.

Roman times. Nowadays the springs are covered by the waters impounded by the Yesa dam during most of the year. However, these springs become exposed frequently during late summer and many people come to benefit from their therapeutic properties. New projects to use these thermal waters again are being proposed. The spring temperature is about 40 °C and the flow rate 200 L/s and they are considered one of the most important geothermal systems in Aragon for its geothermal potential (Sánchez, 2000; Sánchez et al., 2004).

During the development of the ALGECO2 project, conducted by the Spanish Geological Survey (IGME), the Paleocene-Eocene carbonate rocks in this area (which is the most feasible aquifer of the Tiermas waters; see below) were considered a favourable structure for CO<sub>2</sub> geological storage (Leyre-Berdún structure, southwards Leyre Sierra; Suárez et al., 2014). This makes the study of these waters a potential analogue study for the ones expected to be in the proposed CO<sub>2</sub> storage, from which there are not yet hydrochemical data (Suárez et al., 2014; Gaus, 2010).

Despite the well known interest of the system, its hydrological and hydrochemical features are still poorly known due to the complex geology of the zone. Thus, the aim of this work is to fill in this gap with the geochemical characterisation of these waters and the estimation of the reservoir temperature using classical and geothermometrical modelling techniques.

## 2. Geological and hydrological setting

The Tiermas springs are located in the Aragonian pre-Pyrenees, in the northwest of the Zaragoza province (Fig. 1). They emerge in the north shore of the Yesa reservoir, which covers the springs during most of the year. Geologically, the system is located in the Jaca-Pamplona Basin, between the Boltaña anticline and the Pamplona fault, and bounded on the north by the Axial Zone and the Inner Ranges and on the south by the Outer Ranges (Fig. 2). The Jaca-Pamplona Basin is elongated in east-west direction, parallel to the general trend of the Pyrenees. Overall, the structure of the basin is an asymmetric syncline dipping south and filled with Tertiary formations (Larrasoña et al., 1996; Bauluz et al., 2008). The evolution of this basin was conditioned by a compressional context. The South Pyrenean zone was a foreland basin during the Cretaceous and a deep trench opened westwards receiving sediments from a turbiditic system. In the Middle Eocene this basin was transformed in a piggy back basin, with southwards displacement due to the propagation of the South Pyrenean Basal Thrust and, eventually, was filled by tertiary sediments (Payros et al., 1994; Oliva et al., 1996).

The Jaca Basin has a great structural complexity: there are two main structural trends that give rise to two fault systems, one with NNE-SSW direction, due to the reactivation of the tardi-hercynian fault systems, and the other with E-W direction (Fig. 1), which corresponds to the Pyrenean trend (IGME, 1973).

### 2.1. Stratigraphy

Stratigraphically, the Jaca-Pamplona Basin is constituted by Triassic to Miocene formations with a sedimentary and metasedimentary Paleozoic basement (Saura and Teixell, 2006). The Triassic rocks belong to the Bundsandstein and Keuper Facies, with about 400 m of conglomerates, sandstones and lutites, and 150 m of evaporites, lutites and limestones, respectively (Pueyo et al., 2012), although due to the role of the Keuper Facies as detachment level, it is difficult to determine its exact thickness. These Triassic formations are directly overlaid by a marine series deposited in the foreland South Pyrenean basin during the Upper Cretaceous: the Paleocene Alveoline Limestones, the Lower and Middle Eocene Guara Limestones and turbidites of the Hecho Group (IGME, 1973; Faci, 1997). This is followed by a regressive carbonate series in the Middle and Upper Eocene formed in an external platform and a prodelta system constituted by the Sabiñanigo

Sandstones (the Larres Marls in other areas), the Arguis-Pamplona Marls and the Belsué-Atarés marls and sandstones. These formations are overlaid by evaporitic rocks, which indicate the transition to a paralic continental environment, and are constituted by halite, anhydrite and potassium salts (sylvite and carnallite) units (e.g. Ayora et al., 1994, 1995). The potash units are restricted to the depocenter and they are mostly absent in the rest of locations (Ayora et al., 1994); for instance, in the hydrocarbon exploration drilling Sangüesa 1 (Fig. 1) these evaporites are only constituted by anhydrite and halite at depth.

Finally, the last stage of the basin evolution corresponds to the alluvial filling of the Jaca-Pamplona Basin that is represented in the Oligocene and Miocene continental formations (Campodarbe Group and Bernués and Uncastillo Formations; IGME, 1973; Faci, 1997).

In the context of this study, the Upper Cretaceous and the Paleocene-Eocene formations are of special interest as they constitute the potential geothermal formations (FG6 and FG7; Sánchez, 2000; Sánchez et al., 2000, 2004) for the Tiermas thermal springs. The thickness of the Upper Cretaceous is about 200 m in the area and it is constituted, at its base, by dolomitic limestones, marls and sandy limestones and, at the top, by the Marboré Sandstones (calcarenites with sandstones and siliceous conglomerates in the uppermost part; IGME, 1973; Faci, 1997).

In the Paleocene-Eocene formations, the Alveoline Limestones are 120 to 300 m thick, and consist of carbonates and calcarenites, with sparitic or microsparitic cement, bioclasts, quartz grains and, locally, oncoids, ooids and intraclasts (IGME, 1973; Faci, 1997). The Guara Limestones in the area are about 100 m thick and consist of bioclastic limestones with abundant siliciclastic rocks at the bottom that grade to marls towards the top (IGME, 1973; Puigdefàbregas, 1975; Faci, 1997). Exploratory drilling at depths between 2800 and 3700 m shows that these limestones from the Paleocene-Lower Eocene (Alveoline and Guara Limestones) are dolomitic at the bottom (Sánchez Guzmán and García de la Noceda, 2005). Finally, the Hecho Group consists of sets of siliciclastic turbidites and hemipelagic marls with calcite, illite, chlorite and minor albite and dolomite (Bauluz et al., 2008). The most arenitic parts contain lithic fragments and clasts of quartz, plagioclase, K-feldspar and muscovite (Gupta and Pickering, 2008). Embedded in these materials appear the so-called carbonated mega-layers (or mega-turbidites), which are thick and laterally continuous carbonate-cemented breccias and calcarenites, removed from a platform and re-deposited in a deep marine trench. Up to seven mega-layers with up to 200 m of thickness have been identified in the Jaca-Pamplona Basin (IGME, 1973; Payros et al., 1994; Faci, 1997; Bauluz et al., 2008).

These formations, considered as the suitable aquifer of the waters studied here, although mainly constituted by carbonates, they also contain siliciclastic rocks, which will determine the geochemical characteristics of the waters (see below).

### 2.2. Hydrogeology

Sánchez (2000) and Sánchez et al. (2000, 2004) distinguish several geothermal formations in the Pyrenees area defining them as “geological units able to store water or other fluids at a specific temperature and under specific mobility conditions suitable to allow some type of geothermal exploitation”. Two of them, FG6 and FG7, are located in the studied area, the first one corresponds to the Upper Cretaceous formations and the second is formed by the Alveoline Limestones (Paleocene), the Guara Limestones (Paleocene-Eocene) and the megaturbidites from the Eocene Flysch. The second one is considered the potential aquifer of the Tiermas springs (ITGE-DGA, 1994; Faci, 1997; Sánchez, 2000; Sánchez et al., 2000, 2004) and of the geothermal system of Jaca-Serrablo (about 70 km NE from Tiermas; Sánchez Guzmán and García de la Noceda, 2005).

The Tiermas waters are chloride-sodium/calcium-sulphate type with a TDS (total dissolved solids) higher than 10,000 ppm. Other waters also hosted in the Alveoline Limestones show different chemical



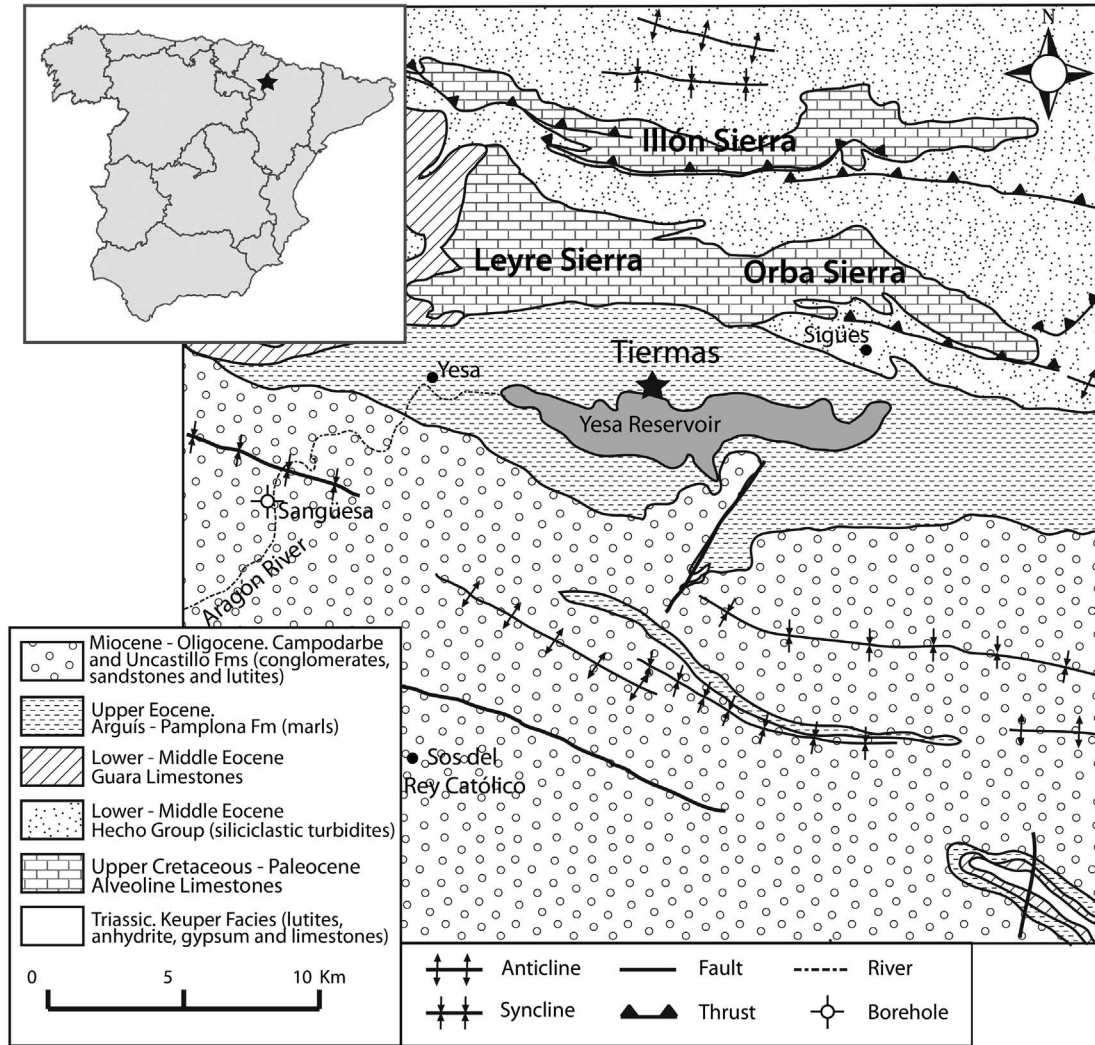


Fig. 1. Location of the TIERMAS geothermal system and geological map of the area (modified from Oliva-Urcia et al., 2012).

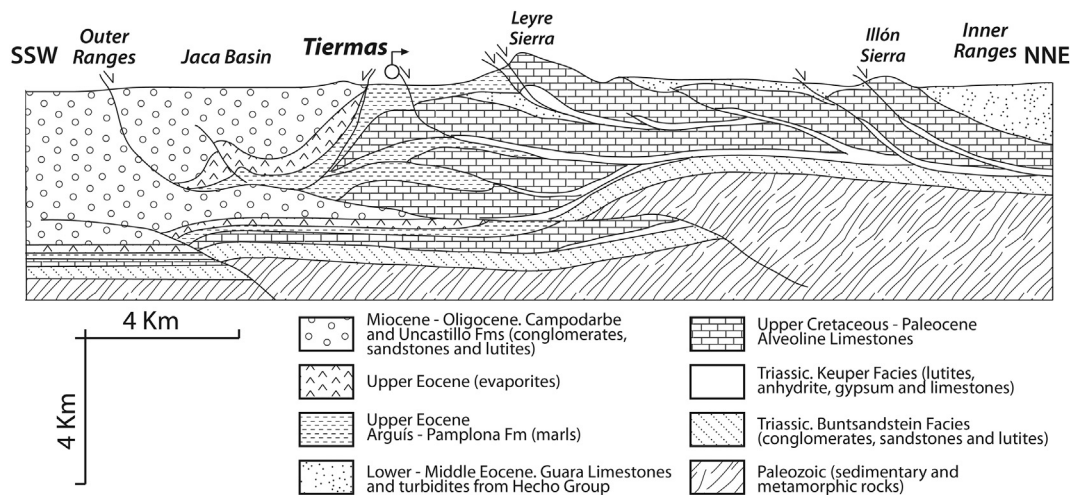


Fig. 2. Cross section showing the general structure of the JACA-PAMPLONA Basin and the location of TIERMAS Springs (modified from ALGECO2 project: <http://info.igme.es/algeco2/>; IGME, 2010).

features. For example, the groundwaters sampled in a piezometric borehole in Romanzado (12 km NW of Tiermas) are calcium-bicarbonate type (Consulnima, 2011) and the waters from the Jaca-Serrablo geothermal system have TDS values around 2000 ppm (Sánchez Guzmán and García de la Noceda, 2005). The lithological features of the potential aquifer of Tiermas springs (the Alveoline Limestones) do not include the presence of suitable rocks to provide a chloride-sodium/calcium-sulphate composition to the waters. One hypothesis is that the waters would acquire these chemical components during their ascent to surface due to the contact with the evaporites from the limit between the Upper Eocene and the Oligocene (ITGE-DGA, 1994). Another possibility could be that the structural complexity of the area (Fig. 2) puts the waters in the deep reservoir into contact with the evaporitic rocks from the Keuper Facies or from the formations of the Eocene-Oligocene limit.

The possible areas proposed as recharge zones for the Tiermas geothermal system are outcrops of Paleocene and Eocene carbonates in the Leyre Sierra (Fig. 1), in the Illon and Orba Sierras (Fig. 1), and in the Inner Ranges (Fig. 2; Auqué, 1993; ITGE-DGA, 1994; Sáenz, 1999; Consulnima, 2011). In any case, these springs result from the upward discharge of a deep (and, therefore, warm) groundwater flow. The rise of these waters to the surface is probably due to the NNE-SSE fractures that interrupt the N-S flow and force this to be vertical, resulting in a flow rate of about 200 L/s (Auqué, 1993; ITGE-DGA, 1994).

The limited information available about the Tiermas geothermal system and the structural complexity of the area makes the characterisation of the possible aquifer lithologies and the hydrological circuit, difficult.

### 3. Methodology

After reviewing the available analytical data about the Tiermas geothermal system, the unpublished results from the sampling campaign carried out in 1985 (Auqué, 1993) were selected because this campaign produced a complete analytical data set including hydrochemical and isotopic data of the spring waters and in situ measurements of temperature, pH, and electrical conductivity. Another sample from 1991 (ITGE-DGA, 1994), taken in a shallow control borehole near the thermal springs, was included in this study to complete the characterisation of the system; in this case the electrical conductivity and pH were measured in the laboratory and there are no data for temperature, although an estimated value has been considered for this parameter. The rest of available chemical analyses since 1991 show a progressive decrease in the salinity of the thermal waters studied here. As they seem to represent a modification of the original situation in the thermal system (e.g. mixing and/or dilution) we decided to not consider them in this work. Table 1 compiles the chemical and physicochemical parameters for the selected samples indicating the laboratories where they were analysed.

The charge imbalance for the water samples was calculated with the PHREEQC code (Parkhurst and Appelo, 2013) and the results showed that all the samples have a charge imbalance lower than  $\pm 5\%$  (Table 1). This value is in the range usually accepted as valid (Nordstrom et al., 1989; Appelo and Postma, 2005) and supports the reliability of the data used in this study. The lack of aluminium data in most of the samples has been solved by fixing the aluminium content in the water imposing equilibrium with an aluminosilicate phase in the geothermometrical modelling (Pang and Reed, 1998; Palandri and Reed, 2001).

#### 3.1. Chemical and isotopic geothermometers

The chemical geothermometers are the classical method to determine the reservoir temperature in geothermal systems. They use empiric or experimental calibrations based on heterogeneous chemical reactions (temperature dependent) from which the equilibrium

**Table 1**

Analytical data of the waters included in this study. Sample B1 was taken in a control borehole in 1991 and the electrical conductivity and pH were measured in the laboratory. The temperature value shown in the table is an estimated value. T1, T2, T3 and T4 correspond to springs sampled in 1985 (Auqué, 1993) and the temperature, pH, and electrical conductivity were measured in situ. Apart from one sample from 1985 (T1, analysed in the Geochemistry Department of the University of Barcelona) the rest of the waters were analysed in the Navarra Provincial Government laboratories and the isotopic determinations were performed in the University of Paris. Sample B1 was analysed in the Spanish Geological Survey laboratories. The TDS values (calculated using PHREEQC) and the concentration of dissolved elements are expressed in ppm.

	B1	T1	T2	T3	T4
Temp. (°C)	38	38.7	38.9	37.3	38.6
TDS	7169.1	7750.3	10,891	10,653	10,905
pH	7.6	6.75	6.84	6.79	6.99
HCO <sub>3</sub> <sup>-</sup>	245	233	225	227	223
Cl <sup>-</sup>	3028	3573	3260	2975	3005
SO <sub>4</sub> <sup>2-</sup>	1300	1035	3500	3650	3800
Ca	330	270	322.6	331.2	318.4
Mg	97	90	83.3	87.8	98.7
Na	2060	2400	3315	3195	3287
K	33	42	31	31	31
B		0.5			
F	1.8	1.9			
Fe	0.033	0.143			
Li		0.77			
Al		0.182			
SiO <sub>2</sub>	22.3	28	28	28	27
% Imbalance	-0.7	-0.24	-0.14	0.02	0.14

temperature can be calculated (e.g. Marini, 2004) using the elemental contents controlled by those heterogeneous reactions and assuming that the contents have not suffered significant changes during the rise of the waters to the surface.

A vast choice of geothermometers with various calibrations and suitable for different systems exists at present (e.g. see the review from D'Amore and Arnórsson, 2000). For example, the use of the cationic geothermometers (e.g. Na-K, K-Mg) has been proven very useful to estimate the reservoir temperature in high temperature systems (> 180 °C), in which the equilibrium between the water and the minerals in the reservoir is generally reached. However, their use in intermediate to low temperature systems or in carbonate-evaporitic reservoirs, as the case studied here, is usually considered inappropriate due to the range of their calibration temperatures, the chemical features of the water used for the calibration and/or the mineral phases involved in the equilibrium situations (Auqué, 1993; Chiodini et al., 1995; D'Amore and Arnórsson, 2000). Despite these limitations, the K-Mg and silica geothermometers and some of their calibrations have been used here as they have provided good results in similar systems (Fernández et al., 1988; Michard and Bastide, 1988; Pastorelli et al., 1999; Wang et al., 2015). Moreover, as shown later, the use of the classical Giggenbach diagram (Giggenbach, 1988) indicates that Tiermas thermal waters fall on the field of the partially equilibrated waters, or near the fully equilibrate waters field, depending on the calibration considered, suggesting that the use of the cationic geothermometers, including the Na-K one, could be adequate.

The geothermometers that are more specific for low temperature carbonate-evaporitic systems and, therefore, more suitable for this study, are the Ca-Mg and the SO<sub>4</sub>-F geothermometers, firstly developed by Marini et al. (1986) and then revised by Chiodini et al. (1995). They are based on the assumption that Ca/Mg and SO<sub>4</sub>/F ratios are mainly controlled by temperature. The Ca-Mg geothermometer assumes the equilibrium of the waters with calcite and dolomite in the reservoir, which is reasonable in this type of systems. However, the results can be affected by the solubility of these mineral phases and whilst the calcite solubility is quite well known, the solubility of the dolomite depends on the degree of order/disorder. With respect to the SO<sub>4</sub>-F geothermometer, it can only be applied to waters fully equilibrated with

Table 2

Chemical geothermometers and calibrations used in this work. Concentration units for the elements involved are all in mg/L except for the calibration proposed by Michard (1979) in which the concentrations are expressed in mol/L.

Geothermometer	Calibration	Author
SiO <sub>2</sub> -quartz	$T = \frac{1315}{5.205 - \log(\text{SiO}_2)} - 273.15$	Truesdell (1976)
	$T = \frac{1309}{5.19 - \log(\text{SiO}_2)} - 273.15$	Fournier (1977); Fournier and Potter (1982)
	$T = \frac{1322}{0.435 - \log(\text{SiO}_2)} - 273.15$	Michard (1979)
SiO <sub>2</sub> -chalcedony	$T = \frac{1032}{4.69 - \log(\text{SiO}_2)} - 273.15$	Fournier (1977); Fournier and Potter (1982)
	$T = \frac{1112}{4.91 - \log(\text{SiO}_2)} - 273.15$	Arnorsson et al. (1983)
Na-K	$T = \frac{1390}{1.75 + \log\left(\frac{\text{Na}}{\text{K}}\right)} - 273.15$	Giggenbach (1988)
	$T = \frac{1217}{1.483 + \log\left(\frac{\text{Na}}{\text{K}}\right)} - 273.15$	Fournier (1979)
K-Mg	$T = \frac{4410}{13.95 - \log\left(\frac{\text{K}^2}{\text{Mg}}\right)} - 273.15$	Giggenbach et al. (1983)
Na-K-Ca	$T = \frac{1647}{\log\left(\frac{\text{Na}}{\text{K}}\right) + \beta \left[ \log\left(\frac{\sqrt{\text{Ca}}}{\text{Na}}\right) + 2.06 \right] + 2.47} - 273.15$	Fournier and Truesdell (1973) <sup>a</sup>
Ca-Mg	$T = \frac{979.8}{3.1170 - \log\left(\frac{\text{Ca}}{\text{Mg}}\right) + 0.07003 \log \sum eq} - 273.15$	Chiodini et al. (1995) <sup>b</sup>
SO <sub>4</sub> -F	$T = \frac{1797.7}{0.7782 + \log\left(\frac{\text{SO}_4}{\text{F}^2}\right) - 0.08653 \log \sum eq} - 273.15$	Chiodini et al. (1995) <sup>b</sup>

<sup>a</sup>  $\beta = 4/3$  should be used if the temperature obtained is lower than 100 °C; if with that value of  $\beta$  the temperature is higher than 100 °C, the temperature should be recalculated considering  $\beta = 1/3$ .

<sup>b</sup>  $\sum eq$  is the summation (in eq/L) of the major dissolved species. Chiodini et al. (1995) performed their calibration for the Ca-Mg geothermometer by using a disordered dolomite.

anhydrite and fluorite in the reservoir (Chiodini et al., 1995), which is not always the case in this type of systems. The chemical geothermometers and calibrations finally selected are listed in Table 2.

Additionally, various isotopic geothermometers have been used

including  $\delta^{13}\text{C}$  CO<sub>2</sub>-HCO<sub>3</sub>,  $\delta^{18}\text{O}$  CO<sub>2</sub>-H<sub>2</sub>O and  $\delta^{18}\text{O}$  SO<sub>4</sub>-H<sub>2</sub>O (Table 3). These geothermometers are based on the assumption that two species are in isotopic equilibrium and the isotope exchange is a function of temperature. These geothermometers could also present problems

Table 3

Isotopic geothermometers and calibrations used in this work.

Geothermometer	Calibration	Author
CO <sub>2(gas)</sub> -HCO <sub>3</sub> <sup>-</sup> ( $\delta^{13}\text{C}_{\text{CO}_2\text{-HCO}_3}$ )	$T = \left( \frac{-9.483 \cdot 10^3}{1000 \ln \alpha_{\text{CO}_2\text{-HCO}_3} - 23.89} \right) - 273.15$	Mook et al. (1974)
	$T = \left( \frac{1.092 \cdot 10^6}{\sqrt{1000 \ln \alpha_{\text{CO}_2\text{-HCO}_3} + 4.54}} \right) - 273.15$	Deines et al. (1974)
CO <sub>2(gas)</sub> -H <sub>2</sub> O ( $\delta^{18}\text{O}_{\text{CO}_2\text{-H}_2\text{O}}$ )	$T = \left( \frac{16.6 \cdot 10^3}{1000 \ln \alpha_{\text{CO}_2\text{-H}_2\text{O}} + 4.69} \right) - 273.15$	O'Neil and Adami (1969)
	$T = \left( \frac{3.97 \cdot 10^6}{\sqrt{1000 \ln \alpha_{\text{CO}_2\text{-H}_2\text{O}} - 0.31}} \right) - 273.15$	Truesdell (1974)
	$T = \left( \frac{17.6 \cdot 10^3}{1000 \ln \alpha_{\text{CO}_2\text{-H}_2\text{O}} + 17.93} \right) - 273.15$	Brennkmeijer et al. (1983)
SO <sub>4</sub> -H <sub>2</sub> O ( $\delta^{18}\text{O}_{\text{HSO}_4\text{-H}_2\text{O}}$ )	$T = \left( \frac{3.26 \cdot 10^6}{\sqrt{1000 \ln \alpha_{\text{HSO}_4\text{-H}_2\text{O}} + 5.81}} \right) - 273.15$	Seal et al. (2000) <sup>a</sup>
	$T = \left( \frac{3.251 \cdot 10^6}{\sqrt{1000 \ln \alpha_{\text{HSO}_4\text{-H}_2\text{O}} + 5.1}} \right) - 273.15$	Friedman and O'Neil (1977)
SO <sub>4</sub> -H <sub>2</sub> O ( $\delta^{18}\text{O}_{\text{SO}_4\text{-H}_2\text{O}}$ )	$T = \left( \frac{2.41 \cdot 10^6}{\sqrt{1000 \ln \alpha_{\text{SO}_4\text{-H}_2\text{O}} + 5.77}} \right) - 273.15$	Halas and Pluta (2000)
	$T = \left( \frac{2.68 \cdot 10^6}{\sqrt{1000 \ln \alpha_{\text{SO}_4\text{-H}_2\text{O}} + 7.45}} \right) - 273.15$	Zeebe (2010)
SO <sub>4</sub> -H <sub>2</sub> O ( $\delta^{18}\text{O}_{\text{CaSO}_4\text{-H}_2\text{O}}$ )	$T = \left( \frac{3.31 \cdot 10^6}{\sqrt{1000 \ln \alpha_{\text{CaSO}_4\text{-H}_2\text{O}} + 4.69}} \right) - 273.15$	Boschetti et al. (2011) <sup>b</sup>

<sup>a</sup> This calibration is the combination of those of Lloyd (1968) and Mizutani and Raftar (1969).

<sup>b</sup> This calibration is the combination of those of Chiba et al. (1981) and Zheng (1999).

associated to reequilibrium processes during the ascent of the waters and to the calibrations. In order to take this into consideration, several calibrations have been used for the geothermometer  $\delta^{18}\text{O}$  in  $\text{SO}_4\text{-H}_2\text{O}$  (Boschetti, 2013): the classical calibrations based in the  $\text{HSO}_4\text{-H}_2\text{O}$  exchange (Friedman and O'Neil, 1977; Seal et al., 2000), and the more recent ones based on the  $\text{SO}_4^{2-}\text{-H}_2\text{O}$  (Halas and Pluta, 2000; Zeebe, 2010) and  $\text{CaSO}_4\text{-H}_2\text{O}$  exchange (Boschetti et al., 2011).

### 3.2. Geothermometrical modelling

This modelling is based on the same assumption as the classical chemical geothermometers: the thermal waters have reached the equilibrium with respect to the minerals in contact with them in the reservoir of the geothermal system. Then, during the ascent to the surface, the waters cool and change the distribution of the dissolved species and, therefore, their saturation states with respect to the various minerals. The modelling consists in reverse the ascent of the waters simulating a progressive increase of the temperature up to a range in which the saturation states of the waters with respect to several minerals (presumably present in the reservoir) coincide in an equilibrium situation.

This technique was initially proposed for its use in alkaline thermal waters by Michard and his co-workers (Michard and Fouillac, 1980; Michard and Roekens, 1983; Michard et al., 1986) and later generalised for other types of thermal systems by Reed and co-workers (Reed and Spycher, 1984; Pang and Reed, 1998; Palandri and Reed, 2001; Peiffer et al., 2014; Spycher et al., 2014). It presents some advantages over the chemical geothermometers: a) it gives a better identification of the mineral set in equilibrium with waters and of the chemical characteristics of the thermal waters at depths (pH, for instance); and b) it allows identifying the action and effects of secondary processes during the ascent of the thermal waters to surface such as mineral reequilibria, mixing with colder waters or outgassing processes (Michard and Fouillac, 1980; Michard and Roekens, 1983; Reed and Spycher, 1984; Michard et al., 1986; Tole et al., 1993; Pang and Reed, 1998; Palandri and Reed, 2001; Asta et al., 2010).

In this study PHREEQC code (Parkhurst and Appelo, 2013) has been used to carry out the geothermometrical modelling, using the LLNL thermodynamic database distributed with the code.

## 4. Results

### 4.1. Chemical characteristics of the waters

The water samples studied here were taken from four springs in 1985 (T1, T2, T3 and T4; Table 1) and from a shallow borehole in 1991 (B1; Table 1), all of them located in an area of 50 m<sup>2</sup>. These samples are separated into two groups: low-sulphate samples, B1 and T1, with low sulphate concentration and low TDS (about 7500 ppm; Table 1) and high-sulphate samples, T2, T3 and T4, with higher sulphate contents and higher TDS values (close to 11,000 ppm; Table 1). These two groups also present differences and similarities in some molar ratios:

- The Na/Cl ratio is near 1 for the samples of the low-sulphate group and higher for the samples of the high-sulphate one (approximately 1.6). This indicates that the Na and Cl concentrations in the low-sulphate group are controlled mainly by halite dissolution. Whereas, the 1.6 value in the high-sulphate group indicates an extra contribution of Na (e.g. associated to cation exchange).
- The Ca/SO<sub>4</sub> ratio in the low-sulphate group is about 0.6, and 0.2 in the high-sulphate. In both cases, as the contents of SO<sub>4</sub> are assumed to be controlled, almost entirely, by anhydrite dissolution, calcium must be removed from the waters by precipitation of other minerals, probably carbonates, or by cation exchange reactions.
- The Ca/HCO<sub>3</sub> and Ca + Mg/HCO<sub>3</sub> ratios are quite similar in both groups (about 2 and 3, respectively), although both are a little higher in the high-sulphate group. These ratios, much higher than 1, would reflect the important contribution of anhydrite dissolution in these waters.
- The Ca + Mg/HCO<sub>3</sub> + SO<sub>4</sub> ratio (in eq/L) ranges between 0.85 and 0.88 (~1) in both groups. This indicates an important participation of interaction processes involving carbonates and sulphates, but with some additional intervention of other water-rock interaction processes.
- The K/Cl ratio is much lower than 1 in both groups (about 0.01) which means that sylvite is not a mineral phase with significant influence in the chemical characteristics of the waters. The same can be said about carnallite since the relation Cl:Mg:K in this phase is 3:1:1 and in the thermal waters is completely different (around 100:4:1). These facts suggest that the waters are not in contact with the evaporitic Eocene-Oligocene or that these rocks do not contain these minerals.
- Finally, the Mg/Ca ratio has similar values in both groups, ranging between 0.42 and 0.55, which could be indicative of a calcite-dolomite equilibrium at similar salinities and temperatures in the reservoir.

These ratios show that the chemical characteristics of both water types are highly influenced by carbonate and sulphate phases. Despite the similar spring temperature in both groups, the differences found in the chemical characteristics could be indicative of the existence of two flow patterns affected by different intensities of water-rock interaction processes.

For the two low-sulphate samples, B1 and T1, (Table 1) the lower concentration of sulphate in T1 could result from sulphate reduction despite the fact that there is not a significant increase in the HCO<sub>3</sub><sup>-</sup> concentration compared to B1. The Tiermas thermal waters usually present a rotten eggs smell and have been described as sulfidic (e.g. Jiménez, 1838); therefore, the influence of sulphate reduction is feasible. A removal of the HCO<sub>3</sub><sup>-</sup> upon sulphate reduction results from the precipitation of a carbonate phase, which would also explain the lower content of calcium in sample T1.

### 4.2. Isotopic characteristics of the waters

The isotopic data used here correspond to two samples from 1985: sample T1 and a sample from the Yesa reservoir (Table 4). The  $\delta^{18}\text{O}$ - $\delta^2\text{H}$  isotopic ratio for these waters (and other unpublished data from the Yesa reservoir in 2012 and one sample from a borehole in Tiermas; Baeza et al., 2000; Fig. 3) is close to the Global Meteoric Water Line  $\delta^2\text{H} = 8\cdot\delta^{18}\text{O} + 10$ , defined by Craig (1961), the Regional Meteoric Water Line for Spain  $\delta^2\text{H} = 8\cdot\delta^{18}\text{O} + 9.27$  (Díaz-Teijeiro et al., 2009) and also to the Local Meteoric Water Line,  $\delta^2\text{H} = 5.6\cdot\delta^{18}\text{O} - 7.6$  (Baeza et al., 2000), which supports a meteoric origin for these waters (Fig. 3). In high-temperature thermal systems, a positive  $\delta^{18}\text{O}$ -shift is observed (e.g. Clark and Fritz, 1997) and since the Tiermas thermal waters do not display such enrichment, this system should be regarded as low-medium temperature.

$\delta^{18}\text{O}$  and  $\delta^2\text{H}$  in meteoric waters are negatively correlated with altitude (e.g. Clark and Fritz, 1997) and therefore, the depleted values

**Table 4**  
Isotopic data of the water and of some dissolved species in sample T1 and Yesa Dam.

	T1				Yesa Dam
	CO <sub>2</sub>	HCO <sub>3</sub> <sup>-</sup>	SO <sub>4</sub> <sup>2-</sup>	Water	Water
$\delta^{18}\text{O}$ (‰ vs SMOW)	19.92	17.05	11.90	-9.87	-8.87
$\delta^2\text{H}$ (‰ vs SMOW)	-	-	-	-70.0	-63.3
$\delta^{13}\text{C}$ (‰ vs PDB)	-8.86	-5.11	-	-	-
$\delta^{34}\text{S}$ (‰ vs CDT)	-	-	18.70	-	-
$^3\text{T}$ (TU)	-	-	-	< 3.4	13

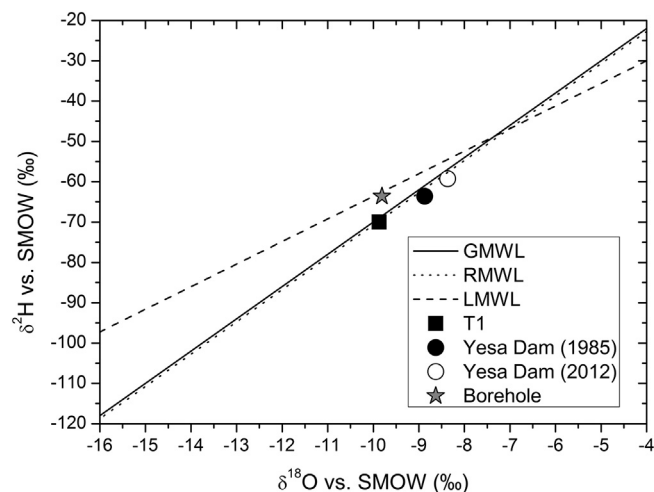


Fig. 3.  $\delta^2\text{H} - \delta^{18}\text{O}$  diagram showing the isotopic composition of sample T1, two samples from the Yesa Reservoir (one taken in 1985 and the other in 2012, this last one still unpublished) and one sample from a borehole in Tiermas from the study performed by Baeza et al. (2000). The Global Meteoric Water Line (GMWL), the Regional Meteoric Water Line (RMWL) and Local Meteoric Water Line (LMWL) are also represented.

for  $^{18}\text{O}$  and  $^2\text{H}$  in the thermal water indicate a higher elevation for its recharge area than for that of the waters in the Yesa reservoir. Unfortunately, there are no available regional data of the isotopic gradient with altitude which would have allowed determining the recharge area more accurately.

Finally, tritium in the thermal waters is below detection limit (Table 4) indicating a recharge prior to 1952 and that they are not affected by mixing with more recent waters (Clark and Fritz, 1997).

Some complementary information exists about the isotopic composition of the sulphates in the evaporites that might be in contact with these thermal waters. The Keuper Facies presents values of 10.9–16.3‰ for the  $\delta^{34}\text{S}$  and 8.9–14.9‰ for  $\delta^{18}\text{O}$  (Utrilla et al., 1987). The isotopic values in the rocks of the limit between the Upper Eocene and the Oligocene are in the range of 12.9–23.6‰ for the  $\delta^{34}\text{S}$  and 9.8–11.9‰ for  $\delta^{18}\text{O}$  (Ayora et al., 1995). The isotopic values in the dissolved sulphate of the thermal waters are within these ranges, except the  $\delta^{34}\text{S}$  in the dissolved sulphate which is slightly higher than the range reported for the Keuper facies (which could be explained by the sulphate reduction process that affects sample T1). In any case, these data support the hypothesis that the waters are in contact with some of these evaporites although, with the available data and considering the structural complexity of the area, it is not clear if they are in contact with the Keuper Facies or with the evaporitic rocks of Upper Eocene-Oligocene limit.

#### 4.3. Saturation states

The results obtained from the speciation-solubility calculations at spring temperature are shown in Table 5. Except for sample B1 that is oversaturated, the waters are close to equilibrium or slightly undersaturated with respect to calcite, and more undersaturated with respect to disordered dolomite. Their  $\text{pCO}_2$  values are higher than the atmosphere and the oversaturation shown by sample B1 (related with its lower  $\text{pCO}_2$ ) is possibly a result of  $\text{CO}_2$  degassing before the pH was measured in laboratory. Waters are almost in equilibrium with chalcedony and are oversaturated with respect to quartz. They are undersaturated with respect to gypsum, anhydrite, fluorite, and also with respect to other evaporitic phases like halite, sylvite and carnallite. T1 is the only sample with aluminium concentration and it is clearly oversaturated with respect to albite, K-feldspar, and other aluminosilicates potentially present in the reservoir such as kaolinite, pyrophyllite, laumontite or clinocllore.

Table 5

Saturation state (SI) of various mineral phases in all the samples considered in this study. The saturation state is the logarithm of the ratio between the ionic activity product, IAP, and the equilibrium constant of the mineral reaction at the indicated temperature, K(T). In this case, the temperature measured in the field for each sample and reported in Table 1 was considered. The equilibrium is reached when  $\text{SI} = 0$ , and positive and negative values indicate oversaturation and undersaturation, respectively.

	B1	T1	T2	T3	T4
$\text{pCO}_2(\text{g})$	-2.26	-1.42	-1.53	-1.49	-1.69
Calcite	0.80	-0.13	-0.11	-0.17	0.01
Dolomite-dis <sup>a</sup>	1.03	-0.76	-0.90	-1.02	-0.58
Anhydrite	-0.62	-0.81	-0.36	-0.34	-0.34
Gypsum	-0.57	-0.76	-0.31	-0.28	-0.29
Fluorite	-0.94	-0.99	-	-	-
Halite	-3.97	-3.83	-3.77	-3.83	-3.81
Sylvite	-5.37	-5.20	-5.42	-5.44	-5.45
Carnallite	-14.06	-13.76	-14.32	-14.41	-14.37
Quartz	0.35	0.45	0.45	0.48	0.44
Chalcedony	0.09	0.19	0.19	0.22	0.18
Albite_low <sup>a</sup>	-	2.73	-	-	-
K-Feldspar	-	3.56	-	-	-
Kaolinite	-	6.45	-	-	-
Pyrophyllite	-	5.85	-	-	-
Laumontite	-	4.08	-	-	-
Clinocllore	-	-1.01	-	-	-
Gibbsite	-	2.38	-	-	-

<sup>a</sup> Dolomite-dis is disordered dolomite and Albite\_low is low temperature albite.

Table 6

Temperatures (°C) obtained with several geothermometers and calibrations for the samples considered in the study.

Geothermometer	Calibration	B1	T1	T2	T3	T4
$\text{SiO}_2$ -quartz	Truesdell (1976)	68	77	77	77	75
	Fournier (1977)	68	77	77	77	75
	Michard (1979)	69	78	78	78	76
$\text{SiO}_2$ -chalcedony	Fournier (1977)	36	45	45	45	44
	Arnorsson et al. (1983)	39	48	48	48	47
Na-K	Giggenbach (1988)	119	123	95	96	95
	Fournier (1979)	98	103	73	75	74
K-Mg	Giggenbach (1988)	66	75	69	68	67
Na-K-Ca	Fournier and Truesdell (1973)	113	120	99	99	99
Ca-Mg	Chiodini et al. (1995)	82	75	88	87	78
$\text{SO}_4$ -F	Chiodini et al. (1995)	-17	-11	-	-	-

#### 4.4. Geothermometrical calculations

##### 4.4.1. Chemical geothermometers

The temperatures calculated (Table 6) with all the silica geothermometers are similar for all samples because their silica contents are also similar. The  $\text{SiO}_2$ -quartz geothermometer yields 75–78 °C (B1 is near 70 °C because its silica content is lower than the rest) whilst the  $\text{SiO}_2$ -chalcedony geothermometer yields lower temperatures, 44–48 °C (38 °C for B1).

The K-Mg geothermometer provides values between 66 and 75 °C for all the samples, closer to those deduced with the  $\text{SiO}_2$ -quartz geothermometer. The results obtained with the other cationic geothermometers show substantial differences depending on the sample considered and in the case of the Na-K geothermometer the temperature predicted also depends on the calibration considered: 1) for the samples of the low-sulphate group (B1 and T1), the temperature is about 120 °C with the Giggenbach (1988) calibration and about 100 °C with the Fournier (1979) one; 2) for the samples of the high-sulphate group, the temperatures are around 95 and 75 °C with the two calibrations, respectively. Given the good agreement between the result obtained with the K-Mg geothermometer and the Fournier (1979) Na-K calibration for the samples from the high-sulphate group (which is coherent with their position closer to the fully equilibrated waters in the Giggenbach diagram, Fig. 4), only the Fournier calibration is considered in the

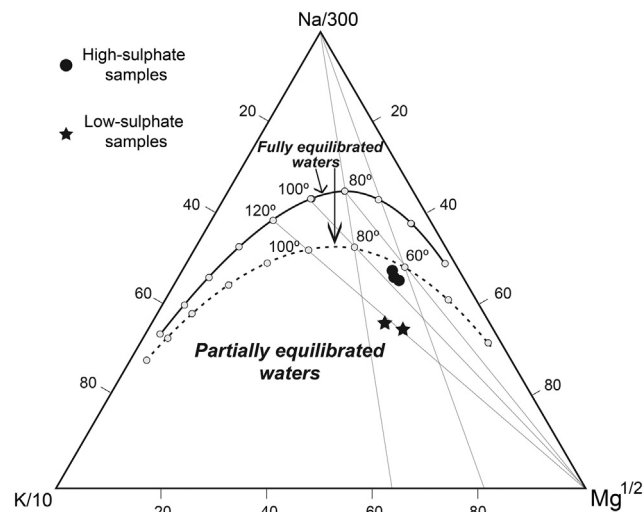


Fig. 4. Location of all the samples in the Giggenbach diagram. The dotted line is calculated with the Na-K Fournier (1979) calibration and with the Giggenbach (1988) one for Mg-K; the solid line is calculated with Na-K and Mg-K calibrations of Giggenbach (1988). If the dotted line is considered, the samples of the group 2 are close of being fully equilibrated.

discussions.

Finally, with respect to the rest of the cationic geothermometers: 1) the Na-K-Ca geothermometer (with  $\beta = 1/3$  as recommended by Fournier and Truesdell, 1973) predicts a temperature close to 100 °C for the samples of the high-sulphate group and slightly higher for the low-sulphate waters; 2) the Ca-Mg geothermometer predicts a temperature in the range between 75 and 88 °C, consistent with the similar Mg/Ca ratios and salinities for all the samples; and 3) the  $\text{SO}_4\text{-F}$  geothermometer provides incoherent results in this case as fluorite has not reached the equilibrium in the reservoir.

As a general trend, the temperatures obtained with most of the chemical geothermometers are more similar to the ones deduced with the quartz geothermometer than to those provided by the chalcedony geothermometer, suggesting that quartz is the phase that probably controls the dissolved silica in the thermal waters of Tiermas.

Despite the slight differences provided by some geothermometers, the temperature values in the two groups of waters are quite similar and a temperature range of  $85 \pm 17$  °C could be proposed for both. This range would include nearly all temperature values obtained (Table 6) and it is acceptable as it is within the uncertainty range for these determinations ( $\pm 20$  °C; Fournier, 1982). Moreover, the 85 °C range is indicated by the Ca-Mg geothermometer, which is specific for low temperature carbonate-evaporite systems and also by various cationic geothermometers with different sensitivity to secondary processes during the water ascent (D'Amore et al., 1987; D'Amore and Arnórsson,

Table 7

Temperatures (°C) obtained with several isotopic geothermometers and calibrations for the sample T1.

Geothermometer	Author	Temperature (°C)
$\text{CO}_{2(\text{gas})}\text{-HCO}_3^-$	Mook et al. (1974).	70
$(\delta^{13}\text{C}_{\text{CO}_2\text{-HCO}_3})$	Deines et al. (1974).	91
$\text{CO}_{2(\text{gas})}\text{-H}_2\text{O}$	O'Neil and Adami (1969)	94
$(\delta^{18}\text{O}_{\text{CO}_2\text{-H}_2\text{O}})$	Truesdell (1974)	96
	Brenninkmeijer et al. (1983)	98
$\text{SO}_4\text{-H}_2\text{O}$	Seal et al. (2000)	71
$(\delta^{18}\text{O}_{\text{HSO}_4\text{-H}_2\text{O}})$	Friedman and O'Neil (1977)	75
$\text{SO}_4\text{-H}_2\text{O}$	Halas and Pluta (2000)	23
$(\delta^{18}\text{O}_{\text{SO}_4\text{-H}_2\text{O}})$	Zeebe (2010)	27
$\text{SO}_4\text{-H}_2\text{O}$	Boschetti et al. (2011)	81
$(\delta^{18}\text{O}_{\text{CaSO}_4\text{-H}_2\text{O}})$		

2000), suggesting that secondary effects are negligible.

#### 4.4.2. Isotopic geothermometers

The results of the isotopic geothermometers calculations for sample T1 (from the low-sulphate group; Table 4) are shown in Table 7.

The  $\delta^{13}\text{C}$   $\text{CO}_2\text{-HCO}_3^-$  geothermometer points towards different temperature values depending on the considered calibration. The Mook et al. (1974) calibration predicts a temperature of 70 °C whilst with the Deines et al. (1974) it is 91 °C. If the  $\delta^{18}\text{O}$   $\text{CO}_2\text{-H}_2\text{O}$  geothermometer is considered, the temperature predicted by various calibrations is quite similar, between 94 and 98 °C (Table 7).

With respect to the  $\delta^{18}\text{O}$   $\text{SO}_4\text{-H}_2\text{O}$  geothermometer, using the classical calibrations (based on the equilibrium exchange between  $\text{HSO}_4^-$  and  $\text{H}_2\text{O}$ ) the temperature ranges from 71 to 75 °C whilst with the recently proposed calibrations based on the equilibrium exchange between  $\text{SO}_4^{2-}$  and  $\text{H}_2\text{O}$  (Halas and Pluta, 2000; Zeebe, 2010), the temperatures obtained are very low (Table 7). Finally, using the calibration proposed in Boschetti et al. (2011; a combination of the calibrations of Chiba et al., 1981 and Zheng, 1999), based on the equilibrium exchange between anhydrite ( $\text{CaSO}_4$ ) and  $\text{H}_2\text{O}$ , the calculated temperature is 81 °C.

The results of the calibrations based on the exchange between waters and various sulphur species, depend on the dominant species in solution (Boschetti, 2013). In low temperature systems with pH close to neutral, as in the Tiermas waters,  $\text{SO}_4^{2-}$  is usually the dominant species (70% of the sulphate, in speciation calculations), nonetheless, these calibrations provide unreasonably low temperatures. This fact is probably due to the lack of equilibrium between  $\text{SO}_4^{2-}$  and  $\text{H}_2\text{O}$  since, in low temperature systems, the  $^{18}\text{O}$  exchange between  $\text{SO}_4^{2-}$  and  $\text{H}_2\text{O}$  is slow and, moreover, the equilibrium can be affected by the sulphate reduction process identified in this sample (Boschetti et al., 2011).

The calibration based on  $\delta^{18}\text{O}$   $\text{CaSO}_4\text{-H}_2\text{O}$  may be the most reliable for this system as it provides a temperature of 81 °C quite similar to the results obtained from the previous calculations. Moreover, as it will be seen with the geothermometrical modelling next, the waters in the reservoir are in equilibrium with anhydrite.

The calibrations based on the  $\delta^{18}\text{O}$   $\text{HSO}_4^- \text{-H}_2\text{O}$  exchange also provide reasonable temperatures despite the fact that they are suitable for acidic waters. This is due to the fact that these calibrations have almost the same position in the  $\delta^{18}\text{O}\text{-T}$  plot, as the one based on the  $\text{CaSO}_4\text{-H}_2\text{O}$  exchange for neutral water (see, for instance, Boschetti, 2013 or Awaleh et al., 2015).

In summary, the values obtained by the isotopic geothermometers are in good agreement with those calculated with the chemical geothermometers.

#### 4.4.3. Geothermometrical modelling

The geothermometrical modelling consists of simulating a progressive increase of water temperature to obtain the value for which a set of minerals, assumed to be present in the reservoir in equilibrium with the waters, simultaneously reach that equilibrium. The selection of the mineral phases is based on the hydrogeochemical characteristics of the studied waters, the reservoir lithology and the results obtained from the chemical geothermometers.

The evolution of these waters is assumed to be controlled by the interaction processes with carbonate and evaporitic rocks. Therefore, phases such as calcite, dolomite and anhydrite are included in the calculations. Other evaporitic minerals, such as halite, may have influenced the water composition but they were not included in the modelling because all the waters are strongly undersaturated with respect to them (Table 5).

The presence of detrital material in the carbonate aquifer diversifies the mineral set to consider. Minerals such as albite, K-feldspar and quartz have been identified in some of these formations and the success of the Na-K geothermometers (based on the existence of a K-feldspar-albite-solution equilibrium) and  $\text{SiO}_2\text{-quartz}$  (based on the existence of

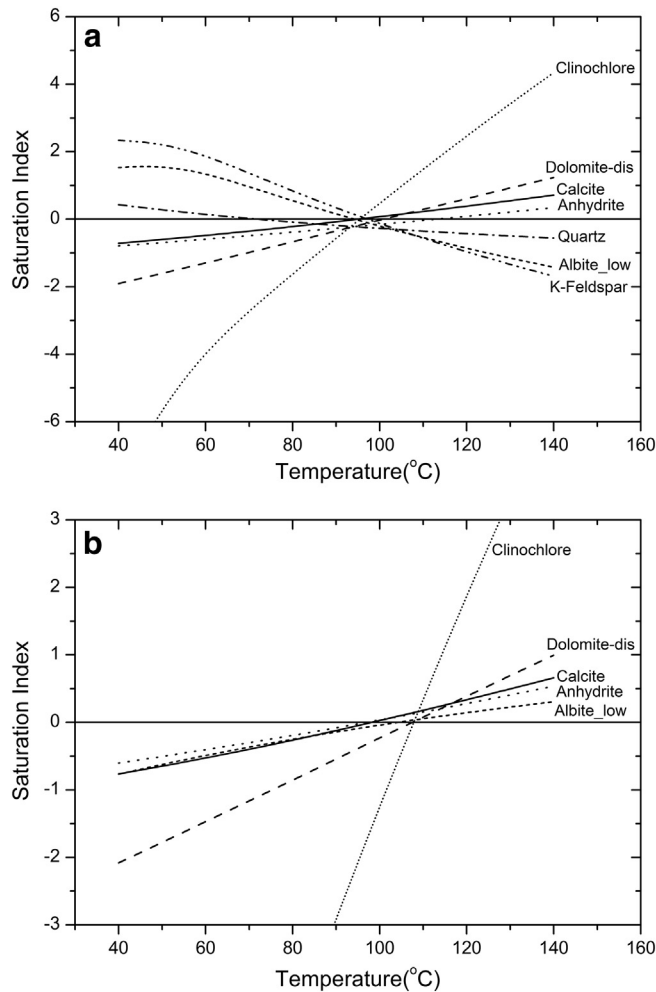


Fig. 5. Evolution with temperature of the saturation indices of the minerals supposed to be in equilibrium with the water of samples T1 (a) and B1 (b) in the reservoir. These results were obtained after the theoretical  $\text{CO}_2$  addition to compensate the  $\text{CO}_2$  outgassing during the ascent of the waters. The modelling for sample B1 (panel b) has been performed by equilibrating the water with quartz and K-feldspar and therefore, they are not shown in the plot. Dolomite-dis is disordered dolomite and Albite\_low is low temperature albite.

a quartz-solution equilibrium) supports that these phases could control some compositional characteristics of the waters.

Other aluminosilicate phases such as smectite, illite, chlorite and kaolinite are common in all types of sedimentary lithologies. Nevertheless, the solubility of such phases presents remarkable uncertainties due to their variability in composition, degree of crystallinity, etc (Merino and Ramson, 1982; Nordstrom et al., 1990; Palandri and Reed, 2001). After testing various aluminium phases, clinocllore was chosen in this study as representative for them, since it provides coherent results.

Some differences were found in the results obtained for the two samples of the low-sulphate group (B1 and T1) and they are shown separately in Fig. 5. The modelling results for the samples from the high-sulphate group are, however, all similar and only T3 is shown as representative in Fig. 6.

The first results obtained for all the waters showed that calcite and dolomite reach equilibrium at temperatures about 50 to 60 °C, lower than the temperatures for the rest of the considered mineral phases. Assuming that these minerals should be in equilibrium in the reservoir in this type of systems, the lack of coincidence with the rest of the minerals in equilibrium could be explained by  $\text{CO}_2$  outgassing during the ascent of the waters to the surface, which is coherent with the high

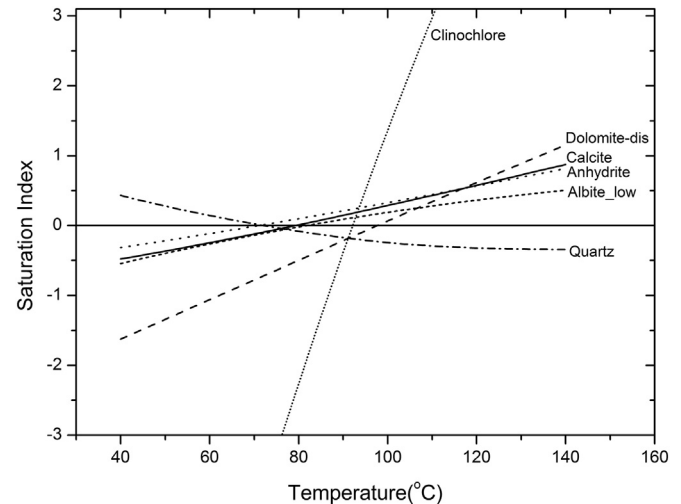


Fig. 6. Evolution with temperature of the saturation indices of the minerals supposed to be in equilibrium with the waters of sample T3 in the reservoir. In this case the modelling has been performed by equilibrating the water with K-feldspar and that is why it is not shown in the plot. These results were obtained after the theoretical  $\text{CO}_2$  addition to compensate the  $\text{CO}_2$  outgassing during the ascent of the waters. Dolomite-dis is disordered dolomite and Albite\_low is low temperature albite.

$\text{pCO}_2$  values in the waters (Table 5). In order to reconstruct the most plausible characteristics of the waters in the reservoir, and to check this hypothesis, an increase of the  $\text{CO}_2$  was simulated (as recommended by Pang and Reed, 1998 or Palandri and Reed, 2001) to obtain an equilibrium temperature for calcite similar to the temperature for the rest of phases. Although dolomite presents more uncertainties than calcite, after adjusting the calcite equilibrium, dolomite also provides coherent results.

The  $\text{CO}_2$  in B1 was increased to about 9.6 mmol/L, which means a pH = 6 in the reservoir, in sample T1 the increase was to 7.5 mmol/L and the pH was 6.15 and, finally, the increase in sample T3 was to about 5.4 mmol/L, which yields pH = 6.45 at depth. The results presented below in Table 8 and Figs. 5 and 6 were obtained after this reconstruction.

The results for sample T1 (Fig. 5a and Table 8) show that the aluminosilicate phases (clinocllore, K-feldspar and albite) reach equilibrium at a temperature around 95 °C, similar to the temperature predicted by dolomite (100 °C). The temperature predicted by quartz is 72 °C and by anhydrite is the highest, 113 °C. Sample B1, with no aluminium data and with silica concentration lower than expected compared to the rest of samples, has been equilibrated with quartz and K-feldspar, as proposed by Palandri and Reed (2001), fixing the dissolved silica and aluminium contents. The results obtained for the rest of the minerals are about 100 °C, (Fig. 5b and Table 8). Even anhydrite reaches equilibrium in the same range as the other minerals since the sulphate content in this sample is higher than in sample T1.

Table 8

Temperatures (°C) at which the selected mineral phases reach the equilibrium in the samples studied in the geothermometrical modelling (both samples of the first group: B1 and T1; and T3 as representative of the second group). These results were obtained after the theoretical  $\text{CO}_2$  addition to compensate the  $\text{CO}_2$  outgassing during the ascent of the waters. Dolomite-dis is disordered dolomite and Albite\_low is low temperature albite.

Mineral phase	B1	T1	T3
Quartz	–	72	73
Anhydrite	96	113	71
Calcite	98	95	79
Dolomite-dis	107	100	97
K-feldspar	–	97	–
Albite_low	104	94	81
Clinocllore	107	95	92

The evolution with the temperature of the saturation indices of the selected minerals for sample T3 (representative of the high-sulphate group) is shown in Fig. 6. Since there is not aluminium data for this sample, its concentration was fixed by imposing the K-feldspar equilibrium (Pang and Reed, 1998; Palandri and Reed, 2001). The results show a remarkable degree of convergence for the saturation indices of quartz and anhydrite which reach equilibrium at the same temperature, 72 and 71 °C, respectively. These phases are highly reliable in geothermometrical determinations (Kharaka and Mariner, 1989; Auqué, 1993; Pastorelli et al., 1999), since they are thermodynamically well characterised and their saturation states are not affected by pH variations during the ascent of thermal waters. On top of that, they are independent of uncertainties from the aluminium concentration of the waters. With respect to the rest of the minerals, albite provides a temperature of 81 °C whilst clinocllore and dolomite slightly higher (probably because these last two minerals can still be affected by some uncertainties due to the order degree in the first case, and the variations in its composition and crystallinity in the second; Helgeson et al., 1978; Palandri and Reed, 2001).

In summary, the temperature range deduced for the samples in the low-sulphate group is  $101 \pm 6$  °C and  $92 \pm 20$  °C for B1 and T1, respectively, and the temperature range predicted for sample T3 (as representative of the high-sulphate group) is somewhat lower,  $84 \pm 13$  °C.

## 5. Discussion

Combining the results obtained with the various geothermometrical techniques, the temperature in the reservoir deduced from each group is slightly different.

Temperature in the low sulphate group is higher, about 90 °C, and although the results show a more widespread temperature range than for the high-sulphate group, they are in a reasonable uncertainty range ( $\pm 20$  °C; Fournier, 1982 and Tole et al., 1993). The SiO<sub>2</sub>-quartz and K-Mg geothermometers predict slightly lower temperatures for sample B1 (68 and 66 °C, respectively), which could be due to secondary processes (e.g. dissolution/precipitation) affecting silica and magnesium contents (D'Amore and Arnórsson, 2000). Anhydrite provides a high temperature (113 °C) for sample T1 (with lower sulphate content probably due to sulphate reduction), whilst for sample B1 (with higher sulphate content), anhydrite reaches equilibrium also close to 90 °C. Therefore, if the temperature indicated by anhydrite in sample T1 is not considered representative of the conditions at depth, the temperature range defined for the waters of the low sulphate group in the reservoir would be  $90 \pm 20$  °C.

The good agreement of the results obtained with chemical geothermometers and geochemical modelling for the waters of the high-sulphate group suggests that the effects of secondary processes are not important and a lower temperature in the reservoir is indicated,  $82 \pm 15$  °C.

A remarkable finding is that equilibrium with albite and K-feldspar in the reservoir is evidenced with the geothermometrical modelling and the chemical geothermometers. This is not a common situation in low temperature carbonate-evaporitic systems. This equilibrium has been identified in some other “complex” carbonate-evaporitic system in which waters were also in contact with metasedimentary rocks (Marini et al., 2000), whilst other authors reported equilibrium with respect to albite but not with respect to K-feldspar in similar geothermal systems (e.g. López-Chicano et al., 2001; Boschetti et al., 2005). The possible explanation for this equilibrium in a carbonate-evaporitic systems is that the aquifer formations contain a significant amount of detrital material, as indicated by López-Chicano et al. (2001), allowing the waters to reach the equilibrium with phases like albite, K-feldspar and other aluminosilicate phases, as also evidenced here in the geothermometrical modelling.

Despite the compositional differences, the waters of both groups

seem to have reached the equilibrium with the same mineral assemblage in the reservoir (calcite, dolomite, quartz, anhydrite, albite, K-feldspar and other aluminosilicate phases) and at quite similar temperatures. Therefore, the compositional differences between the groups must be due to different extent of reaction with the evaporitic minerals and/or to the participation of additional reactions along the flow paths (as reflected in the Na/Cl and Ca/SO<sub>4</sub> ratios).

One of the main conclusions is that the equilibrium of these thermal waters with respect to anhydrite in the reservoir implies they must acquire the chloride-sodium/calcium-sulphate composition at depth and not whilst ascending to surface, otherwise, this equilibrium would not exist. However, with the available data, it is not possible to certainly determine if the evaporitic rocks in contact with the waters in the reservoir are those of the Keuper facies or those of the Eocene-Oligocene limit.

Although the degree of knowledge of this system is not enough to quantify the different intensity in the water-rock interaction processes, two relevant issues can be discussed from these results: 1) the influence of halite dissolution in the chemical characteristics of the waters; and 2) the implications that the chemical character of these waters could have for CO<sub>2</sub> storage in the reservoir formations.

### 5.1. The influence of halite dissolution in the chemical characteristics of the waters

The chemical characteristics of a water in equilibrium with a set of minerals are conditioned by the temperature and the pressure at which this equilibrium is attained; but they also depend on the concentration of elements not controlled by mineral equilibria such as chloride or sulphate, the mobile elements of Michard (1987). The influence of mobile elements, especially chloride, was recognised long ago by Helgeson (1970) and chloride has been considered as an independent master variable in determining the water composition in rock-buffered systems (Hanor, 2001). This importance has been verified in various types of geothermal systems (Michard, 1987; Michard and Bastide, 1988; Michard et al., 1996; Chiodini et al., 1991), in low temperature groundwaters in crystalline systems (Grimaud et al., 1990; Trotignon et al., 1999) and in saline waters in sedimentary basins (Hanor, 1994, 1996, 2001).

The influence of the mobile elements are especially important in carbonate-evaporitic geothermal systems because the waters are likely to be in contact with halite and its dissolution will condition the chemistry of the waters in equilibrium with a specific mineral set. This influence has been tested in the Tiermas thermal waters using the reaction-path capabilities of PHREEQC (Parkhurst and Appelo, 2013).

The water composition in equilibrium with the identified set of minerals was reconstructed to represent the water in the reservoir before halite dissolution starts. To do that, equimolar amounts of chloride and sodium were subtracted from the solution, down to  $\text{Cl}^- = 0$  mol/L, while maintaining the other mineral equilibria (albite, K-feldspar, quartz, anhydrite, calcite and dolomite) at the reservoir temperature (82 °C in the case of the high-sulphate group and 95 °C in the case of the low-sulphate group). From this theoretical solution, the effects of increasing the concentrations of chloride (and Na, through halite dissolution) on the rest of the chemical components controlled by the imposed mineral equilibria, can be discussed. The results obtained for all the samples are similar and therefore, only those from T3 are shown in Fig. 7.

The theoretical evolution of the concentration of the major elements in sample T3 is plotted in Fig. 7a to d against chloride under the situation of equilibrium with the rest of the mineral set. The concentration of all these major elements (Na, K, Ca, Mg and sulphate), although controlled by that equilibrium situation at a constant temperature, increases with sodium and chloride (except for silica whose concentration is almost constant, Fig. 7b).

Dissolved sulphate increases with chloride contents (Fig. 7d) as



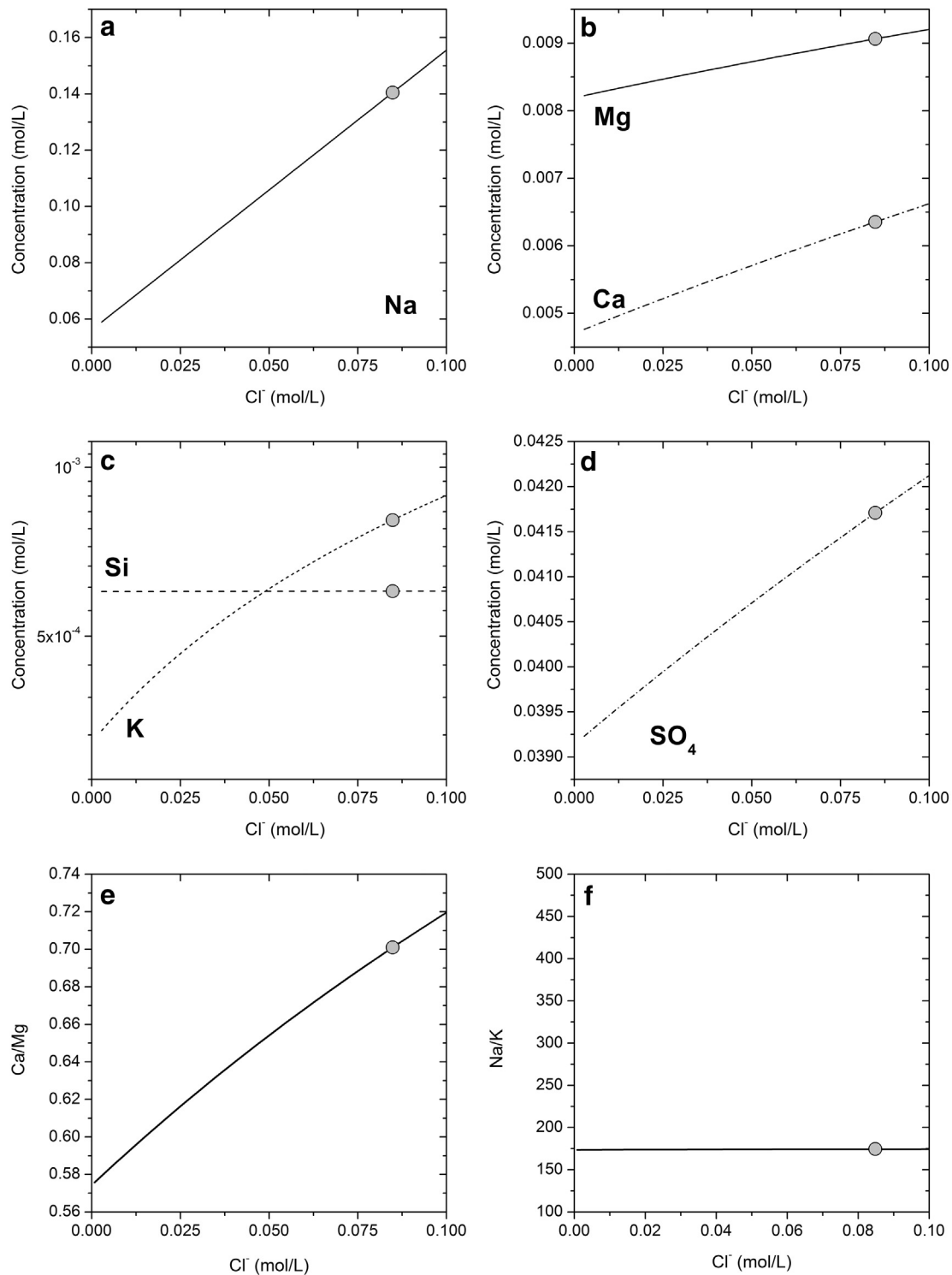
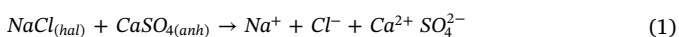
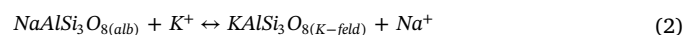


Fig. 7. Variation of the concentration of major elements (Na, Mg, Ca, Si, K and SO<sub>4</sub>, panels a to d) and of the ratios Ca/Mg and Na/K (as total element concentrations; panels e and f) in sample T3 with the variation of the dissolved chloride in the waters at 82 °C and maintaining the mineral equilibria that exist in the reservoir (albite, K-feldspar, quartz, anhydrite, calcite and dolomite). The grey dots in all the plots represent the chemical composition of sample T3.

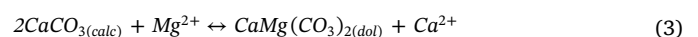
anhydrite solubility is enhanced by the increase of salinity and, therefore, by halite dissolution:



The increase in dissolved sodium promotes, in turn, the displacement of the albite-K-feldspar equilibrium reaction towards the left, increasing the amount of dissolved potassium (Fig. 7c):



And the increase of dissolved calcium promotes the displacement of the calcite-dolomite equilibrium reaction towards the left, increasing the concentrations of dissolved magnesium (Fig. 7b):



The two last panels in Fig. 7 (e and f) show the evolution of the

elemental ratios Ca/Mg and Na/K. The corresponding activity ratios stay constant under the specific temperature in the calculations as they are controlled by the calcite-dolomite and albite-K-feldspar equilibria, respectively (reactions 2 and 3); however, the elemental ratios show a different behaviour. The Na/K elemental ratio is also constant and near the corresponding activity ratio ( $a_{\text{Na}^+}/a_{\text{K}^+} = 185$ ) because these elements are almost unaffected by complexing and the free ion activity coefficients mutually cancel out (Chiodini et al., 1991). The Ca/Mg elemental ratio, however, is different from the activity ratio ( $a_{\text{Ca}^{2+}}/a_{\text{Mg}^{2+}} = 1.59$ ) and slightly increases with  $\text{Cl}^-$  concentrations (Fig. 7e; note the vertical scale) as these elements are more and differentially affected by the effect of complexation and activity coefficient calculations, which cause a deviation between the total contents and the activities (Chiodini et al., 1991).

These results indicate that although the chemistry of the waters is mainly controlled by mineral equilibria at a given temperature, the concentration of mobile elements are, therefore, an important variable in the control of the water composition. In the case studied here, the mobile element participating in the control of the system is chloride. Nonetheless, in other systems in which sulphate is not controlled by equilibrium with anhydrite or gypsum, the concentration of this component may have an influence in the controlled elements of the waters.

### 5.2. Effects of the chemical characteristics of the water in a future $\text{CO}_2$ storage

During the ALGECO2 project (IGME, 2010), a favourable tectonic and sedimentary structure for  $\text{CO}_2$  storage was identified in the studied area (the Leyre-Berdún structure; Suárez et al., 2014) in the Paleocene-Eocene carbonate rocks, which probably is the aquifer of the Tiermas thermal waters. If the features of the waters in that structure are similar to those deduced in the thermal waters, then some important conclusions about some plausible processes effective during the  $\text{CO}_2$  injection could be drawn. For example, in the vicinity of the injection well, the desiccation of the saline waters in contact with dry  $\text{CO}_2$  could easily induce the precipitation of carbonates and sulphates (Gaus, 2010; Gimeno et al., 2011; Gutiérrez et al., 2011) as the waters at depth are in equilibrium with calcite, dolomite and anhydrite. In the long term, injection of  $\text{CO}_2$  will promote the acidification of the saline groundwaters, which will lead to the dissolution of carbonate minerals (calcite and dolomite). In this context, precipitation of sulphates (gypsum or anhydrite) may be triggered as the waters are in equilibrium with anhydrite (e.g. with high concentrations of dissolved sulphate). A similar situation has been found in the Spanish test site for  $\text{CO}_2$  geological storage, located at Hontomin (Burgos), in a limestone reservoir, also with sulphate-rich saline groundwaters in equilibrium with gypsum/anhydrite (García-Ríos et al., 2014).

These processes involving carbonate and sulphate minerals are kinetically fast and their effects on the porosity and permeability of the reservoir rocks or in the well environment should be evaluated in future and more detailed site selection studies.

## 6. Conclusions

Two hydrogeochemical groups of waters have been identified in Tiermas springs: a group with TDS about 7500 ppm and low sulphate contents (low-sulphate group) and other with TDS close to 11,000 ppm and higher sulphate contents (high-sulphate group).

The temperature of the waters in the reservoir has been determined by combining various chemical and isotopic geothermometers with geothermometrical modelling, and a reliable range of temperatures has been established. The temperatures predicted for the waters are also slightly different for each group; being  $90 \pm 20$  °C for the low-sulphate group and slightly lower  $82 \pm 15$  °C for the high-sulphate one.

It is remarkable the good results obtained with some cationic geothermometers, such as the Na/K geothermometer, in a geothermal

system of low temperature and hosted in carbonate- evaporitic rocks like the studied here. This unusual situation may be attributed to the presence of detrital rocks (silicate minerals) in the carbonate- evaporitic aquifer, which provides for equilibrium between albite and K-feldspar as found in the geothermometrical modelling.

The two water groups are in equilibrium with the same mineral assemblage in the reservoir (calcite, dolomite, quartz, anhydrite, albite, K-feldspar and other aluminosilicate phases). However, they show slight differences in the temperature at depth and in the concentration of some chemical elements, which suggests that each group of waters could represent a different flow path with different types and/or intensities of water-rock interaction processes.

The influence of halite dissolution has also been evaluated and the results indicate that apart from temperature, chloride contents of the thermal waters have a significant influence on the concentrations of  $\text{SO}_4$ , Na, K, Ca and Mg measured in these waters. As demonstrated in the simulations presented here, if halite dissolution had occurred during the ascent of the thermal waters (without the influence of the mineral equilibria at depth) their chemical characteristics would be different. These results, along with the fact that anhydrite is included in the mineral assemblage in equilibrium in the reservoir, indicate that the waters should be in contact with an evaporitic facies in the reservoir and not during their ascent to surface.

Finally, as a favourable structure for  $\text{CO}_2$  storage has recently been identified in the Paleocene-Eocene carbonates, the probable aquifer of the Tiermas geothermal system, the groundwaters studied here could be used as analogues to the waters in that site. Therefore, the results of this study are useful for understanding the main processes related to the  $\text{CO}_2$  injection and mixing with this type of water. Near the injection wells, the waters will desiccate causing the precipitation of calcite, dolomite and anhydrite, since the waters are in equilibrium with respect to these phases in the reservoir, affecting the porosity and permeability of the rocks. And in the long term, the water will acidify leading to the carbonate dissolution and sulphate precipitation.

## Acknowledgements

M. Blasco is working in this study thanks to a scholarship from the Ministry of Education, Culture and Sports of Spain, for the Training of University Teachers (ref. FPU14/01523). This study forms part of the activities of the Geochemical Modelling Group (University of Zaragoza; Aragón Government). The comments of Dr. M.H. Reed and an anonymous reviewer have contributed to improve the work and are gratefully appreciated.

## References

- Appelo, C.A.J., Postma, D., 2005. *Geochemistry, Groundwater and Pollution*, 2nd edition. A.A. Balkema, Rotterdam.
- Arnorsson, S., Gunnlaugsson, E., Svavarsson, H., 1983. The chemistry of geothermal waters in Iceland. III. Chemical geothermometry in geothermal investigations. *Geochim. Cosmochim. Acta* 47, 567–577.
- Asta, M.P., Gimeno, M.J., Auqué, L.F., Gómez, J., Acero, P., Lapuente, P., 2010. Secondary processes determining the pH of alkaline waters in crystalline rock systems. *Chem. Geol.* 276, 41–52.
- Auqué, L.F., 1993. *Estudio de Sistemas Geotermales en Aragón. Pautas de Especiación y Reacción Aplicadas a la Modelización de Sistemas de Baja - Media Entalpía*. (Doctoral Thesis) University of Zaragoza, Zaragoza, Spain.
- Awaleh, M.O., Hoch, F.B., Boschetti, T., Soubaneh, Y.D., Egueh, N.M., Elmi, S.K., Mohamed, J., Khaireh, M.A., 2015. The geothermal resources of the Republic of Djibouti - II: geochemical study of the Lake Abhe geothermal field. *J. Geochim. Explor.* 159, 129–147.
- Ayora, C., García-Veigas, J., Pueyo, J., 1994. The chemical and hydrological evolution of an ancient potash-forming evaporite basin as constrained by mineral sequence, fluid inclusion composition and numerical simulation. *Geochim. Cosmochim. Acta* 58, 3779–3794.
- Ayora, C., Taberner, C., Pierre, C., Pueyo, J.J., 1995. Modeling the sulfur and oxygen isotopic composition of sulfates through a halite-potash sequence: implications for the hydrological evolution of the Upper Eocene South Pyrenean Basin. *Geochim. Cosmochim. Acta* 59, 1799–1808.
- Baeza, J., Torrealano, R., Cerezuela, M.A., 2000. Estudio para caracterizar, evaluar y

- proteger las aguas minerales y termales de una comunidad: Aragón. In: López Geta, J.A., Pinuaga, J.L. (Eds.), *Panorama Actual de las Aguas Minerales y Minero-medicinales en España*. Instituto Geológico y Minero de España (IGME), Madrid, pp. 283–303.
- Bauluz, B., González, J.M., Yuste, A., Mayayo, M.J., 2008. Evolución diagenética de las turbiditas del Grupo Hecho (Eoceno) en la Cuenca de Jaca (España). *Macla* 9, 47–48.
- Boschetti, T., 2013. Oxygen isotope equilibrium in sulfate-water systems: a revision of geothermometric applications in low-enthalpy systems. *J. Geochem. Explor.* 124, 92–100.
- Boschetti, T., Giampiero, V., Toscani, L., Barbieri, M., Muchino, C., 2005. The Bagni di Lucca thermal waters (Tuscany, Italy): an example of Ca-SO<sub>4</sub> waters with high Na/Cl and low Ca/SO<sub>4</sub> ratios. *J. Hydrol.* 307, 270–293.
- Boschetti, T., Corceci, G., Toscani, L., Iacumin, P., 2011. Sulfur and oxygen isotope compositions of Upper Triassic sulfates from northern Apennines (Italy): paleogeographic and hydrogeochemical implications. *Geol. Acta* 9 (2), 129–147.
- Brennkmeijer, C.A.M., Kraft, P., Mook, W.G., 1983. Oxygen isotope fractionation between CO<sub>2</sub> and H<sub>2</sub>O. *Isot. Geosci.* 1, 181–190.
- Chiba, H., Kusakabe, M., Hirano, S.I., Matsuo, S., Somiya, A., 1981. Oxygen isotope fractionation factors between anhydrite and water from 100 to 550 °C. *Earth Planet. Sci. Lett.* 53, 55–62.
- Chiodini, G., Cioni, R., Guidi, M., Marini, L., 1991. Chemical geothermometry and geobarometry in hydrothermal aqueous solutions: a theoretical investigation based on a mineral-solution equilibrium model. *Geochim. Cosmochim. Acta* 55, 2709–2727.
- Chiodini, G., Frondini, F., Marini, L., 1995. Theoretical geothermometers and pCO<sub>2</sub> indicators for aqueous solutions coming from hydrothermal systems of medium-low temperature hosted in carbonate-evaporite rocks. Application to the thermal springs of the Etruscan Swell. Italy. *Appl. Geochem.* 10, 337–346.
- Clark, I., Fritz, P., 1997. *Environmental Isotopes in Hydrogeology*. CRC Press/Lewis Publishers, Boca Raton (Florida).
- Consulnima, S.L., 2011. Informe Piezómetro de Romanzado: 090.031.001. Inspección y Vigilancia de las Obras de Construcción de Sondeos para la Adecuación de las Redes de Piezometría y Calidad de las Aguas Subterráneas. Cuenca del Ebro. Confederación Hidrográfica del Ebro, Zaragoza.
- Craig, H., 1961. Isotopic variations in meteoric waters. *Science* 133, 1702–1703.
- D'Amore, F., Arnórsson, S., 2000. Geothermometry. In: Arnórsson, S. (Ed.), *Isotopic and Chemical Techniques in Geothermal Exploration, Development and Use*. International Atomic Agency, Vienna, pp. 152–199.
- D'Amore, F., Fancelli, R., Caboi, R., 1987. Observations of the application of chemical geothermometers to some hydrothermal systems in Sardinia. *Geothermics* 16, 271–282.
- Deines, P., Languir, D., Harmon, R.S., 1974. Stable carbon isotope ratios and the existence of a gas phase in the evolution of carbonate ground water. *Geochim. Cosmochim. Acta* 38, 1147–1168.
- Díaz-Teijeiro, M.F., Rodríguez-Arévalo, J., Castaño, S., 2009. La Red Española de Vigilancia de Isótopos en la Precipitación (REVIP): distribución isotópica espacial y aportación al conocimiento del ciclo hidrológico. *Ing. Civ.* 155, 87–97.
- Faci, E., 1997. (Dir.) *Cartografía Geológica de Navarra*. E. 1:25000. Hoja 175-I: Tiermas. Gobierno de Navarra. Departamento de Obras Públicas, Transportes y Comunicaciones, Navarra.
- Fernández, J., Auqué, L.F., Sánchez Cela, V.S., Guaras, B., 1988. Las aguas termales de Fitero (Navarra) y Arnedillo (Rioja). Análisis comparativo de la aplicación de técnicas geotermométricas químicas a aguas relacionadas con reservorios carbonatado-evaporíticos. *Estud. Geol.* 44, 453–469.
- Fournier, R.O., 1977. Chemical geothermometers and mixing models for geothermal systems. *Geothermics* 5, 41–50.
- Fournier, R.O., 1979. A revised equation for the Na-K geothermometer. *Geotherm. Resour. Counc. Trans.* 3, 221–224.
- Fournier, R.O., 1982. Water geothermometers applied to geothermal energy. In: D'Amore, F., Co-ordinator (Eds.), *Applications of Geochemistry in Geothermal Reservoir Development*. UNITAR/UNDO centre on Small Energy Resources, Rome, pp. 37–69.
- Fournier, R.O., Potter, R.W., 1982. An equation correlating the solubility of quartz in water from 25 to 900 °C at pressures up to 10,000 bars. *Geochim. Cosmochim. Acta* 46, 1975–1978.
- Fournier, R.O., Truesdell, A.H., 1973. An empirical Na-K-Ca geothermometer for natural waters. *Geochim. Cosmochim. Acta* 37, 1255–1275.
- Friedman, I., O'Neil, J.R., 1977. Compilation of stable isotope fractionation factors of geochemical interest. In: *Fleischer, M. (Ed.), Data on Geochemistry*, 6th ed. United States Government Printing Office, Washington Chapter KK. USGS Professional Paper 440-KK.
- García-Ríos, M., Cama, J., Luquot, L., Soler, J.M., 2014. Interaction between CO<sub>2</sub>-rich sulfate solutions and carbonate reservoir rocks from atmospheric to supercritical CO<sub>2</sub> conditions: experiments and modeling. *Chem. Geol.* 383, 107–122.
- Gaus, I., 2010. Role and impact of CO<sub>2</sub>-rock interactions during CO<sub>2</sub> storage in sedimentary rocks. *Int. J. Greenhouse Gas Control* 4, 73–89.
- Giggenbach, W.F., 1988. Geothermal solute equilibria. Derivation of Na-K-Mg-Ca geothermometers. *Geochim. Cosmochim. Acta* 52, 2749–2765.
- Giggenbach, W., Gonfiantini, R., Jangi, B.L., Truesdell, A.H., 1983. Isotopic and chemical composition of Parbati valley geothermal discharges, N.W. Himalaya. *India. Geothermics* 12, 199–222.
- Gimeno, M.J., Acero, P., Gutiérrez, V., Auqué, L.F., Asta, M.P., Gómez, J.B., 2011. Evaluation of thermodynamic data and activity coefficient models for the geochemical modeling of CO<sub>2</sub> storage systems. *Mineral. Mag.* 75 (3), 918.
- Grimaud, D., Beaucaire, C., Michard, G., 1990. Modelling of the evolution of ground waters in a granite system at low temperature: the Stripa ground waters, Sweden. *Appl. Geochem.* 5, 515–525.
- Gupta, K.D., Pickering, K.T., 2008. Petrography and temporal changes in petrofacies of deep-marine Ainsa-Jaca basin sandstone systems, Early and Middle Eocene, Spanish Pyrenees. *Sedimentology* 55, 1083–1114.
- Gutiérrez, V., Acero, P., Auqué, L.F., Gimeno, M.J., 2011. Modelización Geoquímica de la Evolución del Entorno de un Pozo de Inyección de CO<sub>2</sub> y Evaluación de Condicionantes Termodinámicos. *Macla* 15, 111–112.
- Halas, S., Pluta, I., 2000. Empirical calibration of isotope thermometer  $\delta^{18}\text{O}$  (SO<sub>4</sub><sup>2-</sup>)- $\delta^{18}\text{O}$  (H<sub>2</sub>O) for low temperature brines. In: *V Isotope Workshop*. Kraków, Poland, pp. 68–71.
- Hanor, J.S., 1994. Physical and chemical controls on the composition of waters in sedimentary basins. *Mar. Pet. Geol.* 11, 31–45.
- Hanor, J.S., 1996. Variations of chloride as a driving force in siliciclastic diagenesis. *Siliciclastic diagenesis and fluid flow: concepts and applications*. SEPM Spec. Publ. 55, 3–12.
- Hanor, J.S., 2001. Reactive transport involving rock-buffered fluids of varying salinity. *Geochim. Cosmochim. Acta* 65, 3721–3732.
- Helgeson, H.C., 1970. Description and interpretation of phase relations in geochemical processes involving aqueous solutions. *Am. J. Sci.* 268, 415–438.
- Helgeson, H.C., Delany, J.M., Nesbitt, H.W., Bird, D.K., 1978. Summary and critique of the thermodynamic properties of rock-forming minerals. *Am. J. Sci.* 278.
- IGME, 1973. Mapa Geológico de España. E. 1:50000. Hoja 175: Sigües. Instituto Geológico y Minero de España (IGME), Madrid.
- IGME, 2010. Selección y caracterización de áreas y estructuras geológicas favorables para el almacenamiento geológico de CO<sub>2</sub> en España. <http://info.igme.es/algeco2/> (accessed 21-03-2016).
- ITGE-DGA, 1994. Estudio de las Aguas Minero-medicinales, Minero-industriales, Termales y de Bebida Envasada en la Comunidad Autónoma de Aragón. Instituto Geológico y Minero de España (IGME), Madrid.
- Jiménez, M., 1838. *Tratado de Materia Farmacéutica*, 2nd ed. Imprenta de la Viuda de Sanchiz e hijos, Madrid.
- Kharaka, Y.K., Mariner, R.H., 1989. Chemical geothermometers from water-mineral equilibria. In: *Abstracts of the 28th International Geological Congress* (vol. 2), Washington D.C., pp. 184–185.
- Larrasoaña, J.C., Pueyo, E.L., del Valle, J., Millán, H., Pucoví, A., Dinarés, J., 1996. Datos magnetotectónicos del Eoceno de la Cuenca de Jaca - Pamplona: resultados iniciales. *Geogaceta* 30, 1058–1061.
- Lloyd, R.M., 1968. Oxygen isotope behaviour in the sulfate-water system. *J. Geophys. Res.* 73, 6099–6110.
- López-Chicano, M., Cerón, J.C., Vallejos, A., Pulido-Bosch, A., 2001. Geochemistry of thermal springs, Alhama de Granada (southern Spain). *Appl. Geochem.* 16, 1153–1163.
- Marini, L., 2004. *Geochemical Techniques for the Exploration and Exploitation of Geothermal Energy*. Laboratorio di Geochimica, Università degli Studi di Genova, Genova.
- Marini, L., Chiodini, G., Cioni, R., 1986. New geothermometers for carbonate-evaporite geothermal reservoirs. *Geothermics* 15, 77–86.
- Marini, L., Bonaria, V., Guidi, M., Hunziker, J.C., Ottonello, G., Vetusch Zuccolini, M., 2000. Fluid geochemistry of the Acqui Terme-Visone geothermal area (Piemonte, Italy). *Appl. Geochem.* 15, 917–935.
- Merino, E., Ramson, B., 1982. Free energies of formation of illite solid solutions and their compositional dependence. *Clay Clay Miner.* 30, 29–39.
- Michard, G., 1979. Géothermomètres chimiques. In: *B.R.G.M. (2nd Ser.)*, section III, vol. 2, pp. 183–189.
- Michard, G., 1987. Controls of the chemical composition of geothermal waters. In: Helgeson, H.C. (Ed.), *Chemical Transport in Metasomatic Processes*. D. Reidel Publishing Company, Dordrecht (Netherlands), pp. 323–353.
- Michard, G., Bastide, J.P., 1988. Etude Géochimique de la nappe du Dogger du Bassin Parisien. *J. Volcanol. Geotherm. Res.* 35, 151–163.
- Michard, G., Fouillac, C., 1980. Contrôle de la composition chimique des eaux thermales sulfurées sodiques du Sud de la France. In: Tardy, Y. (Ed.), *Géochimie des Interactions Entre les Eaux, les Minéraux et les Roches*. Elements, Tarbes, pp. 147–166.
- Michard, G., Roekens, E., 1983. Modeling of the chemical composition of alkaline hot waters. *Geothermics* 12, 161–169.
- Michard, G., Sanjuan, B., Criaud, A., Pentcheva, E.N., Petrov, P.S., Alexieva, R., 1986. Equilibria and geothermometry in hot waters from granites of SW Bulgaria. *Geochem. J.* 20, 159–171.
- Michard, G., Pearson Jr., F.J., Gautschi, A., 1996. Chemical evolution of waters during long term interaction with granitic rocks in northern Switzerland. *Appl. Geochem.* 11, 757–774.
- Mizutani, Y., Rafta, T.A., 1969. Oxygen isotopic composition of sulphates. 3. Oxygen isotopic fractionation in the bisulfate ion-water system. *N. Z. J. Sci.* 12, 54–59.
- Mook, W.G., Bommerson, J.C., Staverman, W.H., 1974. Carbon isotope fractionation between dissolved bicarbonate and gaseous carbon dioxide. *Earth Planet. Sci. Lett.* 22, 169–176.
- Nordstrom, D.K., Ball, J.W., Donahoe, R.J., Whittemore, D., 1989. Groundwater chemistry and water-rock interactions at Stripa. *Geochim. Cosmochim. Acta* 53, 1727–1740.
- Nordstrom, D.K., Plummer, L.N., Langmuir, L., Busenberg, E., May, H.M., Jones, B.F., Parkhurst, D.L., 1990. Revised chemical equilibrium data for major water-mineral reactions and their limitation. In: Melchior, D.C., Basset, R.L. (Eds.), *Chemical Modeling of Aqueous Systems II*. Symposium Series Vol. 416. American Chemical Society, Washington DC, pp. 398–413.
- Oliva, B., Millán, H., Pucoví, A., Casas, A.M., 1996. Estructura de la Cuenca de Jaca en el sector occidental de las Sierras Exteriores Aragonesas. *Geogaceta* 20, 800–802.
- Oliva-Urcia, B., Casas, A.M., Pueyo, E.L., Pucoví-Juan, A., 2012. Structural and paleomagnetic evidence for non-rotational kinematics of the South Pyrenean Frontal

- Thrust at the western termination of the External Sierras (southwestern central Pyrenees). *Geol. Acta* 10, 125–144.
- O'Neil, J.R., Adami, L.H., 1969. The oxygen isotope partition function ratio of water and the structure of liquid water. *J. Phys. Chem.* 73 (5), 1553–1558.
- Palandri, J.L., Reed, M.H., 2001. Reconstruction of in situ composition of sedimentary formation waters. *Geochim. Cosmochim. Acta* 65, 1741–1767.
- Pang, Z., Reed, M.H., 1998. Theoretical chemical thermometry on geothermal waters: problems and methods. *Geochim. Cosmochim. Acta* 62, 1083–1091.
- Parkhurst, D.L., Appelo, C.A.J., 2013. *Techniques and methods, book 6, chap. A43. In: U.S. Geological Survey (Ed.), Description of Input and Examples for PHREEQC Version 3. A Computer Program for Speciation, Batch-Reaction, One-Dimensional Transport, and Inverse Geochemical Calculations. U.S.G.S., Denver, Colorado available only at* <http://pubs.usgs.gov/tm/06/a43>.
- Pastorelli, S., Marini, L., Hunziker, J.C., 1999. Water chemistry and isotope composition of the Acuarossa thermal system, Ticino, Switzerland. *Geothermics* 28, 75–93.
- Payros, A., Orue-Etxebarria, X., Bacera, J.I., Pujalte, V., 1994. Las “megaturbiditas” y otros depósitos de resedimentación carbonatada a gran escala del Eoceno surpirineico: nuevos datos del área Urrobi-Ultzama (Navarra). *Geogaceta* 16, 94–97.
- Peiffer, L., Wanner, C., Spycher, N., Sonnenthal, E.L., Kennedy, B.M., Iovenitti, J., 2014. Optimized multicomponent vs. classical geothermometry: insights from modeling studies at the Dixie Valley geothermal area. *Geothermics* 51, 154–169.
- Pueyo, E.L., Calvin, P., Casas, A.M., Olivia-Ucria, B., Klimowitz, J., García-Lobón, J.L., Rubio, F.M., Ibarra, P.I., Martínez-Duran, P., Rey-Moral, M.C., Pérez, L., Martín, J.M., 2012. A research plan for a large potential CO<sub>2</sub> reservoir in the Southern Pyrenees. *Geo-Temas* 13, 1970–1973.
- Puigdefàbregas, C., 1975. La sedimentación molásica en la cuenca de Jaca. *Pirineos* 104.
- Reed, M., Spycher, N., 1984. Calculation of pH and mineral equilibria in hydrothermal waters with application to geothermometry and studies of boiling and dilution. *Geochim. Cosmochim. Acta* 48, 1479–1492.
- Sáenz, C., 1999. Patrimonio Geológico del Camino de Santiago. Instituto Tecnológico GeoMinero de España, Madrid.
- Sánchez, J.A., 2000. Las Aguas Termales en Aragón: Estudio Hidrogeotérmico. Consejo de Protección de la Naturaleza de Aragón, Zaragoza.
- Sánchez Guzmán, J., García de la Noceda, C., 2005. Geothermal energy development in Spain - country update report. In: *Proceedings World Geothermal Congress 2005*. Antalya, Turkey, pp. 1–10.
- Sánchez, J.A., Coloma, P., Pérez-García, A., De Leiva, A., 2000. Evaluación del flujo geotérmico en manantiales de Aragón. *Geogaceta* 27, 155–158.
- Sánchez, J.A., Colom, P., Pérez-García, A., 2004. Evaluation of geothermal flow at the springs in Aragón (Spain), and its relation to geologic structure. *Hydrogeol. J.* 12, 601–609.
- Saura, E., Teixell, A., 2006. Inversion of small basins: effects on structural variations at the leading edge of the Axial Zone antiformal stack (Southern Pyrenees, Spain). *J. Struct. Geol.* 28, 1909–1920.
- Seal, R.R.I., Alpers, C.N., Rye, R.O., 2000. Stable isotope systematics of sulfate minerals. In: Alpers, C.N., Jambor, J.L., Nordstrom, D.K. (Eds.), *Sulfate Minerals — Crystallography: Geochemistry and Environmental Significance*. Mineral Society of America, Chantilly (Virginia), pp. 541–602.
- Spycher, N., Peiffer, L., Sonnenthal, E.L., Saldi, G., Reed, M.H., Kennedy, B.M., 2014. Integrated multicomponent solute geothermometry. *Geothermics* 51, 113–123.
- Suárez, I., Arenillas, A., Medaito, J.F., García, J., Molinero, R., Catalina, R., 2014. Atlas de Estructuras del Subsuelo Susceptibles de Almacenamiento Geológico de CO<sub>2</sub> en España. Instituto Geológico y Minero de España (IGME). Instituto para la Reestructuración de la Minería del carbón y desarrollo Alternativo de las Comarcas Mineras, Madrid.
- Tole, M.P., Armannsson, H., Pang, Z., Arnorsson, S., 1993. Fluid/mineral equilibrium calculations for geothermal fluids and chemical geothermometry. *Geothermics* 22, 17–37.
- Trotignon, L., Beaucaire, C., Louvat, D., Aranyosy, J.F., 1999. Equilibrium geochemical modelling of Áspö groundwaters: a sensitivity study of thermodynamic equilibrium constants. *Appl. Geochem.* 14, 907–916.
- Truesdell, A.H., 1974. Oxygen isotope activities and concentrations in aqueous salt solutions at elevated temperatures: consequences for isotope geochemistry. *Earth Planet. Sci. Lett.* 23, 387–396.
- Truesdell, A.H., 1976. Geochemical techniques in exploration. Summary of section III. In: *Proceedings of the Second United Nations Symposium on the Development and Use of Geothermal Resources*. San Francisco, California, pp. iii–xxix.
- Utrilla, R., Pierre, C., Ortí, F., Rosell, L., Inglés, M., Pueyo, J.J., 1987. Estudio Isotópico de los Sulfatos en Formaciones Evaporíticas Mesozoicas y Terciarias Continentales. II Congreso de Geoquímica de España, Soria, pp. 91–94.
- Wang, J., Jin, M., Jia, B., Kang, F., 2015. Hydrochemical characteristics and geothermometry applications of thermal groundwater in northern Jinan, Shandong, China. *Geothermics* 57, 185–195.
- Zeebe, R.E., 2010. A new value for the stable oxygen isotope fractionation between dissolved sulfate ion and water. *Geochim. Cosmochim. Acta* 74, 818–828.
- Zheng, Y.F., 1999. Oxygen isotope fractionation in carbonate and sulfate minerals. *Geochem. J.* 33, 109–126.

## 4.2 Paper 2

### **Low temperature geothermal systems in carbonate-evaporitic rocks: Mineral equilibria assumptions and geothermometrical calculations. Insights from the Arnedillo thermal waters (Spain)**

*Mónica Blasco, María J. Gimeno, Luis F. Auqué*

Science of The Total Environment 615, 526-539 (2018)

Impact Factor (2017): 4.61

Quartile and Category (2017): Q1 (27/241), Environmental Sciences

DOI: 10.1016/j.scitotenv.2017.09.269

Sent: 22 August 2017

Accepted: 25 September 2017

Available online: 5 October 2017

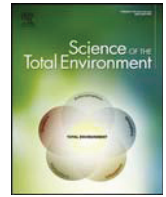
Final publication: 15 February 2018





Contents lists available at ScienceDirect

## Science of the Total Environment

journal homepage: [www.elsevier.com/locate/scitotenv](http://www.elsevier.com/locate/scitotenv)

# Low temperature geothermal systems in carbonate-evaporitic rocks: Mineral equilibria assumptions and geothermometrical calculations. Insights from the Arnedillo thermal waters (Spain)



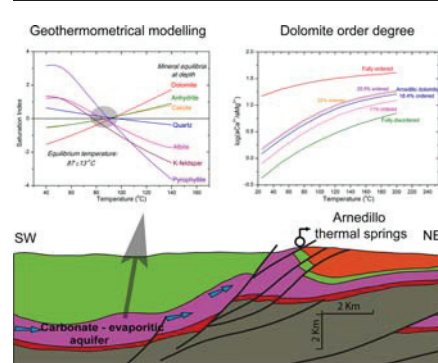
Mónica Blasco\*, María J. Gimeno, Luis F. Auqué

Geochemical Modelling Group, Petrology and Geochemistry Area, Earth Sciences Department, University of Zaragoza, Spain C/ Pedro Cerbuna 12, 50009 Zaragoza, Spain

## HIGHLIGHTS

- Mineral equilibria in low temperature geothermal systems are discussed.
- Consequences on some geothermometrical methods are addressed.
- The order degree of the dolomite present in the aquifer is calculated.
- A low temperature geothermal system hosted in carbonate rocks is used as an example.

## GRAPHICAL ABSTRACT



## ARTICLE INFO

## Article history:

Received 22 August 2017

Received in revised form 24 September 2017

Accepted 25 September 2017

Available online xxx

Editor: D. Barcelo

## Keywords:

Low temperature geothermal system

Geochemical modelling

Geothermometry

Mineral equilibria

Dolomite order/disorder degree

## ABSTRACT

Geothermometrical calculations in low-medium temperature geothermal systems hosted in carbonate-evaporitic rocks are complicated because 1) some of the classical chemical geothermometers are, usually, inadequate (since they were developed for higher temperature systems with different mineral-water equilibria at depth) and 2) the chemical geothermometers calibrated for these systems (based on the Ca and Mg or  $\text{SO}_4$  and F contents) are not free of problems either. The case study of the Arnedillo thermal system, a carbonate-evaporitic system of low temperature, will be used to deal with these problems through the combination of several geothermometrical techniques (chemical and isotopic geothermometers and geochemical modelling).

The reservoir temperature of the Arnedillo geothermal system has been established to be in the range of  $87 \pm 13^\circ\text{C}$  being the waters in equilibrium with respect to calcite, dolomite, anhydrite, quartz, albite, K-feldspar and other aluminosilicates. Anhydrite and quartz equilibria are highly reliable to establish the reservoir temperature. Additionally, the anhydrite equilibrium explains the coherent results obtained with the  $\delta^{18}\text{O}$  anhydrite – water geothermometer. The equilibrium with respect to feldspars and other aluminosilicates is unusual in carbonate-evaporitic systems and it is probably related to the presence of detrital material in the aquifer.

The identification of the expected equilibria with calcite and dolomite presents an interesting problem associated to dolomite. Variable order degrees of dolomite can be found in natural systems and this fact affects the associated equilibrium temperature in the geothermometrical modelling and also the results from the Ca-Mg geothermometer. To avoid this uncertainty, the order degree of the dolomite present in the Arnedillo reservoir has been determined and the results indicate 18.4% of ordered dolomite and 81.6% of disordered dolomite.

\* Corresponding author.

E-mail address: [monicabc@unizar.es](mailto:monicabc@unizar.es) (M. Blasco).

Overall, the results suggest that this multi-technique approach is very useful to solve some of the problems associated to the study of carbonate–evaporitic geothermal systems.

© 2017 Elsevier B.V. All rights reserved.

## 1. Introduction

The study of the chemical and isotopic composition of thermal waters allows identifying the water–rock interaction processes involved in their evolution, determining the possible secondary processes that could affect them during their ascent to surface (e.g. mineral reequilibrium or mixing) and establishing the reservoir temperature by geothermometrical methods. This characterisation is the first step to evaluate the geothermal potential of an area (e.g. D'Amore and Arnórsson, 2000). Nowadays, the use of geothermal energy is diversifying and the technical advances make possible to obtain electrical energy from waters of lower temperature. Additionally, one of the possibilities considered for the CO<sub>2</sub> geological storage is the use of deep saline aquifers, usually hot, hosted in sedimentary rocks (e.g. Auqué et al., 2009, and references therein). These deep storages are inaccessible for their study in an initial stage and, therefore, the information obtained from low to medium temperature thermal systems with similar hydrogeochemical characteristics becomes a suitable and very convenient source of information.

The temperature in the deep reservoirs can be determined by several chemical and isotopic geothermometers and by geothermometrical modelling. However, these techniques present some problems in the case of carbonate–evaporitic aquifers. The classical cationic geothermometers (based on the equilibrium with aluminosilicate phases) are useful in systems with high temperature or with host rocks like granites or basalts in which the waters have reached the equilibrium with various aluminosilicates such as albite or K-feldspar (e.g. Arnórsson et al., 1983; Asta et al., 2012; Auqué et al., 1997; Buil et al., 2006; Choi et al., 2005; D'Amore et al., 1987; Fouillac and Michard, 1981; Fournier, 1981, 1977; Giggenbach et al., 1983; Giggenbach, 1988; Kharaka and Mariner, 1989; Mariner et al., 2006; Mutlu and Güleç, 1998; Stefánsson and Arnórsson, 2000, among much others). These equilibria are not likely to have been attained in carbonate–evaporitic systems and they may provide erroneous results (Chiodini et al., 1995; Karimi and Moore, 2008; Levet et al., 2002; López-Chicano et al., 2001; Sonney and Vuataz, 2010) although, in some cases, the silica and some cationic geothermometers have provided good results (e.g. Apollaro et al., 2012; Blasco et al., 2017; Fernández et al., 1988; Gökgöz and Tarkan, 2006; Michard and Bastide, 1988; Mohammadi et al., 2010; Pastorelli et al., 1999; Wang et al., 2015).

The more suitable geothermometers are, obviously, those developed for this kind of systems, that is, the Ca–Mg and SO<sub>4</sub>–F geothermometers, initially proposed by Marini et al. (1986) and reviewed by Chiodini et al. (1995) afterwards. However, even these might have problems since the former can be affected by the uncertainties in the thermodynamic properties of dolomite (due to non-stoichiometry of order/disorder degree; Chiodini et al., 1995; Frondini, 2008; Helgeson et al., 1978; Marini, 2006; Palandri and Reed, 2001) and the latter will only be suitable if the waters are in equilibrium with anhydrite (or gypsum) and fluorite (Chiodini et al., 1995) which is not always the case.

The isotopic geothermometry is another possible technique although it may also be problematic. For example, the  $\delta^{18}\text{O}$  exchange between CO<sub>2</sub> and H<sub>2</sub>O is easily modified during the ascent of the waters to surface since the kinetics of the exchange reaction is fast and the isotopic reequilibrium takes place even at low temperatures (D'Amore and Arnórsson, 2000). Other common isotopic geothermometer is the  $\delta^{18}\text{O}$  SO<sub>4</sub>–H<sub>2</sub>O, but traditionally its calibrations are based in the HSO<sub>4</sub>–H<sub>2</sub>O exchange, and the HSO<sub>4</sub> is not present in neutral to basic waters (Boschetti, 2013). Some new calibrations have been recently proposed trying to solve this problem, although they are not widely used yet.

Finally, the geothermometrical modelling (or multicomponent solution geothermometry; e.g. Spycher et al., 2014) is very useful since it allows determining the reservoir temperature by studying the saturation states of a vast number of minerals, providing important information about the probable mineral set the waters are in equilibrium with in the reservoir. Additionally it allows evaluating the secondary processes (e.g. mixing, degasification or mineral reequilibrium) that could affect the waters during their ascent to surface (Asta et al., 2010; Auqué et al., 2009; Michard and Fouillac, 1980; Michard and Roekens, 1983; Michard et al., 1986a; Palandri and Reed, 2001; Pang and Reed, 1998; Reed and Spycher, 1984; Tole et al., 1993). Nevertheless, this technique also shows some problems associated to the uncertainties in the mineral solubility of some minerals (Palandri and Reed, 2001).

The study of the low–medium temperature geothermal system of Arnedillo will be used 1) to test all the mentioned geothermometrical techniques, in order to improve their knowledge for their use in further studies; and 2) to characterise hydrogeochemically this natural thermal system for a future exploitation of its geothermal potential.

## 2. Geological and hydrogeological setting

The Arnedillo thermal waters emerge near the Cidacos River, in the Arnedillo village (La Rioja, Spain). Geologically, they are located in the NW of the Iberian Chain, in the contact between the eastern Cameros Range and the tertiary Ebro Basin (Fig. 1; Coloma et al., 1997; Sánchez and Coloma, 1998).

The Cameros Range, constituted mainly by Mesozoic formations, is bounded by two continental basins and two Palaeozoic reliefs: the Ebro and Duero basins in the north and the south, respectively; and the Demanda and Moncayo Ranges at the east and west (Gil et al., 2002). The Triassic is represented by Buntsandstein (sandstones, siltstones and breccias surrounding the Demanda Range), Muschelkalk (mainly dolostones, although the outcrops in the area are scarce) and Keuper facies (gypsum/anhydrite, marls and clays) which is the detachment level for the tertiary thrusting (Coloma, 1998; Gil et al., 2002).

The marine Jurassic formations (up to Kimmeridgian, Upper Jurassic) are the ones found in the rest of the Iberian Chain (Coloma, 1998; Gil et al., 2002; Goy et al., 1976), consisting of dolostones and limestones with some intercalations of marls: Imon (dolostones), Cortes de Tajuña (dolomitic breccias with anhydrite), Cuevas Labradas (limestones and dolostones), Cerro del Pez (marls), Barahona (bioclastic limestones), Turmiel (marls and limestones), Chelva (limestones), Aldealpozo (black limestones) and Torrecilla (limestones with corals). These formations are mainly constituted by carbonates but some terrigenous deposits are also present (Goy et al., 1976). These Triassic and marine Jurassic formations constitute the pre-rift sequence.

A rifting process took place at the end of the Jurassic and during the Cretaceous, resulting in the formation of the Cameros Basin. The corresponding formations are known as the syn-rift sequence, which is constituted by continental sediments from the Upper Jurassic (Tithonian) to the Lower Cretaceous (Albian) (Coloma, 1998; Gil et al., 2002; Mas et al., 1993). These continental sediments have been traditionally divided into five groups (Tischer, 1965): Tera, Oncala, Urbión (fluvial sediments consisting of lutites and sandstones), Enciso and Oliván (lacustrine sediments constituted by limestones, marls and limolites).

The Upper Cretaceous constitutes the post-rift sequence and consists of carbonates from the Urgon Facies, the Utrillas Sandstones and the carbonate sedimentation at the end of this period (Gil et al., 2002).

During the Tertiary the tectonic inversion resulted in the relief of the Cameros Range and the formation of the tertiary basins, which were



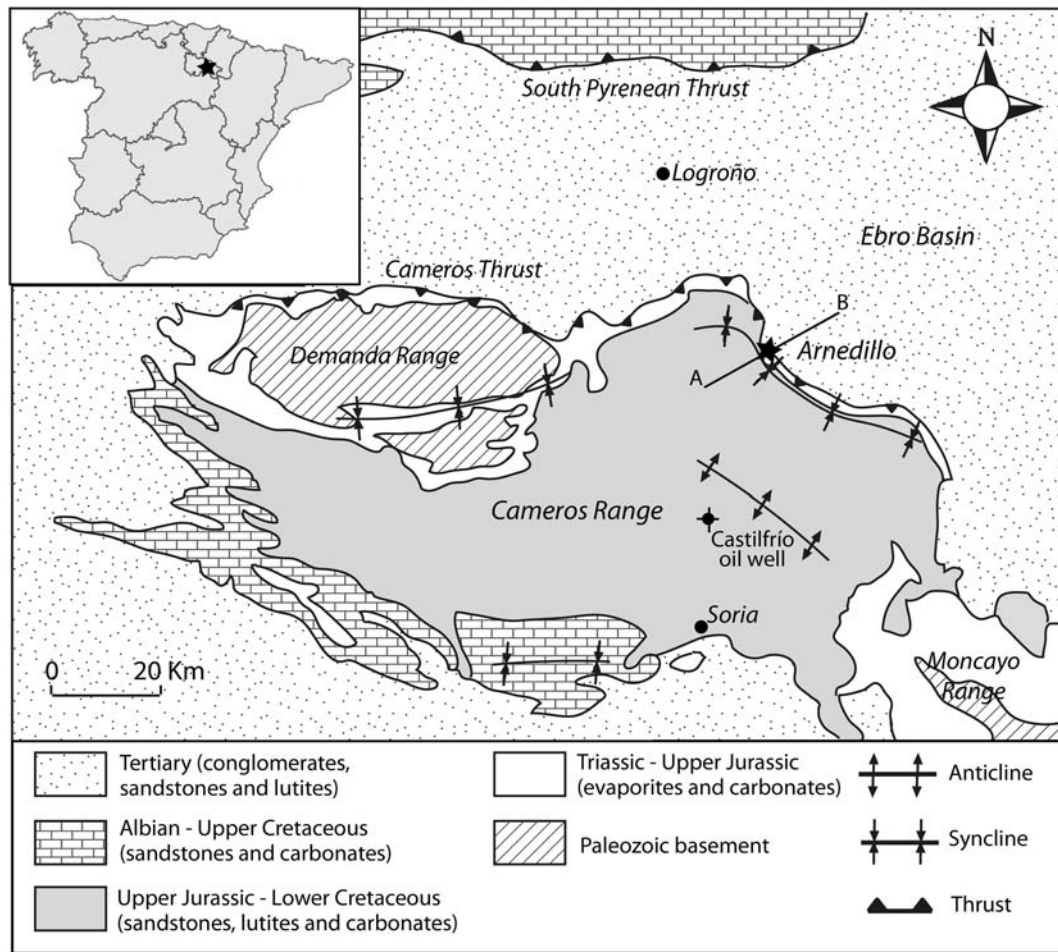


Fig. 1. Geological map of the Arnedillo area and location of the geothermal springs (modified from Gil et al., 2002). A–B indicates the location of the cross section shown in Fig. 2.

filled with detrital material mainly from the Paleogene and Neogene. Compressive structures were generated with E-W or NW-SE direction, being the Cameros thrust one of the most important, which makes the Mesozoic series thrust over the tertiary formations of the Ebro Basin (Coloma, 1998; Gil et al., 2002). Finally, the Quaternary is constituted by alluvial and colluvial deposits due to the glaci – terrace systems developed from the Cameros Range to the Ebro River (Coloma, 1998).

The carbonate formations of the pre-rift sequence (Fig. 2) constitute the main aquifer in this area. These formations are divided in three groups, two permeable ones separated by other less permeable: 1) Imón, Cortes de Tajuña and Cuevas Labradas Formations (the first permeable group); 2) Cerro del Pez, Barahona and Turmiel Formations (the intermediate impermeable group); and 3) Chelva, Aldealpozo and Torrecilla Formations (the second permeable group). Due to the great fracturation affecting them, these formations are interconnected

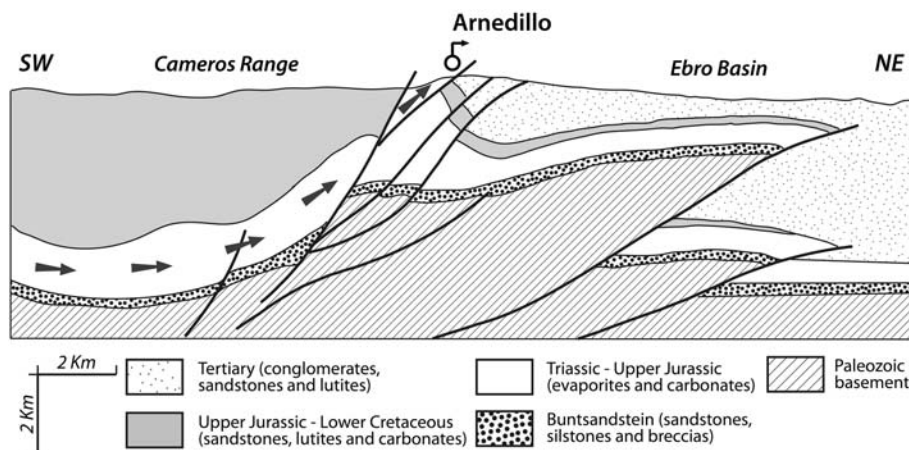


Fig. 2. SW-NE cross section (A–B, in Fig. 1) showing the general tectonic structure of the Arnedillo geothermal system modified from ALGECO2 Project; IGME, 2010). The grey arrows represent the flow direction.

constituting the regional drainage level of the Iberian Chain, although the main flow circulates through the formations of the first permeable group (Coloma et al., 1995; Sánchez and Coloma, 1998; Sánchez et al., 1999).

The Arnedillo thermal waters are of sodium – chloride type and emerge with a temperature of about 50 °C and flow rates of 10–20 L/s (Coloma et al., 1998, 1995; Sánchez and Coloma, 1998). This sodium – chloride affinity, along with the high sulfate contents, is coherent with the circulation of the waters through the first permeable group, since the waters would be in contact to the evaporites of the Keuper Facies and the anhydrite of the Cortes de Tajuña Formation. The discharge takes place in the contact between the Mesozoic and Tertiary formations, in the Cameros thrust (Fig. 2), through which the waters rapidly ascend to surface (Coloma, 1998; Coloma et al., 1996).

The recharge of the waters takes place by three different forms: 1) direct infiltration in the outcrops of the Jurassic rocks; 2) infiltration from permeable stretches of the rivers; and 3) through the rocks of the synrift sequence that, although they have a low permeability, constitute and aquitard and their vast lateral extension actually makes this form of recharge the most important one (Coloma et al., 1997, 1995).

### 3. Methodology

Analytical data of the Arnedillo thermal waters were compiled and reviewed in order to assess possible chemical changes over the time. Apart from the data corresponding to a new sampling campaign performed by the authors of this paper in 2015 (samples AR1 and AR2), other samples were selected after checking their reliability: AR3 from Maraver Eyzaguirre (2003) and AR4 and AR5 from Coloma et al. (1997). The methodological aspects corresponding to the previous sampling campaigns can be found in the original papers. Here we will describe the methods followed for the sampling and analyses in 2015. However, it is important to indicate that the pH was determined in situ in all the samples except in sample AR5 in which the pH value was determined in laboratory, and there is not data of spring temperature for samples AR4 and AR5, therefore it has been estimated.

#### 3.1. Field sampling

With respect to the water sampling conducted on October 2015, samples AR1 and AR2 were collected in two different springs, one inside the spa and the other in the natural pool outside. In both sampling points temperature, pH and conductivity were determined in situ. A Thermo Orion 250A portable pH-meter with combined pH electrode ORION 815600 Ross with temperature compensation was used together with a conductivitymeter Jenway 4200 with automatic correction of temperature.

Separated samples for cation, anion and isotopic analyses were taken. Samples for cation analyses were filtered through 0.1 µm and acidified with ultrapure HNO<sub>3</sub>. Then, they were stored in bottles that had been pre-washed with ultrapure HNO<sub>3</sub>, rinsed with distilled water and air-dried. The samples for <sup>13</sup>C isotope analysis were filtered through 0.1 µm, and were taken in small vials with mercury chloride to avoid the microbial activity. The samples for the analyses of <sup>18</sup>O and <sup>2</sup>H isotopes were filtered through 0.1 µm and those for <sup>34</sup>S isotopes and anions were taken without any special treatment.

#### 3.2. Analysis of the samples

Total alkalinity was measured in the laboratory only a few hours after the sampling. It was determined by titration with a Mettler titrator using H<sub>2</sub>SO<sub>4</sub> 0.02 N up to pH = 4.5 end point. The anions were analysed in 24 h after collection. Chloride and fluoride were determined by a selective ion analyser equipment, using the specific electrodes of chloride ORION 94-17B and fluoride ORION 94-09. Sulfate was determined by

colorimetry using a modification of the Nemeth method (Nemeth, 1963).

The cations and isotopes were analysed in the Scientific and Technological Centre at the University of Barcelona. The determination of Ca, Na, K, Mg, Sr and Si was performed by Inductively Coupled Plasma Emission Spectrometry (ICP-OES) with a Perkin Elmer Optima 3200rl equipment in standard conditions. The rest of the minor cations were analysed through Inductively Coupled Plasma Mass Spectrometry (ICP-MS) with an Agilent 7500ce equipment in standard conditions.

The isotopes, <sup>18</sup>O and <sup>2</sup>H in water, <sup>13</sup>C in DIC (dissolved inorganic carbon), and <sup>34</sup>S and <sup>18</sup>O in dissolved sulfates, were analysed by Continuous Flow Isotope-Ratio Mass Spectrometry (CF-IRMS) with a Delta plus xp Thermofisher equipment. The <sup>18</sup>O, <sup>2</sup>H, <sup>13</sup>C were directly analysed using the secondary standards traceable to certified standards: NBS18, NBS19, SMOW and SLAP. For the <sup>34</sup>S and <sup>18</sup>O measurement in dissolved sulfate this was precipitated as BaSO<sub>4</sub> (0.2 mg in silver capsule for oxygen and 0.3 mg in tin capsule for sulfur) and the secondary standards used were NBS-127, SO-5 and SO-6. The results of <sup>18</sup>O (both in water and in SO<sub>4</sub><sup>2-</sup>) and <sup>2</sup>H (in water) are expressed vs SMOW, <sup>34</sup>S (in SO<sub>4</sub><sup>2-</sup>) vs CDT and <sup>13</sup>C (in CO<sub>2</sub>) vs PDB.

#### 3.3. Geothermometry

Three methods have been used to determine the reservoir temperature: the chemical geothermometers, the isotopic geothermometers and the geothermometrical modelling. These techniques could be considered as complementary giving more accurate results when combined.

##### 3.3.1. Chemical geothermometers

Chemical geothermometry is the classical method used to calculate the temperature of a thermal water in the deep reservoir and it consists of the use of different empiric or experimental calibrations based on temperature dependent heterogeneous chemical reactions. The classical chemical geothermometers use the elemental contents controlled by those reactions to determine the reservoir temperature (e.g. Truesdell, 1976; Marini, 2004) assuming that these contents are representative of reservoir conditions and have not changed during the water ascent to the surface due to water-rock interactions.

There are many chemical geothermometers and calibrations, but not all are suitable for all types of geothermal systems. The classical chemical geothermometers SiO<sub>2</sub>-quartz, SiO<sub>2</sub>-chalcedony, Na-K, K-Mg and Na-K-Mg, with different calibrations, provide good results in high temperature (> 180 °C) systems hosted in rocks with feldspars and aluminosilicates with which the waters have reached the equilibrium (as previously indicated). Although these geothermometers are not expected to be suitable for low temperature and/or carbonate-evaporitic systems (as stated above) in some cases they provide consistent results and, therefore, they have been used in this study (Table 1).

The other chemical geothermometers that will be used here are the Ca-Mg and SO<sub>4</sub>-F geothermometers, firstly developed by Marini et al. (1986) and then improved by Chiodini et al. (1995). Although they were specifically calibrated for low temperature systems hosted in carbonate-evaporitic rocks (Table 1), they may also present problems. They are based on the assumption that in carbonate-evaporitic systems, calcite-dolomite and anhydrite-fluorite equilibria are likely to be attained and Ca/Mg and SO<sub>4</sub>/F ratios will be mainly controlled by temperature (Chiodini et al., 1995). However, the Ca-Mg geothermometer is affected by the order degree of dolomite, since its solubility depends on that and the SO<sub>4</sub>-F geothermometer is only valid if the waters have reached the equilibrium with anhydrite and fluorite, and fluorite is not always present in the carbonate-evaporitic rocks (Chiodini et al., 1995). These problems are taken into account and will be discussed further.

A final consideration when using the chemical geothermometers is that the elemental contents of the waters could be affected by

secondary processes like mixing or reequilibrium during their ascent to surface. However, the simultaneous application of several geothermometers, with different sensitivities to these secondary processes, will help to evaluate their effective presence in the thermal system (e.g. D'Amore and Arnórsson, 2000).

### 3.3.2. Isotopic geothermometers

The isotopic geothermometers are based on the fact that the isotope exchange is a function of temperature between two species which are assumed to be in isotopic equilibrium in the system. The isotopic geothermometers used in this study are the ones based on the  $\delta^{18}\text{O}$  exchange between waters and sulfate species or minerals (Table 2).

These geothermometers are suitable to predict the temperature of low temperature systems (D'Amore and Arnórsson, 2000) however, some problems may also arise. The traditional problem with the use of the  $\text{SO}_4\text{-H}_2\text{O}$  geothermometer is that the classical calibrations are

based on the  $\delta^{18}\text{O}$   $\text{HSO}_4\text{-H}_2\text{O}$  exchange and the  $\text{HSO}_4$  species is only present in acidic waters ( $\text{pH} < 4$ ), while in systems like the studied here the isotopic equilibrium is supposed to be controlled by the  $\delta^{18}\text{O}$   $\text{SO}_4^{2-}\text{-H}_2\text{O}$  (Boschetti, 2013). Therefore, some new calibrations for this geothermometer based on this last assumption will be used here (e.g. Halas and Pluta, 2000 or Zeebe, 2010). Finally, a third geothermometer recently proposed by Boschetti et al. (2011), based on the anhydrite- $\text{H}_2\text{O}$  exchange, will also be used as it provides good results in thermal waters in equilibrium with respect to anhydrite (e.g. Awaleh et al., 2015; Blasco et al., 2017; Boschetti, 2013).

### 3.3.3. Geothermometrical modelling

This method consists of simulating a progressive increase in the temperature of the waters and observe the variation of the saturation states with respect to a group of selected minerals (assumed to be in the reservoir) in order to find a point where the saturation states

**Table 1**  
Chemical geothermometers and calibrations used in this work. Concentration units for the elements involved are in mg/L except for the calibration proposed by Michard (1979) in which they are expressed in mol/L. Temperature is in °C.

Geothermometer	Calibration	Author
SiO <sub>2</sub> -quartz	$T = \frac{1315}{5.205 - \log(\text{SiO}_2)} - 273.15$	Truesdell (1976)
	$T = \frac{1309}{5.19 - \log(\text{SiO}_2)} - 273.15$	Fournier (1977)
	$T = \frac{1322}{0.435 - \log(\text{SiO}_2)} - 273.15$	Michard (1979)
SiO <sub>2</sub> -chalcedony	$T = \frac{1032}{4.69 - \log(\text{SiO}_2)} - 273.15$	Fournier (1977)
	$T = \frac{1112}{4.91 - \log(\text{SiO}_2)} - 273.15$	Arnórsson et al. (1983)
Na-K	$T = \frac{1390}{1.75 + \log(\text{Na}/\text{K})} - 273.15$	Giggenbach (1988)
	$T = \frac{1217}{1.483 + \log(\text{Na}/\text{K})} - 273.15$	Fournier (1979)
	$T = \frac{1289}{1.615 + \log(\text{Na}/\text{K})} - 273.15$	Verma and Santoyo (1997) <sup>a</sup>
K-Mg	$T = \frac{4410}{13.95 - \log\left(\frac{\text{K}^2}{\text{Mg}}\right)} - 273.15$	Giggenbach et al. (1983)
Na-K-Ca	$T = \frac{1647}{\log(\text{Na}/\text{K}) + \beta \left[ \log\left(\frac{\sqrt{\text{Ca}}}{\text{Na}}\right) + 2.06 \right] + 2.47} - 273.15$	Fournier and Truesdell (1973) <sup>b</sup>
Ca-Mg	$T = \frac{979.8}{3.1170 - \log\left(\frac{\text{Ca}}{\text{Mg}}\right) + 0.07003 \log \sum eq} - 273.15$	Chiodini et al. (1995) <sup>c</sup>
SO <sub>4</sub> -F	$T = \frac{1797.7}{0.7782 + \log\left(\frac{\text{SO}_4}{\text{F}^2}\right) - 0.08653 \log \sum eq} - 273.15$	Chiodini et al. (1995) <sup>c</sup>

<sup>a</sup> This is a modification of the previously proposed by Fournier (1979).

<sup>b</sup>  $\beta = 4/3$  should be used if the temperature obtained is lower than 100 °C; if with that value of  $\beta$  the temperature is higher than 100 °C, the temperature should be recalculated considering  $\beta = 1/3$ .  $\beta$  should also be taken to be 1/3 if  $\log(\text{Ca}^{0.5}/\text{Na}) + 2.06$  is negative.

<sup>c</sup>  $\sum eq$  is the summation (in eq/L) of the major dissolved species. Chiodini et al. (1995) performed their calibration for the Ca-Mg geothermometer by using a disordered dolomite.

**Table 2**Isotopic geothermometers and calibrations used in this work (" $\alpha_{A-B}$ " =  $(1000 + \delta^{18}\text{O}_A)/(1000 + \delta^{18}\text{O}_B)$ ). Temperature is in °C.

Geothermometer	Calibration	Author
SO <sub>4</sub> -H <sub>2</sub> O ( $\delta^{18}\text{O}_{\text{HSO}_4\text{-H}_2\text{O}}$ )	$T = \left( \sqrt{\frac{3.26 \cdot 10^6}{1000 \ln \alpha_{\text{HSO}_4^- \text{-H}_2\text{O}} + 5.81}} \right) - 273.15$	Seal et al. (2000) <sup>a</sup>
	$T = \left( \sqrt{\frac{3.251 \cdot 10^6}{1000 \ln \alpha_{\text{HSO}_4^- \text{-H}_2\text{O}} + 5.1}} \right) - 273.15$	Friedman and O'Neil (1977)
SO <sub>4</sub> -H <sub>2</sub> O ( $\delta^{18}\text{O}_{\text{SO}_4\text{-H}_2\text{O}}$ )	$T = \left( \sqrt{\frac{2.41 \cdot 10^6}{1000 \ln \alpha_{\text{SO}_4^{2-} \text{-H}_2\text{O}} + 5.77}} \right) - 273.15$	Halas and Pluta (2000)
	$T = \left( \sqrt{\frac{2.68 \cdot 10^6}{1000 \ln \alpha_{\text{SO}_4^{2-} \text{-H}_2\text{O}} + 7.45}} \right) - 273.15$	Zeebe (2010)
SO <sub>4</sub> -H <sub>2</sub> O ( $\delta^{18}\text{O}_{\text{CaSO}_4\text{-H}_2\text{O}}$ )	$T = \left( \sqrt{\frac{3.31 \cdot 10^6}{1000 \ln \alpha_{\text{CaSO}_4 \text{-H}_2\text{O}} + 4.69}} \right) - 273.15$	Boschetti et al. (2011) <sup>b</sup>

<sup>a</sup> This calibration is the combination of those of Lloyd (1968) and Mizutani and Rafter (1969).<sup>b</sup> This calibration is the combination of those of Chiba et al. (1981) and Zheng (1999).

simultaneously reach equilibrium indicating the reservoir temperature. The same assumption as in the previous methods has to be done: the thermal waters are in equilibrium with the reservoir materials and their elemental contents remain constant during the waters ascent, although the saturation state with respect to different minerals can change due to cooling and redistribution of the dissolved species.

This geothermometrical modelling has been carried out using the PHREEQC geochemical code (Parkhurst and Appelo, 2013) and the LLNL thermodynamic database (distributed with the code). A sensitivity analysis to the thermodynamic data was also performed by using the WATEQ4F thermodynamic database (also distributed with PHREEQC code).

The minerals presumably present in the reservoir and, therefore, considered in the modelling, have been inferred from the mineralogy of the aquifer formation. The aquifer is constituted by carbonate rocks which are in contact with the evaporitic Keuper facies, so, the evolution of the waters would be mainly controlled by calcite, dolomite and anhydrite. As the aquifer also contains terrigenous rocks, some silica and aluminosilicate phases have been included: quartz and chalcedony (as the usual silica controlling phases in thermal waters) and albite, K-feldspar and other aluminosilicates (smectite, illite, chlorite, kaolinite, etc.).

The solubility constants for calcite, chalcedony, quartz and anhydrite are reasonably well known, but there are other minerals with more uncertainties. The solubility of dolomite depends on its degree of order/disorder (Carpenter, 1980; Helgeson et al., 1978; Hyeong and Capuano, 2001; Reeder, 2000). For example, the dolomite considered when using the LLNL database is a completely disordered dolomite as it is usually done in other geothermometrical or geochemical studies in systems related to carbonate-evaporitic rocks (e.g. Blasco et al., 2017; Chiodini et al., 1995). However, the more plausible phase in natural groundwater systems is a more ordered dolomite (Carpenter, 1980; Helgeson et al., 1978; see below) and a partially-ordered dolomite (obtained from a set of water samples taken from gas and oil wells in the sediments of the Oligocene Frio Formation; Hyeong and Capuano, 2001) has been also considered in the sensitivity analysis performed with the WATEQ4F database (Ball and Nordstrom, 2001; see below).

There are also important uncertainties in the thermodynamic data of the aluminosilicate phases due to their degree of crystallinity and their compositional variability (e.g. Merino and Ramson, 1982; Nordstrom et al., 1990; Palandri and Reed, 2001). To reduce this uncertainty,

pyrophyllite, with better known thermodynamic data, has been selected as representative of these phases (as recommended by Helgeson et al., 1978; or Palandri and Reed, 2001). The sensitivity analysis performed with WATEQ4F database includes also the thermodynamic data for pyrophyllite, albite, K-feldspar and chalcedony taken from Michard (1983), which have been used previously in thermal systems obtaining very good results (e.g. Asta et al., 2012; Auqué et al., 1998; Michard and Roekens, 1983; Michard et al., 1989, 1986b).

## 4. Results

### 4.1. Chemical characteristics of the waters

Five water samples have been considered in this study: AR1, AR3 and AR5 (Table 3), taken in the spring inside the spa of Arnedillo and AR2 and AR4 (Table 3) taken in a natural pool built in the Cidacos River. The main chemical characteristics of the waters emerging inside the Arnedillo Spa seem to remain quite constant over time which suggests that they are not likely to be affected by mixing with surficial waters (or the influence of this process is negligible). However, in the case of the waters emerging in the natural pool it seems clear that they can be affected by different proportions of mixing with the cold waters from the Cidacos River.

All the waters are of sodium – chloride type and there are not great chemical differences among them. The pH value in all the samples is in the range of 6.60 to 7.05, except for the sample AR5 which shows a higher value due to the CO<sub>2</sub> outgassing prior to the pH determination in the laboratory (pH was determined in situ in the rest of the samples).

The spring temperature is about 45–50 °C except for the sample AR2 in which it is lower (39.5 °C), probably due to the mixing with the waters of the Cidacos river. Considering these two ranges of temperature and the location of the samples, the temperature value for samples AR4 and AR5, from the pool and the spa, respectively, (not measured) has been estimated as 40 and 48 °C, respectively (Table 3).

The TDS is in the range of 7300 to 7900 ppm in all the samples, except for AR4 in which it is somewhat lower, probably affected by the mixing with the waters of the river in a higher proportion than the other sample taken from the pool, AR2, whose TDS is in the same range as the rest of the samples. The Na/Cl ratios (near 1; Table 3) confirm that halite dissolution is the principal process responsible for the

**Table 3**  
Analytical data of the waters included in this study. TDS (calculated using PHREEQC) and dissolved elements are expressed in ppm and the isotopic contents in %.

	Sampling campaign 2015		Maraver Eyzaguirre (2003)	Coloma et al. (1997)	
	Spa	External pool	Spa	External pool	Spa
	AR1	AR2	AR3	AR4	AR5
Temp. (°C)	45.30	39.50	49.70	40 <sup>a</sup>	48 <sup>a</sup>
TDS	7720.9	7352.1	7912.7	6447.0	7276.5
pH	6.87	7.05	6.90	6.80	8.2
HCO <sub>3</sub> <sup>-</sup>	179.88	181.58	189.10	183.00	149.50
Cl <sup>-</sup>	3220.00	3030.00	3314.60	2556.00	2876.90
SO <sub>4</sub> <sup>-</sup>	1541.00	1537.00	1442.60	1385.30	1549.00
Ca	444.00	443.00	465.10	391.20	459.40
Mg	75.50	73.80	72.70	63.60	76.60
Na	2099.00	1941.00	2267.50	1720.20	2077.10
K	20.60	22.90	21.90	25.00	23.90
Sr	9.90	9.80			
F	2.36	2.30	2.30		
Al	0.0142	0.0643			
Li	0.2901	0.2708	0.60		
SiO <sub>2</sub>	30.87	29.10			
δ <sup>18</sup> O vs SMOW in (H <sub>2</sub> O)	-8.5	-8.8			
δ <sup>2</sup> H vs SMOW (H <sub>2</sub> O)	-65.3	-65.1			
δ <sup>18</sup> O vs SMOW in (SO <sub>4</sub> <sup>2-</sup> )	14.1	14			
δ <sup>34</sup> S vs CDT (in SO <sub>4</sub> <sup>2-</sup> )	14.8	14.8			
δ <sup>13</sup> C vs PDB (in CO <sub>2</sub> )	-4.16	-5.52			
Na/Cl	1.01	0.99	1.05	1.04	1.11
Ca/SO <sub>4</sub>	0.69	0.69	0.77	0.68	0.71
Ca + Mg/HCO <sub>3</sub> + SO <sub>4</sub>	0.81	0.81	0.86	0.76	0.83
% imbalance <sup>b</sup>	-2.41	-3.28	0.42	-2.31	2.72

<sup>a</sup> Estimated temperature.

<sup>b</sup> Imbalance expressed as  $\frac{\text{cations} - \text{anions}}{\text{cations} + \text{anions}} \cdot 100$  (cations and anions in eq.)

sodium – chloride character of these waters. The high dissolved SO<sub>4</sub> contents are consistent with the presence of anhydrite, or gypsum, in the aquifer and the intervention of them in the control of the dissolved SO<sub>4</sub> and Ca. The Ca/SO<sub>4</sub> ratio, lower than 1 (0.68–0.77; Table 3) is indicative of the removal of Ca from waters by other processes, probably carbonate precipitation. The Ca + Mg/HCO<sub>3</sub> + SO<sub>4</sub> ratio (in eq/L), with values near 1 (0.76–0.86), confirms these indications suggesting an important control of anhydrite, calcite and dolomite, although with the contribution of other processes.

There is isotopic information for the samples AR1 and AR2 with respect to <sup>13</sup>C (DIC), <sup>2</sup>H in the water, <sup>18</sup>O in water and in dissolved sulfates and <sup>34</sup>S in dissolved sulfates (Table 3). Only AR5 has a tritium value of 1.1 ± 2.5 TU (Coloma et al., 1997) which is very low compared to the mean tritium content in rainfall measured in the REVIP meteorological station of Zaragoza (the closet monitoring point to the recharge area) from 2000 to 2012 (about 5 TU; Lambán et al., 2015) and indicates that they were recharged before the thermonuclear testings in 1952 or that, at the most, they have been affected by a small proportion of mixing with recent waters (Clark and Fritz, 1997).

The δ<sup>18</sup>O – δ<sup>2</sup>H isotopic ratio for AR1 and AR2 indicates a meteoric origin for these waters since it is close to the Global Meteoric Water Line (δ<sup>2</sup>H = 8 · δ<sup>18</sup>O + 10; Craig, 1961; Fig. 3) and the Spanish Meteoric Water Line (δ<sup>2</sup>H = 8 · δ<sup>18</sup>O + 9.27; Díaz-Teijeiro et al., 2009; Fig. 3).

The δ<sup>13</sup>C values for AR1 and AR2 are -4.16‰ and -5.52‰, respectively. The δ<sup>13</sup>C of the dissolved inorganic carbon (DIC) in groundwaters is controlled by various carbon sources: 1) the organic matter and the concomitant biological degradation processes in the soils of the recharge area; and 2) the carbonate dissolution during the water circulation in the hydrological circuit. The contribution of the atmospheric CO<sub>2</sub> could be neglected (Mook and Tan, 1991). Most of the plants (about the 85%) on terrestrial ecosystems are of type C<sub>3</sub>, with a medium δ<sup>13</sup>C of about -27‰ (Clark and Fritz, 1997; Vogel, 1993). Nonetheless, some agricultural plants are of C<sub>4</sub> type (Clark and Fritz, 1997), with a mean δ<sup>13</sup>C value of -12.5‰ (Vogel, 1993), and they could also be present in the recharge area. The degradation of these plants results in δ<sup>13</sup>C values of the soils of about -23‰ in areas with C<sub>3</sub> plants and close to -9‰ when C<sub>4</sub> plants are present (Clark and Fritz, 1997). Finally, the δ<sup>13</sup>C in

carbonate minerals could be 0‰ (Clark and Fritz, 1997). Therefore, the δ<sup>13</sup>C values found in these thermal waters suggest that, after the recharge of the waters through the soils, their evolution has been highly influenced by the dissolution of carbonates.

Finally, the values of δ<sup>34</sup>S and δ<sup>18</sup>O in the dissolved sulfate are about 14.8‰ and 14‰, respectively, which are similar to the values reported for the Keuper rocks in this area, 13–15.5‰ for the δ<sup>34</sup>S, and 10.9–12.7‰ for the δ<sup>18</sup>O (Alonso-Azcárate et al., 2006), and in the Ebro Basin, 10.9–16.3‰ for the δ<sup>34</sup>S, and 8.9–14.9‰ for the δ<sup>18</sup>O (Utrilla et al., 1987), suggesting that these waters are in contact with the Keuper facies in the reservoir.

#### 4.2. Saturation indices

Most of the samples are in equilibrium or slightly oversaturated with respect to calcite, in equilibrium or close to equilibrium with respect to

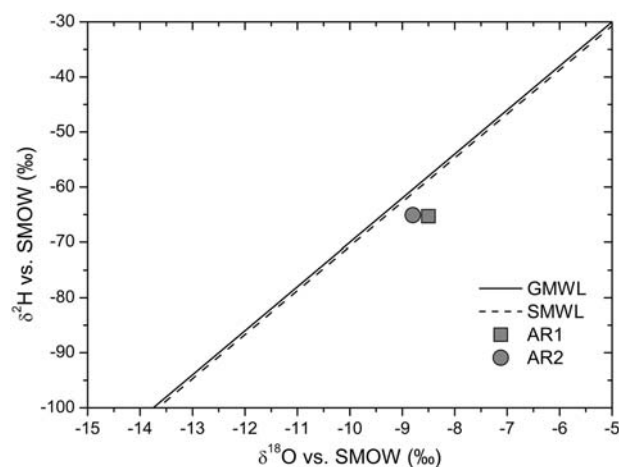


**Fig. 3.** δ<sup>2</sup>H–δ<sup>18</sup>O diagram showing the isotopic composition of samples AR1 and AR2. The Global Meteoric Water Line (GMWL) and the Spanish Meteoric Water Line (SMWL) are also represented.

strontianite and slightly undersaturated with respect to disordered dolomite (Table 4). Only the sample AR5, with the highest pH value (Table 3) is oversaturated with respect to dolomite. Considering that its  $p\text{CO}_2$  value is close to the atmosphere ( $\log p\text{CO}_2 = -3$ ) this behaviour is probably due to the  $\text{CO}_2$  outgassing of the waters after sampling and before measuring the pH in the laboratory.

All the waters are slightly undersaturated with respect to fluorite, anhydrite and gypsum and highly understaturated with respect to halite (Table 4). They are close to equilibrium with chalcedony and oversaturated with respect to quartz (Table 4).

Only samples AR1 and AR2 have aluminium data and the solubility results indicate that they are oversaturated with respect to albite, K-feldspar, and other aluminosilicates like kaolinite, pyrophyllite or laumontite (Table 4).

### 4.3. Geothermometrical results

#### 4.3.1. Chemical geothermometers

The results obtained by applying the selected chemical geothermometers and calibrations to the water samples are shown in Table 5.

The temperature predicted with the silica geothermometers for the samples AR1 and AR2 is about 80 °C with the  $\text{SiO}_2$ -quartz and 50 °C with  $\text{SiO}_2$ -chalcedony.

In order to check whether the use of the cationic geothermometers Na-K, K-Mg, and Na-K-Ca is adequate or not in this system the samples have been plotted in the Giggenbach diagram (Fig. 4). All of them fall in the partially equilibrated waters field and close to the fully equilibrated field, especially using the Fournier (1979) calibration for the Na-K geothermometer. This result indicates that consistent temperatures can be expected when using some of these geothermometers.

The temperatures obtained with the Na-K geothermometer vary depending on the sample and also the calibration considered. The highest results are obtained with the Giggenbach (1988) calibration and in sample AR4 (114 °C). The lowest temperature values are those obtained with the Fournier (1979) calibration in sample AR3 (75 °C). The rest of the values are all close to 90 or 95 °C. The Na-K-Ca geothermometer provides similar results to those obtained with the Na-K geothermometer, being around 90 °C for all the samples.

The temperature predicted with the K-Mg geothermometer is lower than the obtained with the Na-K one, ranging between 60 and 67 °C. This is probably due to secondary processes affecting the dissolved magnesium contents (D'Amore and Arnórsson, 2000) or simply because the phase used in the calibration of the geothermometers is not controlling the magnesium contents of these waters.

The Ca-Mg provides higher temperatures, about 115 °C which might be conditioned by the fact that this geothermometer is affected by the

**Table 4**

Saturation state of the waters with respect to the mineral phases considered in the study. These have been calculated at spring conditions with the LLNL database. Dolomite-dis is the fully disordered dolomite, and Albite-low is the low temperature albite.

	AR1	AR2	AR3	AR4	AR5
$p\text{CO}_2(\text{g})$	-1.60	-1.81	-1.58	-1.54	-3.00
Calcite	0.16	0.27	0.29	0.01	1.45
Dolomite-dis	-0.44	-0.28	-0.17	-0.81	2.15
Strontianite	0.09	0.25			
Anhydrite	-0.38	-0.42	-0.35	-0.47	-0.33
Gypsum	-0.39	-0.38	-0.40	-0.43	-0.37
Fluorite	-0.64	-0.62	-0.66		
Halite	-3.95	-4.00	-3.91	-4.12	-4.01
Quartz	0.39	0.45			
Chalcedony	0.13	0.19			
Albite_low	1.33	2.26			
K-Feldspar	1.81	2.90			
Kaolinite	3.51	5.05			
Pyrophyllite	2.84	4.46			
Laumontite	1.78	3.52			

**Table 5**

Temperatures (°C) obtained with several chemical and isotopic geothermometers and calibrations for the samples considered in the study.

Geothermometer	Calibration	AR1	AR2	AR3	AR4	AR5
$\text{SiO}_2$ -quartz	Truesdell, 1976	81	78			
	Fournier (1977)	80	78			
	Michard (1979)	82	80			
$\text{SiO}_2$ -chalcedony	Fournier (1977)	49	47			
	Arnórsson et al. (1983)	52	50			
Na-K	Giggenbach (1988)	97	105	96	114	107
	Fournier (1979)	75	84	75	93	83
	Verma and Santoyo (1997)	83	91	82	100	90
K-Mg	Giggenbach et al. (1983)	61	64	63	67	64
Na-K-Ca	Fournier and Truesdell (1973)	88	91	90	96	92
Ca-Mg	Chiodini et al. (1995)	116	117	114	112	108
$\text{SO}_4$ -F	Chiodini et al. (1995)	-11	-11	-10		
$\text{SO}_4$ - $\text{H}_2\text{O}$	Seal et al. (2000)	66	64			
$(\delta^{18}\text{O}_{\text{HSO}_4\text{-H}_2\text{O}})$	Friedman and O'Neil (1977)	69	68			
$\text{SO}_4$ - $\text{H}_2\text{O}$	Halas and Pluta (2000)	18	17			
$(\delta^{18}\text{O}_{\text{SO}_4\text{-H}_2\text{O}})$	Zeebe (2010)	25	25			
$\text{SO}_4$ - $\text{H}_2\text{O}$	Boschetti et al. (2011)	75	74			
$(\delta^{18}\text{O}_{\text{CaSO}_4\text{-H}_2\text{O}})$						

degree of order of dolomite in equilibrium with the waters (see below). The  $\text{SO}_4$ -F geothermometer gives incoherent results indicating that it is not applicable in this system probably because fluorite is not likely to be in the reservoir in enough amounts to control the contents of the waters (see Table 5).

The temperatures obtained for all the samples are similar and the most reasonable results are those from  $\text{SiO}_2$ -quartz, Na-K and Na-K-Ca geothermometers. The temperature at depth is  $87 \pm 12$  °C, which is within the uncertainty range usually accepted in geothermometrical calculations ( $\pm 20$  °C; Fournier, 1982). In any case, these results will be integrated with the other geothermometrical techniques.

#### 4.3.2. Isotopic geothermometers

The temperature predicted by the geothermometer  $\delta^{18}\text{O}$   $\text{SO}_4$ - $\text{H}_2\text{O}$  is similar for the two samples with isotopic data (Table 5 and Fig. 5). However, the results depend on the calibration considered:

1. The calibration proposed by Boschetti et al. (2011), based on the equilibrium exchange between anhydrite ( $\text{CaSO}_4$ ) and  $\text{H}_2\text{O}$  is the most reliable for these waters as it is adequate for systems oversaturated or in equilibrium with anhydrite (e.g. Awaleh et al., 2015; Boschetti, 2013; Boschetti et al., 2011), which is the case in

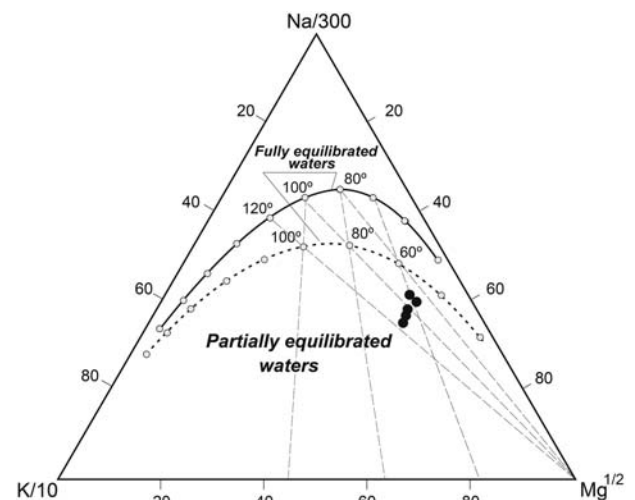


**Fig. 4.** Location of all the samples in the Giggenbach diagram. The dotted line is calculated with the Na-K Fournier (1979) calibration and with the Giggenbach (1988) one for Mg-K; the solid line is calculated with Na-K and Mg-K calibrations of Giggenbach (1988).

Arnedillo (see below). The temperature values predicted are around 75 °C in both samples.

- Although the  $\text{HSO}_4^-$  species is not expected to control the equilibrium in a neutral system like Arnedillo, two calibrations based on the equilibrium exchange between  $\text{HSO}_4^-$  and  $\text{H}_2\text{O}$  have been used. The calibration of Seal et al. (2000) provides temperatures of about 65 °C and the calibration of Friedman and O'Neil (1977) a temperature close to 69 °C. These temperatures coincide with the rest of the results and the reason for that (even not being the dominant species) is shown in Fig. 5: the calibrations based on this exchange are quite close to the one based on the  $\text{CaSO}_4$ - $\text{H}_2\text{O}$  exchange for neutral water.
- Finally, using the calibrations based on the equilibrium exchange between the  $\text{SO}_4$  and  $\text{H}_2\text{O}$  the temperatures obtained are considered incoherent since they are about 20 °C, below the emergence temperature of the thermal waters. This can be due to the slow process of  $^{18}\text{O}$  exchange between  $\text{SO}_4^{2-}$  and  $\text{H}_2\text{O}$  in low temperature systems preventing the equilibrium between  $\text{SO}_4^{2-}$  and  $\text{H}_2\text{O}$  to be attained (Boschetti et al., 2011).

#### 4.3.3. Geothermometrical modelling

Samples AR1 and AR2, with the more complete chemical analysis, have been selected to perform the geothermometrical modelling as the results from the chemical geothermometers have been similar for all the samples.

Using the LLNL thermodynamic database the results show that calcite, dolomite (disordered-dolomite) and chalcedony reach equilibrium at lower temperature than the rest of the phases (Fig. 6). While most of the minerals predict temperatures of about 80–95 °C, chalcedony reaches equilibrium at 65 °C, dolomite at 50 °C in AR1 and 60 °C in AR2, and calcite even at lower temperature.

The lower temperature predicted by chalcedony was also found with the  $\text{SiO}_2$ -chalcedony chemical geothermometer, while the results obtained for quartz (the equilibrium temperature and the  $\text{SiO}_2$ -quartz geothermometer) are more reasonable and in agreement with the rest of the minerals. These results indicate that the phase controlling the silica equilibrium in this system is quartz and no chalcedony.

Calcite and dolomite are expected to be in equilibrium with the reservoir waters in systems hosted in carbonate rocks and, therefore, the fact that the equilibrium temperature predicted for them is too low can be the result of a  $\text{CO}_2$  outgassing process during the ascent of the

waters to surface, since the  $p\text{CO}_2$  of the waters (between –1.8 and –1.3) is much higher than the atmosphere. A theoretical reconstruction of the characteristics in the reservoir was simulated to check this assumption. Following the recommendations from Pang and Reed (1998) and Palandri and Reed (2001), the  $\text{CO}_2$  content of the waters was increased in the simulation up to a value that made the carbonate phases (mainly calcite since it is less affected by uncertainties in the thermodynamic data) reach equilibrium in a temperature range similar to the rest of the phases. In this case the equilibrium temperature of calcite was adjusted to 87 °C (deduced with the chemical geothermometers and in agreement with the rest of the minerals) by adding between 1.56 and 2.27 mmol/L of  $\text{CO}_2$  to the waters.

In Fig. 7 and Table 6 the results obtained in the geothermometrical modelling after the  $\text{CO}_2$  reconstruction are shown. The modelling was performed with the LLNL and the WATEQ4F thermodynamic databases to evaluate the problems related with the uncertainties in the thermodynamic data and to determine an uncertainty range for the results.

The results obtained for each sample with the two databases are similar and they reach equilibrium at a temperature around 90 °C. A reliable range of  $93 \pm 14$  °C for the temperature in the reservoir could be proposed from the modelling results, which is in the accepted uncertainty range ( $\pm 20$  °C; Tole et al., 1993).

## 5. Discussion

Overall, the results presented in the previous section show a remarkable degree of coincidence in the results obtained with the different geothermometrical methodologies. Some of these results are coherent with the mineral equilibria expected in reservoirs of systems hosted in carbonate-evaporitic rocks and, therefore, are highly reliable. However, the good results obtained with the cationic geothermometers (mainly the Na-K) are unusual in this type of systems. Finally, other geothermometers as the Ca-Mg (or the calcite – dolomite equilibrium in which it is based), a priori well suited for these systems, display different type of problems. These aspects are discussed below.

Anhydrite and quartz (or chalcedony) equilibrium have been considered highly reliable in geothermometrical calculations (e.g. Alçiçek et al., 2016; Kharaka and Mariner, 1989; Levet et al., 2002; Pastorelli et al., 1999) since their thermodynamic data are quite well-known, their saturation states are not affected by pH variations during the ascent of thermal waters and they display different thermodynamic behaviour (retrograde and prograde solubility, respectively; e.g. Alçiçek et al., 2016 or Levet et al., 2002). Therefore, the good agreement in the temperatures predicted by these phases (80 to 90 °C with LLNL and 87 to 97 °C with WATEQ4F; Fig. 7 and Table 6) in the modelling and with the results of the  $\text{SiO}_2$ -quartz geothermometer (Table 5) reinforces the reliability of the results as reservoir temperature. The results obtained with the isotopic geothermometer  $\delta^{18}\text{O}$   $\text{SO}_4^{2-}$ - $\text{H}_2\text{O}$  with the  $\text{CaSO}_4$  calibration agree with the anhydrite equilibrium in the reservoir and provides a very similar temperature, which supports the findings by Awaleh et al. (2015), Boschetti (2013) or Boschetti et al. (2011) and the reliability of this new isotopic calibration.

Although usually inappropriate in low temperature and carbonate-evaporitic systems, the cationic geothermometers (mainly the Na-K) have provided reasonable results. They are also consistent with those obtained from the modelling which show that the waters have reached the equilibrium with albite and K-feldspar (Fig. 7 and Table 6). This equilibrium situation has also been identified in the Giggenbach diagram (Fig. 2) where these waters fall close to the field of the fully equilibrated waters. The explanation to this unusual situation could be the presence of some detrital material in the aquifer, as found in other studies (e.g. Blasco et al., 2017; Boschetti et al., 2005; López-Chicano et al., 2001), which allows the waters attaining the equilibrium with aluminosilicates.

In summary, the integration of the results obtained with the several geothermometrical techniques, excluding the less reliable results

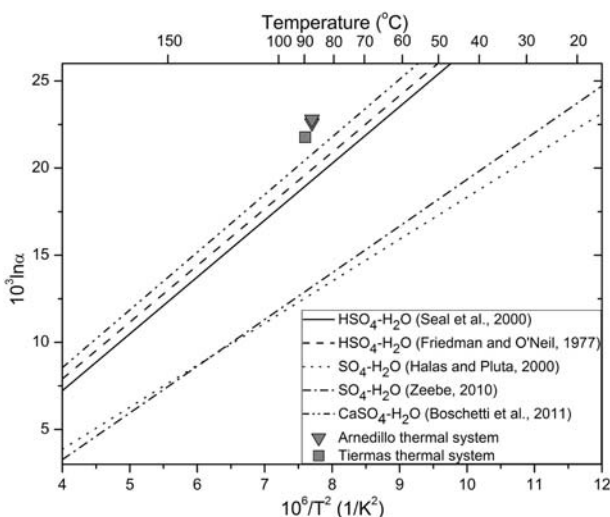


**Fig. 5.** Sulfate – water oxygen isotope fractionation ( $10^3 \ln \alpha = 10^3 \ln[(1000 + \delta^{18}\text{O}_{\text{sulphate}}) / (1000 + \delta^{18}\text{O}_{\text{H}_2\text{O}})]$ ) versus temperature for the Arnedillo thermal waters (AR1 and AR2) and considering the different calibrations. A sample from other low temperature carbonate-evaporitic system, hosted in Paleocene-Eocene carbonates in the pre-Pyrenees, the Tiermas thermal system, also in equilibrium with anhydrite, has also been plotted for comparative purposes (Blasco et al., 2017). The temperature considered for the samples has been the temperature deduced from the rest of geothermometrical techniques used.

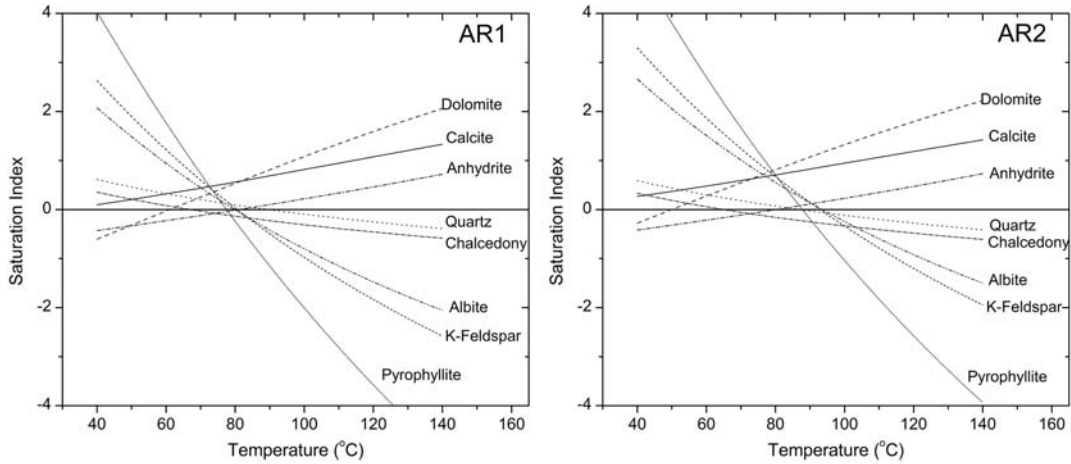


**Fig. 6.** Evolution with temperature of the saturation indices of the minerals supposed to be in equilibrium with the water samples AR1 and AR2 in the reservoir. This calculation has been performed by using the LLNL thermodynamic database and prior to the reconstruction of the reservoir characteristics. The dolomite used is the disordered dolomite and the albite is the low temperature albite.

discussed along this work, allow determining that the temperature range for the Arnedillo thermal waters in the reservoir is  $87 \pm 13$  °C. Moreover, the good convergence of the saturation index of the considered mineral phases in the line of  $SI = 0$  (Fig. 7) indicates that these thermal waters have not been affected by a significant mixing process. A mixing process would modify the temperature results since the

convergence point would be shifted to undersaturated values (Pang and Reed, 1998).

The depth of the reservoir of these thermal waters can be approximated using the temperature estimated for them. Assuming that the thermal gradient in the Cameros Range is  $18$  °C/km (as determined in the Castilfrío oil well; Fig. 1; Fernández et al., 1998), and the mean

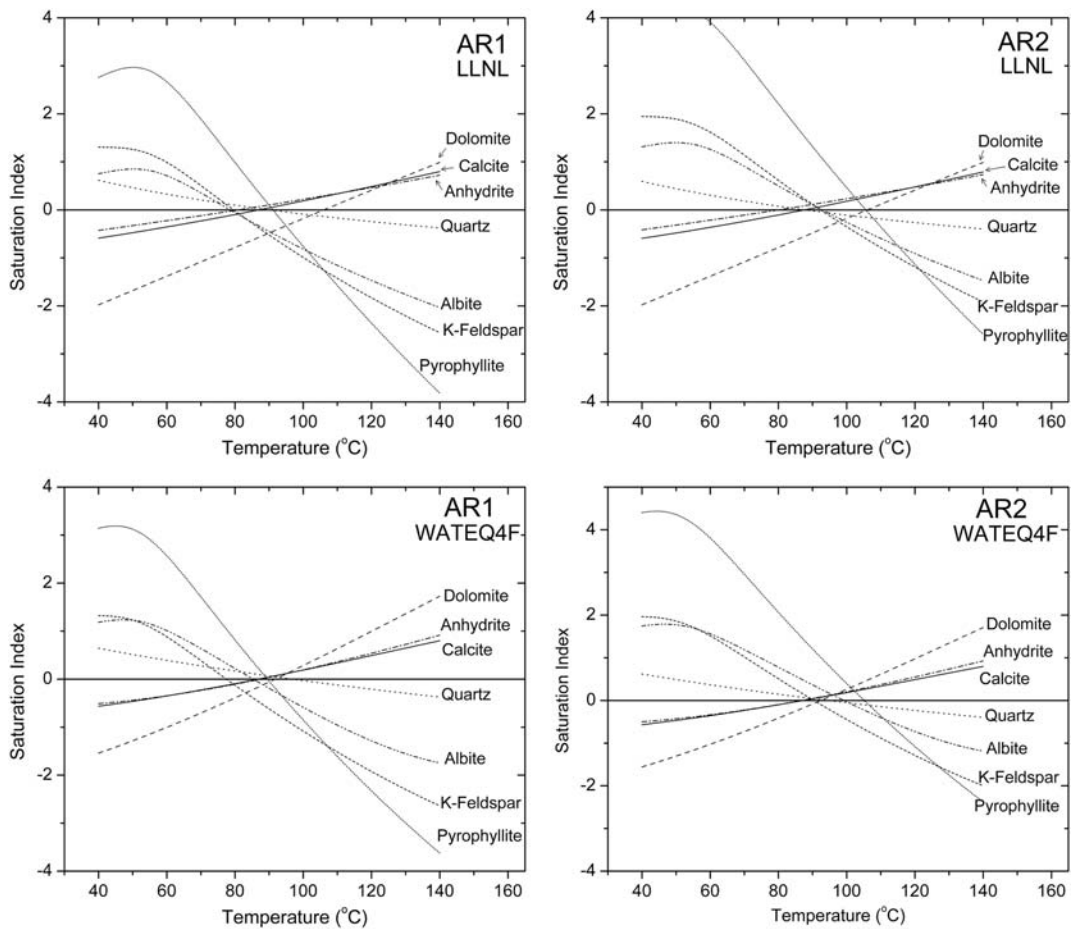


**Fig. 7.** Evolution with temperature of the saturation indices of the minerals supposed to be in equilibrium with the water samples AR1 and AR2 after the reconstruction of the reservoir characteristics by adding  $CO_2$ . The results obtained with two different thermodynamic databases, LLNL and WATEQ4F, are shown. In the case of the LLNL database the disordered dolomite and low temperature albite have been used. In the case of the WATEQ4F the thermodynamic data for the partially ordered dolomite from Hyeong and Capuano (2001) and albite, K-feldspar and pyrophyllite from Michard (1983) have been added to the database.



**Table 6**

Temperatures (°C) at which the mineral phases considered reach equilibrium in the samples AR1 and AR2 and calculated with the LLNL and WATEQ4F databases. In the case of the LLNL database, the dolomite and albite considered are the fully disordered dolomite and the low temperature albite, respectively. In the case of the WATEQ4F, the thermodynamic data correspond to the dolomite deduced by Hyeong and Capuano (2001) and the albite, K-feldspar and pyrophyllite have been taken from Michard (1983).

Mineral phase	AR1		AR2	
	LLNL	WATEQ4F	LLNL	WATEQ4F
Calcite	87	87	87	87
Dolomite	106	92	107	92
Quartz	90	97	88	94
Anhydrite	81	88	80	87
Albite	79	85	94	99
K-feldspar	80	78	93	91
Pyrophyllite	91	90	106	106

surface temperature in Spain is 16 °C (Chamorro et al., 2014), the reservoir should be located at about 4000 m depth, coincident with the depth of the Jurassic rocks that constitute the aquifer of these waters (Fig. 2). Overall, this result reinforces the reliability of the geothermometrical results.

Finally, as mentioned at the beginning of this discussion, some comments are needed with respect to the problems associated to the calcite-dolomite equilibrium. This equilibrium is expected to be attained by the waters at depth in systems hosted in carbonate rocks (like the one studied here) due to the high temperatures and the long residence time. However, this equilibrium is not always easy to verify in geothermometrical modelling due to the outgassing of the waters and the subsequent modification of the saturation states of carbonate phases (as shown in Section 4.3.3). An additional complication is that, while the thermodynamic data of calcite are quite well defined, the dolomite solubility is conditioned by its degree of order which in the end affects the equilibrium temperature of this phase (e.g. Frondini, 2008; Hyeong and Capuano, 2001; Vespasiano et al., 2014).

The results found for the Arnedillo system indicate that the temperature obtained for the fully disordered dolomite used in the LLNL database is too high with respect to the one obtained with calcite (Table 6) while the partially-ordered dolomite proposed by Hyeong and Capuano (2001) and introduced in the WATEQ4F database (calculated to be 11% of ordered dolomite, see below) gives a more similar temperature although still a few degrees higher (Table 6). The influence of the order degree of dolomite in geothermometrical calculations is evident and the results suggest that the dolomite in the Arnedillo reservoir should be of higher order degree than the dolomites used in the modelling.

To delimit this issue some additional calculations on the order of the dolomite have been done as proposed by Vespasiano et al. (2014) for aquifers in dolomitic rocks affected by metamorphism. In this case, assuming that dolomite should be in equilibrium with calcite at 87 °C in the Arnedillo aquifer, the corresponding degree of order has been determined. From the results obtained in the speciation – solubility calculations, a  $\log K = 1.1237$  (for the dissolution reaction:  $\text{CaMg}(\text{CO}_3)_2 + 2\text{H}^+ = \text{Ca}^{2+} + \text{Mg}^{2+} + 2\text{HCO}_3^-$ ) has been calculated for the dolomite at 87 °C. This  $\log K$  yields the Gibbs free energy of the reaction (Eq. (1)). With that value and with the Gibbs free energy of formation of the species ( $\text{Ca}^{2+}$ ,  $\text{Mg}^{2+}$  and  $\text{HCO}_3^-$ ), the Gibbs free energy of formation ( $\Delta G_f$ ) for the dolomite at 87 °C can be obtained (Eq. (2)):

$$\log K = \frac{-\Delta G_R}{2.303RT} \quad (1)$$

<sup>1</sup> The values of  $\Delta G_f$  of the different species needed to calculate the  $\Delta G_f$  of the dolomite in the Arnedillo system and the values of  $\Delta G_{f,ord}$  and  $\Delta G_{f,dis}$  at the temperature of interest, have been obtained from <http://geopig3.la.asu.edu:8080/GEOPIG/pigopt1.html>

$$\Delta G_R = \sum \Delta G_{f,products} - \sum \Delta G_{f,reactants} \quad (2)$$

where R is the constant of the ideal gases and T the temperature in K. The value obtained is  $\Delta G_{f,Arn} = -519.06$  Kcal. Knowing the  $\Delta G_f$  value for the ordered dolomite ( $\Delta G_{f,ord} = -520.298$  Kcal)<sup>1</sup> and the disordered dolomite ( $\Delta G_{f,dis} = -518.362$  Kcal)<sup>1</sup> (all at 87 °C), the proportion of order and disorder dolomite present in the dolomite from Arnedillo can be determined using the following equation (Anderson and Crerar, 1993):

$$\Delta G_{f,Arn} = X_{ord} \cdot \Delta G_{f,ord} + X_{dis} \cdot \Delta G_{f,dis} + RT(X_{ord} \cdot \ln X_{ord} + X_{dis} \cdot \ln X_{dis}) \quad (3)$$

where  $X_{ord}$  is the molar ratio of the ordered dolomite and  $X_{dis}$  the molar ratio of the disordered dolomite.

The result is that the dolomite present in the aquifer of the Arnedillo thermal system is constituted by 18.4% of ordered dolomite and 81.6% of disordered dolomite, which is a partially-disordered dolomite but with a higher order degree than the dolomite obtained by Hyeong and Capuano (2001). This is consistent with the interpretation done from the results of the geothermometrical modelling.

Going a step forward, from the values of order and disorder obtained and using the Eq. (3), the  $\Delta G_{f,Arn}$ , and therefore the  $\log K$ , at different temperatures can also be calculated (Eqs. (2) and (1)). The results at standard conditions (25 °C) for the  $\log K$  of the Arnedillo dolomite is 3.55 for the dissolution reaction  $\text{CaMg}(\text{CO}_3)_2 + 2\text{H}^+ = \text{Ca}^{2+} + \text{Mg}^{2+} + 2\text{HCO}_3^-$ . The corresponding values for the ordered and disordered dolomite are 4.01 and 2.61, respectively.

Fig. 8 shows the calcite/dolomite equilibria in a  $\log(a\text{Ca}^{2+}/a\text{Mg}^{2+})$  vs temperature plot for different dolomites: the fully ordered and fully disordered dolomites, the Arnedillo dolomite and some other partially-ordered dolomites from the literature deduced from natural systems as there are no experimental data for dolomites of intermediate order. The fully ordered and fully disordered dolomites have been taken from the LLNL thermodynamic database. Data from natural groundwater systems from studies where calcite-dolomite equilibrium has been verified in a wide range of temperatures have also been included. Hyeong and Capuano (2001) studied the equilibrium situation between calcite and dolomite in the groundwaters of the Oligocene Frio Formation in the Texas Gulf Coast, between 40 and 150 °C, and the order has been calculated to be 11%. Busby et al. (1991) also studied the calcite-dolomite equilibrium in the groundwaters of the Carboniferous Madison Aquifer, between 10 and 100 °C, and the order has been calculated to be 23.5%. Finally, data from Vespasiano et al. (2014) corresponding to a dolomite in the Triassic rocks affected by a low-grade metamorphism in Calabria (Italy) have also been included (order of 22%).

The  $\log(a\text{Ca}^{2+}/a\text{Mg}^{2+})$  for the different dolomites at different temperatures has been calculated from the  $\log K$  at those temperatures and using the Eq. (4) (the calcite data was taken from the LLNL thermodynamic database).

$$\log\left(\frac{a\text{Ca}^{2+}}{a\text{Mg}^{2+}}\right) = 2 \cdot \log K_{calcite} - \log K_{dolomite} \quad (4)$$

The comparison shown in Fig. 8 evidences the great importance of the order/disorder degree of dolomite in the geothermometrical determinations as small changes can yield to representative differences in the equilibrium temperature of this phase.

The problem stands on the difficulties to know the order degree of the dolomite present in a specific aquifer since in groundwater systems hosted in sedimentary rocks calcite-dolomite equilibrium usually involve Ca- or Fe-rich partially ordered dolomites (Carpenter, 1980; Helgeson et al., 1978; Hyeong and Capuano, 2001; Land, 1985; Reeder, 2000) that remain with variable disorder degree for hundreds of millions of years of burial diagenesis (Kaczmarek and Duncan, 2011;

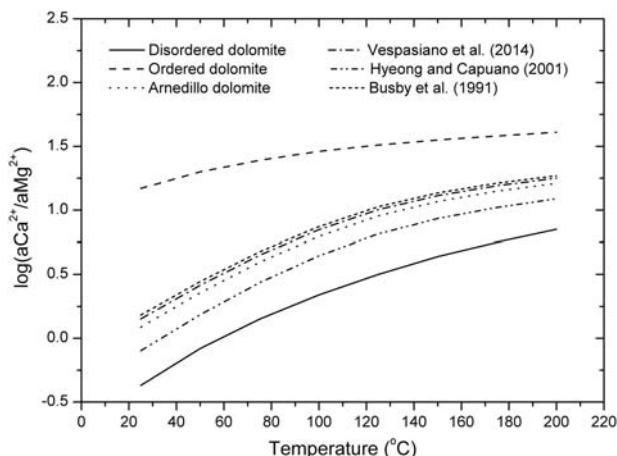


**Fig. 8.** Log ( $a\text{Ca}^{2+}/a\text{Mg}^{2+}$ ) vs temperature for different data of calcite/dolomite equilibria considering different degrees of order for dolomite.

Lumsden and Chimahusky, 1980; Sperber et al., 1984). Therefore this type of calculations is not only useful in dolomitic aquifers affected by metamorphism (as applied by Vespasiano et al., 2014) but also in sedimentary/diagenetic carbonate or carbonate-evaporitic aquifers.

In summary, with respect to the calcite-dolomite equilibrium uncertainties, it is important to keep in mind that although the consideration of the fully disordered dolomite will provide, at least, a maximum temperature for the waters in the deep reservoir, a careful approach, like the one done in this work, is needed to interpret and improve the results of the geothermometrical calculations based on the calcite-dolomite equilibria.

## 6. Conclusion

In this study a multi-technique approach to determine the temperature in the reservoir of carbonate-evaporitic and low temperature thermal systems is applied to a study case in La Rioja (Spain). This methodology and its application to a specific case has resulted to be very helpful to deal with some of the problems that the geothermometrical calculations present in this kind of systems.

The integration of the results obtained with chemical geothermometers, isotopic geothermometers and geochemical modelling has given a reservoir temperature for the Arnedillo thermal system of  $87 \pm 13$  °C. At this temperature the waters are in equilibrium with respect to calcite, dolomite, anhydrite, quartz, albite, K-feldspar and other aluminosilicates. Considering the geothermal gradient in the studied area, the approximate depth of the reservoir seems to be at about 4000 m depth, which is coincident with the depth of the suggested aquifer formations.

It is also remarkable the coherent results obtained with the Na-K geothermometer since it is considered inadequate for this type of systems. However the presence of a significant amount of detrital material in the carbonate aquifer seems to be enough to allow the water reaching the equilibrium with respect the phases in which it is based (albite and K-feldspar).

Finally, the effects of the thermodynamic uncertainties related to dolomite have been evaluated and the order degree of the dolomite present in the reservoir of the Arnedillo thermal waters has been determined, resulting in 18.4% of ordered dolomite and 81.6% of disordered dolomite, with a log  $K = 3.55$  at standard conditions (for the reaction  $\text{CaMg}(\text{CO}_3)_2 + 2\text{H}^+ = \text{Ca}^{2+} + \text{Mg}^{2+} + 2\text{HCO}_3^-$ ).

The need of this kind of calculations and of the integration of all the geothermometrical techniques is proposed here as a methodological procedure to be used in similar kind of studies.

## Acknowledgement

M. Blasco has worked in this study thanks to a scholarship from the Ministry of Education, Culture and Sports of Spain, for the Training of University Teachers (ref. FPU14/01523). This study forms part of the activities of the Geochemical Modelling Group (University of Zaragoza; Aragón Government).

We thank the staff of the Arnedillo spa for allowing us to sample and their help during the sampling campaign. We are also grateful to Giovanni Vespasiano for his guidelines in the thermodynamic calculations. The technical assistance of Enrique Oliver, from the Earth Science Department of the University of Zaragoza, is also thankful. The comments of two anonymous reviewers are gratefully acknowledged.

## References

- Alçiçek, H., Bülbül, A., Alçiçek, M.C., 2016. Hydrogeochemistry of the thermal waters from the Yenice Geot Field (Denizli Basin, Southwestern Anatolia, Turkey). *J. Volcanol. Geotherm. Res.* 309, 118–138.
- Alonso-Azcárate, J., Bottrell, S.H., Mas, J.R., 2006. Synsedimentary versus metamorphic control of S, O and Sr isotopic compositions in gypsum evaporites from the Cameros Basin, Spain. *Chem. Geol.* 234, 46–57.
- Anderson, G.M., Crerar, D.A., 1993. Thermodynamics in geochemistry. The Equilibrium Model. Oxford University Press, Oxford.
- Apollaro, C., Dotsika, E., Marini, L., Barca, D., Bloise, A., de Rosa, R., Doveri, M., Lelli, M., Muto, F., 2012. Chemical and isotopic characterization of the thermomineral water of Terme Sibarite springs (Northern Calabria, Italy). *Geochim. J.* 46, 117–129.
- Arnórsson, S., Gunnlaugsson, E., Svavarsson, H., 1983. The chemistry of geothermal waters in Iceland. III. Chemical geothermometry in geothermal investigations. *Geochim. Cosmochim. Acta* 47, 567–577.
- Asta, M.P., Gimeno, M.J., Auqué, L.F., Gómez, J., Acero, P., Lapuente, P., 2010. Secondary processes determining the pH of alkaline waters in crystalline rock systems. *Chem. Geol.* 273, 41–52.
- Asta, M.P., Gimeno, M.J., Auqué, L.F., Gómez, J., Acero, P., Lapuente, P., 2012. Hydrochemistry and geothermometrical modeling of low-temperature Panticosa geothermal system (Spain). *J. Volcanol. Geotherm. Res.* 235–236, 84–95.
- Auqué, L.F., Mandado, J., López, P.L., Lapuente, P.L., Gimeno, M.J., 1997. Los sistemas geotermiales del Pirineo Central. II. Resultados de la aplicación de técnicas geotermométricas. *Estud. Geol.* 53, 45–54.
- Auqué, L.F., Mandado, J., López, P.L., Lapuente, P.L., Gimeno, M.J., 1998. Los sistemas geotermiales del Pirineo Central. III. Evaluación de las condiciones en profundidad y evolución de las soluciones hidrotermales durante su ascenso. *Estud. Geol.* 54, 25–37.
- Auqué, L.F., Acero, P., Gimeno, M.J., Gómez, J.B., Asta, M.P., 2009. Hydrogeochemical modeling of a thermal system and lessons learned for CO<sub>2</sub> geologic storage. *Chem. Geol.* 268, 324–336.
- Awaleh, M.O., Hoch, F.B., Boschetti, T., Soubaneh, Y.D., Egueh, N.M., Elmi, S.K., Mohamed, J., Khaireh, M.A., 2015. The geothermal resources of the Republic of Djibouti – II: geochemical study of the Lake Abhe geothermal field. *J. Geochem. Explor.* 159, 129–147.
- Ball, J.W., Nordstrom, D., 2001. User's manual for WATEQ4F with revised thermodynamic database and test cases for calculating speciation of major, trace and redox elements in natural waters. In: U.S. Geological Survey (Ed.), Water-Resources Investigation Report. U.S. Geological Survey, Menlo Park (California), pp. 91–183.
- Blasco, M., Auqué, L.F., Gimeno, M.J., Acero, P., Asta, M.P., 2017. Geochemistry, geothermometry and influence of the concentration of mobile elements in the chemical characteristics of carbonate-evaporitic thermal systems. The case of the Tiermas geothermal system (Spain). *Chem. Geol.* 466, 696–709.
- Boschetti, T., 2013. Oxygen isotope equilibrium in sulfate-water systems: a revision of geothermometric applications in low-enthalpy systems. *J. Geochem. Explor.* 124, 92–100.
- Boschetti, T., Giampiero, V., Toscani, L., Barbieri, M., Mucchino, C., 2005. The Bagni di Lucca thermal waters (Tuscany, Italy): an example of Ca-SO<sub>4</sub> waters with high Na/Cl and low Ca/SO<sub>4</sub> ratios. *J. Hydrol.* 307, 273–293.
- Boschetti, T., Cortecchi, G., Toscani, L., Iacumin, P., 2011. Sulfur and oxygen isotope compositions of Upper Triassic sulfates from northern Apennines (Italy): paleogeographic and hydrogeochemical implications. *Geol. Acta* 9, 129–147.
- Buil, B., Gómez, P., Turrero, M.J., Garralón, A., Lago, M., Arranz, E., de la Cruz, B., 2006. Factors that control the geochemical evolution of hydrothermal systems of alkaline water in granites in Central Pyrenees (Spain). *J. Iber. Geol.* 32, 283–302.
- Busby, J.F., Plummer, L.N., Lee, R.W., Hanshaw, B.B., 1991. Geochemical Evolution of Water in the Madison Aquifer in Parts of Montana, South Dakota, and Wyoming, in: U.S. Geological Survey Professional Paper 1273-F. United States Government Printing Office, Washington, p. 89.
- Carpenter, A.B., 1980. The chemistry of dolomite formation I: the stability of dolomite. In: Zenger, D.H., Dunham, J.B., Ethington, R.L. (Eds.), Concepts and Models of Dolomitization. Society of Economic Paleontologists and Mineralogists Spec. Publ. Vol. 28, pp. 111–121.
- Chamorro, C.R., García-Cuesta, J.L., Mondéjar, M.E., Linares, M.M., 2014. An estimation of the enhanced geothermal systems potential for the Iberian Peninsula. *Renew. Energy* 66, 1–14.

- Chiba, H., Kusakabe, M., Hirano, S.I., Matsuo, S., Somiya, A., 1981. Oxygen isotope fractionation factors between anhydrite and water from 100 to 550 °C. *Earth Planet. Sci. Lett.* 53, 55–62.
- Chiodini, G., Frondini, F., Marini, L., 1995. Theoretical geothermometers and pCO<sub>2</sub> indicators for aqueous solutions coming from hydrothermal systems of medium-low temperature hosted in carbonate-evaporite rocks. Application to the thermal springs of the Etruscan Swell, Italy. *Appl. Geochem.* 10, 337–346.
- Choi, H.S., Koh, Y.K., Bae, D.K., Park, S.S., Hutcheon, I., Yun, S.T., 2005. Estimation of deep-reservoir temperature of CO<sub>2</sub>-rich springs in Kangwon district, South Korea. *J. Volcanol. Geotherm. Res.* 141, 77–89.
- Clark, I., Fritz, P., 1997. *Environmental Isotopes in Hydrogeology*. CRC Press/Lewis Publishers, Boca-Raton (Florida).
- Coloma, P., 1998. El agua subterránea en La Rioja. *Zubía Monográfico* 10, 63–132.
- Coloma, P., Sánchez, J.A., Martínez, F.J., 1995. El drenaje subterráneo de la cordillera Ibérica en la depresión terciaria del Ebro (sector Riojano). *Geogaceta* 17, 68–71.
- Coloma, P., Sánchez, J.A., Martínez, F.J., 1996. Procesos geotérmicos causados por la circulación del agua subterránea en el contacto entre la Sierra de Cameros y la Depresión Terciaria del Ebro. *Geogaceta* 20, 749–753.
- Coloma, P., Sánchez, J.A., Martínez, F.J., 1997. Sistemas de flujo subterráneo regional en el acuífero carbonatado mesozoico de la Sierra de Cameros. Sector Oriental. *Estud. Geológicos* 53, 159–172.
- Coloma, P., Sánchez, J.A., Jorge, J.C., 1998. Simulación matemática del flujo y transporte de calor del sector oriental de la Cuenca de Cameros. *Zubía Monográfico* 10, 45–61.
- Craig, H., 1961. Isotopic variations in meteoric waters. *Science* (80-) 133, 1702–1703.
- D'Amore, F., Arnórsson, S., 2000. *Geothermometry*. In: Arnórsson, S. (Ed.), *Isotopic and Chemical Techniques in Geothermal Exploration, Development and Use*. International Atomic Agency, Vienna.
- D'Amore, F., Fancelli, R., Caboi, R., 1987. Observations of the application of chemical geothermometers to some hydrothermal systems in Sardinia. *Geothermics* 16, 271–282.
- Díaz-Tejedor, M.F., Rodríguez-Arévalo, J., Castaño, S., 2009. La Red Española de Vigilancia de Isótopos en la Precipitación (REVIP): distribución isotópica espacial y aportación al conocimiento del ciclo hidrológico. *Ing. Civ.* 155, 87–97.
- Fernández, J., Auqué, L.F., Sánchez Cela, V.S., Guaras, B., 1988. Las aguas termales de Fitero (Navarra) y Arnedillo (Rioja). Análisis comparativo de la aplicación de técnicas geotermométricas químicas a aguas relacionadas con reservorios carbonatado-evaporíticos. *Estud. Geol.* 44, 453–469.
- Fernández, M., Marzán, I., Correia, A., Ramalho, E., 1998. Heat flow, heat production, and lithospheric thermal regime in the Iberian Peninsula. *Tectonophysics* 291.
- Fouillat, C., Michard, G., 1981. Sodium/lithium ratio in water applied to geothermometry of geothermal reservoirs. *Geothermics* 10, 55–70.
- Fournier, R.O., 1977. Chemical geothermometers and mixing models for geothermal systems. *Geothermics* 5, 41–50.
- Fournier, R.O., 1979. A revised equation for the Na-K geothermometer. *Geotherm. Resour. Coun. Trans.* 3, 221–224.
- Fournier, R.O., 1981. Application of water geochemistry to geothermal exploration and reservoir engineering. In: L. R., M. L.J.P. (Eds.), *Geothermal Systems: Principles and Case Histories*. John Wiley & Sons Ltd., New York, pp. 109–141.
- Fournier, R.O., 1982. Water geothermometers applied to geothermal energy. In: D'Amore, F. (Ed.), *Applications of Geochemistry in Geothermal Reservoir Development*. UNITAR/UNDO centre on Small Energy Resources, Rome, Italy, pp. 37–69.
- Fournier, R.O., Truesdell, A.H., 1973. An empirical Na-K-Ca geothermometer for natural waters. *Geochim. Cosmochim. Acta* 37, 1255–1275.
- Friedman, I., O'Neil, J.R., 1977. Compilation of stable isotope fractionation factors of geochemical interest. In: Fleischer, M. (Ed.), *Data on Geochemistry*, USGS Professional Paper 440-KK. United States Government Printing Office, Washington, p. 109.
- Frondini, F., 2008. Geochemistry of regional aquifers hosted by carbonate-evaporite formations in Umbria and southern Tuscany (Central Italy). *Appl. Geochem.* 23, 2091–2104.
- Giggenbach, W.F., 1988. Geothermal solute equilibria. Derivation of Na-K-Mg-Ca geothermometers. *Geochim. Cosmochim. Acta* 52, 2749–2765.
- Giggenbach, W.F., Gonfiantini, R., Jangi, B.L., Truesdell, A.H., 1983. Isotopic and chemical composition of Parbat valley geothermal discharges, N.W. Himalaya. *India. Geothermics* 12, 199–222.
- Gil, A., Villalán, J.J., Barbero, L., González, G., Mata, P., Casas, A.M., 2002. Aplicación de Técnicas geoquímicas, geofísicas y mineralógicas al estudio de la Cuenca de Cameros. Implicaciones geométricas y evolutivas. *Zubía Monográfico* 14, 65–98.
- Gökgöz, A., Tarkan, G., 2006. Mineral equilibria and geothermometry of the Dalaman-Köyceğiz thermal springs, southern Turkey. *Appl. Geochem.* 21, 253–268.
- Goy, A., Gómez, J.J., Yébenes, A., 1976. El Jurásico de la Rama Castellana de la Cordillera Ibérica (Mitad norte) I. Unidades litoestratigráficas. *Estud. Geol.* 32, 391–423.
- Halas, S., Pluta, I., 2000. Empirical Calibration of Isotope Thermometer  $\delta^{18}\text{O}$  (SO<sub>4</sub><sup>2-</sup>)– $\delta^{18}\text{O}$  (H<sub>2</sub>O) for Low Temperature Brines, in: V Isotope Workshop. European Society for Isotope Research, Kraków, Poland, pp. 68–71.
- Helgeson, H.C., Delany, J.M., Nesbitt, H.W., Bird, D.K., 1978. Summary and critique of the thermodynamic properties of rock forming minerals. *Am. J. Sci.* 278A (229 pp.).
- Hyeong, K., Capuano, R., 2001. Ca/Mg of brines in Miocene/Oligocene clastic sediments of the Texas Gulf Coast: buffering by calcite/disordered dolomite equilibria. *Geochim. Cosmochim. Acta* 65, 3065–3080.
- IGME, 2010. ALGECO2 Project: elección y caracterización de áreas y estructuras geológicas favorables para el almacenamiento geológico de CO<sub>2</sub> en España. [WWW Document]. URL: <http://info.igme.es/algeco2/>, Accessed date: 24 May 2017.
- Kaczmarek, S.E., Duncan, F.S., 2011. On the evolution of dolomite stoichiometry and cation order during high-temperature synthesis experiments: an alternative model for the geochemical evolution of natural dolomites. *Sediment. Geol.* 240, 30–40.
- Karimi, H., Moore, F., 2008. The source and heating mechanism for the Ahram, Mirahmad and Garu thermal springs, Zagros Mountains, Iran. *Geothermics* 37, 84–100.
- Kharaka, Y.K., Mariner, R.H., 1989. Chemical geothermometers and their application to formation waters from sedimentary basins. In: Naeser, N.D., McCollon, T.H. (Eds.), *Thermal History of Sedimentary Basins*. Springer, Berlin, pp. 99–117.
- Land, L.S., 1985. The origin of massive dolomite. *J. Geol. Educ.* 33, 112–125.
- Lambán, L.J., Jódar, J., Custodio, E., Soler, A., Sapriza, G., Soto, R., 2015. Isotopic and hydrogeochemical characterization of high-altitude karst aquifers in complex geological settings. The Ordesa and Monte Perdido National Park (Northern Spain) case study. *Sci. Total Environ.* 506, 466–479.
- Levet, S., Toutain, J.P., Munoz, M., Berger, G., Negrel, P., Jendrzewski, N., Agrinier, P., Sortino, F., 2002. Geochemistry of the Bagnères-de-Bigorre thermal waters from the North Pyrenean Zone sedimentary environment (France). *Geofluids* 2, 1–16.
- Lloyd, R.M., 1968. Oxygen isotope behaviour in the sulfate-water system. *J. Geophys. Res.* 73, 6099–6110.
- López-Chicano, M., Cerón, J.C., Vallejos, A., Pulido-Bosch, A., 2001. Geochemistry of thermal springs, Alhama de Granada (southern Spain). *Appl. Geochem.* 16, 1153–1163.
- Lumsden, D.N., Chimahusky, J.S., 1980. Relationship between dolomite nonstoichiometry and carbonate facies parameters. In: Dunham, J.B., Ethington, R.L. (Eds.), *Concepts and Models of Dolomitization: Special Publication*. Vol. 28. Society of Economic Paleontologists and Mineralogists (SEPM), pp. 123–137.
- Maraver Eyzaguirre, F. (Ed.), 2003. *Vademécum de Aguas Mineromedicinales Españolas*. Instituto de Salud Carlos III, Madrid.
- Mariner, R.H., Evans, W.C., Young, H.W., 2006. Comparison of circulation times of thermal waters discharging from the Idaho batholith based on geothermometer temperatures, helium concentrations, and <sup>14</sup>C measurements. *Geothermics* 35, 3–25.
- Marini, L., 2004. *Geochimical Techniques for the Exploration and Exploitation of Geothermal Energy*. Laboratorio di Geochemia, Università degli Studi di Genova, Genova.
- Marini, L., 2006. Geological sequestration of carbon dioxide. *Thermodynamics, Kinetics, and Reaction Path Modeling*. Elsevier Science, Amsterdam.
- Marini, L., Chiodini, G., Cioni, R., 1986. New geothermometers for carbonate-evaporite geothermal reservoirs. *Geothermics* 15, 77–86.
- Mas, J.R., Alonso, A., Guimera, J., 1993. Evolución tectonosedimentaria de una cuenca extensional intraplaca: la cuenca finijurásica-eocretácica de los Cameros (La Rioja-Soria). *Rev. Soc. Geol. Esp.* 6, 129–144.
- Merino, E., Ramson, B., 1982. Free energies of formation of illite solid solutions and their compositional dependence. *Clay Clay Miner.* 30, 29–39.
- Michard, G., 1979. *Geothermomètres Chimiques*. Bur. Rech. Géologiques Minières (2nd Ser.), Sect. III 2. pp. 183–189.
- Michard, G., 1983. *Recueil de Données Thermodynamiques Concernant les Équilibres Eau-Minéraux dans les Réservoirs Géothermaux*. Commission des Communautés Européennes, Luxembourg.
- Michard, G., Bastide, J.P., 1988. Géochimie de la nappe du Dogger du Bassin de Paris. *J. Volcanol. Geotherm. Res.* 35, 151–163.
- Michard, G., Fouillat, C., 1980. Contrôle de la composition chimique des eaux thermales sulfurées sodiques du Sud de la France. In: Tardy, Y. (Ed.), *Geochemie Des Interactions Entre Les Eaux Le Minéraux et Les Roches*. Elements, Tarbes, pp. 147–166.
- Michard, G., Roekens, E., 1983. Modelling of the chemical composition of alkaline hot waters. *Geothermics* 12, 161–169.
- Michard, G., Sanjuan, B., Criaud, A., Fouillat, C., Pentcheva, E.N., Petrov, P.S., Alexieva, R., 1986a. Equilibria and geothermometry in hot waters from granites of SW Bulgaria. *Geochem. J.* 1 (20), 159–171.
- Michard, G., Sanjuan, B., Criaud, A., Fouillat, C., Pentcheva, E.N., Petrov, P.S., Alexieva, R., 1986b. Equilibria and geothermometry in hot alkaline waters from granites of S.W. Bulgaria. *Geochem. J.* 20, 159–171.
- Michard, G., Grimaud, D., D'Amore, F., Fancelli, R., 1989. Influence of mobile ion concentration on the chemical composition of geothermal waters in granitic areas. Example of hot springs from Piemonte (Italy). *Geothermics* 18, 729–741.
- Mizutani, Y., Rafter, T.A., 1969. Oxygen isotopic composition of sulphates, part 3. Oxygen isotopic fractionation in the bisulfate ion-water system. *New Zel. J. Sci.* 22, 169–176.
- Mohammadi, Z., Bagheri, R., Jahanshahi, R., 2010. Hydrogeochemistry and geothermometry of Chaghal thermal springs, Zagros region, Iran. *Geothermics* 39, 242–249.
- Mook, W.G., Tan, F.C., 1991. Stable carbon isotopes in rivers and estuaries. In: Degens, E.T., Kempe, S., Richey, J.E. (Eds.), *Biogeochemistry of Major World Rivers*, Scope Report 42. Wiley, New York, pp. 245–263.
- Mutlu, H., Güleç, N., 1998. Hydrogeochemical outline of thermal waters and geothermometry applications in Anatolia (Turkey). *J. Volcanol. Geotherm. Res.* 85, 495–515.
- Nemeth, K., 1963. Photometric determination of sulphate in soil extracts. *Z. Pflernähr. Dung.* 103, 193–196.
- Nordstrom, D.K., Plummer, L.N., Langmuir, L., Busenberg, E., May, H.M., Jones, B.F., Parkhurst, D.L., 1990. Revised chemical equilibrium data for major water-mineral reactions and their limitation. In: Melchior, D.C., Basset, R.L. (Eds.), *Chemical Modeling of Aqueous Systems II*. Symposium Series 416. American Chemical Society, Washington.
- Palandri, J.L., Reed, M.H., 2001. Reconstruction of in situ composition of sedimentary formation waters. *Geochim. Cosmochim. Acta* 65, 1741–1767.
- Pang, Z., Reed, M.H., 1998. Theoretical chemical thermometry on geothermal waters: Problems and methods. *Geochim. Cosmochim. Acta* 62.
- Parkhurst, D.L., Appelo, C.A.J., 2013. Description of input and examples for PHREEQC version 3. A computer program for speciation, batch reaction, one dimensional transport, and inverse geochemical calculations. In: U.S. Geological Survey (Ed.), *Techniques and Methods*. U.S. Geological Survey, Denver, Colorado (Book 6, Chap. A43).
- Pastorelli, S., Marini, L., Hunziker, J.C., 1999. Water chemistry and isotope composition of the Acquarossa thermal system, Ticino, Switzerland. *Geothermics* 28, 75–93.

- Reed, M., Spycher, N., 1984. Calculation of pH and mineral equilibria in hydrothermal waters with application to geothermometry and studies of boiling and dilution. *Geochim. Cosmochim. Acta* 48, 1479–1492.
- Reeder, R.J., 2000. Constraints on cation order in calcium-rich sedimentary dolomite. *Aquat. Geochem.* 6, 213–226.
- Sánchez, J.A., Coloma, P., 1998. Hidrogeología de los manantiales termales de Arnedillo. *Zubia Monográfico* 10, 11–25.
- Sánchez, J.A., Coloma, P., Pérez, A., 1999. Sedimentary processes related to the groundwater flows from the Mesozoic Carbonate Aquifer of the Iberian Chain in the Tertiary Ebro Basin, northeast Spain. *Sediment. Geol.* 129, 201–213.
- Seal, R.R.I., Alpers, C.N., Rye, R.O., 2000. Stable isotope systematics of sulfate minerals. In: Alpers, C.N., Jambor, J.L., Nordstrom, D. (Eds.), *Sulfate Minerals – Crystallography: Geochemistry and Environmental Significance*. Mineral Society of America, Chantilly (Virginia), pp. 541–602.
- Sonney, R., Vuataz, F.D., 2010. Validation of chemical and isotopic geothermometers from low temperature deep fluids of Northern Switzerland. *Proceedings World Geothermal Congress 2010*. Bali, Indonesia, Indonesia, pp. 25–29.
- Sperber, C.M., Wilkinson, B.H., Peacor, D.R., 1984. Rock composition, dolomite stoichiometry, and rock/water reactions in dolomitic carbonate rocks. *J. Geol.* 92, 609–622.
- Spycher, N., Peiffer, L., Sonnenthal, E.L., Saldi, G., Reed, M.H., Kennedy, B.M., 2014. Integrated multicomponent solute geothermometry. *Geothermics* 51, 113–123.
- Stefánsson, A., Arnórsson, S., 2000. Feldspar saturation state in natural waters. *Geochim. Cosmochim. Acta* 64, 2567–2584.
- Tischer, G., 1965. Über die Wealden-Ablagerung und die Tektonik der östlichen Sierra de los Cameros in den nordwestlichen Iberischen Ketten (Spanien). *Beihefte zum Geol. Jahrb.* 44, 123–164.
- Tole, M.P., Arnórsson, H., Pang, Z., Arnórsson, S., 1993. Fluid/mineral equilibrium calculations for geothermal fluids and chemical geothermometry. *Geothermics* 12, 17–37.
- Truesdell, A.H., 1976. *Geochemical techniques in exploration. Summary of section III. Proceedings of the Second United Nations Symposium on the Development Y Use of Geothermal Resources*. San Francisco (California), pp. iii–xxix.
- Utrilla, R., Pierre, C., Ortí, F., Rosell, L., Inglés, M., Pueyo, J.J., 1987. Estudio isotópico de los sulfatos en formaciones evaporíticas mesozoicas y terciarias continentales. Aplicación a la Cuenca del Tajo. *II Congreso de Geoquímica de España*. Soria, pp. 91–94.
- Verma, S.P., Santoyo, E., 1997. New improved equations for Na/K, Na/Li and SiO<sub>2</sub> geothermometers by outlier detection and rejection. *J. Volcanol. Geotherm. Res.* 79, 9–24.
- Vespasiano, G., Apollaro, C., Muto, F., Dotsika, E., de Rosa, R., Marini, L., 2014. Chemical and isotopic characteristics of the warm and cold waters of the Luigiane Spa near Guardia Piemontese (Calabria, Italy) in a complex faulted geological framework. *Appl. Geochem.* 41:73–88. <https://doi.org/10.1016/j.apgeochem.2013.11.014>.
- Vogel, J.C., 1993. Variability of carbon isotope fractionation during photosynthesis. In: Ehleringer, J.R., Hall, A.E., Farquhar, G.D. (Eds.), *Stable Isotopes and Plant Carbon – Water Relations*. Academic Press, San Diego (California), pp. 29–38.
- Wang, J., Jin, M., Jia, B., Kang, F., 2015. Hydrochemical characteristics and geothermometry applications of thermal groundwater in northern Jinan, Shandong, China. *Geothermics* 57, 185–195.
- Zeebe, R.E., 2010. A new value for the stable oxygen isotope fractionation between dissolved sulfate ion and water. *Geochim. Cosmochim. Acta* 74, 818–828.
- Zheng, Y.F., 1999. Oxygen isotope fractionation in carbonate and sulfate minerals. *Geochem. J.* 33, 109–126.

### 4.3 Paper 3

#### **Geochemical evolution of thermal waters in carbonate – evaporitic systems: the triggering effect of halite dissolution in the dedolomitisation and albitisation processes**

*Mónica Blasco, Luis F. Auqué, María J. Gimeno*

Journal of Hydrology 570, 623-636 (2019)

Impact Factor (2017): 3.727

Quartile and Category (2017): Q1 (7/128), Engineering Civil; Water Resources; Q1 (27/189), Geosciences.

DOI: 10.1016/j.jhydrol.2019.01.013

Sent: 30 August 2018

Accepted: 12 January 2019

Available online: 16 January 2019

Final publication: March 2019





Contents lists available at ScienceDirect

Journal of Hydrology

journal homepage: [www.elsevier.com/locate/jhydrol](http://www.elsevier.com/locate/jhydrol)

## Research papers

# Geochemical evolution of thermal waters in carbonate – evaporitic systems: The triggering effect of halite dissolution in the dedolomitisation and albitisation processes



Mónica Blasco\*, Luis F. Auqué, María J. Gimeno

Geochemical Modelling Group, Petrology and Geochemistry Area, Earth Sciences Department, University of Zaragoza, Spain C/ Pedro Cerbuna 12, 50009 Zaragoza, Spain

## ARTICLE INFO

This manuscript was handled by Huaming Guo, Editor-in-Chief, with the assistance of Prosun Bhattacharya, Associate Editor

**Keywords:**

Geothermal system  
Geothermometry  
Geochemical modelling  
Dedolomitisation  
Albitisation  
Halite dissolution triggering effects

## ABSTRACT

The Fitero and Arnedillo geothermal systems are located in the NW part of the Iberian Range (Northern Spain). The geothermal reservoir is hosted in the Lower Jurassic carbonates, in contact with the evaporitic Keuper Facies. Thermal waters are of chloride-sodium type with discharge temperature of about 45 °C and near neutral pH. The Arnedillo waters are more saline with higher Na, Cl and sulphate contents, but lower Ca and Mg than the Fitero waters. All waters have attained mineral equilibrium at depth with calcite, dolomite, anhydrite, quartz, albite, K-feldspar and other aluminosilicates, except for the Fitero waters, which have not reached the equilibrium with the aluminosilicates. The calculated reservoir temperature is  $81 \pm 11$  °C in Fitero and  $87 \pm 13$  °C in Arnedillo. In order to identify the reasons for the differences found between the two systems some inverse and forward geochemical calculations were performed and the main water-rock interaction processes responsible for the chemical evolution of these waters have been evaluated.

Halite dissolution has been found to be the triggering factor for the two most important geochemical processes in the system: a) albitisation process, due to the common ion effect (Na); and b) dedolomitisation process, associated with the salinity increase, which enhance the dissolution of anhydrite and, in turn, produces the precipitation of calcite (common ion effect, Ca) and the concomitant dissolution of dolomite.

Halite dissolution may be an important driving force in the geochemical evolution of groundwater systems in contact with carbonates and evaporites, where equilibrium with K-feldspar, albite and anhydrite has already been attained. The evolution of the processes at pH, temperature and salinity ranges wider than those in the Fitero-Arnedillo system has been theoretically examined with additional reaction-path simulations, in order to generalise the geochemical behaviour of these processes in other environments.

## 1. Introduction

Fitero and Arnedillo are two small villages in Navarra and La Rioja regions (Spain) respectively, which have well known spas functioning for a long time (e.g. Gutiérrez, 1801; Mezquíriz, 2004) for its medicinal and therapeutic benefits. Arnedillo is about 35 Km NW of Fitero, and the waters that emerge in both villages belong to the same carbonate-evaporitic reservoir. The discharge temperature of the thermal waters at both sites is similar, but their chemistry is different.

The hydrogeochemical characterisation of these thermal waters started with the study of the Arnedillo system (Blasco et al., 2018) and it is completed in this paper with the characterisation of the Fitero thermal waters. Moreover, following the same methodology as for the Arnedillo waters, the temperature in the reservoir of the Fitero system has been determined by using the chemical and isotopic

geothermometers and the geothermometrical modelling. The use of classical chemical geothermometers (cationic geothermometers and silica geothermometers) in low-temperature and carbonate-evaporitic systems is rather controversial, since they were developed to be used in waters of higher temperature and with a different mineral assemblage in contact to the waters in the reservoir. However, although not completely free of uncertainties or limitations, there are some chemical geothermometers specifically calibrated for this type of systems (Ca-Mg and SO<sub>4</sub>-F; Chiodini et al., 1995). These issues were thoroughly treated in the previous study on the Arnedillo waters (Blasco et al., 2018) and, therefore, only some observations are included here. In any case, as both systems belong to the same reservoir, the study of the Fitero thermal waters will improve the general understanding in the particularities of the use of these geothermometers (as explained in Blasco et al., 2017).

\* Corresponding author.

E-mail address: [monicabc@unizar.es](mailto:monicabc@unizar.es) (M. Blasco).<https://doi.org/10.1016/j.jhydrol.2019.01.013>

Received 30 August 2018; Received in revised form 4 January 2019; Accepted 12 January 2019

Available online 16 January 2019

0022-1694/ © 2019 Elsevier B.V. All rights reserved.

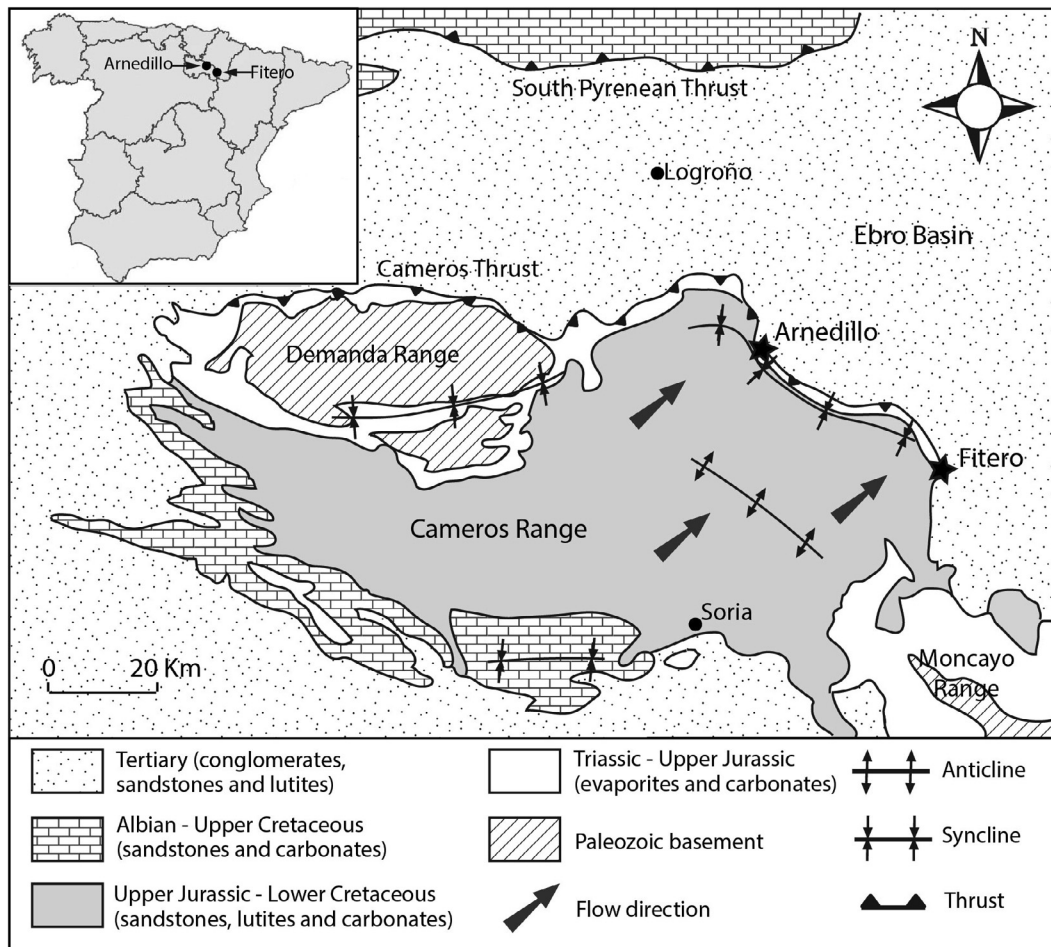


Fig. 1. Location of the Arnedillo and the Fitero geothermal springs and geological map of the area (modified from Blasco et al. 2018).

Finally, the geochemical characterisation of the whole system allows assessing, by mass balance and reaction paths calculations, the main reactions (and their extent) that condition the evolution of these thermal waters. This evaluation has evidenced the important role played by halite dissolution in the geochemical evolution of this type of systems through its effects on several water-mineral equilibria.

## 2. Geology and hydrogeology

The Fitero and Arnedillo thermal springs are located in the NW of the Iberian Chain, in the contact between the eastern Cameros Range and the tertiary Ebro Basin (Fig. 1; Coloma et al., 1997a,b; Sánchez and Coloma, 1998). These springs are aligned in a NW-SE thrust that separates the aforementioned two units (Albert, 1979; Auqué et al., 1988). They are located in the Fitero (Navarra, Spain) and Arnedillo (La Rioja, Spain) villages, respectively, which are separated by about 35 km.

The Cameros Range, constituted mainly by Mesozoic rocks, is limited by two continental basins and two Paleozoic reliefs (Fig. 1): the Ebro and Duero basins in the north and the south, respectively; and the Demanda and Moncayo Ranges at the east and west (Gil et al., 2002). The formations of this area range from the Paleozoic up to the Quaternary. The Triassic and the marine Jurassic carbonate rocks (up to Kimmeridgian) constitute the pre-rift sequence, and they are represented by the formations normally found in the Iberian Chain (Coloma, 1998; Gil et al., 2002; Goy et al., 1976). At the end of the Jurassic and during the Cretaceous time a rifting process resulted in the creation of the Cameros Basin and the sedimentation of this period constitutes the syn-rift sequence. These are continental sediments from

Upper Jurassic to Upper Cretaceous (Tithonian to Lower Albian; Coloma, 1998; Gil et al., 2002; Mas et al., 1993) and they are constituted by an intercalation of fluvial and lacustrine sediments. Finally, the post-rift sequence is constituted by the Upper Cretaceous carbonates (Urgon Facies) and sandstones (Utrillas Formation) and the carbonates of the Later Cretaceous (Santa María de la Hoyas, Picofrentes, Muñecas, Hortezielos, Hontoria Pinar, Burgo de Osma, Santo Domingo de Silos and Santibañez del Val Formations; Gil et al., 2002, 2004). The Cameros Range relief and the tertiary basin were created during the tertiary tectonic inversion when E-W and NW-SE compressive structures, such as the Cameros thrust, were generated (Coloma, 1998; Gil et al., 2002).

The geothermal reservoir associated with these thermal waters is located in the Jurassic carbonates of the pre-rift sequence. Based on their permeability, these materials have been divided in three groups, two permeable ones separated by other less permeable (Coloma et al., 1995; Sánchez and Coloma, 1998; Sánchez et al., 1999), although they are interconnected due to the intense fracturation:

- 1) Group 1 (the first permeable group): Imón (dolostones), Cortes de Tajuña (dolomitic carnioles) and Cuevas Labradas (limestones and dolostones) Formations.
- 2) Group 2 (the intermediate less permeable group): Cerro del Pez (marls), Barahona (bioclastics limestones) and Turmiel (marls and limestones) Formations.
- 3) Group 3 (the second permeable group): Chelva (limestones), Aldealpozo (black limestones) and Torrecilla (limestones with corals) Formations.



All these formations constitute the regional drainage level of the Iberian Chain, although the main flow occurs through the materials of the first permeable group (Coloma et al., 1995; Sánchez and Coloma, 1998; Sánchez et al., 1999).

The recharge occurs through the outcrops of Jurassic rocks and the syn-rift sequence and from the infiltration from rivers (Coloma et al., 1995; Sánchez et al., 1999). Then, the ascent of the thermal waters to surface takes place through the Cameros thrust (Coloma, 1998; Coloma et al., 1996; Fig. 1). The discharges are associated with the Keuper facies and the Lower Jurassic formations (Auqué et al., 1988; Coloma, 1998; Coloma et al., 1996). The thermal waters are of chloride-sodium type and the discharge temperature is close to 50 °C in both cases, however, the flow rate is higher in Fitero (about 50 L/s) than in Arnedillo (up to 20 L/s; Coloma et al., 1998, 1997b, 1995; Sánchez and Coloma, 1998).

### 3. Methodology

#### 3.1. Field sampling and analyses

A sampling campaign was conducted in October 2015 and four water samples were taken and analysed. Two of them were collected in Arnedillo, one inside the Arnedillo spa (AR1) and the other in a spring in a pool built in the Cidacos River (AR2). The other two samples were taken in Fitero in two different spas, one in the Bequer spa (F1) and the other in the Palafox spa (F2).

The field sampling procedures and analytical methodology were described in detail in Blasco et al. (2018). Briefly, temperature, pH and electrical conductivity were determined in situ in all these samples; alkalinity was determined by titration with H<sub>2</sub>SO<sub>4</sub> 0.02 N and endpoint monitoring by pH-meter, chloride and fluoride by selective electrodes and sulphates by colorimetry. The major cations (Ca, Na, K, Mg, Sr and Si) were analysed by ICP-OES, the minor cations by ICP-MS and the isotopes ( $\delta^{18}\text{O}$ ,  $\delta^2\text{H}$ ,  $\delta^{13}\text{C}$ , and  $\delta^{34}\text{S}$  and  $^{18}\text{O}$  in dissolved sulphates) by CF-IRMS.

#### 3.2. Geothermometers

The use of chemical and isotopic geothermometers for determining the reservoir temperature of a thermal system can be considered complementary to the geothermometrical modelling and through the combination of the three techniques the temperature is more precisely established. The characteristics of the chemical and isotopic geothermometers used here and their application to these thermal waters were detailed in Blasco et al. (2018), so here only the most relevant information is highlighted.

##### 3.2.1. Chemical geothermometers

Chemical geothermometers are the classical technique used for determining the reservoir temperature of thermal waters. They consist of empiric or experimental calibrations based on chemical heterogeneous reactions which depend on temperature and control the elemental contents dissolved in waters (e.g. Marini, 2004; Truesdell, 1976). There are some geothermometers that have been specifically calibrated for carbonate-evaporitic and low temperature thermal systems and they have been used in this study: the Ca-Mg and the SO<sub>4</sub>-F geothermometers (Chiodini et al. 1995).

However, most of the existing geothermometers (cationic and silica geothermometers) have been calibrated for waters of high temperature (> 180 °C) and hosted in different rocks than the ones present in the studied area (e.g. Arnórsson et al., 1983; Asta et al., 2010; Auqué et al., 1997; Buil et al., 2006; Choi et al., 2005; D'Amore et al., 1987; Fouillac and Michard, 1981; Fournier, 1981, 1977; Giggenbach et al., 1983; Giggenbach, 1988; Kharaka and Mariner, 1989; Mariner et al., 2006; Mutlu and Güleç, 1998; Stefánsson and Arnórsson, 2000). These geothermometers have provided coherent results in some systems similar

to the ones studied here (e.g. Apollaro et al., 2012; Blasco et al., 2018, 2017; Fernández et al., 1988; Gökğöz and Tarkan, 2006; Michard and Bastide, 1988; Mohammadi et al., 2010; Pastorelli et al., 1999; Wang et al., 2015) and, therefore, their applicability in the Fitero – Arnedillo geothermal system is tested. Classical chemical geothermometers and calibrations used in this study are: SiO<sub>2</sub>-quartz (calibrations: Fournier, 1977; Michard, 1979; Truesdell, 1976), SiO<sub>2</sub>-chalcedony (calibrations: Arnórsson et al., 1983; Fournier, 1977) Na-K (calibrations: Fournier, 1977; Giggenbach, 1988; Verma and Santoyo, 1997), K-Mg (Giggenbach et al., 1983 calibration) and Na-K-Ca (Fournier and Truesdell, 1973 calibration).

##### 3.2.2. Isotopic geothermometers

Isotopic geothermometers are similar to chemical geothermometers as they consist of reactions dependent on temperature, however they are based on the isotopic equilibrium between two species. The isotopic geothermometers used in this study are the ones based on the  $\delta^{18}\text{O}$  exchange between waters and sulphate. The traditional calibrations for this geothermometer are based on the  $\delta^{18}\text{O}$  HSO<sub>4</sub>-H<sub>2</sub>O exchange and the calibrations used here are those from Friedman and O'Neil (1977) and Seal et al. (2000). However as isotopic equilibrium in waters of neutral pH is supposed to be controlled by the  $\delta^{18}\text{O}$  SO<sub>4</sub><sup>2-</sup>-H<sub>2</sub>O exchange (Boschetti, 2013), additional calibrations based on this assumption have also been used (Halas and Pluta, 2000; Zeebe, 2010). Finally, the calibration based on  $\delta^{18}\text{O}$  CaSO<sub>4</sub>-H<sub>2</sub>O exchange (Boschetti et al., 2011) provides good results in systems oversaturated or in equilibrium with anhydrite (e.g. Awaleh et al., 2015; Boschetti, 2013; Boschetti et al., 2011) and it has also been used here.

#### 3.3. Geochemical modelling

The geochemical calculations have been performed by using the PHREEQC geochemical code (Parkhurst and Appelo, 2013) and the WATEQ4F thermodynamic database (Ball and Nordstrom, 2001) with some additional thermodynamic data which are detailed below:

- pyrophyllite, laumontite, albite, K-feldspar and chalcedony data from Michard (1983). These data have been selected because they have provided good results in geothermal systems previously (e.g. Asta et al., 2012; Auqué et al., 1998; Michard and Roekens, 1983; Michard et al., 1989, 1986) and their reliability in this system was proven by Blasco et al. (2018); and
- dolomite data from Blasco et al. (2018), which was calculated from the data of the Arnedillo geothermal system. This is a partially ordered dolomite which consists of 18.4% of ordered dolomite and 81.6% of disordered dolomite.

##### 3.3.1. Speciation-solubility calculations

These calculations provide the distribution of the different species in the water, determining their concentrations and activities. They also give the saturation states of waters with respect to the mineral phases and the partial pressure of gasses (e.g. pCO<sub>2</sub>). The saturation state (SI) is the logarithm of the ratio between the ionic activity product (IAP) and the equilibrium constant of the mineral reaction at the indicated temperature (K(T)):

$$SI = \log \left( \frac{IAP}{K(T)} \right) \quad (1)$$

When SI = 0 the solution is in equilibrium with the mineral phase, a positive value indicates oversaturation and a negative value undersaturation. These determinations will be the basic part of the geothermometrical modelling.

##### 3.3.2. Geothermometrical modelling

As mentioned above, in order to compare the results, the

geothermometrical techniques used here are the same as the ones used to estimate the reservoir temperature of the Arnedillo thermal waters (Blasco et al., 2018): chemical and isotopic geothermometers (previously described) and geothermometrical modelling (or multi-component solute geothermometry; e.g. Spycher et al., 2014). With this last technique, the temperature of the reservoir is determined by simulating an increase of the temperature of the thermal water to find the temperature range at which the saturation states of a previously selected mineral set (according to the reservoir mineralogy and assuming that they will be in equilibrium in the reservoir) reach equilibrium simultaneously. A more detailed explanation of this method and the minerals selected for the modelling can be found in Blasco et al. (2018).

### 3.3.3. Inverse and direct modelling

Mass-balance calculations (inverse modelling) provide the mass transfer for the selected or assumed reactions between two connected points of the system along a flow path but without taking into account the thermodynamic feasibility of those reactions (Back et al., 1983; Busby et al., 1991; Hanshaw and Back, 1985; Plummer and Back, 1980; Plummer, 1977; Plummer et al., 1990, 1983; Román-Mas and Lee, 1987; Zhu and Anderson, 2002). In this case the assumption is that Fitero and Arnedillo are geochemically related and, although they are not strictly in the same flow path, they represent two different evolution stages, that is, Fitero will be considered as the initial solution and Arnedillo the final one. The mass transfers that will be obtained with this assumption will be used in a qualitative way to assess the differences in the intensity of the reactions controlling the chemistry of the thermal waters. To solve a mass balance calculation the necessary data include: the chemical composition of the initial and the final waters and the mineral and gas phases which the waters can react with while moving from the initial to the final point. The most feasible model obtained with this calculation will be selected according to the geochemical characteristics of waters and the thermodynamic feasibility of the mass transfers obtained, which is then checked with a reaction-path simulation.

Reaction path-modelling (forward or direct modelling) checks the thermodynamic feasibility of the previous mass balance models. The initial water from the mass balance is taken as the starting point and its evolution is simulated imposing the reactions obtained previously. The results indicate the theoretical composition of the final water together with the amount of precipitated or dissolved phases. The coherence of the inverse and direct modelling results will support the conclusion on which are the most feasible reactions taking place in the system.

## 4. Results and discussion

### 4.1. Chemical and isotopic characteristics of the waters

The four samples collected in 2015 have been considered in this study, two from Fitero and two from Arnedillo. The detailed study of the Arnedillo samples can be found in Blasco et al. (2018) and they will be discussed here in comparison with the Fitero waters.

All these thermal waters are of chloride – sodium type, with pH between 6.86 and 7.11 and spring temperature about 45 °C (except for AR2 which is 39.5 °C due to its location in the Cidacos river with which some mixing happens; Table 1). The most important differences between the Fitero and the Arnedillo waters are those related to their salinity and their Al contents, in general lower in Fitero:

1. The total dissolved solids (TDS) in Fitero thermal waters is about 4800 ppm while in Arnedillo is higher, about 7500 ppm.
2. Dissolved Cl and Na contents are almost half in Fitero (about 1600 and 1000 ppm, respectively; Table 1) than in Arnedillo (about 3000 and 2000 ppm, respectively; Table 1).
3. The aluminium is lower in the samples from Fitero than in the samples from Arnedillo.

**Table 1**

Chemical and isotopic data of the thermal waters included in this study. TDS (calculated using PHREEQC) and dissolved elements are expressed in ppm. The molar ratios are also shown, the Ca + Mg/HCO<sub>3</sub> + SO<sub>4</sub> is in eq/L.

	AR1	AR2	F1	F2
Temp. (°C)	45.30	39.50	45.50	45.10
TDS	7720.9	7352.1	4820.2	4854.7
pH	6.87	7.05	6.86	7.11
HCO <sub>3</sub> <sup>-</sup>	179.88	181.58	174.02	175.36
Cl <sup>-</sup>	3220.00	3030.00	1610	1620
SO <sub>4</sub> <sup>-</sup>	1541.00	1537.00	1376	1401
Ca	444.00	443.00	469	476
Mg	75.50	73.80	92.10	94.60
Na	2099.00	1941.00	981	982
K	20.60	22.90	30.20	31.80
Sr	9.90	9.80	11.10	11.20
F	2.36	2.30	0.992	1.02
Al	0.0142	0.0643	0.0059	0.0075
Li	0.2901	0.2708	0.4755	0.4836
SiO <sub>2</sub>	30.87	29.10	23.75	24.39
δ <sup>18</sup> O vs. SMOW in (H <sub>2</sub> O)	-8.5	-8.8	-8.7	-9.6
δ <sup>2</sup> H vs. SMOW (H <sub>2</sub> O)	-65.3	-65.1	-63.9	-64.3
δ <sup>18</sup> O vs. SMOW in (SO <sub>4</sub> <sup>2-</sup> )	14.1	14	14.2	13.9
δ <sup>34</sup> S vs. CDT (in SO <sub>4</sub> <sup>2-</sup> )	14.8	14.8	14.9	14.9
δ <sup>13</sup> C vs. PDB (in CO <sub>2</sub> )	-4.16	-5.52	-8.42	-8.1
Na/Cl	1.01	0.99	0.94	0.93
Ca/SO <sub>4</sub>	0.69	0.69	0.82	0.81
Ca + Mg/HCO <sub>3</sub> + SO <sub>4</sub>	0.81	0.81	0.98	0.98
Ca/HCO <sub>3</sub>	3.76	3.71	4.10	4.13
Ca + Mg/HCO <sub>3</sub>	4.81	4.73	5.43	5.49
Mg/Ca	0.27	0.28	0.32	0.33
% imbalance	-2.41	-3.28	-1.7	-1.8

4. Dissolved F, SO<sub>4</sub> and SiO<sub>2</sub> are higher in the Arnedillo samples.
5. Only dissolved Ca, Mg and K are higher in the Fitero samples.

With respect to the molar ratios, the main observations are:

1. Despite the difference in the salinity of the waters the Na/Cl molar ratio is close to 1 in all the samples (Table 1) which indicates that the Na and Cl concentrations are mainly controlled by halite dissolution, although, considering the concentration values, the amount of dissolution is higher in the Arnedillo waters.
2. The Ca/SO<sub>4</sub> and Ca + Mg/HCO<sub>3</sub> + SO<sub>4</sub> ratios (the last one in eq/L) are quite similar for all samples although slightly higher in Fitero.
3. The Ca/SO<sub>4</sub> molar ratio is about 0.82 in Fitero and about 0.69 in Arnedillo (Table 1). Considering that anhydrite is the main control for the SO<sub>4</sub> contents, the value of this ratio lower than 1 means that Ca is being removed from the waters by carbonate precipitation, which (based on the value) would be higher in the case of Arnedillo.
4. The values for the Ca + Mg/HCO<sub>3</sub> + SO<sub>4</sub> ratio (in eq/L) are 0.98 in Fitero and 0.81 in Arnedillo (Table 1). The fact that this ratio is lower than 1, mainly in the Arnedillo thermal waters, means that, apart from the role played by calcite, dolomite and anhydrite, other processes should be involved in the control of this ratio.
5. Finally, the similar values found in the two systems for the Mg/Ca molar ratios (0.28 in Fitero and 0.24 in Arnedillo) and the aMg/aCa activity ratios (0.29 in Fitero and 0.26 in Arnedillo) suggest a similar calcite – dolomite equilibrium temperature in the reservoir.

The differences found between the Fitero and the Arnedillo samples, along with their similarities, are coherent with the fact that the thermal waters from both sites belong to the same geothermal reservoir, although with a more evolve stage of water-rock interaction in the case of Arnedillo thermal waters.

This hypothesis is also supported by some of the isotopic data of the waters. Tritium was not analysed in these samples, but Coloma et al. (1997a) reported values of 0.8 ± 2.5 TU and 7 ± 1.5 TU in the Fitero spas and 1.1 ± 2.5 TU in the Arnedillo spa. This low content of tritium

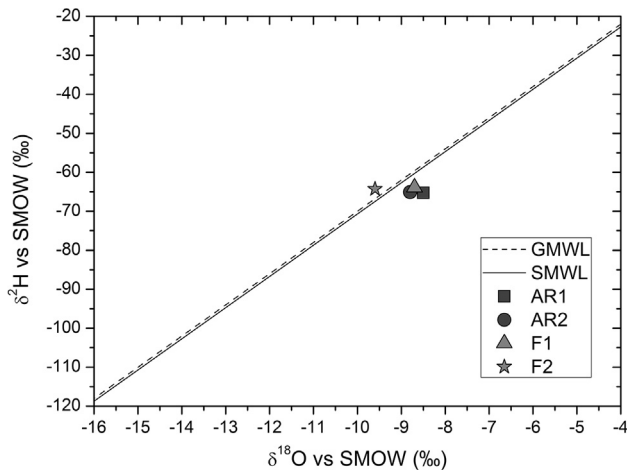


Fig. 2.  $\delta^2\text{H} - \delta^{18}\text{O}$  diagram showing the isotopic composition of the samples from Arnedillo and Fitero. The Global Meteoric Water Line (GMWL) and the Spanish Meteoric Water Line (SMWL) are also shown.

suggests that the recharge of the waters was prior to 1952, when the thermonuclear testing began, and are not affected by mixing with recent waters, except for the sample from Fitero with  $7 \pm 1.5$  TU, in which a low proportion of mixing can exist (Clark and Fritz, 1997).

The values of  $\delta^{18}\text{O} - \delta^2\text{H}$  in these samples (Table 1) indicate a meteoric origin of the waters since the  $\delta^{18}\text{O} - \delta^2\text{H}$  ratio represented in Fig. 2 is close to the Global Meteoric Water Line ( $\delta^2\text{H} = 8 \cdot \delta^{18}\text{O} + 10$ ; Craig, 1961) and to the Spanish Meteoric Water Line calculated from the data of the Spanish Network for the control of the isotopes in the rainfall (Díaz-Teijeiro et al. 2009;  $\delta^2\text{H} = 8 \cdot \delta^{18}\text{O} + 9.27$ ). The similar  $\delta^{18}\text{O}$  and  $\delta^2\text{H}$  values for all the water samples suggest that their recharge area is the same, supporting the hypothesis of Fitero and Arnedillo waters belonging to the same geothermal reservoir.

The main sources for the  $\delta^{13}\text{C}$  of the waters are: 1) the organic matter present in the soil through which the waters recharge, which has values that range from  $-24$  to  $-30\text{‰}$  for the C3 plants (the most likely ones to exist in the area, promoting a mean  $\delta^{13}\text{C}$  value for the soil  $\text{CO}_2$  of  $-23\text{‰}$ ; Clark and Fritz, 1997) and 2) the interaction with carbonates, whose  $\delta^{13}\text{C}$  is approximated to be  $0\text{‰}$  (see Blasco et al., 2018 and references therein for a more complete explanation). Therefore, the higher the  $\delta^{13}\text{C}$  value, the higher the interaction with the dissolved carbonates of the waters. The  $\delta^{13}\text{C}$  in the dissolved inorganic carbon (DIC) in the Arnedillo waters is higher than in the Fitero ones (about  $-5\text{‰}$  and  $-8.4\text{‰}$  respectively; Table 1) indicating that the thermal waters from Arnedillo have had a greater (or longer) interaction with carbonates than the thermal waters from Fitero.

Finally, the values of  $\delta^{34}\text{S}$  and  $\delta^{18}\text{O}$  in the dissolved sulphate are nearly the same for the Fitero and Arnedillo waters, being of about  $14.8\text{‰}$  for the  $\delta^{34}\text{S}$  and  $14\text{‰}$  for the  $\delta^{18}\text{O}$  (Table 1). As explained in Blasco et al. (2018) these values agree with those reported for the Keuper facies in the surrounding areas indicating that these thermal waters have been in contact with these rocks in the reservoir.

#### 4.2. Saturation indices

The speciation-solubility results obtained at spring temperature for the Fitero thermal waters are very similar to the ones obtained for the Arnedillo samples discussed in Blasco et al. (2018). The main results concerning the carbonate phases, fluorite, evaporitic phases and silica and aluminosilicate phases, are described and compared next.

Thermal waters are almost in equilibrium (slightly oversaturated) with respect to calcite except for the sample F2 which is more oversaturated (Table 2). Dolomite is oversaturated in F2, less oversaturated in F1 and AR2 and slightly undersaturated in AR1. The log  $p\text{CO}_2$  is

Table 2

Saturation state of the waters with respect to different mineral phases.

	AR1	AR2	F1	F2
Log $p\text{CO}_2(\text{g})$	-1.59	-1.81	-1.58	-1.84
Calcite	0.08	0.20	0.14	0.39
Dolomite	-0.29	0.13	0.14	0.64
Anhydrite	-0.48	-0.50	-0.41	-0.40
Gypsum	-0.37	-0.36	-0.31	-0.30
Fluorite	-0.31	-0.27	-0.98	-0.95
Halite	-3.96	-4.01	-4.56	-4.56
Quartz	0.57	0.63	0.31	0.32
Chalcedony	0.30	0.35	0.03	0.05
Albite	1.84	2.73	0.36	0.53
K-Feldspar	1.91	2.95	0.93	1.13
Kaolinite	4.04	5.57	2.79	2.58
Pyrophyllite	3.22	4.81	1.43	1.25
Laumontite	1.18	2.81	-0.54	-0.24

higher than the atmospheric value in all the cases,  $-1.6$  in F1 and AR1 and about  $-1.81$  in F2 and AR2, which might produce  $\text{CO}_2$  outgassing process with variable intensity and carbonate phases saturation states with variable values in the springs.

All the waters are undersaturated with respect to fluorite and to the evaporitic phases. However, fluorite is more undersaturated in Fitero while the saturation states of anhydrite and gypsum are quite similar in both systems (between  $-0.4$  and  $-0.5$  in the case of anhydrite and between  $-0.3$  and  $-0.37$  in the case of gypsum). All the samples are highly undersaturated with respect to halite.

Quartz and chalcedony are slightly oversaturated in all thermal waters, although the Fitero samples are closer to equilibrium, especially with chalcedony ( $IS = 0.02$  and  $0.03$ ). Finally, all the samples are also oversaturated with respect to the aluminosilicate phases considered in the calculations: albite, K-feldspar, kaolinite, pyrophyllite and laumontite. The only exception is the case of laumontite which is undersaturated in the Fitero samples. In all cases, the saturation states of the aluminosilicate phases are higher in the Arnedillo waters, probably associated with their higher dissolved aluminium contents (Table 1).

#### 4.3. Geothermometry

##### 4.3.1. Chemical geothermometers

Table 3 shows the results obtained for the samples considered in this study by using various chemical geothermometers. Compared with the Arnedillo results, the temperatures obtained with the silica geothermometers are lower in the Fitero samples. The  $\text{SiO}_2$ -quartz geothermometer provides a temperature of about  $80^\circ\text{C}$  for the Arnedillo samples and about  $70^\circ\text{C}$  for the Fitero ones. A similar situation occurs with the  $\text{SiO}_2$ -chalcedony geothermometers, giving a temperature of  $50^\circ\text{C}$  for Arnedillo and of  $40^\circ\text{C}$  for Fitero. This temperature is similar or lower than the discharge temperature and therefore, the phase most likely controlling the dissolved silica contents is quartz and not chalcedony in both systems.

Despite having provided coherent results in Arnedillo thermal waters, some of the cationic geothermometers provide too high temperatures in the case of Fitero. The calibrations considered for the Na-K geothermometer provide temperatures in the range of  $133 - 160^\circ\text{C}$ . This geothermometer is usually considered inappropriate for low temperature carbonate evaporitic systems because waters are not expected to reach the equilibrium with the mineral phases on which they are based. This situation has been checked with the Giggenbach diagram (Fig. 3), where Arnedillo thermal waters are plotted in the field of partially equilibrated waters whereas Fitero thermal waters are close to the immature waters field. This different behaviour supports again the hypothesis of different local flow paths or residence times in the geothermal reservoir.

From the cationic geothermometers only the K-Mg provides

**Table 3**  
Temperatures (°C) obtained with different chemical and isotopic geothermometers and calibrations for the Arnedillo and Fitero samples.

Geothermometer	Calibrate	AR1	AR2	F1	F2
SiO <sub>2</sub> -quartz	Truesdell, 1976	81	78	70	71
	Fournier (1977)	80	78	70	71
	Michard (1979)	82	80	71	72
SiO <sub>2</sub> -chalcedony	Fournier (1977)	49	47	38	40
	Arnórsson et al. (1983)	52	50	42	43
Na-K	Giggenbach (1988)	97	105	153	160
	Fournier (1979)	75	84	133	136
	Verma and Santoyo (1997)	83	91	139	142
K-Mg	Giggenbach et al. (1983)	61	64	67	68
Na-K-Ca	Fournier and Truesdell (1973)	88	91	91	92
Ca-Mg	Chiodini et al. (1995)	116	117	108	107
SO <sub>4</sub> -F	Chiodini et al. (1995)	-10	-11	-36	-35
SO <sub>4</sub> -H <sub>2</sub> O ( $\delta^{18}\text{O}_{\text{HSO}_4\text{-H}_2\text{O}}$ )	Seal et al. (2000) <sup>1</sup>	66	64	64	60
	Friedman and O'Neil (1977)	69	68	66	64
SO <sub>4</sub> -H <sub>2</sub> O ( $\delta^{18}\text{O}_{\text{SO}_4\text{-H}_2\text{O}}$ )	Halas and Pluta (2000)	18	17	17	14
	Zeebe (2010)	25	25	24	21
SO <sub>4</sub> -H <sub>2</sub> O ( $\delta^{18}\text{O}_{\text{CaSO}_4\text{-H}_2\text{O}}$ )	Boschetti et al. (2011) <sup>2</sup>	75	74	73	70

<sup>1</sup> This calibration is the combination of those of Lloyd (1968) and Mizutani and Rafter (1969).

<sup>2</sup> This calibration is the combination of those of Chiba et al. (1981) and Zheng (1999).

temperatures similar to those obtained with the SiO<sub>2</sub>-quartz geothermometers, close to 70 °C. These two geothermometers have been identified in previous studies as the most suitable for low temperature carbonate-evaporitic systems (e.g. Apollaro et al., 2012; Pastorelli et al., 1999; Wang et al., 2015).

The results obtained with the rest of the geothermometers (Na-K-Ca and Ca-Mg) indicate higher temperatures. The Na-K-Ca (with  $\beta = 4/3$

as recommended by Fournier and Truesdell, 1973) provides results of 91 and 92 °C for the Fitero waters which are higher than expected (according to the results obtained with the SiO<sub>2</sub>-quartz geothermometers the expected results should be lower than in the Arnedillo waters); however, these results are in the accepted uncertainty range for these calculations ( $\pm 20$  °C; Fournier, 1982) and, therefore, they will be taken into account. The Ca-Mg geothermometer provides even higher temperatures (close to 110 °C) which are not coherent with the rest of values despite the fact that in a carbonate evaporitic system the equilibrium calcite-dolomite is expected to exist. Therefore, this higher temperature is probably due to the uncertainties associated with the order degree of dolomite (Chiodini et al., 1995) or to other secondary processes affecting the dissolved Ca or Mg contents. Finally, as previously indicated in Blasco et al. (2018), the SO<sub>4</sub>-F geothermometer provides incoherent results (negative temperatures; Table 3) since fluorite is not likely to be in the reservoir in amounts enough to control the contents of the waters.

Considering all these results and excluding the higher and the lower results previously mentioned, the temperature obtained for the Fitero reservoir with the chemical geothermometers is of  $81 \pm 11$  °C, which is slightly lower than the temperature previously deduced for Arnedillo thermal waters ( $87 \pm 13$  °C).

#### 4.3.2. Isotopic geothermometers

The results provided by the isotopic geothermometers are very similar for Fitero and Arnedillo thermal waters (Table 3), since the isotopic values are also very similar (Table 1):

1. The temperatures obtained with the calibrations based on the equilibrium exchange between HSO<sub>4</sub><sup>-</sup> and H<sub>2</sub>O are in the range of 60–69 °C for the four samples.
2. The calibrations based on the equilibrium exchange between the SO<sub>4</sub><sup>2-</sup> and H<sub>2</sub>O provide too low and incoherent temperatures, between 14 and 25 °C.

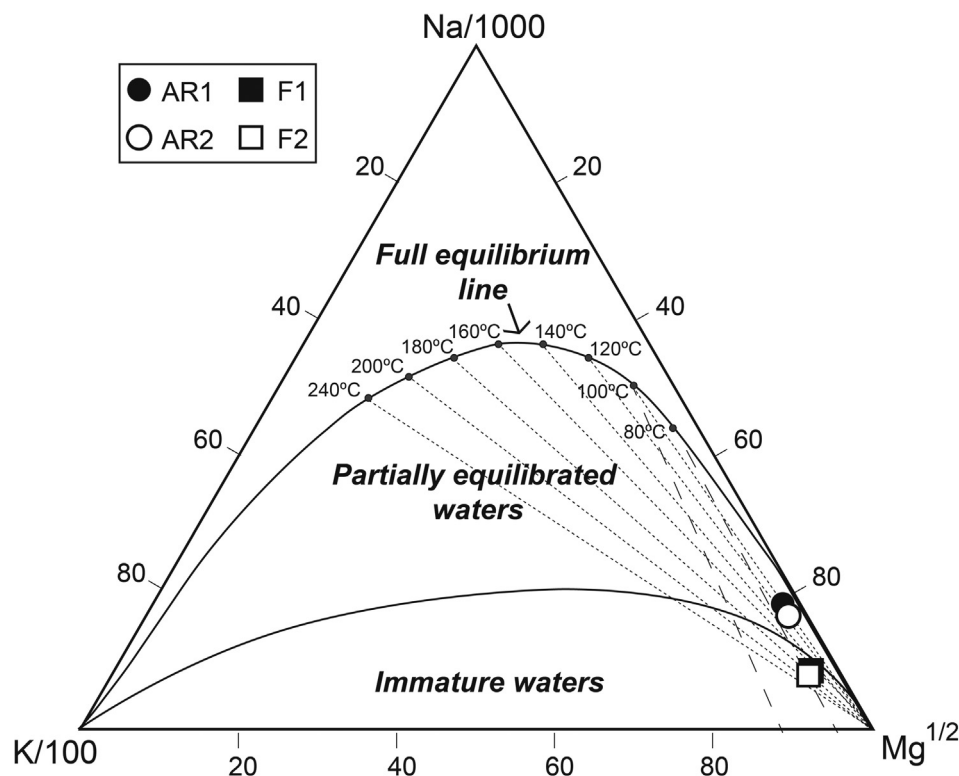


**Fig. 3.** Location of the Fitero and Arnedillo samples in the Giggenbach diagram. The dotted line is calculated with the Na-K Fournier (1979) calibration and with the Giggenbach (1988) one for Mg-K; the solid line is calculated with Na-K and Mg-K calibrations of Giggenbach (1988).

3. The calibration based on the equilibrium exchange between anhydrite ( $\text{CaSO}_4$ ) and  $\text{H}_2\text{O}$  (Boschetti, 2013), provides temperatures between 70 and 75 °C.

The temperatures obtained with this last calibration ( $\text{CaSO}_4\text{-H}_2\text{O}$  exchange) are the most reasonable ones since anhydrite is in equilibrium in the system (see below) and they are in the range previously defined with the chemical geothermometers. The bad results obtained with the calibration based on  $\text{SO}_4^{2-}$  (despite being the dominant sulphur species in this type of waters), are probably due to the lack of equilibrium between  $\text{SO}_4^{2-}$  and  $\text{H}_2\text{O}$  (Blasco et al., 2018, 2017; Boschetti et al., 2011). On the contrary, although, the  $\text{HSO}_4^-$  is not the main species, the calibration based on it provides good results because it is very similar to the  $\text{CaSO}_4\text{-H}_2\text{O}$  calibration in a  $10^3 \ln \alpha - 10^6/T^2$  plot (see Blasco et al., 2018).

#### 4.3.3. Geothermometrical modelling

The geothermometrical modelling of the Fitero waters shows that most of the minerals reach equilibrium at the range temperature between 71 and 82 °C, which agrees with the previous results obtained with the chemical and isotopic geothermometers. However, as already observed in the case of the Arnedillo samples (Blasco et al., 2018), calcite, dolomite and chalcedony reach equilibrium at a lower temperature: chalcedony indicates a temperature of about 50 °C, calcite of 29 °C for F1 and a negative temperature for F2, and dolomite of 47 °C for F1 and 23 °C for F2. Albite and K-feldspar also reach equilibrium at low temperature, about 50 and 60 °C, respectively. The lower equilibrium temperature obtained for chalcedony confirms that the phase controlling the dissolved silica in these thermal waters is quartz. Considering that calcite and dolomite should be in equilibrium in this geothermal system, the lack of agreement with the rest of the mineral assemblage must be related to an outgassing process during the ascent of thermal waters to surface, as it also occurs in the Arnedillo system (the  $\log p\text{CO}_2$ , is much higher than the atmospheric value, Table 2; Blasco et al., 2018). To reconstruct the conditions of thermal waters at depth an increase of the  $\text{CO}_2$  contents from 3.4 mmol/l in F1 and 3.2 mmol/L in F2 up to 4.9 mmol/L ( $\text{pH} = 6.3$ ) has been simulated as it was done in Arnedillo (5 mmol/L in that case; Blasco et al., 2018) following the recommendations from Pang and Reed (1998) and Palandri and Reed (2001). The amount of  $\text{CO}_2$  added is the necessary to adjust the calcite equilibrium temperature in the same range as the rest of the minerals (calcite is used instead of dolomite since it is less affected by

**Table 4**

Temperatures (°C) at which the different mineral phases considered converge towards equilibrium in the geothermometrical modelling for the Fitero and Arnedillo samples.

Mineral phase	F1	F2	AR1	AR2
Calcite	79	79	91	92
Dolomite	74	74	83	83
Quartz	71	72	97	94
Anhydrite	82	82	88	87
Albite	50	53	85	99
K-feldspar	60	62	78	91
Pyrophyllite	60	71	91	107

thermodynamic uncertainties). Fig. 4 and Table 4 show the results obtained with the geothermometrical modelling after the reconstruction of the water conditions at depth (the Arnedillo results have also been included in the table).

The results obtained from the aluminosilicate phases for the Fitero thermal waters are almost the same for both samples and slightly lower than those obtained for Arnedillo. The phases considered in the modelling (albite, K-feldspar and pyrophyllite) provide a low temperature (Fig. 4 and Table 4). One possible reason for this result can be related to the very low aluminium concentration in the Fitero waters. In order to ascertain whether this lower aluminium concentration was due to an analytical error, the aluminium analyses were repeated in a different laboratory obtaining the same range of values. Additionally several theoretical simulations have been performed increasing the aluminium content of the waters (Figure S1 of the Supplementary Material) and the results suggest that thermal waters are in real disequilibrium with respect to the aluminosilicate phases, since the amount of aluminium necessary to make the saturation state to converge with albite and K-feldspar (providing a temperature about 100 °C), would be 0.4 ppm (see the explanation presented in the Supplementary Material) which is much higher than the concentrations measured in the Arnedillo waters (0.01 to 0.06 ppm), where these phases are close to equilibrium. This is coherent with the results obtained with the chemical geothermometers, which also suggest the disequilibrium of Fitero thermal waters with respect to the aluminosilicate phases.

After this discussion the main results indicate that, without considering the aluminosilicate phases, since they do not represent an equilibrium situation, the temperature predicted for the Fitero samples

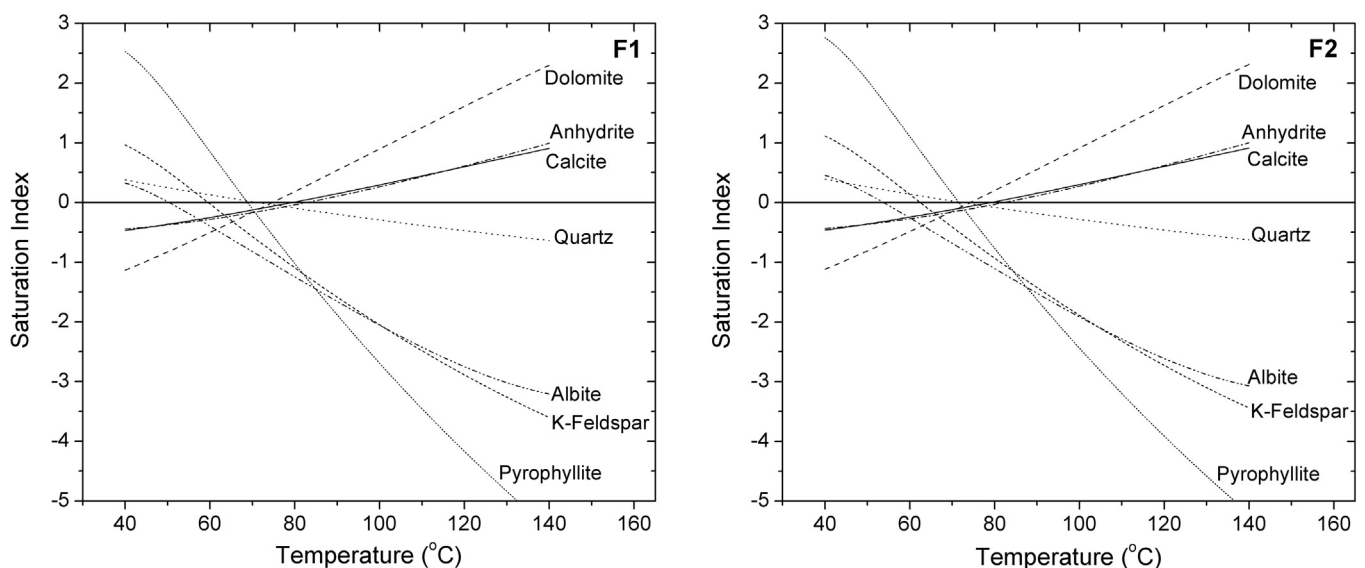


**Fig. 4.** Evolution with temperature of the saturation indices of the different minerals supposed to be in equilibrium with the water of the Fitero samples. These results were obtained after the theoretical reconstruction of the waters at depth by adding  $\text{CO}_2$  to compensate the  $\text{CO}_2$  outgassing during the ascent of the waters.

is in a range between 71 and 84 °C, that is,  $78 \pm 7$  °C. This result is in clear agreement with the previously obtained with the chemical and isotopic geothermometers. Combining all the results, a reliable range of temperature of  $81 \pm 11$  °C for the reservoir of the Fitero thermal waters can be established. This temperature is similar, although slightly lower, than the temperature deduced for the reservoir of Arnedillo thermal waters,  $87 \pm 13$  °C, by Blasco et al. (2018).

#### 4.3.4. Geochemical modelling

As mentioned above, thermal waters that emerge in the Fitero and Arnedillo springs show similar chemical and physico-chemical characteristics but also some differences suggesting that, although belonging to the same reservoir, their exact flow paths and/or their residence times differ and they undergo different intensities of water-rock interaction processes. According to the results shown in this paper, the Fitero thermal waters are less saline and more immature than thermal waters in Arnedillo. Thus, although they are not directly connected, an evolutionary geochemical path from the chemical characteristics represented by the Fitero thermal waters towards the more evolved Arnedillo thermal waters is interpreted to exist in the reservoir.

Inverse and direct modelling calculations have been performed (using one sample from each system, AR1 and F1) to assess the possible water-rock interaction processes responsible for the evolution and their intensities. The simplest calculation is the inverse modelling (mass balance) only considering the chemical characteristics of the waters (see Table 1 and compare the chemical values of the samples), which identify the most probable mass transfers in the reservoir. Then the results obtained with this calculation and their interpretation will be checked and completed with the direct modelling (reaction path). These two types of calculations have been performed considering the following assumptions:

- The mineral phases which the waters can interact with are: halite, anhydrite, calcite, dolomite, quartz, albite and K-feldspar.
- Cation exchange involving Na, Ca and Mg is also considered in the models.
- In order to reproduce the conditions at depth, the characteristics of the thermal waters have been adjusted according to the following: a) the calculations have been performed at the temperatures calculated for the reservoir; b) the amount of CO<sub>2</sub> (and, therefore, the pH values) has been modified to avoid the effect of the CO<sub>2</sub> outgassing in surface; and c) the waters have been equilibrated with the minerals found in equilibrium at the reservoir temperature (i.e. the Fitero water has been equilibrated with calcite, dolomite, anhydrite and quartz at 81 °C, and the Arnedillo water has been equilibrated with calcite, dolomite, anhydrite, quartz, albite and K-feldspar at 87 °C).

#### 4.3.5. Mass-balance calculations

These calculations have been performed with the inverse modelling capacities of PHREEQC taking the Fitero waters (F1) as initial solution and the Arnedillo waters (AR1) as final solution. The uncertainty allowed in the calculations is 3% (see Parkhurst and Appelo, 2013 for more details). Sixteen models have been obtained (Table 5) indicating the following mass transfers:

1. The highest mass transfer found in the models is the dissolution of about 45 mmol/L of halite.
2. About 1.4 mmol/L of anhydrite dissolve.
3. 0.56 mmol/L of albite precipitate in all models and almost the same amount of K-feldspar dissolves indicating an albitisation process.
4. Some models do not show any mass transfer affecting quartz but in others, a small dissolution occurs (0.07 mmol/L).
5. The results for calcite and dolomite are more variable in the various models: a) no mass transfer for calcite but dolomite dissolution (lower than 0.05 mmol/L); b) no mass transfer for dolomite but calcite dissolution (always lower than 0.1 mmol/L); c) calcite

dissolution (about 1.2 mmol/L) and dolomite precipitation (about 0.5 mmol/L); and d) dolomite dissolution and calcite precipitation (a dedolomitisation process), which are the cases in which the higher mass transfer takes place (about 2.5 mmol/L of dissolved dolomite and 5 mmol/L of precipitated calcite).

6. Finally, the Na exchanger (NaX) releases about 6 mmol/L and the Ca and Mg exchangers (CaX<sub>2</sub> and MgX<sub>2</sub>), in some cases, remove these elements from the waters in different ways: a) CaX<sub>2</sub> removes about 2.4 mmol/L and MgX<sub>2</sub> about 0.6 mmol/L; b) CaX<sub>2</sub> removes about 3 mmol/L and there is no transfer affecting MgX<sub>2</sub>; and c) MgX<sub>2</sub> removes about 3 mmol/L and there is no transfer affecting CaX<sub>2</sub>.

Compared with the expected mass transfers and reactions that can be deduced from the elemental differences between the initial and final solutions (Table 1), the following conclusions can be indicated:

- Chloride content in Arnedillo is 46 mmol/L higher than in Fitero and halite is assumed to be the only control of this element. The results obtained in all the models agree with this.
- Sulphate content in the Arnedillo water is about 2 mmol/L higher than in Fitero, and anhydrite seems to be the only controlling mineral for dissolved sulphate. Therefore, although the waters in both systems are in equilibrium with respect to anhydrite, this mineral seems to be dissolving due to the changes in salinity produced by halite dissolution (e.g. Li and Duan, 2011).
- Anhydrite dissolution will increase the calcium content of waters leading to the oversaturation and precipitation of calcite, which will explain the slightly lower contents of calcium in the Arnedillo waters (Table 1). Calcite precipitation causes an increase in the H<sup>+</sup> and the pCO<sub>2</sub> producing the dissolution of dolomite. This situation will explain the lower pH and higher pCO<sub>2</sub> (when the conditions at depth are theoretically reconstructed) in Arnedillo thermal waters. As a result, only the models that consider a dedolomitisation process seem to be plausible (Table 5).
- The dedolomitisation would also produce an increase in the dissolved magnesium in Arnedillo thermal waters which is not observed (Table 1). Therefore, an additional process should be removing the magnesium from the waters. The Mg sink that other authors have considered as the most likely in systems where dedolomitisation was also the driving process (e.g. Madison Aquifer; Busby et al., 1991; Jacobson and Wasserburg, 2005; Plummer et al., 1990) is the existence of a cationic exchange process where Na is released to the waters while Mg or Mg + Ca are uptaken. This situation also seems to be the most probable one in this system and it is coherent with some of the models obtained (those in which the dedolomitisation also takes place; Table 5).
- Finally, the increase of the Na dissolved contents as a result of halite dissolution can produce the albite precipitation which is associated with the K-feldspar dissolution (albitisation process).

In summary, the main processes responsible for the chemical evolution of these waters in the geothermal reservoir seem to be the dedolomitisation and albitisation processes and their thermodynamic feasibility will be checked with the reaction-path calculations.

#### 4.3.6. Reaction-path calculations

These calculations will consider the dedolomitisation and albitisation processes triggered by halite and anhydrite dissolution; to make the calculations simple, the cationic exchange is not included because the information that would be necessary (amount of exchangers and their exchange capacity) is not available and its consideration is not decisive for the verification of the feasibility of the main processes.

The first reaction-path calculation consisted of forcing the Fitero waters (F1), at 81 °C, to dissolve 46 mmol/L of halite while mineral equilibria with calcite, dolomite, quartz, anhydrite, albite and K-feldspar is maintained.

**Table 5**

Different models obtained in the mass balance calculation between samples F1 and AR1 as initial and final solutions, respectively. The mass transfer of the mineral phases and the cationic exchanges are given in mmol/L (negative means precipitation whilst positive means dissolution). The models selected as most plausible are: model 5, model 6, model 12 and model 15.

Model	Halite	Calcite	Anhydrite	Dolomite	Quartz	Albite	K-feldspar	NaX	CaX <sub>2</sub>	MgX <sub>2</sub>
1	44.51	0.00	1.38	0.04	0.07	-0.56	0.56	5.97	-2.39	-0.59
2	44.51	0.00	1.38	0.02	0.00	-0.54	0.56	5.95	-2.40	-0.57
3	44.51	1.19	1.38	-0.55	0.07	-0.56	0.56	5.97	-2.99	0.00
4	44.51	1.14	1.38	-0.55	0.00	-0.54	0.56	5.95	-2.97	0.00
5	44.51	-4.78	1.38	2.43	0.07	-0.56	0.56	5.97	0.00	-2.99
6	44.51	-4.74	1.38	2.39	0.00	-0.54	0.56	5.95	0.00	-2.97
7	44.51	0.00	1.38	0.02	0.00	-0.54	0.56	5.95	-2.40	-0.57
8	44.51	0.09	1.38	0.00	0.07	-0.56	0.56	5.97	-2.43	-0.55
9	44.51	0.04	1.38	0.00	0.00	-0.54	0.56	5.95	-2.39	-0.58
10	44.51	0.00	1.38	0.04	0.07	-0.56	0.56	5.97	-2.39	-0.59
11	44.51	1.14	1.38	-0.55	0.00	-0.54	0.56	5.95	-2.97	0.00
12	44.51	-4.74	1.38	2.39	0.00	-0.54	0.56	5.95	0.00	-2.97
13	44.51	0.04	1.38	0.00	0.00	-0.54	0.56	5.95	-2.39	-0.58
14	44.51	1.19	1.38	-0.55	0.07	-0.56	0.56	5.97	-2.99	0.00
15	44.51	-4.78	1.38	2.43	0.07	-0.56	0.56	5.97	0.00	-2.99
16	44.51	0.09	1.38	0.00	0.07	-0.56	0.56	5.97	-2.43	-0.55

**Table 6**

Results obtained in the reaction-path calculation. The composition of the resulting water is shown and, for comparison, the composition of the Arnedillo water. The mass transfers of the considered phases are also shown (positive values mean precipitation whilst negative values mean dissolution).

	Final water (mmol/L)	Arnedillo water (mmol/L)	Mineral phase	Mass transfer (mmol/L)
HCO <sub>3</sub> <sup>-</sup>	2.84	2.92	Calcite	0.5
SO <sub>4</sub>	16.2	15.5	Dolomite	-0.25
Cl	91.6	91.5	Anhydrite	-2.1
Na	88.5	92	Albite	0.4
Ca	14.4	11.5	K-feldspar	-0.4
Mg	2.9	2.1	Quartz	0.01
Si	0.5	0.6		
K	1.2	1.3		

The thermodynamic results show a small precipitation of quartz (0.01 mmol/L), dissolution of anhydrite, K-feldspar and dolomite, and precipitation of albite and calcite. That is, the simulations evidence that the addition of NaCl (i.e. halite dissolution) produces albitisation and, especially, dedolomitisation, supporting the conclusions obtained previously from the mass balance calculations and excluding the rest of the obtained mass balance models. The obtained mass transfers are shown in Table 6 and Fig. 5, and the changes produced in the elemental contents are shown in Fig. 6. The composition of the final water obtained after the reaction path calculation (Table 6) is quite similar to the composition of the Arnedillo water at depth. Dedolomitisation processes have been identified in groundwater systems at very different depths and conditions: in shallow, low temperature and fresh water environments (e.g. Bischoff et al., 1994; Cañaveras et al., 1996; López-Chicano et al., 2001; Moral et al., 2008), in deeper aquifers and thermal waters with variable salinity (e.g. Auqué et al., 2009; Back et al., 1983; Blasco et al., 2017; Frondini, 2008; Plummer et al., 1990; Prado-Pérez

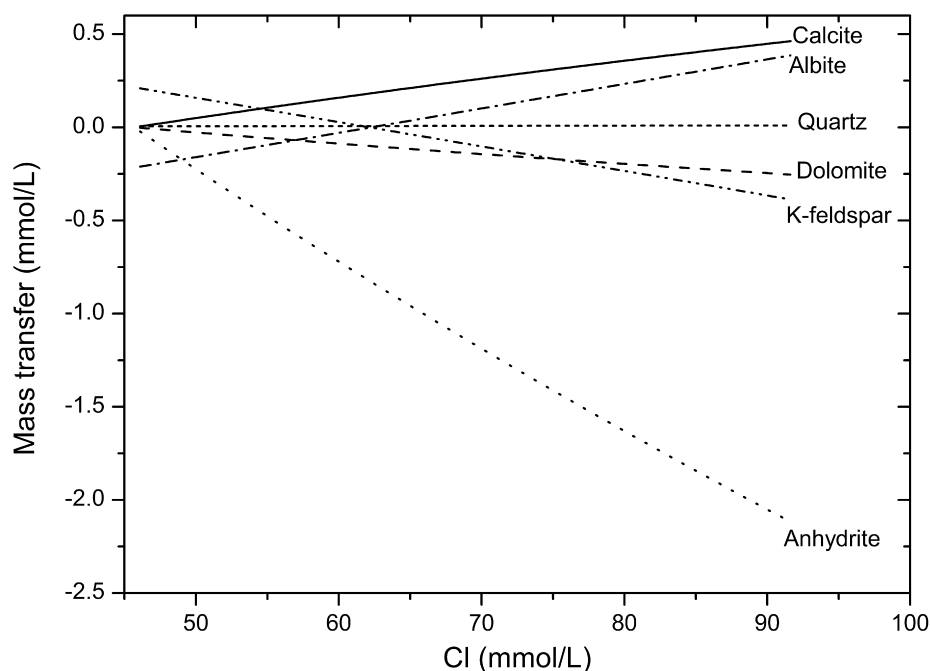


**Fig. 5.** Mass transfers of the different mineral phases when the water of the Fitero sample, with Cl<sup>-</sup> = 45.6 mmol/L, dissolves 46 mmol/L of halite (represented by the increase in the Cl<sup>-</sup> concentration) Negative and positive slopes indicate dissolution and precipitation, respectively.

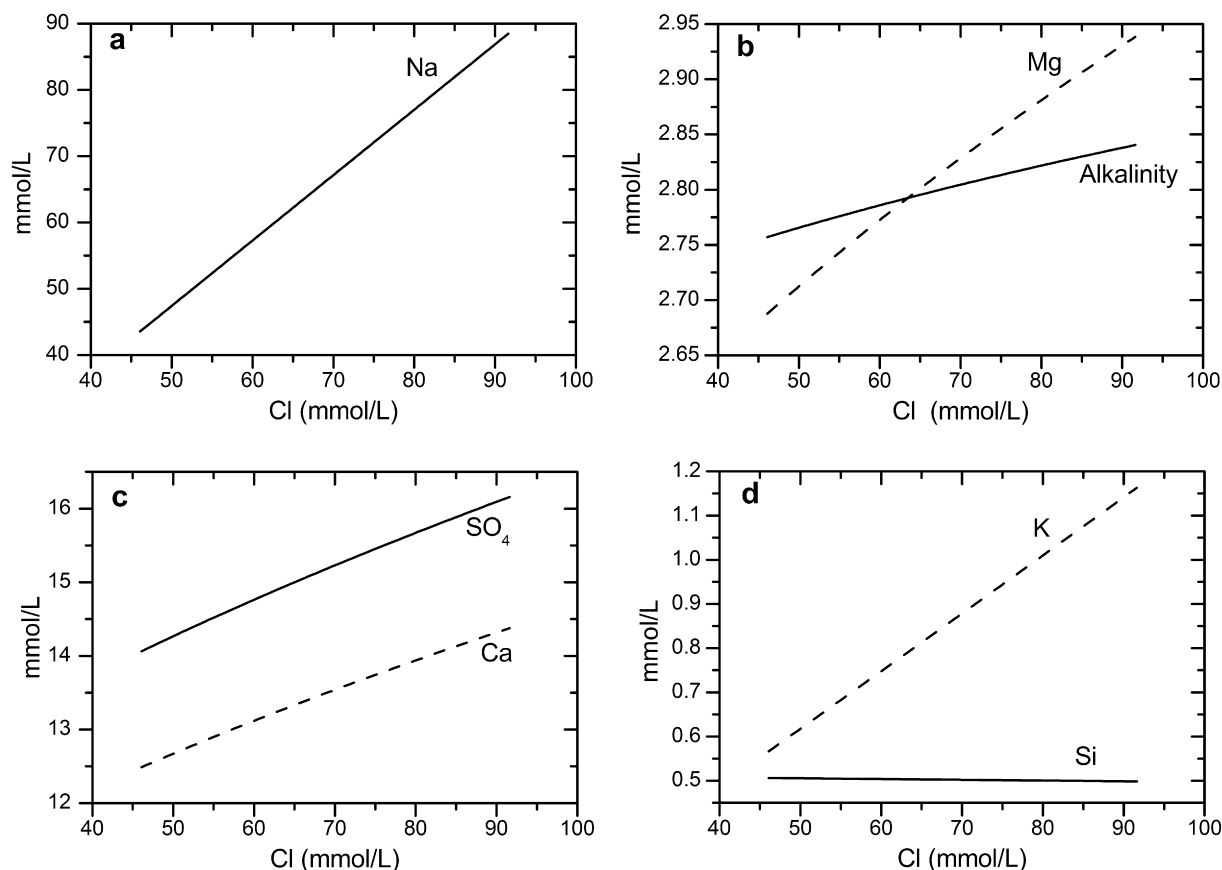


Fig. 6. Changes in the elemental contents in the Fitero waters, with  $\text{Cl}^- = 45.6 \text{ mmol/L}$ , when  $46 \text{ mmol/L}$  of halite are dissolved (represented by the increase in the  $\text{Cl}^-$  concentration).

and Pérez del Villar, 2011) and even in brines during burial diagenesis (e.g. Budai et al., 1984; Stoessell et al., 1987; Woo and Moore, 1996 and references therein).

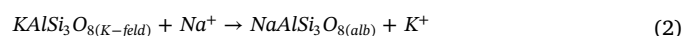
Albitisation processes (like the K-feldspar albitisation deduced in this study) are usually developed in groundwater systems at temperatures higher than  $60^\circ\text{C}$  (e.g. Aagaard et al., 1990) but they have also been observed in thermal waters at similar temperatures (around  $85^\circ\text{C}$ ) and salinities (TDS about  $8000 \text{ ppm}$ ) to the ones studied here (Blasco et al., 2017) or, more often, in more saline formation or interstitial waters in sedimentary basins at higher temperatures (e.g. Aagaard et al., 1990; Dias Lima and De Ros, 2002; Egeberg and Aagaard, 1989; Hanor, 1996; Saigal et al., 1988 and references therein). That is, the two main processes identified in this system can take place in other situations and under different pH ( $\text{pCO}_2$ ), temperature and salinity conditions.

In order to make these findings more general, some additional simulations have been performed to assess the effects of different physicochemical conditions on the main processes identified (dedolomitisation and albitisation). For this, sample F1 has been considered as the initial solution and it has been forced to dissolve up to  $2000 \text{ mmol/L}$  of halite (ionic strength close to 2). Then the various conditions considered have been 1) a variation of pH between 6 and 8, since this is the most common range of pH in natural systems, and 2) a range of temperature from  $25$  to  $200^\circ\text{C}$ . The LLNL database (using low albite and the same dolomite as in the WATEQ4F database) has been used to carry out this calculation because the WATEQ4F database was developed to be used up to  $100^\circ\text{C}$  and at higher temperatures the results should be carefully considered (Ball and Nordstrom, 2001), while temperature range of the LLNL database is up to  $300^\circ\text{C}$  (Johnson et al., 2000).

The most important results are shown in Table 7, Fig. 7 and Figure S2 (in the Supplementary Material; Fig. 7 contains the results obtained

at  $\text{pH} = 6$  and the results obtained at  $\text{pH} = 7$  and  $\text{pH} = 8$  are in the Supplementary Material since they are almost the same as those for  $\text{pH} = 6$ ). Albitisation and dedolomitisation processes, along with anhydrite dissolution, are more intense as salinity increases in all the simulations. Dolomite dissolution and calcite precipitation, that is, the dedolomitisation process, is more intense at lower temperatures (Fig. 7a and Figure S2a-b) as it was also pointed out by Escorcia et al. (2013). The effect of pH is of minor importance and almost imperceptible in Fig. 7a and Figure S2a-b, and while dolomite dissolution is almost the same with the increase of pH, the calcite precipitation is somewhat higher being most important at higher temperatures (Table 7). The dissolution of anhydrite is more intense at low temperatures and it is almost unaffected by the variation of the pH (Fig. 7b, Figure S2c-d, Table 7). Finally, the albitisation process displays the opposite behaviour (Table 7, Fig. 7c and Figure S2 e-f): the amount of albite precipitated is always the same as the amount of dissolved K-feldspar being more intense at higher temperatures and not affected by the pH variations.

Considering all these results it is clear that halite dissolution and, therefore, the increase of the salinity of the waters, can be a relevant controlling factor for the hydrochemical evolution of the waters. Halite dissolution increases the Na dissolved contents and by the ion-common effect the albitisation process takes place (Eq. (2)):



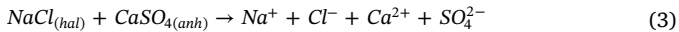
On the other hand, anhydrite solubility is highly influenced by the salinity of the waters due to the salting-in effect (Langmuir, 1997), in the way that the increase in the salinity will lead to a higher solubility of anhydrite (e.g. Li and Duan, 2011; Raines and Dewers, 1997). Therefore, halite dissolution enhances anhydrite dissolution (Eq. (3)):



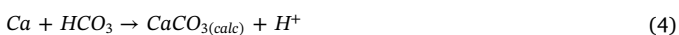
**Table 7**

Total mass transfers obtained in the reaction-path calculation when 2000 mmol/L of halite are dissolved at pH of 6, 7 and 8 and temperatures of 25, 100 and 200 °C. The results are expressed in mmol/L (positive values mean precipitation and negative values mean dissolution).

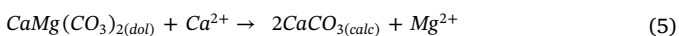
	pH = 6			pH = 7			pH = 8		
	25 °C	100 °C	200 °C	25 °C	100 °C	200 °C	25 °C	100 °C	200 °C
Calcite	48.9	5.2	0.5	51.2	5.6	0.6	51.3	5.6	0.8
Dolomite	-23.4	-2.9	-0.4	-26.6	-2.8	-0.4	-26.3	-2.8	-0.4
Anhydrite	-61.3	-21.5	-4.9	-63	-21.7	-4.9	-63	-21.7	-4.9
Albite	1.9	16	77	1.9	16	77	1.9	16	77
K-Feldspar	-1.9	-16	-77	-1.9	-16	-77	-1.9	-16	-77



Anhydrite dissolution increases the calcium content of the waters (as shown in Eq. (3)) and, given that waters are in equilibrium with respect to calcite, the excess of Ca will produce the oversaturation of calcite and, therefore, its precipitation (common-ion effect; Eq. (4)):



At the same time calcite precipitation leads to a decrease in calcium and  $\text{HCO}_3^-$  in the solution (Eq. (4)) and to an increase in the  $\text{H}^+$  and the  $\text{pCO}_2$  which triggers the dissolution of dolomite (dedolomitisation process; Eq. (5)):



This dedolomitisation process, triggered by anhydrite (or gypsum) dissolution, has been reported in other carbonate aquifers, containing dolostones and in contact with anhydrite or gypsum (Appelo and Postma, 2005; Auqué et al., 2009; Back et al., 1983; Capaccioni et al., 2001; Cardenal et al., 1994; Choi et al., 2012; Deike, 1990; Frondini, 2008; Leybourne et al., 2009; López-Chicano et al., 2001; Plummer, 1977; Plummer et al., 1990; Prado-Pérez and Pérez del Villar, 2011; Sacks et al., 1995). However, in the case presented here, although anhydrite dissolution is the direct triggering reaction for the dedolomitisation, the process actually responsible of it is the dissolution of halite. Halite dissolution keeps the dedolomitisation process ongoing even when the waters reach the equilibrium with anhydrite (or gypsum).

Finally, the dissolution of halite also triggers the albitisation process and, although this had previously been identified in diagenetic environments (Egeberg and Aagaard, 1989; Hanor, 1996; Saigal et al., 1988), the results shown in this paper indicate that this process is also feasible in groundwater (thermal) systems at lower temperatures and salinities.

Overall, these results are also relevant for the geological  $\text{CO}_2$  storage in saline aquifers or, even, for enhanced geothermal systems (EGS) where saline waters, initially in equilibrium with the reservoir rocks, are usually involved. The evolution of the dedolomitisation processes has been identified as a critical point in assessing carbonate formations for potential  $\text{CO}_2$  storage (e.g. Auqué et al., 2009; Prado-Pérez and Pérez del Villar, 2011 and references therein). And albitisation processes have been identified in  $\text{CO}_2$ -brine-rock interaction experiments at in situ P-T conditions of the pilot  $\text{CO}_2$  storage site at Ketzin in Germany (Fischer et al., 2010) and in the experiments with hydrothermal Na-Cl solutions on fracture surfaces in the geothermal reservoir of the Upper Rhine Graben (Schmidt et al., 2017). Therefore, the evolution and consequences of the processes identified in this paper should be further explored.

## 5. Conclusions

The spring waters of the Fitero-Arnedillo geothermal system are located in the localities of the same name and separated about 35 km. They are hosted in carbonate-evaporitic materials and they are of chloride-sodium type with near neutral pH and discharge temperature of about 45 °C. The main differences between these waters are the

higher salinity of those emerging in Arnedillo, the slightly higher Ca and Mg contents in Fitero and the calculated reservoir temperature ( $81 \pm 11$  °C in Fitero and  $87 \pm 13$  °C in Arnedillo). All these together with the mineral equilibria in the reservoir indicate that, although the waters belong to the same geothermal reservoir, they evolve along different flow paths with different intensities of water-rock interaction processes which would justify a more evolved stage of the Arnedillo system compared to the Fitero thermal waters.

Mass-balance and reaction path calculation have been used to assess the main reactions responsible for the chemical differences and evolution of these waters and the results indicate that the triggering process is the halite dissolution, which leads to an albitisation process and to the dissolution of anhydrite, which, in turn, triggers the calcite precipitation and the dolomite dissolution (dedolomitisation process). The processes identified in this system (dedolomitisation and albitisation) have been identified in different environments under different conditions of temperature, pH and/or salinities, and how these parameters affect them has also been evaluated in this paper. The extension of these processes is higher as the salinity of the waters increases. However, the effect of pH (assessed between 6 and 8) is almost negligible in terms of the mass transfers of the involved phases. Temperature also causes significant variations in a way that the dedolomitisation and anhydrite dissolution are higher at low temperatures and the albitisation is more intense at high temperatures.

These calculations have evidenced the importance that the changes in the salinity of the waters (through halite dissolution) have over the geochemical evolution of waters due to its effect in the water-mineral equilibria attained. Halite dissolution has been proven to trigger a dedolomitisation process even when the waters have reached the equilibrium with respect to anhydrite, calcite and dolomite. Moreover it has been shown that these processes are more general than what was known up to date and deserve future studies, mainly considering their feasibility in particularly relevant situations such as the enhanced geothermal systems and the geological  $\text{CO}_2$  storage sites.

## Acknowledgements

M. Blasco has worked in this study thanks to a scholarship from the Ministry of Science, Innovation and Universities of Spain, for the Training of University Teachers (ref. FPU14/01523). This study forms part of the activities of the Geochemical Modelling Group (University of Zaragoza; Aragón Government).

We are grateful to the staff of the Fitero and Arnedillo spas for their disposition and assistance during the sampling campaign. The technical assistance of Enrique Oliver, from the Earth Sciences Department of the University of Zaragoza, is acknowledged. The comments from two anonymous reviewers are also appreciated.

## Appendix A. Supplementary data

Supplementary data to this article can be found online at <https://doi.org/10.1016/j.jhydrol.2019.01.013>.

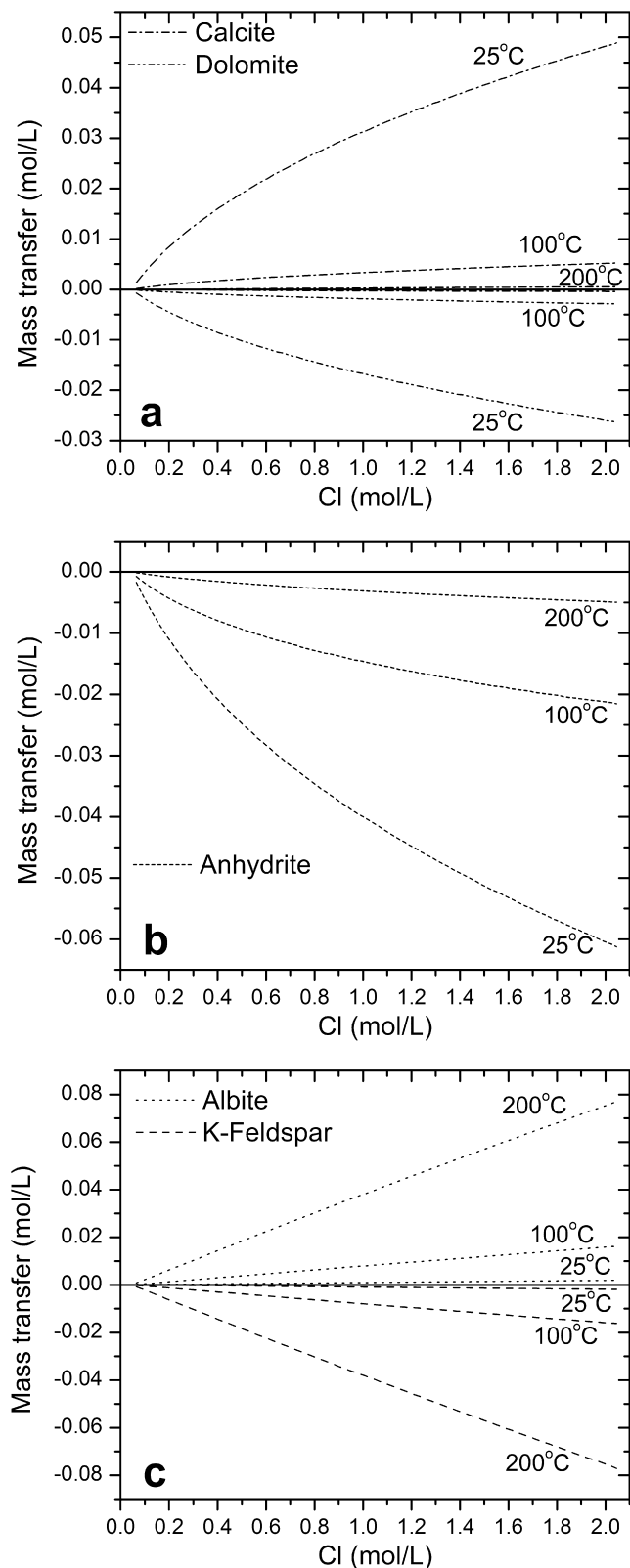


Fig. 7. Evolution of a) calcite precipitation and dolomite dissolution (dedolomitisation process); b) anhydrite dissolution; and c) albite precipitation and K-feldspar dissolution (albitisation process) with the increase of salinity (dissolution of halite) at different temperatures (25, 100 and 200 °C) and a pH = 6.

## Reference

Aagaard, P., Egeberg, P.K., Saigal, G.C., Morad, S., Bjorlykke, K., 1990. Diagenetic

- albitisation of detrital K-feldspar in Jurassic, Lower Cretaceous and Tertiary clastic reservoir rocks from offshore Norway, II. Formation water chemistry and kinetic considerations. *J. Sediment. Petrol.* 60, 575–581.
- Albert, J.F., 1979. Estudio geoquímico preliminar de Navarra. In: *II Simposio Nacional de Hidrogeología. Hidrogeología Y Recursos Hidráulicos IV. Sección Quinta: Técnicas Especiales. 22-26 de Octubre de 1979. Pamplona (España)*, pp. 511–531.
- Apollaro, C., Dotsika, E., Marini, L., Barca, D., Bloise, A., de Rosa, R., Doveri, M., Lelli, M., Muto, F., 2012. Chemical and isotopic characterization of the thermomineral water of Terme Sibarite springs (Northern Calabria, Italy). *Geochem. J.* 46, 117–129.
- Appelo, C.A.J., Postma, D., 2005. *Geochemistry, Groundwater and Pollution*, 2<sup>nd</sup> ed. A.A. Balkema, Rotterdam.
- Arnórsson, S., Gunnlaugsson, E., Svavarsson, H., 1983. The chemistry of geothermal waters in Iceland. III. Chemical geothermometry in geothermal investigations. *Geochim. Cosmochim. Acta* 47, 567–577.
- Asta, M.P., Gimeno, M.J., Auqué, L.F., Gómez, J., Acero, P., Lapuente, P., 2012. Hydrochemistry and geothermometrical modeling of low-temperature Panticosa geothermal system (Spain). *J. Volcanol. Geotherm. Res.* 235–236, 84–95.
- Asta, M.P., Gimeno, M.J., Auqué, L.F., Gómez, J., Acero, P., Lapuente, P., 2010. Secondary processes determining the pH of alkaline waters in crystalline rock systems. *Chem. Geol.* 273, 41–52.
- Auqué, L.F., Acero, P., Gimeno, M.J., Gómez, J.B., Asta, M.P., 2009. Hydrogeochemical modeling of a thermal system and lessons learned for CO<sub>2</sub> geologic storage. *Chem. Geol.* 268, 324–336.
- Auqué, L.F., Fernández, J., Tena Calvo, J.M., 1988. Las aguas termales de Fitero (Navarra) y Arnedillo (Rioja). I. Análisis geoquímico de los estados de equilibrio-desde equilibrio en las surgencias. *Estud. geológicos* 44, 285–292.
- Auqué, L.F., Mandado, J., López, P.L., Lapuente, P.L., Gimeno, M.J., 1998. Los sistemas geotermiales del Pirineo Central. III. Evaluación de las condiciones en profundidad y evolución de las soluciones hidrotermales durante su ascenso. *Estud. geológicos* 54, 25–37.
- Auqué, L.F., Mandado, J., López, P.L., Lapuente, P.L., Gimeno, M.J., 1997. Los sistemas geotermiales del Pirineo Central. II. Resultados de la aplicación de técnicas geotermométricas. *Estud. geológicos* 53, 45–54.
- Awaleh, M.O., Hoch, F.B., Boschetti, T., Soubaneh, Y.D., Egueh, N.M., Elmi, S.K., Mohamed, J., Khairah, M.A., 2015. The geothermal resources of the Republic of Djibouti – II: Geochemical study of the Lake Abhe geothermal field. *J. Geochemical Explor.* 159, 129–147.
- Back, W., Hanshaw, B.B., Plummer, L.N., Rahn, P.H., Rightmire, C.T., Rubin, M., 1983. Process and rate of dedolomitization: mass transfer and <sup>14</sup>C dating in a regional carbonate aquifer. *Geol. Soc. Am. Bull.* 94, 1415–1429.
- Ball, J.W., Nordstrom, D., 2001. User's manual for WATEQ4F with revised thermodynamic database and test cases for calculating speciation of major, trace and redox elements in natural waters. In: *U.S. Geological Survey (Ed.), Water-Resources Investigation Report. U.S. Geological Survey, Menlo Park (California)*, pp. 91–183.
- Bischoff, J.L., Juliá, R., Shanks III, W.C., Rosenbauer, R.J., 1994. Karstification without carbonic-acid: bedrock dissolution by gypsum-driven dedolomitization. *Geology* 22, 995–998.
- Blasco, M., Auqué, L.F., Gimeno, M.J., Acero, P., Asta, M.P., 2017. Geochemistry, geothermometry and influence of the concentration of mobile elements in the chemical characteristics of carbonate-evaporitic thermal systems. The case of the Tiermas geothermal system (Spain). *Chem. Geol.* 466, 696–709.
- Blasco, M., Gimeno, M.J., Auqué, L.F., 2018. Low temperature geothermal systems in carbonate-evaporitic rocks: Mineral equilibria assumptions and geothermometrical calculations. Insights from the Arnedillo thermal waters (Spain). *Sci. Total Environ.* 615, 526–539.
- Boschetti, T., 2013. Oxygen isotope equilibrium in sulfate-water systems: A revision of geothermometric applications in low-enthalpy systems. *J. Geochemical Explor.* 124, 92–100.
- Boschetti, T., Cortecci, G., Toscani, L., Iacumin, P., 2011. Sulfur and oxygen isotope compositions of Upper Triassic sulfates from northern Apennines (Italy): paleogeographic and hydrogeochemical implications. *Geol. Acta* 9, 129–147.
- Budai, J.M., Lohmann, K.C., Owen, R.M., 1984. Burial dedolomite in the Mississippian Madison Limestone, Wyoming and Utah Thrust Belt (USA). *J. Sediment. Petrol.* 54, 276–288.
- Buil, B., Gómez, P., Turrero, M.J., Garralón, A., Lago, M., Arranz, E., de la Cruz, B., 2006. Factors that control the geochemical evolution of hydrothermal systems of alkaline water in granites in Central Pyrenees (Spain). *J. Iber. Geol.* 32, 283–302.
- Busby, J.F., Plummer, L.N., Lee, R.W., Hanshaw, B.B., 1991. *Geochemical Evolution of Water in the Madison Aquifer in Parts of Montana, South Dakota, and Wyoming*, in: *U.S. Geological Survey Professional Paper 1273-F. United States Government Printing Office, Washington*, p. 89.
- Cañaveras, J.C., Sánchez-Moral, S., Calvo, J.P., Hoyos, M., Ordóñez, S., 1996. Dedolomites associated with karstification. An example of early dedolomitization in lacustrine sequences from the Tertiary Madrid Basin, Central Spain. *Carbonates Evaporites* 11, 85–103.
- Capaccioni, B., Didero, M., Paletta, C., Salvadori, P., 2001. Hydrogeochemistry of groundwaters from carbonate formations with basal gypsiferous layers: an example from the Mt Catria Mt Nerone ridge (Northern Apennines, Italy). *J. Hydrol.* 253, 14–26.
- Cardenal, J., Benavente, J., Cruz-Sanjulián, J.J., 1994. Chemical evolution of groundwater in triassic gypsum-bearing carbonate aquifers (Las Alpujarras, southern Spain). *J. Hydrol.* 161, 3–30.
- Chiodini, G., Frondini, F., Marini, L., 1995. Theoretical geothermometers and pCO<sub>2</sub> indicators for aqueous solutions coming from hydrothermal systems of medium-low temperature hosted in carbonate-evaporite rocks. Application to the thermal springs of the Etruscan Swell. Italy. *Appl. Geochemistry* 10, 337–346.

- Choi, B.Y., Yun, S.T., Mayer, B., Hong, S.Y., Kim, K.H., Jo, H.Y., 2012. Hydrogeochemical processes in clastic sedimentary rocks, South Korea: a natural analogue study of the role of dedolomitization in geologic carbon storage. *Chem. Geol.* 306–307, 103–113.
- Choi, H.S., Koh, Y.K., Bae, D.K., Park, S.S., Hutcheon, I., Yun, S.T., 2005. Estimation of deep-reservoir temperature of CO<sub>2</sub>-rich springs in Kangwon district, South Korea. *J. Volcanol. Geotherm. Res.* 141, 77–89.
- Clark, I., Fritz, P., 1997. *Environmental Isotopes in Hydrogeology*. CRC Press/Lewis Publishers, Boca-Raton (Florida).
- Coloma, P., 1998. El agua subterránea en La Rioja. *Zubía Monográfico* 10, 63–132.
- Coloma, P., Sánchez, J.A., Jorge, J.C., 1998. Simulación matemática del flujo y transporte de calor del sector oriental de la Cuenca de Cameros. *Zubía Monográfico* 10, 45–61.
- Coloma, P., Sánchez, J.A., Martínez, F.J., 1997a. Sistemas de flujo subterráneo regional en el acuífero carbonatado mesozoico de la Sierra de Cameros. *Sector Oriental. Estud. geológicos* 53, 159–172.
- Coloma, P., Sánchez, J.A., Martínez, F.J., 1996. Procesos geotérmicos causados por la circulación del agua subterránea en el contacto entre la Sierra de Cameros y la Depresión Terciaria del Ebro. *Geogaceta* 20, 749–753.
- Coloma, P., Sánchez, J.A., Martínez, F.J., 1995. El drenaje subterráneo de la cordillera Ibérica en la depresión terciaria del Ebro (sector Riojano). *Geogaceta* 17, 68–71.
- Coloma, P., Sánchez, J.A., Martínez, F.J., Pérez, A., 1997b. El drenaje subterráneo de la Cordillera Ibérica en la Depresión terciaria del Ebro. *Rev. la Soc. Geológica España* 10, 205–218.
- Craig, H., 1961. Isotopic variations in meteoric waters. *Science* (80-), 133, 1702–1703.
- ÁMore, F., Fancelli, R., Caboi, R., 1987. Observations of the application of chemical geothermometers to some hydrothermal systems in Sardinia. *Geothermics* 16, 271–282.
- Deike, R.G., 1990. Dolomite dissolution rates and possible Holocene dedolomitization of water-bearing units in the Edwards aquifer, south-central Texas. *J. Hydrol.* 112, 335–373.
- Dias Lima, R., De Ros, L.F., 2002. The role of depositional setting and diagenesis on the reservoir quality of Devonian sandstones from Solimoes Basin, Brazilian Amazonia. *Mar. Pet. Geol.* 19, 1047–1071.
- Díaz-Teijeiro, M.F., Rodríguez-Arévalo, J., Castaño, S., 2009. La Red Española de Vigilancia de Isótopos en la Precipitación (REVIP): distribución isotópica espacial y aportación al conocimiento del ciclo hidrológico. *Ing. Civ.* 155, 87–97.
- Egeberg, P.K., Aagaard, P., 1989. Origin and evolution of formation waters from oil fields on the Norwegian shelf. *Appl. Geochemistry* 4, 131–142.
- Escorcía, L.C., Gomez-Rivas, E., Daniele, L., Corbella, M., 2013. Dedolomitization and reservoir quality: Insights from reactive transport modelling. *Geofluids* 13, 221–231.
- Fernández, J., Aqueú, L.F., Sánchez Cela, V.S., Guaras, B., 1988. Las aguas termales de Fitero (Navarra) y Arnedillo (Rioja). II. Análisis comparativo de la aplicación de técnicas geotermométricas químicas a aguas relacionadas con reservorios carbonatado-evaporíticos. *Estud. geológicos* 44, 453–469.
- Fischer, S., Liebscher, A., Wandrey, M., 2010. CO<sub>2</sub>-brine-rock interaction - first results of long-term exposure experiments at in situ P-T conditions of the Ketzin CO<sub>2</sub> reservoir. *Chemie der Erde* 70, 155–164.
- Fouillac, G., Michard, G., 1981. Sodium/lithium ratio in water applied to geothermometry of geothermal reservoirs. *Geothermics* 10, 55–70.
- Fournier, R.O., 1982. Water geothermometers applied to geothermal energy. In: D'Amore, F. (Ed.), *Applications of Geochemistry in Geothermal Reservoir Development*. UNITAR/UNDO centre on Small Energy Resources, Rome, Italy, Italy, pp. 37–69.
- Fournier, R.O., 1981. *Application of water geochemistry to geothermal exploration and reservoir engineering*. In: Rybach, L. and Muffler, L.J.P. (Eds.), *Geothermal Systems: Principles and Case Histories*. John Wiley & Sons Ltd., New York, pp. 109–141.
- Fournier, R.O., 1977. Chemical geothermometers and mixing models for geothermal systems. *Geothermics* 5, 41–50.
- Fournier, R.O., 1979. A revised equation for the Na-K geothermometer. *Geotherm. Resour. Coun. Trans.* 3, 221–224.
- Fournier, R.O., Truesdell, A.H., 1973. An empirical Na–K–Ca geothermometer for natural waters. *Geochim. Cosmochim. Acta* 37, 1255–1275.
- Friedman, I., O'Neil, J.R., 1977. Compilation of stable isotope fractionation factors of geochemical interest. In: Fleischer, M. (Ed.), *Data on Geochemistry*, USGS Professional Paper 440-KK. United States Government Printing Office, Washington, pp. 109.
- Froncini, F., 2008. Geochemistry of regional aquifers hosted by carbonate-evaporite formations in Umbria and southern Tuscany (central Italy). *Appl. Geochemistry* 23, 2091–2104.
- Giggenbach, W.F., 1988. Geothermal solute equilibria. Derivation of Na-K-Mg-Ca geothermometers. *Geochim. Cosmochim. Acta* 52, 2749–2765.
- Giggenbach, W.F., Gonfiantini, R., Jangi, B.L., Truesdell, A.H., 1983. Isotopic and chemical composition of Parbati valley geothermal discharges, NW Himalaya. *India. Geothermics* 12, 199–222.
- Gil, A., Villalain, J.J., Barbero, L., González, G., Mata, P., Casas, A.M., 2002. Aplicación de Técnicas geoquímicas, geofísicas y mineralógicas al estudio de la Cuenca de Cameros. Implicaciones geométricas y evolutivas. *Zubía Monográfico* 14, 65–98.
- Gil, J., Arenas, B., Segura, M., García-Hidalgo, J.F., García, A., 2004. Revisión y correlación de las unidades litoestratigráficas del Cretácico Superior en la región central y oriental de España. *Rev. la Soc. Geológica España* 17, 249–266.
- Gökgöz, A., Tarkan, G., 2006. Mineral equilibria and geochemistry of the Dalaman-Köycegiz thermal springs, southern Turkey. *Appl. Geochemistry* 21, 253–268.
- Goy, A., Gómez, J.J., Yébenes, A., 1976. El Jurásico de la Rama Castellana de la Cordillera Ibérica (Mitad norte) I. Unidades litoestratigráficas. *Estud. geológicos* 32, 391–423.
- Gutiérrez, P., 1801. Descripción de los Reales Baños de Arnedillo y análisis de sus aguas. Imprenta Fermín Villalpando, Madrid.
- Halas, S., Pluta, I., 2000. Empirical calibration of isotope thermometer  $\delta^{18}\text{O}(\text{SO}_4^{2-})-\delta^{18}\text{O}(\text{H}_2\text{O})$  for low temperature brines. In: *V Isotope Workshop*. European Society for Isotope Research, Kraków, Poland, pp. 68–71.
- Hanor, J.S., 1996. Variations in chloride as a driving force in siliclastic diagenesis. *Siliclastic Diagenesis. Fluid Flow Concepts Appl. SEPM Spec. Publ.* 55, 3–12.
- Hanshaw, B.B., Back, W., 1985. Deciphering hydrological systems by means of geochemical processes. *Hydrological Sci. J.* 30, 257–271.
- Jacobson, A.D., Wasserburg, G.J., 2005. Anhydrite and the Sr isotope evolution of groundwater in a carbonate aquifer. *Chem. Geol.* 214, 331–350.
- Johnson, J., Anderson, G., Parkhurst, D., 2000. Database “thermo.com.V8.R6.230,” Rev. 1.11. Livermore, California.
- Kharaka, Y.K., Mariner, R.H., 1989. Chemical geothermometers and their application to formation waters from sedimentary basins. In: Naeser, N.D., McCollon, T.H. (Eds.), *Thermal History of Sedimentary Basins*. Springer, Berlin, pp. 99–117.
- Langmuir, D., 1997. *Aqueous environmental geochemistry*. Prentice Hall, Upper Saddle River, New Jersey.
- Leybourne, M.I., Betcher, R.N., McRitchie, W.D., Kaszycki, C.A., Boyle, D.R., 2009. Geochemistry and stable isotopic composition of tufa waters and precipitates from the Interlake Region, Manitoba. *Chem. Geol.* 260, 221–233.
- Li, J., Duan, Z., 2011. A thermodynamic model for the prediction of phase equilibria and speciation in the H<sub>2</sub>O–CO<sub>2</sub>–NaCl–CaCO<sub>3</sub>–CaSO<sub>4</sub> system from 0 to 250 °C, 1 to 1000 bar with NaCl concentrations up to halite saturation. *Geochim. Cosmochim. Acta* 75, 4351–4376.
- López-Chicano, M., Bouamama, M., Vallejos, A., Pulido-Bosch, A., 2001. Factors which determine the hydrogeochemical behaviour of karstic springs. A case study from the Betic Cordilleras, Spain. *Appl. Geochemistry* 16, 1179–1192.
- Mariner, R.H., Evans, W.C., Young, H.W., 2006. Comparison of circulation times of thermal waters discharging from the Idaho batholith based on geothermometer temperatures, helium concentrations, and 14C measurements. *Geothermics* 35, 3–25.
- Marini, L., 2004. *Geochemical techniques for the exploration and exploitation of geothermal energy*. Laboratorio di Geochimica, Università degli Studi di Genova, Genova.
- Mas, J.R., Alonso, A., Guimera, J., 1993. Evolución tectono-sedimentaria de una cuenca extensional intraplaca: la cuenca finijurásica-eocretácica de los Cameros (La Rioja-Soria). *Rev. la Soc. Geológica España* 6, 129–144.
- Mezquizar, M.A., 2004. Las termas romanas de Fitero. *Trab. Arqueol. Navarra* 17, 273–286.
- Michard, G., 1983. Recueil de données thermodynamiques concernant les équilibres eaux-minéraux dans les réservoirs géothermaux. Commission des Communautés Européennes, Luxembourg.
- Michard, G., 1979. *Geothermomètres chimiques*. Bur. Rech. Géologiques Minières (2nd Ser.). Sect. III 2, 183–189.
- Michard, G., Bastide, J.P., 1988. Géochimie de la nappe du Dogger du Bassin de Paris. *J. Volcanol. Geotherm. Res.* 35, 151–163.
- Michard, G., Grimaud, D., D'Amore, F., Fancelli, R., 1989. Influence of mobile ion concentration on the chemical composition of geothermal waters in granitic areas. Example of hot springs from Piemonte (Italy). *Geothermics* 18, 729–741.
- Michard, G., Roekens, E., 1983. Modelling of the chemical composition of alkaline hot waters. *Geothermics* 12, 161–169.
- Michard, G., Sanjuan, B., Criaud, A., Fouillac, C., Pentcheva, E.N., Petrov, P.S., Alexieva, R., 1986. Equilibria and geothermometry in hot alkaline waters from granites of S.W. Bulgaria. *Geochim. J.* 20, 159–171.
- Mohammadi, Z., Bagheri, R., Jahanshahi, R., 2010. Hydrogeochemistry and geothermometry of Changan thermal springs, Zagros region. *Iran. Geothermics* 39, 242–249.
- Moral, F., Cruz-Sanjulián, J.J., Ollás, M., 2008. Geochemical evolution of groundwater in the carbonate aquifers of Sierra de Segura (Betic Cordillera, southern Spain). *J. Hydrol.* 360, 281–296.
- Mutlu, H., Güleç, N., 1998. Hydrogeochemical outline of thermal waters and geothermometry applications in Anatolia (Turkey). *J. Volcanol. Geotherm. Res.* 85, 495–515.
- Palandri, J.L., Reed, M.H., 2001. Reconstruction of in situ composition of sedimentary formation waters. *Geochim. Cosmochim. Acta* 65, 1741–1767.
- Pang, Z., Reed, M.H., 1998. Theoretical chemical thermometry on geothermal waters: problems and methods. *Geochim. Cosmochim. Acta* 62.
- Parkhurst, D.L., Appelo, C.A.J., 2013. *Description of Input and Examples for PHREEQC Version 3. A Computer Program for Speciation, Batch Reaction, One Dimensional Transport, and Inverse Geochemical Calculations*. In: U.S. Geological Survey (Ed.), *Techniques and Methods*, Book 6, Chap. A43. U.S. Geological Survey, Denver, Colorado.
- Pastorelli, S., Marini, L., Hunziker, J.C., 1999. Water chemistry and isotope composition of the Acquarossa thermal system, Ticino, Switzerland. *Geothermics* 28, 75–93.
- Plummer, L.N., 1977. Defining reactions and mass transfer in part of the Floridan aquifer. *Water Resour. Res.* 13, 801–812.
- Plummer, L.N., Back, W., 1980. The mass balance approach: application to interpreting the chemical evolution of hydrologic systems. *Am. J. Sci.* 280, 130–142.
- Plummer, L.N., Busby, J.F., Lee, R.W., Hanshaw, B.B., 1990. Geochemical modelling of the Madison aquifer in parts of Montana, Wyoming, and South-Dakota. *Water Resour. Res.* 26, 1981–2014.
- Plummer, L.N., Parkhurst, D.L., Thorstenson, D.C., 1983. Development of reaction models for ground-water systems. *Geochim. Cosmochim. Acta* 47, 665–686.
- Prado-Pérez, A.J., Pérez del Villar, L., 2011. Dedolomitization as an analogue process for assessing the long-term behaviour of a CO<sub>2</sub> deep geological storage: The Alicún de las Torres thermal system (Betic Cordillera, Spain). *Chem. Geol.* 289, 98–113. <https://doi.org/10.1016/j.chemgeo.2011.07.017>.
- Raines, M.A., Dewers, T.A., 1997. Dedolomitization as a driving mechanism for kars formation in Permian blaine Formation, southwestern Oklahoma, USA. *Carbonates and Evaporites* 12, 24–31.
- Román-Mas, A., Lee, R.W., 1987. Geochemical evolution of waters within the North Coast limestone aquifers of Puerto Rico: a conceptualization based on a flow path in the

- Barceloneta area, in: U.S. Geological Survey Water-Resources Investigations Report 86-4080. U.S. Geological Survey, San Juan, Puerto Rico, p. 28.
- Sacks, L.A., Herman, J.S., Kauffman, S.J., 1995. Controls on high sulfate concentrations in the upper Floridan aquifer in southwest Florida. *Water Resour. Res.* 31, 2541–2551.
- Saigal, G.C., Sadoon, M., Bjorlykke, K., Egeberg, P.K., Aagaard, P., 1988. Diagenetic albitization of detrital K-feldspar in Jurassic, Lower Cretaceous and Tertiary clastic reservoir rocks from offshore Norway, I. Textures and origin. *J. Sediment. Petrol.* 58, 1003–1013.
- Sánchez, J.A., Coloma, P., 1998. Hidrogeología de los manantiales termales de Arnedillo. *Zubia Monográfico* 10, 11–25.
- Sánchez, J.A., Coloma, P., Pérez, A., 1999. Sedimentary processes related to the groundwater flows from the Mesozoic Carbonate Aquifer of the Iberian Chain in the Tertiary Ebro Basin, northeast Spain. *Sediment. Geol.* 129, 201–213.
- Schmidt, R.B., Bucher, K., Drüppel, K., Stober, I., 2017. Experimental interaction of hydrothermal Na-Cl solution with fracture surfaces of geothermal reservoir sandstone of the Upper Rhine Graben. *Appl. Geochemistry* 81, 36–52.
- Seal, R.R.I., Alpers, C.N., Rye, R.O., 2000. Stable isotope systematics of sulfate minerals. In: Alpers, C.N., Jambor, J.L., Nordstrom, D. (Eds.), *Sulfate Minerals — Crystallography: Geochemistry and Environmental Significance*. Mineral Society of America, Chantilly (Virginia), pp. 541–602.
- Spycher, N., Peiffer, L., Sonnenthal, E.L., Saldi, G., Reed, M.H., Kennedy, B.M., 2014. Integrated multicomponent solute geothermometry. *Geothermics* 51, 113–123.
- Stefánsson, A., Arnórsson, S., 2000. Feldspar saturation state in natural waters. *Geochim. Cosmochim. Acta* 64, 2567–2584.
- Stoessell, R.K., Klimentidis, R.E., Prezbindoski, D.R., 1987. Dedolomitization in Na-Cl-Ca brines from 100°C to 200°C at 300 bar. *Geochim. Cosmochim. Acta* 51, 847–855.
- Truesdell, A.H., 1976. *Geochemical Techniques in Exploration. Summary of Section III. In: Proceedings of the Second United Nations Symposium on the Development & Use of Geothermal Resources. San Francisco (California)*, pp. iii–xxix.
- Verma, S.P., Santoyo, E., 1997. New improved equations for Na/K, Na/Li and SiO<sub>2</sub> geothermometers by outlier detection and rejection. *J. Volcanol. Geotherm. Res.* 79, 9–24.
- Wang, J., Jin, M., Jia, B., Kang, F., 2015. Hydrochemical characteristics and geothermometry applications of thermal groundwater in northern Jinan, Shandong, China. *Geothermics* 57, 185–195.
- Woo, K.S., Moore, C.H., 1996. Burial dolomitization and dedolomitization of the late Cambrian Wagok Formation, Yeongweol, Korea. *Carbonates Evaporites* 11, 104–112.
- Zeebe, R.E., 2010. A new value for the stable oxygen isotope fractionation between dissolved sulfate ion and water. *Geochim. Cosmochim. Acta* 74, 818–828.
- Zhu, C., Anderson, G., 2002. *Environmental Applications of Geochemical Modeling*. Cambridge University Press.

#### 4.4 Paper 4

### **Mineral equilibria and thermodynamic uncertainties in the geothermometrical characterisation of carbonate geothermal systems of low temperature. The case of the Alhama-Jaraba system (Spain)**

*Mónica Blasco, Luis F. Auqué, María J. Gimeno, Patricia Acero, Javier Gómez, Maria P. Asta*

*Geothermics* 78, 170-182 (2019)

Impact Factor (2017): 2.693

Quartile and Category (2017): Q2 (57/189), Geosciences; Q2 (47/97), Energy & Fuels.

DOI: 10.1016/j.geothermics.2018.11.004

Sent: 11 May 2018

Accepted; 19 November 2018

Available online: 22 December 2018

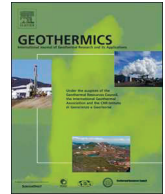
Final publication: March 2019





Contents lists available at ScienceDirect

## Geothermics

journal homepage: [www.elsevier.com/locate/geothermics](http://www.elsevier.com/locate/geothermics)

# Mineral equilibria and thermodynamic uncertainties in the geothermometrical characterisation of carbonate geothermal systems of low temperature. The case of the Alhama-Jaraba system (Spain)

Mónica Blasco<sup>a,\*</sup>, Luis F. Auqué<sup>a</sup>, María J. Gimeno<sup>a</sup>, Patricia Acero<sup>a</sup>, Javier Gómez<sup>a</sup>,  
 Maria P. Asta<sup>b</sup>

<sup>a</sup> Geochemical Modelling Group, Petrology and Geochemistry Area, Earth Science Department, University of Zaragoza, Spain C/ Pedro Cerbuna 12, 50009, Zaragoza, Spain

<sup>b</sup> Environmental Microbiology Laboratory (EML), École Polytechnique Fédérale de Lausanne (EPFL), EPFL-ENAC-IIE-EML, Station 6, 1015, Lausanne, Switzerland

### ARTICLE INFO

#### Keywords:

Low temperature geothermal system  
 Geothermometry  
 Geothermometrical modelling  
 Calcite-dolomite equilibrium  
 Carbonate aquifer

### ABSTRACT

Geothermometrical characterisation of low-temperature, carbonate-evaporitic geothermal systems is usually hampered by the lack of appropriate mineral equilibria to successfully use most of the classical geothermometers and/or by the thermodynamic uncertainties affecting some of the most probable mineral equilibria in low temperature conditions. This situation is further hindered if the thermal waters are additionally affected by secondary processes (e.g., CO<sub>2</sub> loss) during their ascent to surface.

All these problems cluster together in the low-temperature Alhama-Jaraba thermal system, hosted in carbonate rocks, with spring temperatures about 30 °C and waters of Ca-Mg–HCO<sub>3</sub>/SO<sub>4</sub> type. This system, one of the largest naturally flowing (600 L/s) low temperature thermal systems in Europe, is used in this paper as a suitable frame to assess the problems in the application of chemical geothermometrical techniques (classical geothermometers and geothermometrical modelling) and to provide a methodology that could be used in this type of geothermal system or in potential CO<sub>2</sub> storage sites in similar aquifers.

The results obtained have shown that the effects of the secondary processes can be avoided by selecting the samples unaffected by such processes and, therefore, representative of the conditions at depth, or by applying existing methodologies to reconstruct the original composition, as is usually done for medium to high temperature systems.

The effective mineral equilibria at depth depend on the temperature, the residence time and the specific lithological/mineralogical characteristics of the system studied. In the present case, the mineral equilibria on which classical cation geothermometers are based have not been attained. The low proportion of evaporitic minerals in the hosting aquifer prevents the system from reaching anhydrite equilibrium, otherwise common in carbonate-evaporitic systems and necessary for the specific SO<sub>4</sub>-F geothermometer or the specially reliable quartz (or chalcidony) – anhydrite equilibrium in the geothermometrical modelling of these geothermal systems.

Under these circumstances, the temperature estimation must rely on quartz (or chalcidony), clay minerals and, especially, calcite and dolomite. However, clay minerals and dolomite present important thermodynamic uncertainties related to possible variations in composition or crystallinity degree for clays and order/disorder degree for dolomite. To deal with these problems, a sensitivity analysis to the thermodynamic data for clay minerals has been carried out, comparing the results obtained when considering different solubility data. The uncertainties associated with dolomite have been addressed by reviewing the solubility data available for dolomites with different order degrees and performing specific calculations for the order degree of the dolomite in the aquifer. This approach can be used to find the most adequate dolomite thermodynamic data for the system under consideration, including medium-high temperature geothermal systems.

Finally, the temperature estimation of the Alhama-Jaraba waters in the deep reservoir has been obtained from simultaneous equilibria of quartz, calcite, partially disordered dolomite and some aluminosilicate phases. The obtained value of 51 ± 14 °C is within the uncertainty range normally affecting this type of estimations and is coherent with independent estimations from geophysical data.

\* Corresponding author at: Geochemical Modelling Group, Petrology and Geochemistry Area, Earth Sciences Department, University of Zaragoza, Spain.  
 E-mail address: [monicabc@unizar.es](mailto:monicabc@unizar.es) (M. Blasco).

<https://doi.org/10.1016/j.geothermics.2018.11.004>

Received 11 May 2018; Received in revised form 8 November 2018; Accepted 19 November 2018

0375-6505/ © 2018 Elsevier Ltd. All rights reserved.

## 1. Introduction

A wide variety of geothermometrical techniques are available to evaluate the reservoir temperature of thermal waters: various chemical and isotopic solute geothermometers and the geothermometrical modelling (or multicomponent solute geothermometry; e.g. Spycher et al., 2014). However, not all of them are always applicable to all thermal systems and they should be carefully selected according to the different equilibria expected at depth.

In the case of low temperature thermal systems hosted in carbonate rocks, a series of problems arise when applying the geothermometrical techniques due to three main reasons: 1) the low temperatures usually make difficult the attainment of the mineral and/or isotopic equilibria; 2) the mineral set present in the reservoir is usually more limited (mainly calcite and dolomite) than in other type of geothermal systems; and 3) the thermodynamic properties of dolomite and clays are uncertain.

An additional complication in the evaluation of the reservoir temperature in any thermal system is the presence of secondary processes during the rising of the thermal waters to surface (e.g. mixing with colder and shallower waters, re-equilibrium processes through mineral-water reactions and/or CO<sub>2</sub> outgassing).

The work presented in this paper is focused on the use and evaluation of several geothermometrical tools in order to calculate the reservoir temperature of the geothermal system of Alhama de Aragón – Jaraba (from now on, Alhama–Jaraba). The characteristics of this thermal system provide the opportunity to deal with almost all the aforementioned complexities (Tena et al., 1995; Auqué et al., 2009; Blasco et al., 2016): 1) the reservoir is hosted mainly in carbonate rocks

(limestones and dolostones), 2) the temperature is, a priori, low and 3) there are different secondary processes (mixing, CO<sub>2</sub> outgassing) affecting the chemistry of some of the waters. There are other reasons why the study of this system presents a special interest. One is the importance of the system as a natural resource with very high flow rates (550 L/s in Alhama and 600 L/s in Jaraba; IGME, 1980; De Toledo and Arqued, 1990; Sánchez et al., 2004) comparable to those found in the area considered the Europe's largest naturally flowing thermal system in Budapest (discharge of ca. 580 L/s; Goldscheider et al., 2010 and references therein). The other reason is related to its special geological and hydrogeochemical features which have given it the consideration of a natural analogue for the CO<sub>2</sub> geological storage (Auqué et al., 2009).

In summary, this study gives a suitable natural frame to test different geothermometrical techniques and the associated uncertainties in low temperature systems hosted in carbonate rocks. From this, a general methodology can be established to be applied in this type of geothermal systems and even in the characterisation of some potential CO<sub>2</sub> storage sites in similar aquifers.

## 2. Geological, hydrogeological and hydrogeochemical setting

The Alhama de Aragón and Jaraba springs (NE Spain, Fig. 1) belong to one of the main thermal systems in Spain. There are several thermal resorts and water bottling plants in the area at present. The Jaraba thermal complex, close to the Mesa River, consists of 14 catalogued springs flowing at an elevation of 737 m.a.s.l. and the Alhama thermal complex, located close to the Jalón River bank, is formed by a dozen of catalogued springs flowing at an elevation of 660 m. Apart from these well-known spring complexes, there are another two minor hot springs

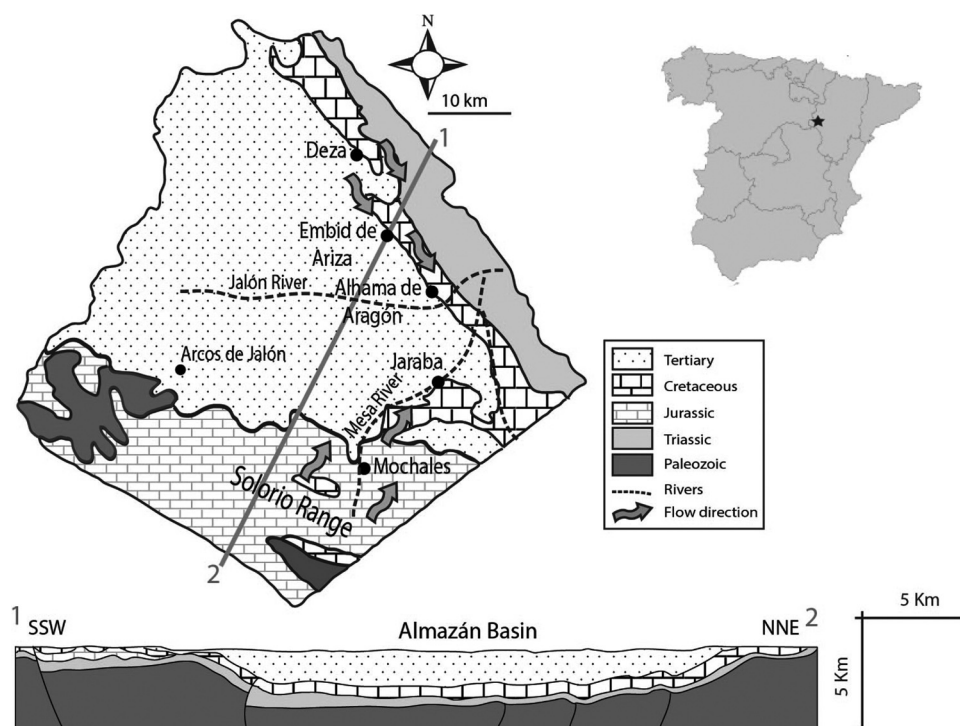


Fig. 1. Location of the Alhama de Aragón and Jaraba geothermal systems in the geological map (modified from Sánchez et al., 2004) and a cross section showing the main structural and lithological characteristics of the area studied (modified from the ALGECO2 project; IGME, 2010).



in the nearby area, Embid and Deza springs (Tena et al., 1995; Sanz and Yelamos, 1998; Sánchez et al., 2004; Auqué et al., 2009; Fig. 1), which have not been included in this study.

Geologically, the Alhama-Jaraba thermal system is located on the border of the Western Iberian Range and the tertiary Almazán Basin (Fig. 1). There are two main aquifers in this area: 1) the Solorio aquifer, hosted in the Jurassic carbonate formations; and 2) the Alhama aquifer, hosted in the Upper Cretaceous carbonate rocks. The hydrological model of the region is not completely clear, but the most accepted hypothesis states that there are two possible recharge areas located 1) in the Solorio Range with a flow direction SW-NE towards Jaraba and Alhama (Fig. 1) and 2) in the vicinity of Deza, with a NW-SE flow direction towards Embid and Alhama (Fig. 1; IGME, 1980, 1987; De Toledo and Arqued, 1990; Sanz and Yelamos, 1998; Sánchez et al., 2004). The fact that the rocks in the Solorio recharge area are mainly Jurassic and that all the thermal springs are associated with the Upper Cretaceous formations (Sánchez et al., 2004) suggests that both aquifers could be connected and that their emergence would be related to the presence of vertical or near vertical layers that allow a rapid ascent of the water from depth (Sánchez et al., 2004).

The mineralogy of the Jurassic and Cretaceous carbonate rocks is quite similar. The rocks are mainly dolostones and limestones with dispersed anhydrite/gypsum intercalations (Meléndez et al., 1985; Alonso et al., 1993; Aurell et al., 2002). The Cretaceous formations are locally affected by a silicification processes with development of authigenic quartz crystals (Meléndez et al., 1985) and there are also intercalations of terrigenous rocks, mainly at the base of the Utrillas Formation, consisting of sandstones, claystones, siltstones, dolomitic siltstones, dolomitic marls, limestones and dolomitic limestones, with a mineralogy comprising calcite, dolomite, quartz, K-feldspar, lithic fragments and clay minerals (IGME, 1991).

The isotope  $\delta^{18}\text{O}$  and  $\delta^2\text{H}$  data available (IGME, 1982, 1994; Sanz

and Yelamos, 1998; Pinuaga et al., 2004) indicate a clear meteoric origin. The tritium data available are also from the aforementioned works and they show the absence of tritium or levels close to the detection limit ( $\approx 1$  TU) in the hottest springs. The most common interpretation for these results is that the thermal groundwaters have residence times longer than 50 years and that some of them are affected by minor mixing with shallow modern waters (Clark and Fritz, 1997).

### 3. Methodology

#### 3.1. Field sampling and analysis

Six and nine springs were sampled in the Alhama and Jaraba thermal sites, respectively. Field sampling procedures and analytical methodology were mostly as described by Auqué et al. (2009). Briefly, at each sampling point, temperature, pH and conductivity were determined in situ and separated samples for anion and cation analysis were taken in 1 N HCl pre-washed polyethylene bottles. Samples for cation analysis were filtered through 0.1  $\mu\text{m}$  and acidified to pH less than 1 with ultrapure  $\text{HNO}_3$ . Anions were determined within 24 h after collection. Total alkalinity was determined by titration with a Mettler titrator with an end-point electrode. Chloride and fluoride concentrations were determined by a selective ion analyser equipment, using the selective electrodes for chloride ORION 94-17B and fluoride ORION 94-09. Sulphate was determined by colorimetry using a modification of the Nemeth method (Nemeth, 1963). Potassium concentrations were analysed by Flame Photometry and aluminium concentrations were determined by Electrothermal Atomisation Atomic Absorption Spectrometry with Zeeman-effect background correction. Inductively Coupled Plasma-Atomic Emission Spectrometry was used for the analysis of the rest of the elements (Ca, Mg, Na, Li, and Si). The average analytical error was estimated  $< 5\%$  for alkalinity, chloride, fluoride, sulphate,

**Table 1**

Calibrations used in this work for the different classical geothermometers. Geothermometrical functions provide the temperature values in degrees Celsius. The concentration units corresponding to the different expressions are also indicated (usually mg/L or mol/L).

Geothermometer	Authors of calibration	Expression	Units
SiO <sub>2</sub> -quartz	Michard (1979)	$T = \frac{1322}{0.435 - \log(\text{SiO}_2)} - 273.15$	mol/L
	Fournier and Potter (1982)	$T = \frac{1309}{5.19 - \log(\text{SiO}_2)} - 273.15$	mg/L
Na-K	Giggenbach (1988)	$T = \frac{1390}{1.75 + \log\left(\frac{\text{Na}}{\text{K}}\right)} - 273.15$	mg/L
	Fournier (1979)	$T = \frac{1217}{1.483 + \log\left(\frac{\text{Na}}{\text{K}}\right)} - 273.15$	mg/L
Na-K-Ca <sup>1</sup>	Fournier and Truesdell (1973)	$T = \frac{1647}{\log\left(\frac{\text{Na}}{\text{K}}\right) + \beta \left[ \log\left(\frac{\sqrt{\text{Ca}}}{\text{Na}}\right) + 2.06 \right] + 2.47} - 273.15$	mg/L
Ca-K	Fournier and Truesdell (1973) <sup>2</sup>	$T = \frac{2920}{3.02 + \log\left(\frac{\text{Ca}}{\text{K}^2}\right)} - 273.15$	mol/L
	Michard (1990)	$T = \frac{3030}{3.94 + \log\left(\frac{\text{Ca}}{\text{K}^2}\right)} - 273.15$	mol/L
K-Mg	Giggenbach et al. (1983)	$T = \frac{4410}{13.95 - \log\left(\frac{\text{K}^2}{\text{Mg}}\right)} - 273.15$	mg/L
Na-Li	Fouillac and Michard, 1981	$T = \frac{1000}{0.33 + \log\left(\frac{\text{Na}}{\text{Li}}\right)} - 273.15$	mol/L
Li	Fouillac and Michard, 1981	$T = \frac{2258}{1.44 + \log(\text{Li})} - 273.15$	mol/L
Mg-Li	Kharaka and Mariner, 1988	$T = \frac{2200}{5.47 + \log\left(\frac{\sqrt{\text{Mg}}}{\text{Li}}\right)} - 273.15$	mg/L
Ca-Mg <sup>3</sup>	Chiodini et al. (1995)	$T = \frac{979.8}{3.1170 - \log\left(\frac{\text{Ca}}{\text{Mg}}\right) + 0.07003 \log \sum \text{eq}} - 273.15$	mol/L

<sup>1</sup>  $\beta = 4/3$  should be used if the temperature obtained is lower than 100 °C; if the temperature obtained, using that value of  $\beta$ , is higher than 100 °C, it should be recalculated considering  $\beta = 1/3$ . Mg-correction proposed by Fournier and Potter (1979) for the Na-K-Ca geothermometer cannot be applied to the studied springs, according to the criteria indicated by those authors.

<sup>2</sup> Derived from Fournier and Truesdell (1973) in Michard (1990).

<sup>3</sup>  $\sum \text{eq}$  is the summation (in eq/L) of the major dissolved species.

potassium and aluminium, < 4% for Ca, Mg, Na and Si, and < 9% for Li.

The calculated charge balance error for the analyses reported, as calculated with the PHREEQC code (Parkhurst and Appelo, 2013), is below 5%.

### 3.2. Methodology for geothermometrical calculations

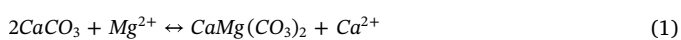
Various geothermometrical techniques are used in this work to ascertain the reservoir temperature in the Alhama-Jaraba system: classical and specific chemical geothermometers and geothermometrical modelling calculations. The integration of the results has helped to propose a temperature range in the reservoir. The general features of these methodologies in their application to the system studied are detailed below.

#### 3.2.1. Chemical geothermometers

Two main types of chemical geothermometers have been used (Table 1):

- Classical geothermometers, which include the dissolved silica geothermometer and several cationic geothermometers (Na-K, Na-K-Ca, Ca-K, K-Mg, Na-Li, Li and Mg-Li, some of them with several calibrations; Table 1). Most of these geothermometers have been proved to be very useful for estimating subsurface temperature in high temperature systems (> 180 °C) where equilibria between aqueous solutions and minerals in the geothermal reservoirs are easily attained (e.g. Fournier, 1977, 1981; Fouillac and Michard, 1981; Arnorsson et al., 1983; Giggenbach et al., 1983; D'Amore et al., 1987; Nieva and Nieva, 1987; Giggenbach, 1988; Kharaka and Mariner, 1988; Chiodini et al., 1995; Mutlu and Güleç, 1998; Stefánsson and Arnórsson, 2000; Mariner et al., 2006; Sonney and Vuataz, 2010; Nicholson, 2012). However, in low to medium temperature hydrothermal systems (40–180 °C) hosted in carbonate-evaporitic rocks, these geothermometrical techniques encounter problems frequently related to the mineral assemblage expected to govern the water chemistry and to the attainment of equilibrium in the reservoir (Chiodini et al., 1995; Levet et al., 2002; Sonney and Vuataz, 2010). Nevertheless, some of these geothermometers have occasionally given good results in this type of system (e.g. Michard and Bastide, 1988; Minissale and Duchi, 1988; Pastorelli et al., 1999; Gökgöz and Tarcan, 2006; Mohammadi et al., 2010; Apollaro et al., 2012; Wang et al., 2015; Blasco et al., 2017, 2018) and, therefore, their performance will be assessed at the studied sites.
- Specific geothermometers, which were developed to be used in low-temperature carbonate-evaporitic systems, like the SO<sub>4</sub>-F and the Ca-Mg geothermometers (Marini et al., 1986; Chiodini et al., 1995). The application of these geothermometers requires the existence of anhydrite/gypsum – fluorite equilibrium, and calcite – dolomite equilibrium, respectively. Equilibrium with anhydrite or gypsum is easily attained in systems with evaporitic rocks in the host formations since these are the most common phases; however, the presence of fluorite is not so common in these environments (Chiodini et al., 1995).

The calcite–dolomite equilibrium can be represented by the following overall reaction and equilibrium equation (e.g. Appelo and Postma, 2005):



$$K = \frac{a_{\text{Ca}^{2+}}}{a_{\text{Mg}^{2+}}} = \frac{(K_{\text{calcite}})^2}{K_{\text{dolomite}}} \quad (2)$$

where  $a_{\text{Ca}^{2+}}/a_{\text{Mg}^{2+}}$  represents the activity ratio of dissolved calcium and magnesium in the target solution and  $K_{\text{calcite}}$  and  $K_{\text{dolomite}}$  represent the equilibrium constants for calcite and dolomite, respectively. As can

be deduced from Eq. (2), one of its advantages is that the  $a_{\text{Ca}^{2+}}/a_{\text{Mg}^{2+}}$  ratio mainly depends on temperature and it is not significantly influenced by variations in the CO<sub>2</sub> partial pressure or pH during the ascent of thermal waters towards spring conditions (Hyeong and Capuano, 2001). However, this geothermometer can also be problematic due to the uncertainties in the solubility of dolomite which make its use in geothermometry very difficult (e.g. Hyeong and Capuano, 2001; Palandri and Reed, 2001; Blasco et al., 2018). These uncertainties will be further evaluated.

#### 3.2.2. Geothermometrical modelling

Geochemical modelling calculations provide a more generalised approach than the classical chemical geothermometry. This technique consists of simulating a process of a progressive water temperature increase to obtain a temperature range in which the saturation state of the waters with respect to a selected mineral set (assumed to be present in the reservoir) simultaneously reaches equilibrium. When most of the minerals selected indicate about the same equilibrium temperature, the average temperature can be considered as the best estimate (e.g. Michard and Roekens, 1983; Reed and Spycher, 1984; D'Amore et al., 1987; Pang and Reed, 1998).

The geochemical modelling approach shows different advantages over the classical geothermometers. It helps to evaluate the secondary processes during the ascent of the thermal waters, such as 1) the extension of mineral re-equilibrium reactions (Michard and Fouillac, 1980; Michard and Roekens, 1983; Michard et al., 1986), 2) the amount of lost gas and/or 3) the proportion of cold waters in mixtures (Pang and Reed, 1998; Palandri and Reed, 2001). It can also be advantageous to distinguish between equilibrated and non-equilibrated waters, as non-equilibrated waters result in a large range of calculated mineral equilibrium temperatures (e.g. Tole et al., 1993). However, this approach also has some uncertainties with respect to 1) the attainment of water-mineral equilibrium, 2) the mineral solubility data input in calculations, and 3) the aluminium concentrations, which are low and can be easily affected by cooling during the ascent of thermal waters (Pang and Reed, 1998; Peiffer et al., 2014).

For the Alhama-Jaraba system, these geothermometrical modelling calculations have been carried out with the assistance of the PHREEQC geochemical code (version 3.4.0; Parkhurst and Appelo, 2013) and using two of the thermodynamic databases distributed with this version, WATEQ4F and LLNL, in order to perform a sensitivity analysis to the thermodynamic data.

Based on the mineralogy identified in the aquifer, the mineral phases selected for these calculations include: calcite, dolomite, quartz, gypsum/anhydrite and some aluminosilicates. Whereas the solubility constants for calcite, quartz, gypsum and anhydrite are fairly well known, there are some uncertainties related to the solubility dependence on temperature (K(T)) for the rest of the mineral phases. To evaluate their effects on the results obtained, the following procedures have been adopted:

- The solubility data for illite and smectites (beidellite, montmorillonite) are affected by potential problems such as their wide compositional variability, the variable degree of crystallinity, particle size effect, and some order/disorder phenomena (e.g. Merino and Ranson, 1982; Nordstrom et al., 1990; Palandri and Reed, 2001). However, illite has been used in geothermometrical calculations with some success (e.g. Pang and Reed, 1998 and Palandri and Reed, 2001), and, therefore, it is also used in this study to verify its performance and uncertainties. Also, the approach recommended by Helgeson et al. (1978) and Palandri and Reed (2001) has been followed and pyrophyllite and paragonite have been used as proxies for the whole set of clay minerals.
- The thermodynamic data for K-feldspar, kaolinite (two types with different crystallinity degrees: poorly crystalline and crystalline) and pyrophyllite from Michard et al. (1979) and Michard (1983)

have been added to the WATEQ4F database for comparison with the data included in the LLNL.

- The solubility of dolomite is strongly affected by non-stoichiometry and order/disorder in Ca and Mg site occupancies (Helgeson et al., 1978; Carpenter et al., 1980; Reeder, 1990, 2000; Hyeong and Capuano, 2001) but experimental data on these effects do not exist. Therefore, in order to consider this uncertainty, we have tested the influence of several solubility values on the geothermometrical calculation results. For this purpose, the values included in the LLNL database, corresponding to fully-disordered and to fully-ordered dolomite were considered in the calculations together with the solubility value proposed for “dolomite” in the WATEQ4F database (Nordstrom et al., 1990; Dolomite\_W from now on), which represents a partially-ordered dolomite (Helgeson et al., 1978; Carpenter et al., 1980). Additionally, some natural dolomites with different degree of order/disorder have been included in the comparison: 1) the dolomite reported by Hyeong and Capuano (2001), from the Oligocene Frio Formation (Texas Gulf Coast) with an order of 11% (Dolomite\_H&C); 2) the dolomite considered by Busby et al. (1991) from the Carboniferous Madison Aquifer and an order of 23.5% (Dolomite\_B); 3) the dolomite used by Vespasiano et al. (2014) from the Triassic of Calabria (Italy) and an order of 22% (Dolomite\_V); and 4) the dolomite reported by Blasco et al. (2018) from the Jurassic of the Cameros Basin (Spain) with an order of 18.4% (Dolomite\_BL).

For comparative purposes, the solubility values at 25 °C and the K (T) function for the different mineral phases considered in the geothermometrical simulations are summarised in Table S1 (Supplementary Material).

## 4. Results

### 4.1. Hydrochemical characteristics of the thermal waters

There are remarkable compositional differences among the springs studied. The thermal waters from Jaraba are mainly of Ca-Mg–HCO<sub>3</sub>-type whilst in Alhama, the waters show a more distinct SO<sub>4</sub>-Cl character with higher conductivity values and higher concentrations of Ca, Mg, Na, SO<sub>4</sub> and Cl (Table 2 and Fig. 2). The alkalinity values are lower in Alhama than those determined in the Jaraba waters and the dissolved silica concentrations are similar in all waters although slightly lower in Jaraba waters.

The measured temperatures in the Alhama springs are always higher than 30 °C and their values are rather homogeneous

(temperature variability smaller than 2.3 °C; Table 2) as it is also the case with the hydrochemical variability which is generally within the analytical error. The Jaraba springs, however, exhibit a larger compositional variability and temperature range (between 21 and 32 °C; Table 2) although the highest temperature is similar to those in Alhama. The combined variability of temperature and compositional characteristics in the Jaraba thermal waters has been attributed to mixing between deep thermal groundwaters and superficial and colder waters along the shallower parts of the upflow towards the Jaraba springs (Tena et al., 1995; Auqué et al., 2009; Blasco et al., 2016).

Results of speciation-solubility calculations (Table 3) indicate that most of the springs studied in the Alhama and Jaraba sites are close to equilibrium or slightly oversaturated with respect to calcite and partially disordered dolomite (Dolomite\_W or Dolomite\_H&C; see above). The differences obtained in the saturation state of the waters with respect to calcite and dolomite are mainly related to the different extent of CO<sub>2</sub> outgassing along the shallowest parts of the flow paths (see Auqué et al., 2009 for further explanation and calculations on this issue). The highest values are found in sample ZA-45, from Alhama, which is the sample with the highest pH and a relative low log pCO<sub>2</sub> and, therefore, the one with the most intense outgassing.

The studied waters are undersaturated with respect to all silica minerals, except quartz, and also with respect to gypsum, anhydrite, fluorite, halite and albite and slightly undersaturated or near equilibrium with respect to K-feldspar (Table 3 and Fig. 3). They are, however, clearly oversaturated with respect to the rest of the aluminosilicates potentially present in the deep reservoir, kaolinite, illite, paragonite and pyrophyllite. As mentioned above, knowing the uncertainties associated to the thermodynamic data for the aluminosilicates, these results have been checked using different thermodynamic data (Table 3 and Fig. 3) and the variations found do not change the over- or undersaturation results commented above significantly.

Based on the combination of ion-ion plots, speciation-solubility calculations, mass-balance and reaction-path modelling, Auqué et al. (2009) suggested that the most important geochemical processes determining the geochemical evolution, along one of the possible flow directions from the Solorio recharge zone through Mochales, Jaraba and Alhama groundwaters (see Fig. 1), are: 1) halite dissolution (note the 1:1 relation for Cl and Na contents both in the Jaraba and Alhama thermal waters; Table 2) and 2) dedolomitisation (dolomite dissolution and concomitant calcite precipitation triggered by gypsum/anhydrite dissolution).

The extent of the halite and gypsum/anhydrite dissolution processes seems to be constrained only by the water-rock interaction time and/or by the availability of these minerals in the system. However, the

**Table 2**  
General hydrochemistry of the Alhama-Jaraba thermal waters included in this study.

Sample Number	Jaraba									Alhama de Aragón					
	ZA-22	ZA-23	ZA-24	ZA-25	ZA-26	ZA-27	ZA-28	ZA-29	ZA-30	ZA-39	ZA-40	ZA-41	ZA-43	ZA-44	ZA-45
T (°C)	26.6	27.3	27.2	21.0	29.4	32.0	31.8	26.1	21.8	30.1	31.9	32.4	30.2	31.6	30.7
pH (field)	7.40	7.40	7.30	7.40	6.80	7.05	7.25	7.30	7.30	7.15	6.90	7.05	7.15	7.45	7.85
Cond. (µS/cm)	865	864	850	755	890	910	905	859	745	1181	1154	1161	1152	1122	1122
mmol/L															
HCO <sub>3</sub> <sup>-</sup>	4.73	4.72	4.72	4.92	4.65	4.62	4.68	4.68	4.81	4.38	4.47	4.39	4.49	4.47	4.58
Cl <sup>-</sup>	1.41	1.41	1.37	1.05	1.72	1.67	1.69	1.37	0.94	2.85	2.75	2.88	2.74	2.69	2.69
SO <sub>4</sub> <sup>2-</sup>	1.32	1.37	1.28	0.88	1.58	1.54	1.5	1.36	1	2.6	2.56	2.6	2.44	2.44	2.52
Ca <sup>2+</sup>	2.31	2.31	2.30	2.09	2.10	2.41	2.39	2.10	2.27	3.05	2.97	3.08	3.06	2.73	2.98
Mg <sup>2+</sup>	1.74	1.67	1.61	1.35	1.92	1.68	1.55	1.76	1.44	2.08	2.07	2.13	2.17	2.21	2.22
Na <sup>+</sup>	1.4	1.4	1.3	1	1.7	1.5	1.5	1.3	0.8	2.6	2.6	2.6	2.6	2.6	2.3
µmol/L															
SiO <sub>2</sub>	0.15	0.15	0.15	0.11	0.15	0.15	0.14	0.14	0.13	0.17	0.17	0.17	0.13	0.16	0.17
K <sup>+</sup>	30	30	25	25	30	30	30	30	15	40	40	40	40	40	70
Li <sup>+</sup>	5.0	5.0	5.0	5.0	5.0	6.1	6.1	6.1	1.0	12.0	9.9	9.9	9.9	6.1	7.9
Sr <sup>2+</sup>	1.5	3.0	1.9		4.0	4.5	4.5	1.9		10	9.5	10	9.5	9.5	9.5
B	0.19						0.28			1.00	0.83	0.74	0.74	0.56	0.46
Al						0.64		0.36		0.41	0.74	0.82			
F <sup>-</sup>	9.2	9.5	8.5	4.8	9.7	12.0	12.0	8.7	7.7	17.0	16.0	17.0	15.0	16.0	16.0

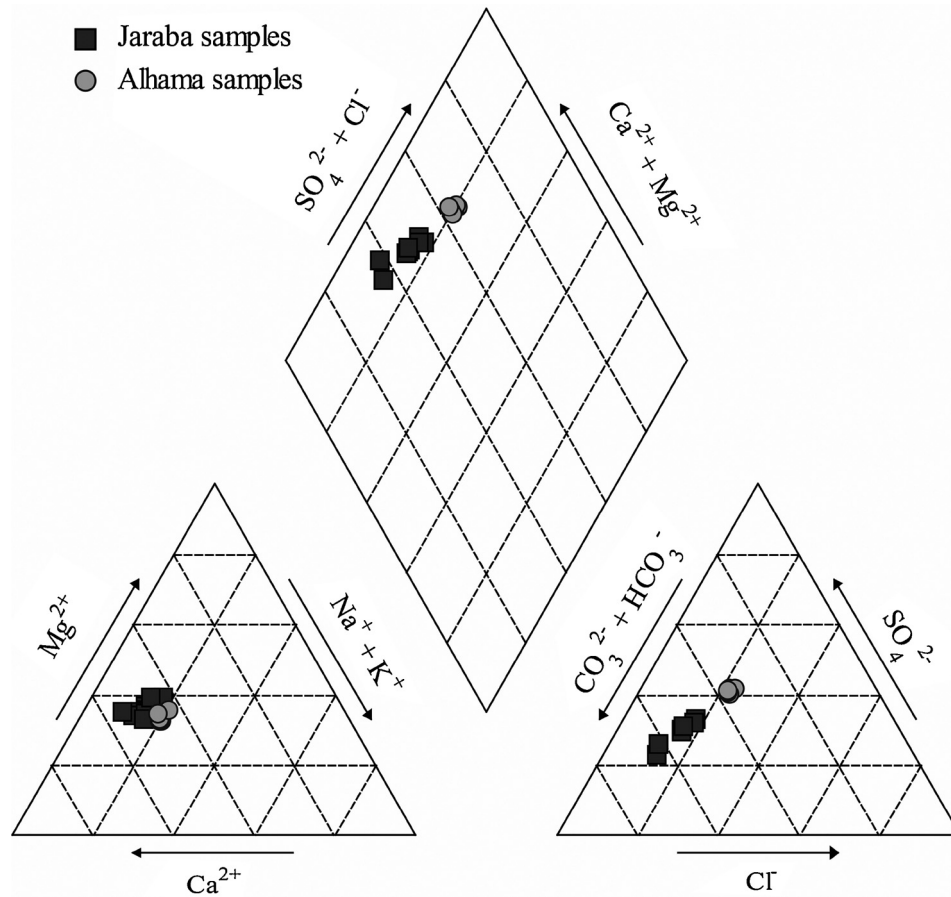


Fig. 2. Representation of the composition of the water samples included in this study in a Piper–Hill diagram.

Table 3

Summary of results from speciation-solubility calculations in the Alhama-Jaraba thermal system. The calculations have been performed with the PHREEQC code (Parkhurst and Appelo, 2013) and the thermodynamic database WATEQ4F with some additional thermodynamic data included. Other results for aluminosilicate phases obtained using the LLNL thermodynamic database have been included for comparison.

Sample Number	Jaraba									Alhama de Aragón					
	ZA-22	ZA-23	ZA-24	ZA-25	ZA-26	ZA-27	ZA-28	ZA-29	ZA-30	ZA-39	ZA-40	ZA-41	ZA-43	ZA-44	ZA-45
Temperature (°C)	26.6	27.3	27.2	21.	29.4	32.0	31.8	26.1	21.8	30.1	31.9	32.4	30.2	31.6	30.7
pH (field)	7.4	7.4	7.3	7.4	6.80	7.05	7.23	7.31	7.29	7.13	6.89	7.04	7.15	7.47	7.87
TIC (mmol/L)	5.06	5.05	5.15	5.30	6.04	5.36	5.16	5.10	5.30	4.94	5.47	5.07	5.04	4.70	4.60
log pCO <sub>2</sub>	-1.96	-1.96	-1.86	-1.97	-1.34	-1.57	-1.76	-1.88	-1.87	-1.71	-1.45	-1.6	-1.72	-2.03	-2.44
Calcite	0.3	0.31	0.21	0.22	-0.32	0.02	0.21	0.16	0.15	0.11	-0.1	0.06	0.16	0.43	0.86
Dolomite_H&C	0.54	0.55	0.33	0.30	-0.61	-0.02	0.31	0.31	0.12	0.14	-0.26	0.05	0.25	0.87	1.67
Dolomite_W	0.62	0.63	0.42	0.35	-0.52	0.08	0.41	0.39	0.18	0.24	-0.16	0.15	0.34	0.97	1.77
Dolomite_dis	0.07	0.09	-0.12	-0.21	-1.05	-0.44	-0.11	-0.15	-0.39	-0.29	-0.68	-0.37	-0.19	0.44	1.24
Gypsum	-1.51	-1.48	-1.5	-1.67	-1.47	-1.44	-1.44	-1.51	-1.58	-1.18	-1.18	-1.17	-1.2	-1.25	-1.2
Anhydrite	-1.72	-1.69	-1.71	-1.9	-1.67	-1.63	-1.62	-1.73	-1.81	-1.37	-1.37	-1.35	-1.39	-1.44	-1.39
Halite	-7.4	-7.4	-7.43	-7.67	-7.24	-7.3	-7.3	-7.43	-7.82	-6.85	-6.85	-6.84	-6.87	-6.87	-6.92
Fluorite	-2.54	-2.52	-2.61	-3.04	-2.58	-2.37	-2.35	-2.62	-2.6	-2.	-2.08	-2.02	-2.1	-2.11	-2.07
Chalcedony	-0.29	-0.3	-0.3	-0.36	-0.32	-0.35	-0.38	-0.32	-0.3	-0.28	-0.3	-0.3	-0.39	-0.32	-0.29
Quartz	0.13	0.12	0.12	0.08	0.09	0.06	0.03	0.11	0.14	0.14	0.11	0.11	0.02	0.09	0.12
Kaolinite	—	—	—	—	—	2.81	—	2.42	—	2.57	3.31	3.06	—	—	—
Kaolinite (crys) <sup>1</sup>	—	—	—	—	—	4.05	—	3.68	—	3.81	4.56	4.31	—	—	—
Kaolinite (poor crys) <sup>1</sup>	—	—	—	—	—	3.28	—	2.96	—	3.06	3.79	3.53	—	—	—
Kaolinite <sup>2</sup>	—	—	—	—	—	3.85	—	3.50	—	3.62	4.33	4.11	—	—	—
K-Feldspar <sup>1</sup>	—	—	—	—	—	-0.24	—	-0.11	—	-0.01	0.10	0.11	—	—	—
Albite <sup>1</sup>	—	—	—	—	—	-1.01	—	-0.97	—	-0.67	-0.56	-0.54	—	—	—
Albite <sup>2</sup>	—	—	—	—	—	-0.96	—	-0.90	—	-0.62	-0.52	-0.49	—	—	—
Paragonite <sup>2</sup>	—	—	—	—	—	2.83	—	2.35	—	2.75	3.62	3.46	—	—	—
Pyrophyllite <sup>1</sup>	—	—	—	—	—	2.12	—	1.83	—	2.04	2.75	2.48	—	—	—
Pyrophyllite <sup>2</sup>	—	—	—	—	—	2.43	—	2.19	—	2.36	3.02	2.79	—	—	—

<sup>1</sup> Thermodynamic data from Michard et al. (1979) and Michard (1983).

<sup>2</sup> LLNL thermodynamic database distributed with PHREEQC.

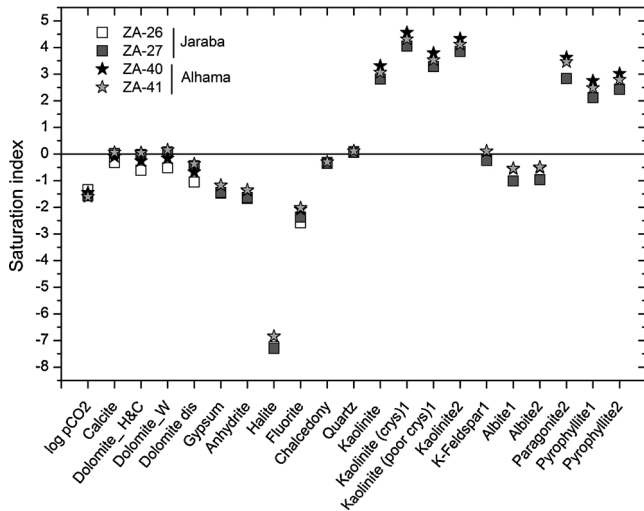


**Fig. 3.** Computed saturation indices for the mineral phases considered. Results shown are for two samples from each site, those with lower pH and higher temperature and, therefore, considered most suitable for geothermometrical calculations. The calculations have been performed with the PHREEQC code (Parkhurst and Appelo, 2013) and the thermodynamic database WATEQ4F with some additional thermodynamic data included. Other results for aluminosilicate phases obtained using the LLNL thermodynamic database have been included for comparison. The thermodynamic data for mineral phases marked with the number 1 are from Michard et al. (1979) and Michard (1983), and those with the number 2 from the LLNL database.

dolomite dissolution and calcite precipitation (dedolomitisation) appear to evolve through partial equilibrium or near partial equilibrium between calcite and dolomite along the entire flow path and all over the system. This situation is consistent with the very similar Mg/Ca ratio, around 0.7, found in the Jaraba and Alhama thermal waters (considering the ZA-27 sample from Jaraba as it is not affected by the mixing process) which is indicative of the existence of a calcite-dolomite equilibrium (or near equilibrium) at similar temperatures in the aquifer. A more detailed description of the hydrogeochemistry and evolution of the Alhama-Jaraba thermal system can be found in Auqué et al. (2009).

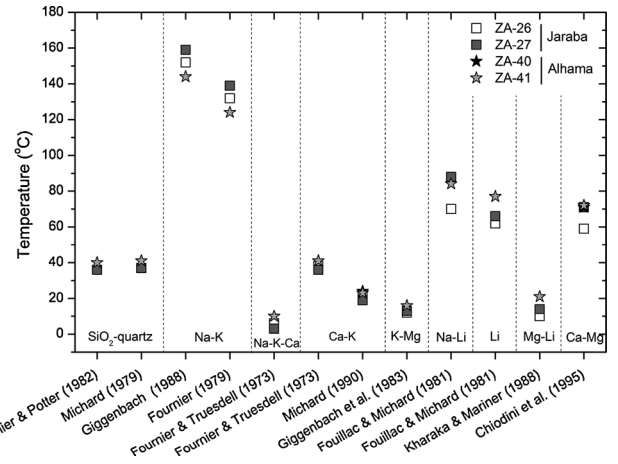


**Fig. 4.** Results obtained with some classical chemical geothermometers. Two samples from each site have been chosen. These samples are the ones with lower pH and higher temperature and, therefore, considered less affected by degassing and/or mixing and thus most suitable for geothermometrical calculations (see text).

4.2. Geothermometrical calculations

4.2.1. Chemical geothermometers

Table 4 and Fig. 4 summarise the results obtained with the various chemical geothermometers. Prior to the application of the classical cation geothermometers, the main cation concentrations of the water samples were plotted in the classical Giggenbach ternary Na-K-Mg diagram (Giggenbach, 1988) in order to check their applicability in this system. All the samples fall in the field of immature waters (almost in the Mg vertex; see Figure S1 in the Supplementary material) indicating that they have not attained equilibrium with respect to the phases on which the classical cation geothermometers are based and, therefore, making their use unsuitable for this system. The spring waters from this system are undersaturated with respect to all silica phases except quartz and therefore, this geothermometer is the only silica geothermometer that provides temperatures higher than spring temperatures, with maximum values around 40 °C for the Alhama waters and 37 °C for the

**Table 4**

Temperature results (in °C) obtained with some classical chemical geothermometers for the Alhama - Jaraba thermal waters. Shaded rows correspond to the most suitable samples from Alhama and Jaraba sites (highest temperatures and lowest pH values) for the geothermometrical calculations (ZA-26 and ZA-27 for Jaraba; ZA-40 and ZA-41 for Alhama).

	Sample Number	Jaraba				Alhama										
		ZA-22	ZA-23	ZA-24	ZA-25	ZA-26	ZA-27	ZA-28	ZA-29	ZA-30	ZA-39	ZA-40	ZA-41	ZA-43	ZA-44	ZA-45
Spring Temp. (°C)		27	27	27	21	29	32	32	26	22	30	32	32	30	32	31
SiO <sub>2</sub> -quartz	Fournier & Potter (1982)	36	36	36	26	36	36	34	34	31	40	40	40	31	38	40
	Michard (1979)	37	37	37	28	37	37	35	35	33	41	41	41	33	39	41
Na-K	Giggenbach (1988)	163	163	156	172	152	159	159	167	159	144	144	144	144	144	185
	Fournier (1979)	143	143	137	153	132	139	139	148	139	124	124	124	124	124	166
Na-K-Ca	Fournier & Truesdell (1973)	3	3	-1	-1	6	3	3	4	-14	10	10	10	10	11	21
	Fournier and Truesdell (1973)	37	37	31	33	38	36	36	38	18	41	41	41	41	43	58
Ca-K	Michard (1990)	20	20	15	16	21	19	19	21	4	24	24	23	23	25	38
K-Mg	Giggenbach et al. (1983)	13	13	10	11	12	13	14	12	3	16	16	16	15	15	25
Na-Li	Fouillac & Michard (1981)	81	81	85	100	70	88	88	96	34	95	84	84	84	59	78
Li	Fouillac & Michard (1981)	62	62	62	62	62	66	66	66	30	82	77	77	77	66	72
Mg-Li	Kharaka & Mariner (1988)	11	11	12	13	10	14	15	14	-11	24	21	21	20	12	17
Ca-Mg	Chiodini et al. (1995)	69	69	72	75	59	71	78	61	80	71	71	72	70	63	68

Jaraba ones. The rest of the cation geothermometers indicate excessively high or low temperatures, as expected from the application of the Giggenbach diagram: high in the case of the Na-K geothermometer and lower than the temperatures measured under spring conditions, in the case of the K-Mg geothermometer (Table 4 and Fig. 4). The Na-K-Ca geothermometer also provides too low temperatures. The temperatures obtained with the Ca-K geothermometer depend on the calibration considered (Table 4 and Fig. 4): the calibration proposed by Fournier and Truesdell (1973) provides reasonable temperatures about 40 °C, whilst the calibration from Michard (1990) estimates a temperature lower than the spring temperature, about 20 °C. This situation, along with the fact that this Ca-K geothermometer is deduced from the Na-K-Ca geothermometer, whose results are also inconsistent, suggests that the Ca-K geothermometer's results are affected by important uncertainties and therefore, they will not be considered in this study. Finally, the Mg-Li geothermometer provides temperatures below the spring temperature and, although the other two lithium geothermometers (Na-Li and Li) provide higher temperatures (62–108 °C), their results are uncertain (e.g. D'Amore et al., 1987) as they were not specifically calibrated for waters with Li concentrations below 1 ppm (which is the case of the Alhama-Jaraba waters).

It is not surprising that the application of most of these cation geothermometers leads to erroneous results, but what is interesting is that in other similar carbonate-evaporitic systems, where some detrital components are also present, these classical cation geothermometers have provided reliable results (e.g. Fernández et al., 1988; Michard and Bastide, 1988; Pastorelli et al., 1999; Gökgöz and Tarcan, 2006; Mohammadi et al., 2010; Apollaro et al., 2012; Wang et al., 2015;

Blasco et al., 2017, 2018). This different performance will be discussed later.

The Ca-Mg geothermometer proposed by Chiodini et al. (1995), based on a disordered dolomite, provides temperatures ranging from 61 to 75 °C, slightly higher than the temperatures obtained with the SiO<sub>2</sub>-quartz geothermometer. However, one has to take into account that this geothermometer is based on the simultaneous equilibrium calcite-dolomite and therefore, the results are strongly affected by the solubilities of both minerals, and as the solubility of calcite is fairly well-constrained, the main effects come from the uncertainties in the dolomite solubility. There is a wide range of proposed solubilities for dolomite depending mainly on the degree of crystallographic order assumed for this phase and as a result this can lead to different temperature results depending on the order degree of the dolomite considered. This issue will be addressed further in this study.

With respect to the use of the geothermometers developed for this type of system (SO<sub>4</sub>-F and Ca-Mg; Marini et al., 1986; Chiodini et al., 1995) some problems have also been found. The SO<sub>4</sub>-F geothermometer cannot be used in the studied system as it is only applicable in the cases where equilibria anhydrite-fluorite or gypsum-fluorite are fulfilled, which is not the case for the Alhama-Jaraba system neither under spring conditions nor in the deep aquifer (see below).

#### 4.2.2. Geothermometrical modelling results

As mentioned above, this type of modelling consists of simulating a process of progressive water temperature increase to obtain the temperature range at which a set of minerals (assumed to be present in the reservoir in equilibrium with the waters) simultaneously reaches

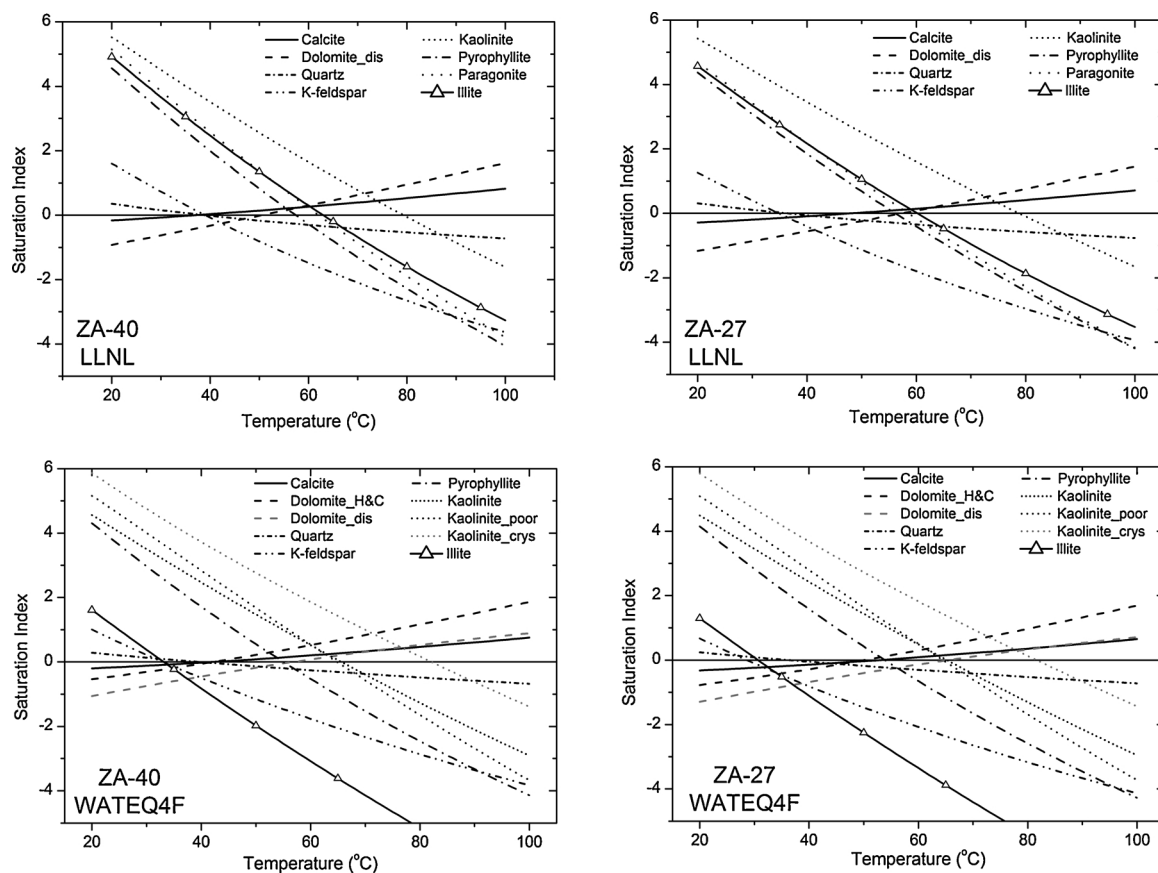


Fig. 5. Evolution with temperature of the saturation indices of the minerals presumed to be in equilibrium with the waters in the reservoir. The waters shown here correspond to sample ZA-27 from Jaraba and ZA-40 from Alhama. The calculations have been performed with two different thermodynamic databases, LLNL (upper two plots) with the original data and WATEQ4F (lower plots) with additional data for many of the minerals of interest: the thermodynamic data for the partially ordered dolomite were taken from Hyeong and Capuano (2001; Dolomite\_H&C) and the data for crystalline kaolinite (Kaolinite\_crys), poorly crystalline kaolinite (Kaolinite\_poor), K-feldspar and pyrophyllite were taken from Michard (1983). Dolomite\_dis represents in both cases the disordered dolomite included in each database.

equilibrium. One of the main difficulties when reconstructing the equilibrium situation at depth through heating simulations is related to the possible hydrogeochemical modifications by secondary processes that may have affected the chemistry of the waters during their ascent to the surface (Pang and Reed, 1998; Peiffer et al., 2014). That is why the selection of the spring water with which the simulations are going to be performed is crucial.

In previous works, mixing with cooler and shallower waters and CO<sub>2</sub> outgassing have been reported as the main secondary processes affecting the hydrogeochemistry of the system studied (see Tena et al., 1995; Auqué et al., 2009 and Blasco et al., 2016 for details). In order to minimise their effects in the modelling, the water samples selected for the geothermometrical simulations are those with the highest temperatures (less probability of have been affected by mixing) and with the lowest pH values (less probability of have been affected by CO<sub>2</sub> outgassing). The two samples are:

- sample ZA-40 (Alhama) which almost fulfils both conditions, the lowest pH of the site and a spring temperature only 0.5 °C lower than the maximum measured temperature spring in Alhama, ZA-41 (Table 2); and
- sample ZA-27 (Jaraba) with the highest measured spring temperature and not affected by mixing (evident process in the Jaraba set; Tena et al., 1995; Pinuaga et al., 2004; Auqué et al., 2009; Blasco et al., 2016) as the chemical composition is very constant with time and it belongs to the group of waters without tritium in the Jaraba group (Tena et al., 1995; Blasco et al., 2016). The problem with this sample is that the pH value (pH = 7.05; Table 2) is not the lowest among the Jaraba waters probably due to some CO<sub>2</sub> outgassing. Therefore, in order to correct the possible effects of this, a theoretical addition of CO<sub>2</sub> (as recommended by Pang and Reed, 1998 and Palandri and Reed, 2001) has been simulated with PHREEQC up to the point at which the lowest pH value measured in the area is obtained (pH = 6.80 in sample ZA-26, adding 0.6 mmol/L of CO<sub>2</sub>).

The results of the geothermometrical simulations with the PHREEQC geochemical code, using the LLNL and WATEQ4F thermodynamic databases are shown in Fig. 5 and Table 5. The general results indicate that these thermal waters are highly undersaturated with respect to albite, gypsum, anhydrite and fluorite not only under spring conditions (as seen above) but within the whole temperature range considered in the simulations.

Quartz equilibrium is reached at rather similar temperatures (37–40 °C) in both waters (Fig. 5 and Table 5) and coincides with the equilibrium for calcite and dolomite in Alhama, especially when considering the partially-ordered dolomite from Hyeong and Capuano (2001; Dolomite\_H&C). Average equilibrium temperatures between the two databases with respect to calcite and dolomite are 41.5 ± 1.5 °C in Alhama and 50.5 ± 2.5 °C in Jaraba when considering the partially-ordered Dolomite\_H&C only. The range in the equilibrium temperatures is increased if fully-disordered dolomite is considered (48 ± 8 °C for Alhama and 56 ± 8 °C for the Jaraba thermal waters) although the temperature provided by this phase, which is more soluble than the others, should be considered as a maximum temperature (Blasco et al., 2018). As a conclusion, it can be said that the good convergence among the temperatures estimated using quartz, calcite and dolomite equilibria (unaffected by possible CO<sub>2</sub> outgassing problems in the case of quartz, but affected for the carbonates) confirm that the samples selected for the geothermometrical simulations are not significantly affected by CO<sub>2</sub> outgassing during the rise of these thermal waters to the surface (e.g. Pang and Reed, 1998).

To verify the previous determinations, the modelling has been repeated for another sample presumably only affected by CO<sub>2</sub> outgassing, sample ZA-39 but reconstructing the characteristics of the waters at depth before the CO<sub>2</sub> loss (Palandri and Reed, 2001; Pang and Reed, 1998). For this purpose, about 0.45 mmol/L of CO<sub>2</sub> have been added to

the ZA-39 sample, giving a pH value identical to that in sample ZA-40 (6.90). The equilibrium temperatures obtained for the mineral phases are almost the same as those presented above for sample ZA-40, without CO<sub>2</sub> outgassing, which suggests that the CO<sub>2</sub> outgassing is the main process affecting the waters at this site and that the effects of other secondary processes such as dissolution/precipitation are negligible, if any.

With regard to the results obtained with the aluminosilicate minerals included in the calculations (K-feldspar, pyrophyllite, paragonite, illite and kaolinite), the temperature values depend strongly on the thermodynamic data used.

- 1 For K-feldspar, the temperature ranges between 13 and 39 °C depending on the thermodynamic data and the sample considered (Table 5 and Fig. 5). K-feldspar solubility depends on the range of composition of the alkali-feldspar solid solutions and on the degree of Al-Si order/disorder (Stefánsson and Arnórsson, 2000). These uncertainties make it very difficult to figure out the possible participation of this phase at equilibrium at depth and, therefore, these results will be disregarded.
- 2 The reservoir temperature values indicated by the equilibrium of illite, pyrophyllite and paragonite are in all cases between 40 and 62 °C (except in the case of the temperature obtained with illite and WATEQ4F in the Jaraba sample which is only 31 °C), in good agreement with the results obtained for calcite, dolomite and quartz.
- 3 Finally, the equilibrium temperature for kaolinite depends on the assumed degree of crystallinity for this mineral (Michard et al., 1979; Sanjuan et al., 1988; Nordstrom et al., 1990), ranging from 49 to 82 °C. The lowest values correspond to a poorly crystalline kaolinite and the highest temperatures to more crystalline varieties (Table 5). This implies that, if kaolinite participates in the equilibrium assemblage of the Alhama-Jaraba thermal waters, which suggests temperatures mostly lower than 60 °C, it will be a poorly-crystalline phase (as also found in other low-temperature carbonate aquifers; Michard and Bastide, 1988).

These results are also affected by the problems associated with the analytical determination of low aluminium concentrations and/or the formation of colloids and the possible precipitation of Al-bearing phases during the ascent of the thermal waters (Pang and Reed, 1998; Peiffer et al., 2014). To evaluate the potential effects of these uncertainties the FixAl method proposed by Pang and Reed (1998) has been applied and K-feldspar equilibrium was imposed in the geothermometrical modelling (Figure S2 in Supplementary Material). The results indicate that in

**Table 5**

Equilibrium temperatures (in °C) for the minerals considered in the geothermometrical simulations for the selected samples from Alhama and Jaraba thermal waters. Results with the WATEQ4F and LLNL thermodynamics databases are shown.

	ZA-27 (Jaraba)		ZA-40 (Alhama)	
	WATEQ4F	LLNL	WATEQ4F	LLNL
Calcite	53	48	43	40
Dolomite (dis)	64	57	56	51
Dolomite_H&C	51	—	42	—
Quartz	37	37	40	40
K-Feldspar	29 <sup>1</sup>	35	33 <sup>1</sup>	39
Kaolinite	65	79	63	79
Kaolinite (poor crys)	64 <sup>1</sup>	—	65 <sup>1</sup>	—
Kaolinite (crys)	81 <sup>1</sup>	—	82 <sup>1</sup>	—
Illite	31	60	44	63
Pyrophyllite	54 <sup>1</sup>	56	56 <sup>1</sup>	57
Paragonite	—	59	—	62

<sup>1</sup> Using the thermodynamic data from Michard et al. (1979) and Michard (1983).

doing so, Al concentrations in the waters would be higher than the measured ones and that there is a lack of convergence of the SI values for the rest of the aluminosilicate phases, which is worse than the previous results (compare the results in Fig. 5 and Figure S2). Similar situations have been obtained when imposing equilibria with other aluminosilicate phases (e.g. kaolinite, muscovite; Pang and Reed, 1998) in the calculations (not shown), suggesting that dissolved aluminium in the waters studied is not meaningfully affected by secondary processes (e.g. re-equilibria with respect to Al-bearing phases) during the ascent of the thermal waters.

Overall, a value of  $51 \pm 14$  °C is indicated from the equilibria with respect to quartz, calcite, dolomite (Dolomite\_H&C, partially disordered; Hyeong and Capuano, 2001), pyrophyllite, paragonite and low crystalline kaolinite, as the most probable temperature range at depth in the Alhama-Jaraba thermal system. This range takes into account the thermodynamic uncertainties for the key minerals and encloses the temperature values deduced by the quartz geothermometer.

## 5. Discussion

The combination of different geothermometrical approaches and sensitivity analysis to thermodynamic data has allowed defining a probable temperature range for the Alhama-Jaraba thermal waters in the aquifer at depth.

The results presented here support the expected unsuitability of most cationic geothermometers for the estimation of the reservoir temperatures in low temperature environments and/or in carbonate-evaporitic reservoirs (Henley et al., 1984; D'Amore et al., 1987; Minissale and Duchi, 1988; Mutlu and Güleç, 1998; López-Chicano et al., 2001; Levet et al., 2002; Karimi and Moore, 2008; Sonney and Vuataz, 2010). The application of these classical geothermometers to the Alhama-Jaraba thermal waters leads to temperatures either too high (compared with the combined results of other methodologies) or too low (below spring temperature). The question that arises here is why these geothermometers have provided coherent results in other similar low temperature systems hosted in carbonate–evaporitic rocks and not in this particular one. Blasco et al. (2017, 2018) have studied some examples of this situation and they indicate that the good results found in those systems are conditioned by the existence of detrital rocks in the carbonate–evaporitic reservoir, allowing the waters to reach equilibrium with respect to the phases on which these geothermometers are based. In this case, their unsuitability, despite the presence of some detrital formations in the aquifer, seems to be related to the shorter residence time of the waters or the less homogeneous distribution of this specific mineralogy.

The  $\text{SO}_4\text{-F}$  chemical geothermometer, based on the anhydrite–fluorite equilibria, was developed specifically for carbonate–evaporitic systems; however, it is not always applicable in them as fluorite is not a common mineral in these aquifers (e.g. Blasco et al., 2017, 2018). This is also the situation in the Alhama–Jaraba system and therefore this geothermometer cannot be applied here. Additionally, dispersed anhydrite has been identified in the aquifer studied although in a clear undersaturation state that produces its dissolution and the associated dedolomitisation process that controls the geochemical evolution of these thermal waters (Auqué et al., 2009). The disequilibrium of the waters with respect to anhydrite prevents the use of one of the most reliable equilibria in the geothermometrical modelling of this type of system, which is the equilibrium quartz/chalcedony–anhydrite (see below).

The results obtained with the Ca–Mg geothermometer (Marini et al., 1986; Chiodini et al., 1995), also developed for carbonate–evaporitic rocks, range between 63 and 78 °C, but the uncertainties related to the crystallinity and solubility of dolomite prevent it from obtaining a unequivocal estimation of the reservoir temperature. As already explained, this is one of the main difficulties in the geothermometrical calculations developed for this type of carbonate system and it

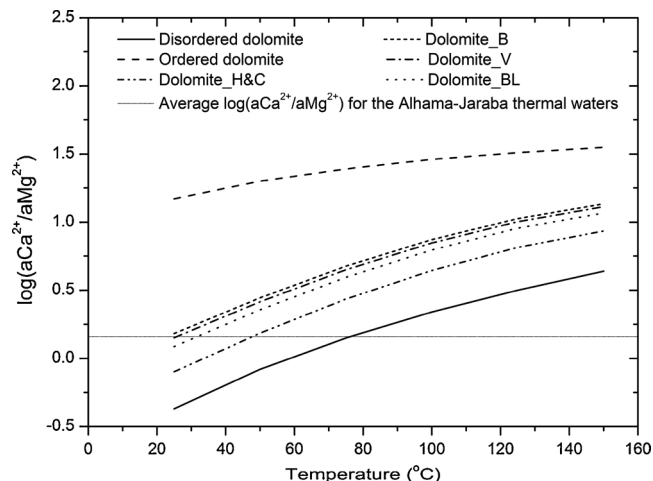


Fig. 6.  $\log(a\text{Ca}^{2+}/a\text{Mg}^{2+})$  vs. temperature plot for the calcite–dolomite equilibrium using different dolomites, from 25 to 150 °C. The equilibria with respect to calcite and fully-disordered dolomite and with respect to calcite and fully-ordered dolomite, have been calculated with the thermodynamic data in the LLNL database. The equilibria with respect to calcite and some partially ordered dolomites present in natural systems are also shown (see text). The  $\log(a\text{Ca}^{2+}/a\text{Mg}^{2+})$  average value (0.146) calculated with PHREEQC for the Jaraba and Alhama thermal waters is also represented as a horizontal grey line.

constitutes a major limitation for their application to natural systems. In order to avoid these uncertainties, various dolomites have been used here in the geothermometrical modelling and the most consistent result (i.e. the best convergence between calcite and dolomite towards  $\text{SI} = 0$ ) has been obtained considering the dolomite provided by Hyeong and Capuano (2001), which indicates that the dolomite present in the reservoir of the Alhama-Jaraba thermal waters should be of a similar order as Dolomite\_H&C, which is 11%.

To explore the importance of the order of dolomite on the classical geothermometrical results,  $\log(a\text{Ca}^{2+}/a\text{Mg}^{2+})$  values have been calculated from Eq. (2) for the different dolomites included in the WATEQ4F and LLNL databases, and also for other dolomites present in natural systems, at different temperatures. As shown in Fig. 6, there is a wide variability field of  $\log(a\text{Ca}^{2+}/a\text{Mg}^{2+})$  values (and, therefore, of possible estimated temperatures) depending on the type of dolomite assumed in the calculations. The average  $\log(a\text{Ca}^{2+}/a\text{Mg}^{2+})$  values calculated with PHREEQC are very similar for Alhama and Jaraba thermal waters (around 0.16; when considering the sample without mixing in Jaraba) and this value corresponds to reservoir temperatures about 77 °C when considering the fully-disordered dolomite (Fig. 6). The presence of this type of dolomite is quite improbable in old rocks from the Jurassic-Cretaceous, but, in any case, this temperature can be considered as a maximum estimate (Blasco et al., 2018). On the other hand, the calculations indicate the impossibility of occurrence of a fully-ordered dolomite in equilibrium with the waters studied (which would imply values of  $\log(a\text{Ca}^{2+}/a\text{Mg}^{2+})$  above 1.2; see Fig. 6). In agreement with the results of the geothermometrical modelling, the most consistent result is the one obtained when this calculation is carried out considering the partially ordered dolomite with an order degree of 11% (dolomite\_H&C). Finally, following the methodology suggested by Blasco et al. (2018) to deal with these uncertainties, the approximate order degree of the dolomite present in this system was calculated considering samples ZA-27, from Jaraba, and ZA-40, from Alhama. The order degree obtained for the dolomite in the reservoir of this thermal system is similar for both samples: 11.3% in the case of Jaraba and 14.7% in the case of Alhama, as expected close to the value for the dolomite studied by Hyeong and Capuano (2001).

Quartz equilibrium in the geothermometrical simulations (and quartz geothermometer results) provides reasonable values, in the



lower range of the estimated temperature ( $51 \pm 14^\circ\text{C}$ ).

Quartz (or chalcedony) – anhydrite equilibrium has been shown to be a reliable indication of the reservoir temperature (e.g. Pastorelli et al., 1999; Levet et al., 2002; Alçiçek et al., 2016, 2017; Blasco et al., 2017, 2018). Unfortunately, as mentioned above, this equilibrium is not applicable to this system because anhydrite equilibrium is not reached.

For other key minerals (K-feldspar and aluminosilicate phases), the estimated reservoir temperature range in geothermometrical simulations depends strongly on the thermodynamic data selected and Al concentration. However, using reasonable solubility “end-members” for these minerals (covering differences due to the degree of crystallinity, particle size effects or the order/disorder phenomena), a relatively narrow temperature range of  $\pm 20^\circ\text{C}$  can be obtained, in agreement with one of the scarce earlier uncertainty estimations for geothermometrical modelling, carried out by Tole et al. (1993).

Taking into account all the geothermometrical techniques applied in this study and the usual uncertainties considered in the temperatures obtained with classical geothermometers ( $\pm 5$  to  $\pm 10^\circ\text{C}$  and may be greater than  $20^\circ\text{C}$ ; Fournier, 1982), or geochemical modelling ( $\pm 20^\circ\text{C}$ ; Tole et al., 1993), the temperature estimate of  $51 \pm 14^\circ\text{C}$  for the Alhama-Jaraba thermal waters can be considered quite probable. This common temperature range at depth for the Alhama and Jaraba thermal waters would be in agreement with the idea that their origin is from the same aquifer.

Furthermore, the results of the studies carried out in the context of the ALGECO2 project (IGME, 2010) in the area of the Almazán Basin, indicate that the carbonate aquifer reaches a depth of about 1200 m. The geothermal gradient for the Almazán Basin is about  $30^\circ\text{C}/\text{Km}$  (Fernández et al., 1998) and, thus, considering an average air temperature of about  $14\text{--}15^\circ\text{C}$  in this area (López et al., 2007), the estimated temperature at these depths would be  $52^\circ\text{C}$ , in close agreement with the average temperature obtained from the combined techniques used in this study.

## 6. Conclusions

The waters of the low temperature Alhama-Jaraba geothermal system, hosted in carbonate rocks and one of the largest naturally flowing thermal systems in Europe, have been characterised in this study, and various chemical geothermometrical techniques have been tested.

The thermal waters in the Jaraba springs are of Ca-Mg –  $\text{HCO}_3$  type whilst they are more  $\text{SO}_4\text{-Cl}$  type in Alhama. The range of emerging temperatures in the Alhama springs is quite narrow, between  $30$  and  $32.4^\circ\text{C}$ , while in Jaraba the temperatures range between  $21$  and  $32^\circ\text{C}$ , due to the effects of mixing with shallower and cooler waters. Variable  $\text{CO}_2$ -outgassing processes affect different springs at both sites, promoting changes in the pH values of the waters. In summary, the Alhama-Jaraba system, as a whole, brings together almost all drawbacks and possible difficulties for the application of the geothermometrical methods in this type of low temperature geothermal system: problems related to the existence of secondary processes during the ascent of the thermal waters and problems related to the effective mineral equilibria in the reservoir at low temperatures.

The effects of the secondary processes identified can be minimised with 1) a careful selection of the adequate samples for the geothermometrical calculations (e.g. discarding those samples affected by mixing) and/or 2) using the reconstruction methodologies available when applying the multicomponent geothermometrical methods (e.g. adding  $\text{CO}_2$  to reverse the effects of  $\text{CO}_2$ -outgassing during the ascent of the thermal waters).

The mineralogical/lithological characteristics of the aquifer importantly constrain the mineral equilibria at depth and, therefore, the results obtained with the classical geothermometers or with the multicomponent geothermometry. Cation geothermometers have been successfully used in some carbonate-evaporitic geothermal systems

with presence of detrital rocks in the aquifer. These detrital rocks are also present in the Alhama-Jaraba system but the lower residence times, the lower temperature at depth and/or the more disperse distribution of siliciclastic materials in the aquifer prevent the waters from attaining the mineral equilibria on which these geothermometers are based (e.g. albite and K-feldspar). This has also been confirmed in the results of the geothermometrical modelling.

The aquifer studied is dominated by carbonates with only a slight evaporitic character reflected by the low abundance of gypsum/anhydrite in the rocks and by the disequilibrium of the waters with respect to these phases. Due to this disequilibrium, the  $\text{SO}_4\text{-F}$  geothermometer (specifically developed for carbonate-evaporitic geothermal systems) and the equilibrium quartz (or chalcedony)–anhydrite (one of the most reliable equilibria in the geothermometrical modelling), cannot be used for this system.

Therefore, the only possible mineral equilibria available for the geothermometrical calculations in systems like the one presented here are silica polymorphs, calcite, dolomite and clay minerals. After evaluating the results obtained with different silica phases, the  $\text{SiO}_2$ -quartz geothermometer appears to provide consistent results in the system studied. The evaluation of the dolomite and clay mineral equilibria, however, shows important uncertainties in the solubility values available related to degree of crystallinity, particle size effects and/or the order/disorder phenomena.

Although the waters are in equilibrium with respect to calcite and dolomite, the uncertainties associated with the order degree of dolomite affect the Ca-Mg geothermometer and the evaluation of this equilibrium by geothermometrical modelling. To deal with these uncertainties a possible strategy is the one applied in this paper, consisting of evaluating the results obtained with different dolomites (with the Ca-Mg geothermometer and the geochemical modelling).

Finally, clay mineral equilibria in the geothermometrical modelling provide consistent results within a reasonable uncertainty range, as long as proper sensitivity analysis is performed in order to evaluate the effects of the thermodynamic data selected.

By applying all these methods, the reservoir temperature for the Alhama-Jaraba system has been established to be  $51 \pm 14^\circ\text{C}$ , with waters in equilibrium with quartz, calcite, partially-ordered dolomite and some aluminosilicate phases. This temperature is in close agreement with that deduced from the results of geophysical studies in the area.

## Acknowledgements

M. Blasco has worked on this study thanks to a scholarship from the Ministry of Education, Culture and Sports of Spain, for the Training of University Teachers (ref. FPU14/01523). This study forms part of the activities of the Geochemical Modelling Group (University of Zaragoza; Aragón Government). The technical assistance of Enrique Oliver, from the Earth Sciences Department of the University of Zaragoza, is also acknowledged. The comments and suggestions of Dr. N. Spycher and of two anonymous reviewers have contributed to improve the work and are gratefully appreciated.

## Appendix A. Supplementary data

Supplementary data associated with this article can be found, in the online version, at <https://doi.org/10.1016/j.geothermics.2018.11.004>.

## References

- Alçiçek, H., Bülbül, A., Alçiçek, M.C., 2016. Hydrogeochemistry of the thermal waters from the Yenice Geot Field (Denizli Basin, Southwestern Anatolia, Turkey). *J. Volcanol. Geotherm. Res.* 309, 118–138.
- Alçiçek, H., Bülbül, A., Brogi, A., Liotta, D., Ruggieri, G., Capezzuoli, E., Meccheri, M., Yavuzer, I., Alçiçek, M.C., 2017. Origin, evolution and geothermometry of the thermal waters in the Gölemezli Geothermal Field, Denizli Basin (SW Anatolia,

- Turkey). *J. Volcanol. Geotherm. Res.* 349, 1–30.
- Alonso, A., Floquet, M., Mas, R., Melendez, A., 1993. Late cretaceous carbonate platforms: origin and evolution, Iberian range, Spain. In: Masse, J.P. (Ed.), *AAPG Spec. Publ.* 56, pp. 297–316.
- Apollaro, C., Dotsika, E., Marini, L., Barca, D., Bloise, A., de Rosa, R., Doveri, M., Lelli, M., Muto, F., 2012. Chemical and isotopic characterization of the thermomineral water of Terme Sibarite springs (Northern Calabria, Italy). *Geochem. J.* 46, 117–129.
- Appelo, C.A.J., Postma, D., 2005. *Geochemistry, groundwater and pollution*. In: Balkema, A.A. (Ed.), Rotterdam, 2<sup>nd</sup> ed. .
- Arnorsson, S., Gunnlaugsson, E., Svavarsson, H., 1983. The chemistry of geothermal waters in Iceland. III. Chemical geothermometry in geothermal investigations. *Geochim. Cosmochim. Acta* 47, 567–577.
- Auqué, L.F., Acero, P., Gimeno, M.J., Gómez, J., Asta, M.P., 2009. Hydrogeochemical modeling of a thermal system and lessons learned for CO<sub>2</sub> geologic storage. *Chem. Geol.* 268, 324–336.
- Aurell, M., Melendez, G., Oloriz, F., Badenas, B., Caracuel, J.E., Garcia-Ramos, J.C., Goy, A., Linares, A., Quesada, S., Robles, S., Rodríguez-Tovar, F.J., Rosales, I., Sandoval, J., Suarez de Centi, C., Tavera, J.M., Valenzuela, M., 2002. Jurassic. In: Gibbons, W., Moreno, T. (Eds.), *The Geology of Spain*. Geological Society of London, London, UK.
- Blasco, M., Auqué, L.F., Gimeno, M.J., 2016. Caracterización geoquímica del proceso de mezcla de aguas termales y no termales en los manantiales de Jaraba (Aragón, España). *Geotemas* 16, 531–534.
- Blasco, M., Auqué, L.F., Gimeno, M.J., Acero, P., Asta, M.P., 2017. Geochemistry, geothermometry and influence of the concentration of mobile elements in the chemical characters of carbonate-evaporitic thermal systems. The case of the Tiermas geothermal system (Spain). *Chem. Geol.* 466, 696–709.
- Blasco, M., Gimeno, M.J., Auqué, L.F., 2018. Low temperature geothermal systems in carbonate-evaporitic rocks: mineral equilibria assumptions and geothermometrical calculations. Insights from the Arnedillo thermal waters (Spain). *Sci. Total Environ.* 615, 526–539.
- Busby, J.F., Plummer, L.N., Lee, R.W. and Hanshaw, B.B., 1991. *Geochemical evolution of water in the Madison Aquifer in parts of Montana, South Dakota, and Wyoming*. U.S. Geological Survey Professional Paper 1273-F, 89.
- Carpenter, A.B., 1980. The chemistry of dolomite formation I: the stability of dolomite. In: Zenger, D.H., Dunham, J.B., Ethington, R.L. (Eds.), *Concepts and Models of Dolomitization*, vol. 28. Society of Economic Paleontologists and Mineralogists Spec. Publ., pp. 111–121.
- Chiodini, G., Frondini, F., Marini, L., 1995. Theoretical geothermometers and PCO<sub>2</sub> indicators for aqueous solutions coming from hydrothermal systems of medium-low temperature hosted in carbonate-evaporite rocks. Application to the thermal springs of the Etruscan Swell. Italy. *Appl. Geochem.* 10, 337–346.
- Clark, I., Fritz, P., 1997. *Environmental Isotopes in Hydrogeology*. CRC Press/Lewis Publishers, Boca-Raton (Florida).
- D'Amore, F., Fancelli, R., Caboi, R., 1987. Observations of the application of chemical geothermometers to some hydrothermal systems in Sardinia. *Geothermics* 16, 271–282.
- De Toledo, F.O., Arqued, V., 1990. Estudio de los recursos hidráulicos subterráneos de los acuíferos relacionados con la provincia de Zaragoza. Unidad Hidrogeológica 43, Sierra del Solorio. MOPU, 09.803.183/0411, pp. 224.
- Fernández, J., Auqué, L.F., Sánchez Cela, V.S., Guaras, B., 1988. Las aguas termales de Fitero (Navarra) y Arnedillo (Rioja). Análisis comparativo de la aplicación de técnicas geotermométricas químicas a aguas relacionadas con reservorios carbonatado-evaporíticos. *Estudios Geológicos* 44, 453–469.
- Fernández, M., Marzán, I., Correia, A., Ramalho, E., 1998. Heat flow, heat production, and lithospheric thermal regime in the Iberian Peninsula. *Tectonophysics* 291, 29–53.
- Fouillac, C., Michard, G., 1981. Sodium/Lithium ratio in water applied to geothermometry of geothermal reservoirs. *Geothermics* 10, 55–70.
- Fournier, R.O., 1977. Chemical geothermometers and mixing models for geothermal systems. *Geothermics* 5, 41–50.
- Fournier, R.O., 1979. A revised equation for the Na-K geothermometer. *Geotherm. Resour. Coun. Trans.* 3, 221–224.
- Fournier, R.O., 1981. Application of water geochemistry to geothermal exploration and reservoir engineering. In: Rybach, L., Muffler, L.J.P. (Eds.), *Geothermal Systems: Principles and Case Histories*. John Wiley & Sons Ltd., pp. 109–141.
- Fournier, R.O., 1982. Water geothermometers applied to geothermal energy. In: D'Amore, F. (Ed.), *Co-Ordinator*, Applications of Geochemistry in Geothermal Reservoir Development. UNITAR/UNDO centre on Small Energy Resources, Rome, Italy, pp. 37–69.
- Fournier, R.O., Potter II, R.W., 1982. A revised and expanded silica (quartz) geothermometer. *Geotherm. Res. Coun. Bull.* 11, 3–12.
- Fournier, R.O., Potter II, R.W., 1979. Magnesium correction to Na-K-Ca geothermometer. *Geochim. Cosmochim. Acta* 43, 1543–1550.
- Fournier, R.O., Truesdell, A.H., 1973. An empirical Na-K-Ca geothermometer for natural waters. *Geochim. Cosmochim. Acta* 37, 1255–1275.
- Giggenbach, W.F., 1988. Geothermal solute equilibria. Derivation of Na-K-Mg-Ca geothermometers. *Geochim. Cosmochim. Acta* 52, 2749–2765.
- Giggenbach, W.F., Gonfiantini, R., Jangi, B.L., Truesdell, A.H., 1983. Isotopic and chemical composition of Parbati Valley geothermal discharges, NW-Himalaya, India. *Geothermics* 12, 199–222.
- Gökgöz, A., Tarcan, G., 2006. Mineral equilibria and geothermometry of the Dalaman-Köyceğiz thermal springs, southern Turkey. *Appl. Geochem.* 21, 253–268.
- Goldscheider, N., Mádl-Szönyi, J., Eröss, A., Schill, E., 2010. Review: thermal water resources in carbonate rock aquifers. *Hydrogeol. J.* 18, 1303–1318.
- Helgeson, H.C., Delany, J.M., Nesbitt, H.W., Bird, D.K., 1978. Summary and critique of the thermodynamic properties of rock-forming minerals. *Am. J. Sci.* 278, 229.
- Henley, R.W., Truesdell, A.H., Barton, P.B., Whitney, T., 1984. Fluid Mineral Equilibria in Hydrothermal Systems. *Reviews in Economic Geology I*. Published by the Soc. of Economic Geologists.
- Hyeong, K., Capuano, R.M., 2001. Ca/Mg of brines in Miocene/Oligocene clastic sediments of the Texas Gulf Coast: buffering by calcite/disordered dolomite equilibria. *Geochim. Cosmochim. Acta* 65, 3065–3080.
- IGME, 1980. Informe Hidrogeológico Del Subsistema Acuífero Sierra Del Solorio (Sistema Acuífero 57).
- IGME, 1982. Estudio De Las Manifestaciones Termiales De Extremadura, Salamanca, Aragón Y Rioja, Orientados a Su Posible Explotación Como Recursos Geotérmicos. Informe Interno Número 747. Ministerio de Industria y Energía, Madrid.
- IGME, 1987. Estudio De Detalle Del Borde Septentrional De La Sierra Del Solorio (Sistema Acuífero 57).
- IGME, 1991. Daroca. Mapa Geológico De España. Escala 1: 200.000. Instituto Tecnológico Geominero de España, pp. 239.
- IGME, 1994. Estudio De Las Aguas Minero-medicinales, Minero-industriales, Termiales Y De Bebida Envasada En La Comunidad Autónoma De Aragón. IGME, Madrid, pp. 1500.
- IGME, 2010. Selección Y Caracterización De Áreas Y Estructuras Geológicas Favorables Para El Almacenamiento Geológico De CO<sub>2</sub> En España. From: <http://info.igme.es/algeco2/>.
- Karimi, H., Moore, F., 2008. The source and heating mechanism for the Ahram, Mirahmad and Garu thermal springs, Zagros Mountains. Iran. *Geothermics* 37, 84–100.
- Kharaka, Y.K., Mariner, R.H., 1988. Chemical geothermometers and their application to formation waters from sedimentary basins. In: Naeser, N.D., McCollon, T.H. (Eds.), *Thermal History of Sedimentary Basins; Methods and Case Histories*. Springer, Berlin Heidelberg New York, pp. 99–117.
- Levet, S., Toutain, J.P., Munoz, M., Berger, G., Negrel, P., Jendrzewski, N., Agrinier, P., Sortino, F., 2002. Geochemistry of the Bagnères-de-Bigorre thermal waters from the North Pyrenean Zone sedimentary environment (France). *Geofluids* 2, 1–16.
- López-Chicano, M., Cerón, J.C., Vallejos, A., Pulido-Bosch, A., 2001. Geochemistry of thermal springs, Alhama de Granada (southern Spain). *Appl. Geochem.* 16, 1153–1163.
- López, F., Cabrera, M., Cuadrat, J.M., 2007. Atlas Climático de Aragón. Gobierno de Aragón. 291.
- Mariner, R.H., Evans, W.C., Young, H.W., 2006. Comparison of circulation times of thermal waters discharging from the Idaho batholith based on geothermometer temperatures, helium concentrations, and <sup>14</sup>C measurements. *Geothermics* 35, 3–25.
- Marini, L., Chiodini, G., Cioni, R., 1986. New geothermometers for carbonate-evaporite geothermal reservoirs. *Geothermics* 15, 71–86.
- Meléndez, A., Meléndez, F., Portero, J., Ramírez del Pozo, J., 1985. Stratigraphy, sedimentology and paleogeography of Upper cretaceous evaporitic-carbonate platform in the central part of the Sierra Iberica. In: Milá, M.D., Rosell, J. (Eds.), *Sixth European Regional Meeting. Excursion Guidebook*, pp. 189–211.
- Merino, E., Ranson, B., 1982. Free energies of formation of illite solid solutions and their compositional dependence. *Clays Clay Min.* 30, 29–39.
- Michard, G., 1979. *Geothermomètres chimiques*. Bur. Rech. Géologiques Minières (2nd Ser.), Sect. III 2, pp. 183–189.
- Michard, G., 1983. *Recueil De Données Thermodynamiques Concernant Les Équilibres Eaux-minéraux Dans Les Réservoirs Géothermaux*. Rapp. Comm. Eur. Brussels EUR 8590 FR.
- Michard, G., Bastide, J.P., 1988. *Géochimie de la nappe du Dogger du Bassin de Paris*. J. Volcanol. Geotherm. Res. 35, 151–163.
- Michard, G., Fouillac, C., 1980. Contrôle de la composition chimique des eaux thermales sulfurées sodiques du Sud de la France. In: Tardy, Y. (Ed.), *Geochimie Des Interactions Entre Les Eaux, Les Minéraux Et Les Roches*. Elements, Tarbes, pp. 147–166.
- Michard, G., Roekens, E., 1983. Modelling of the chemical composition of alkaline hot waters. *Geothermics* 12, 161–169.
- Michard, G., 1990. Behaviour of major elements and some trace elements (Li, Rb, Cs, Sr, Fe, Mn, W, F) in deep hot waters from granitic areas. *Chem. Geol.* 89, 117–134.
- Michard, G., Ouzounian, G., Fouillac, C., Sarazin, G., 1979. Contrôle des concentrations en aluminium dissous dans les eaux des sources thermales. *Geochim. Cosmochim. Acta* 43, 147–156.
- Michard, G., Sanjuan, B., Criaud, A., Fouillac, C., Pentcheva, E.N., Petrov, P.S., Alexieva, R., 1986. Equilibria and geothermometry in hot waters from granites of S.W. Bulgaria. *Geochem. J.* 20, 159–171.
- Minissale, A.A., Duchi, V., 1988. Geothermometry on fluids circulating in a carbonate reservoir in north-central Italy. *J. Volcanol. Geotherm. Res.* 35, 237–252.
- Mohammadi, Z., Bagheri, R., Jahanshahi, R., 2010. Hydrogeochemistry and geothermometry of Changal thermal springs, Zagros region. Iran. *Geothermics* 39, 242–249.
- Mutlu, H., Gülec, N., 1998. Hydrogeochemical outline of thermal waters and geothermometry applications in Anatolia (Turkey). *J. Volcanol. Geotherm. Res.* 85, 495–515.
- Nemeth, K., 1963. Photometric determination of sulphate in soil extracts. *Z. Pflernähr. Dung.* 103, 193–196.
- Nicholson, K., 2012. *Geothermal Fluids: Chemistry and Exploration Techniques*. Springer, Berlin Heidelberg, pp. 263.
- Nieva, D., Nieva, R., 1987. Developments in geothermal energy in Mexico, part twelve. A cationic composition geothermometer for prospection of geothermal resources. *Heat Recovery Syst. Chp* 243–258 CHP 7.
- Nordstrom, D.K., Plummer, L.N., Langmuir, L., Busenberg, E., May, H.M., Jones, B.F., Parkhurst, D.L., 1990. Revised chemical equilibrium data for major water-mineral reactions and their limitation. In: Melchior, D.C., Basset, R.L. (Eds.), *Chemical Modeling of Aqueous Systems 1/ 416*. ACS Symp. Series, pp. 398–413.
- Palandri, J.L., Reed, M.H., 2001. Reconstruction of in situ composition of sedimentary formation waters. *Geochim. Cosmochim. Acta* 65, 1741–1767.
- Pang, Z., Reed, M.H., 1998. Theoretical chemical thermometry on geothermal waters:

- problems and methods. *Geochim. Cosmochim. Acta* 62, 1083–1091.
- Parkhurst, D.L., Appelo, C.A.J., 2013. Description of input and examples for PHREEQC version 3. A computer program for speciation, batch reaction, one dimensional transport, and inverse geochemical calculations. In: Geological Survey, U.S. (Ed.), *Techniques and Methods, Book 6*. U.S. Geological Survey, Denver, Colorado Chap. A43.
- Pastorelli, S., Marini, L., Hunziker, J.C., 1999. Water chemistry and isotope composition of the Acquarossa thermal system, Ticino, Switzerland. *Geothermics* 28, 75–93.
- Peiffer, L., Wanner, C., Spycher, N., Sonnenthal, E.L., Kennedy, B.M., Iovenitti, J., 2014. Optimized multicomponent vs. classical geothermometry: Insights from modeling studies at the Dixie Valley geothermal area. *Geothermics* 51, 154–169.
- Pinuaga, J.I., Garrido, E., Ramírez, A., 2004. Geología, Hidrogeología y protección de los Bañeros de Jaraba (Zaragoza). *Anales de la Real Academia Nacional de Farmacia* 70, 597–610.
- Reed, M.H., Spycher, N.F., 1984. Calculation of pH and mineral equilibria in hydrothermal water. *Geochim. Cosmochim. Acta* 48, 1479–1490.
- Reeder, R.J., 1990. Crystal chemistry of rhombohedral carbonates. In: Reeder, R.J. (Ed.), *Carbonates: Mineralogy and Chemistry. Reviews in Mineralogy*, vol. 11. Mineralogical Society of America, pp. 1–47.
- Reeder, R.J. (2000). Constraints on cation order in calcium-rich sedimentary dolomite. *Aquat. Geochemistry* 6, 213–226. Sánchez, J.A., Coloma, P. and Perez-García, A. (2004). Evaluation of geothermal flow at the springs in Aragon (Spain), and its relation to geologic structure. *Hydrol. J.*, 12, 601–609.
- Sánchez, J.A., Coloma, P., Pérez-García, A., 2004. Evaluation of geothermal flow at the springs in Aragón (Spain), and its relation to geologic structure. *Hydrogeol. J.* 12, 601–609.
- Sanjuan, B., Michard, A., Michard, G., 1988. Influence of the temperature of CO<sub>2</sub>-rich springs on their Al and REE contents. *Chem. Geol.* 68, 57–68.
- Sanz, E., Yelamos, J.G., 1998. Methodology for the study of unexploited aquifers with thermal waters: application to the aquifer of the Alhama de Aragon Hot Spring. *Ground Water* 6, 913–923.
- Sonney, R., Vuataz, F.D., 2010. Validation of chemical and isotopic geothermometers from low temperature deep fluids of Northern Switzerland. *Proceedings World Geothermal Congress 2010* 25–29.
- Spycher, N., Peiffer, L., Sonnenthal, E.L., Saldi, G., Reed, M.H., Kennedy, B.M., 2014. Integrated multicomponent solute geothermometry. *Geothermics* 51, 113–123.
- Stefánsson, A., Arnórsson, S., 2000. Saturation state of feldspars in natural waters. *Geochim. Cosmochim. Acta* 64, 2567–2584.
- Tena, J.M., Auqué, L.F., Gimeno, M.J., Mandado, J., 1995. Evolución fisicoquímica y geotermometría del sistema hidrotermal de Alhama-Jarba. *Institución Fernando el Católico* 178.
- Tole, M.P., Armannsson, H., Pang, Z., Arnórsson, S., 1993. Fluid/mineral equilibrium calculations for geothermal fluids and chemical geothermometry. *Geothermics* 22, 17–37.
- Vespasiano, G., Apollaro, C., Muto, F., Dotsika, E., de Rosa, R., Marini, L., 2014. Chemical and isotopic characteristics of the warm and cold waters of the Luigiane Spa near Guardia Piemontese (Calabria, Italy) in a complex faulted geological framework. *Appl. Geochem.* 41, 73–88.
- Wang, J., Jin, M., Jia, B., Kang, F., 2015. Hydrochemical characteristics and geothermometry applications of thermal groundwater in northern Jinan, Shandong, China. *Geothermics* 57, 185–195.



## 4.5 Paper 5

### **Characterisation of recent aragonite travertine deposits associated to the Fitero thermal waters (Spain) I: stable isotopes equilibrium evaluation**

*Mónica Blasco, Luis F. Auqué, María J. Gimeno, María P. Asta, Juan Mandado*

Sedimentary Geology

Impact Factor (2017): 2.575

Quartile and Category (2017): Q1 (9/47), Geology

Sent: 02 May 2019

Currently under review



# Characterisation of recent aragonite travertine deposits associated to the Fitero thermal waters (Spain) I: stable isotopes equilibrium evaluation

Under review in *Sedimentary Geology*

Mónica Blasco<sup>a,\*</sup>, Luis F. Auqué<sup>a</sup>, María J. Gimeno<sup>a</sup>, María P. Asta<sup>b</sup>, Juan Mandado<sup>a</sup>

<sup>a</sup> Geochemical Modelling Group. Petrology and Geochemistry Area, Earth Sciences Department, University of Zaragoza, Spain C/ Pedro Cerbuna 12, 50009 Zaragoza, Spain.

<sup>b</sup> Institut des Ciencias de la Terre (ISTerre). Université Grenoble Alpes - CNRS. 1381 Rue de la Piscine, 38610, Gières (France)

\* Corresponding author: Geochemical Modelling Group. Petrology and Geochemistry Area, Earth Sciences Department, University of Zaragoza, Spain. e-mail: monicabc@unizar.es; Tel.: +34 976761071; Fax: +34 976761106

## Abstract

The aragonite travertine deposits of the Fitero thermal springs, with a proportion of aragonite higher than 98 % in most of the samples, are studied in this paper. The main objective is to improve the general understanding of the aragonite precipitation since the deposits of almost pure aragonite are very scarce. The study has been focus on obtaining a complete mineralogical and isotopic characterisation of these solids, including the evaluation of the  $\delta^{18}\text{O}$  and  $\delta^{13}\text{C}$  fractionation during their precipitation, as a valuable information for paleoclimate and paleoenvironmental studies.

The Fitero thermal waters, from which these solids precipitate, are of chloride-sodium type, with spring temperature about 45 °C and near neutral pH. One travertine sample of almost pure aragonite (98 %) was taken from a pipe discharging the exceeding water from the cooling pool inside the spa. The water temperature was about 40 °C and it suffered an important process of  $\text{CO}_2$  loss, as suggested by the geochemical calculations and by the  $\delta^{13}\text{C}$  values measured in the travertines and the waters. This  $\text{CO}_2$  outgassing is the triggering factor for the oversaturation and concomitant precipitation of carbonate phases, and the temperature seems to be the main factor controlling the precipitation of aragonite or calcite in different proportions. This temperature effect has been checked by studying another travertine sample with a higher proportion of calcite (40%), precipitated in another pipe at the end of all the spa circuit where the water discharges at variable temperatures, from 33 to 40 °C.

Various  $\delta^{18}\text{O}$  isotope fractionation equations for aragonite and for calcite were used to evaluate the data in the travertine samples. The results indicate that the precipitation took place close to equilibrium according to some of these equations and the calculated temperature fits very well with the measured one; moreover, no differences have been found between the calcite–water and aragonite–water oxygen fractionation. The fact that the equilibrium is maintained during precipitation in a natural system with an important  $\text{CO}_2$  loss is quite surprising. However, it can be explained by an oxygen isotopic equilibrium between dissolved  $\text{HCO}_3^-$  and water and a direct transfer of the  $\text{HCO}_3^-$  isotope signal to the precipitating carbonate without fractionation due to the fast  $\text{CO}_2$  loss and precipitation. This would result in a  $\delta^{18}\text{O}$  equilibrium between travertines and water and, therefore, accurate temperature results could be expected using the  $\delta^{18}\text{O}$  fractionation equations.

The temperature– $\delta^{18}\text{O}$  values of the aragonite deposits in Fitero fit with the available data in other aragonite travertines from the literature (always with aragonite proportions higher than 90 %). Overall, they define a fractionation equation for natural aragonite in the temperature range of 23 to 80 °C near the experimental equation of Kim et al. (2007), suggesting that the existence of equilibrium, or apparent equilibrium, situations is not uncommon.

**Keywords:** geothermal system; travertine; aragonite; stable isotope; isotope equilibrium

## 1. Introduction

The Fitero thermal springs (Navarra region, Spain) are quite well known and their waters are used in two spas in the village for their medicinal and therapeutic properties. They have been studied by different authors (e.g. Blasco et al., 2019, Auqué et al., 1989, 1988, Coloma et al., 1998, 1997a, 1996, 1995; Fernández et al., 1988) obtaining the temperature in the deep reservoir, a complete chemical and isotopic characterisation of the hydrogeochemical system and a good knowledge of the main processes controlling the evolution of the waters.

Despite this broad characterisation of the thermal waters, the travertines precipitating from them are still almost unstudied. That is why the first objective of this research is the in-depth study of these travertines<sup>1</sup>. The fact that some of the Fitero travertines consist of almost pure aragonite

---

<sup>1</sup> The terminology that will be used here is the one proposed by Ford and Pedley (1996) in which the term travertine is used to refer to the carbonates precipitated from thermal (hot) waters, while the term tufa is reserved for the carbonates precipitated from cold waters (e.g. rivers).



(with less than 2 % of calcite) makes this system even more interesting because there are very few studies about pure or almost pure aragonite travertines or tufas, as most of them are mixtures of calcite and aragonite and they are studied as a whole. Therefore, the study of the aragonite travertine will help to improve the general understanding of the aragonite precipitation process and, the study of another more calcite-rich travertine (60% of calcite) precipitated from the same thermal waters will serve for comparative purposes and to evaluate the main controlling factors responsible for the precipitating mineral phases.

The thermal springs in the Fitero spa are currently controlled for their use in the balneotherapeutic facilities and the travertines studied here are generated inside water discharging pipes; however, their study will still be useful for the objectives of this work as it has already been done by other authors such as Asta et al. (2017) in travertines collected in the facilities of other spas, Rodríguez-Berriguete et al. (2018) in tufas precipitated in a pipe used for irrigation or Arenas et al. (2018) in a tufa generated in a pipe that diverted water from a river.

The study and characterisation of the Fitero aragonite travertines will be addressed from two different points of view which will be presented and discussed in two complementary papers: one dealing with the mineralogical and isotopic characterisation of the travertines (the present paper) and the other which will address their textural and geochemical characterisation, together with the distribution coefficients of some trace elements.

The relevance of the isotope characterisation of these solids lies on the fact that the stable  $\delta^{18}\text{O}$  isotope signature of travertines, tufas and speleothems precipitated under equilibrium conditions depends on the temperature and, therefore, it can be used for paleoenvironmental and paleoclimatic reconstructions (e.g. Andrews, 2006; Capezzuoli et al., 2014; Ford and Pedley, 1996; Fouke et al., 2000; Garnett et al., 2004; Jones and Renaut, 2010; Kele et al., 2011, 2008; Lachniet, 2015; Liu et al., 2006, 2010; Osácar et al., 2016, 2013; Pedley, 2009; Pentecost, 2005) by using empirical and experimental temperature-dependant equations assumed to represent the isotopic equilibrium between travertine and water. However, the paleothermometrical interpretation of the stable isotopes in carbonates is not always straightforward due to several reasons: 1) the isotopic signature of the old travertines parental water is unknown; 2) the equilibrium is not always attained, or maintained, during the travertine precipitation due to the kinetic isotope effects related to  $\text{CO}_2$  outgassing and high precipitation rates (e. g. Fouke et al., 2000; Kele et al., 2008; 2011; among others); and 3) the representativeness of those equations with respect to the real equilibrium is not always warranted (e.g. Kele et al., 2015; Lachniet, 2015). All these difficulties make the study of actively precipitating travertines an interesting subject that will help to interpret the isotope composition in old travertines.

## 2. Geological and hydrological setting

The Fitero thermal waters emerge in the NW part of the Iberian Chain, in the contact between the Cameros Range and the tertiary Ebro Basin (a NW-SW thrust; Figure 1; Coloma et al., 1997a; Sánchez and Coloma, 1998). The Cameros Range consists mainly of Mesozoic rocks which are divided in three different sequences: 1) the pre-rift sequence represented by Triassic and marine Jurassic rocks (with the classic formations of the Iberian Chain; Coloma, 1998; Gil et al., 2002; Goy et al., 1976); 2) the syn-rift sequence deposited during a rifting process initiated at the end of Jurassic and constituted by fluvial and lacustrine sediments from Upper Jurassic (Tithonian) to Upper Cretaceous (Lower Albian) (Coloma, 1998; Gil et al., 2002; Mas et al., 1993); and 3) the post-rift sequence which is constituted by the Upper Cretaceous carbonates and sandstones and the Later Cretaceous carbonate rocks (Gil et al., 2002). Finally, during the Tertiary a tectonic inversion created the Cameros Range and the Ebro basin (Coloma, 1998; Gil et al., 2002).

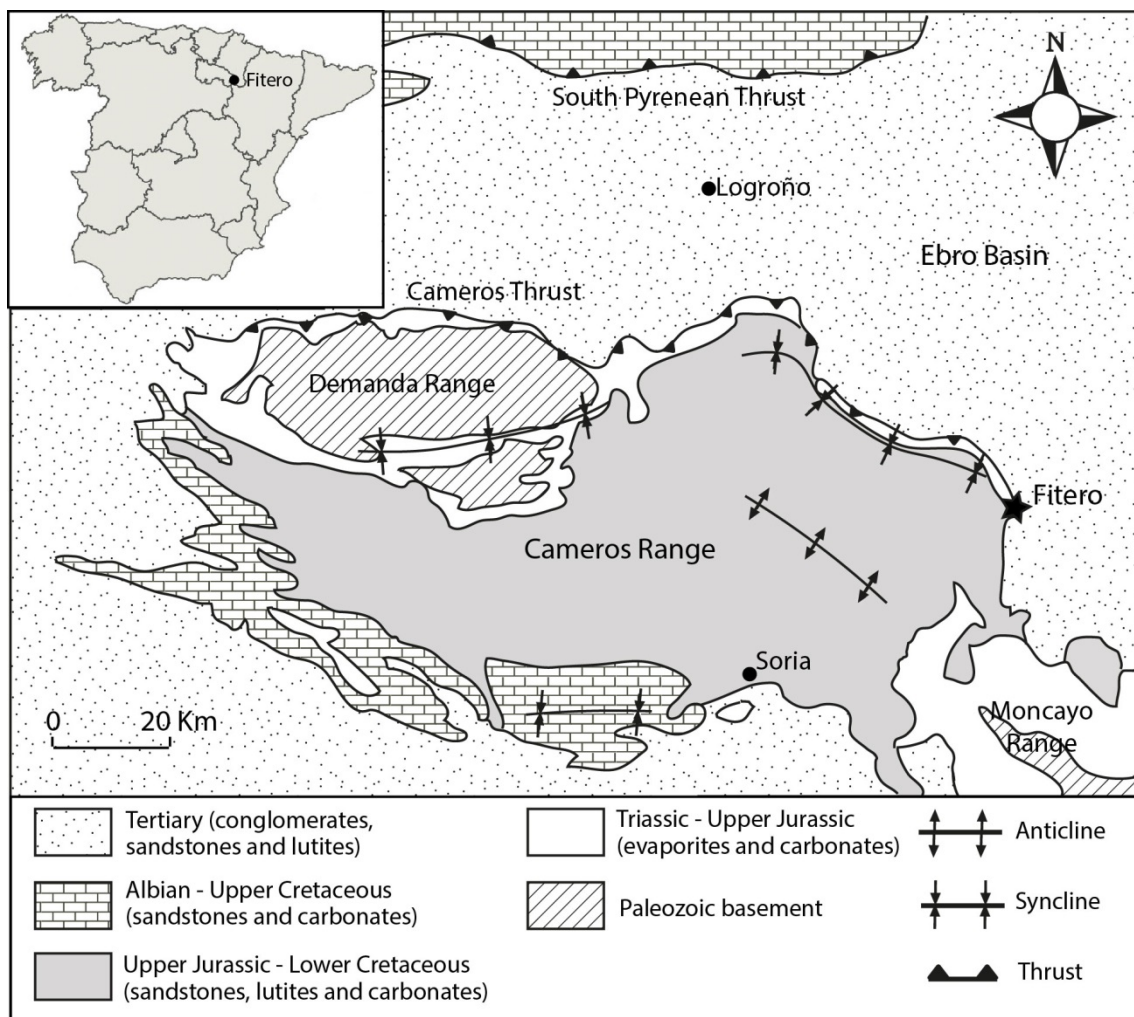


**Figure 1.** Location of the Fitero geothermal springs and geological map of the area (modified from Blasco et al., 2018).

The reservoir of the Fitero thermal waters is located in the carbonates of the pre-rift sequence (see Blasco et al., 2018 or Blasco et al., 2019 for more details about the geology and hydrogeology of this area) from which they ascend to surface through the Cameros thrust. The springs are associated to the Keuper facies and the Lower Jurassic carbonates (Auqué et al., 1988; Coloma, 1998; Coloma et al., 1996), their flow rate is about 50 L/s and the reservoir temperature is close to 50 °C (Coloma et al., 1998, 1997b, 1995; Sánchez and Coloma, 1998).

### 3. Methodology

#### 3.1. Field sampling

A sample of the thermal water, F1, was taken in a spring inside the Becquer spa, in Fitero (Navarra, Spain). For its use in the spa, this water is cooled down to 40 °C in a pool from where it is distributed to the different balneotherapeutic facilities at that temperature or even lower.

A travertine sample named FTOP (Fitero Travertine Old Pipe) was taken in an old pipe that drained the thermal water from the cooling pool in the moments of exceeding water (Figure 2) and, therefore, the water circulating through it was at a constant temperature of 40 °C. The diameter of this old pipe was about 30 cm and the inclination close to 30° with a height difference of 20 m from the pool to the exit point of the pipe. The travertine precipitation was so important that the pipe was almost completely clogged and it had to be removed, which gave the chance to get the solids sample but not the directly related water.

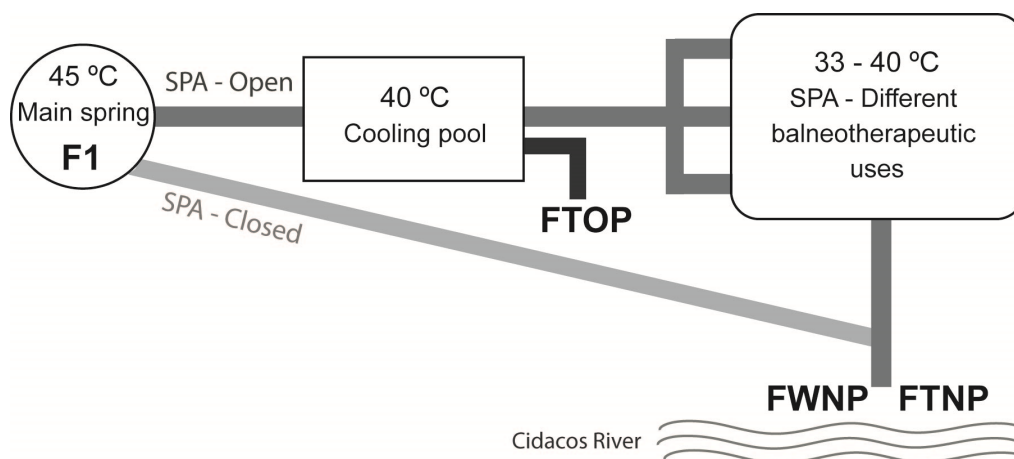


**Figure 2.** Idealised scheme of the Spa facilities showing the location where the different samples were taken.

Another travertine sample, FTNP, (Fitero Travertine New Pipe) was taken at the end of a currently active pipe that collects the final discharge water from the spa and pours it into the Cidacos river (Figure 2). The temperature of this discharge water oscillates between 33 and 40 °C during the spa operation times (depending on the different balneotherapeutic uses) and, when the spa is closed, it comes directly from the main spring undergoing a natural cooling. As this is an active pipe, a sample of the discharging water, FWNP, was taken at the same time as the travertine FTNP when the spa was closed and the measured water temperature was 33 °C.

### 3.2. Analytical determinations

Temperature, pH and electrical conductivity were measured in situ and separated samples for cation, anion and isotopic analyses were taken (the detailed procedure of sampling was described in Blasco et al. (2018)). The anions were analysed in the Geochemistry Laboratory of the Department of Earth Sciences at the University of Zaragoza: alkalinity was determined by titration, sulphate by colorimetry and chloride and fluoride by selective electrodes. The major cations were analysed by ICP-OES, the minor cations by ICP-MS, and  $\delta^{18}\text{O}$  and  $\delta^2\text{H}$  in water, and  $\delta^{13}\text{C}$  in the dissolved inorganic carbon, were analysed by CF-IRMS, all in the Scientific and Technological Centre of the University of Barcelona. More details about the analytical procedures can be found in (Blasco et al., 2018).

Petrographical and mineralogical observations of the travertines were conducted using conventional optical microscope on polished thin sections, and field emission scanning electron microscope (FESEM, using a Carl Zeiss MERLIN<sup>TM</sup>) on carbon-coated samples. Thin sections and FESEM analysis were performed at the facilities of the Research Support Services at the University of Zaragoza.

A small drill was used to separate the material from the different layers in the travertine deposits and the obtained solid samples were crushed in a steel jaw crusher and ground to a size fraction below 60  $\mu\text{m}$ . The bulk mineralogical composition was determined by X-ray diffractometry (XRD) using a PANalytical X'Pert PRO MPD powder diffractometer in Bragg-Brentano  $\theta/2\theta$  geometry of 240 millimetres of radius with a focalizing Ge (111) primary monochromator, a X'Celerator detector and using  $\text{CuK}\alpha_1$  radiation:  $\lambda = 1.5406 \text{ \AA}$  at the X-Ray Diffraction Unit in the Scientific and Technological Center of the University of Barcelona (Spain). Semi-quantitative phase analysis of the identified crystalline phases was performed by the Rietveld method (Rietveld, 1969).

Carbon and oxygen isotope analyses of six bulk layer subsamples from FTOP (the travertine from the old pipe) were determined at the Stable Isotope Analysis Service of the University of Salamanca (Spain). Extraction of  $\text{CO}_2$  for isotopic analyses followed standard techniques (McCrea, 1950) using an ISOCARB device connected to a SIRA series 10 mass spectrometer

from VG Isotech. The isotope analysis of the other travertine samples (FTNP from the new pipe) was performed at the Laboratory of Biogeochemistry of Stable Isotopes of the Andalusian Institute of Earth Sciences of Granada (CSIC). The methodology for CO<sub>2</sub> extraction was the same but the analyses were done using the GasBench II connected to the Finnigan DeltaPLUS XP isotope ratio mass spectrometer (IRMS). The overall analytical reproducibility, as determined on replicate measurements of laboratory standards, is routinely better than  $\pm 0.12$  ‰. Results are reported in the familiar  $\delta$ ‰ notation relative to V-PDB and V-SMOW.

### 3.3. Applications of the stable isotopes fractionation

The use of the stable isotopes fractionation equations for paleoclimatic and paleoenvironmental reconstructions is based on the fact that the isotope fractionation between a mineral phase and the water from which it is precipitating is a function of the temperature as long as the precipitation takes place in thermodynamic equilibrium (e.g. Zheng, 2011, 1999, and references therein) and therefore, the isotopic values of the solids represent the water temperature in the moment of precipitation (e.g. Capezzuoli et al., 2014; Fouke et al., 2000; Gabitov, 2013; Kele et al., 2015, 2011, 2008; Lachniet, 2015; Liu et al., 2006; Osácar et al., 2016, 2013; Pedley, 2009; Pentecost, 2005; Zhou and Zheng, 2003).

In the case of the  $\delta^{13}\text{C}$  isotope data, this paleotemperature indication can only be obtained using the  $\delta^{13}\text{C}$  fractionation between calcite–aragonite and the dissolved CO<sub>2</sub>, since this fractionation is temperature–dependent (e.g. Chacko et al., 2001; Romanek et al., 1992; Scheele and Hoefs, 1992). The problem in the present study is that the  $\delta^{13}\text{C}$  value in CO<sub>2</sub> is not available in the analysed waters, instead, the  $\delta^{13}\text{C}$  value was measured in the dissolved inorganic carbon (DIC), which, in these waters could be assumed to mostly be as HCO<sub>3</sub><sup>-</sup> (see below). The  $\delta^{13}\text{C}$  fractionation between the carbonate solids (calcite or aragonite) and the HCO<sub>3</sub><sup>-</sup> is independent of the temperature (Rubinson and Clayton, 1969; Turner, 1982; Romanek et al., 1992) and for the range between 10 and 40 °C, the reported values are  $2.7 \pm 0.6$  ‰ for aragonite-HCO<sub>3</sub> fractionation and  $1 \pm 0.2$  ‰ for calcite-HCO<sub>3</sub> fractionation. In summary, the measured  $\delta^{13}\text{C}$  cannot be used to make a temperature estimation in the Fitero system but it can help to evaluate the  $\delta^{13}\text{C}$  fractionation during the travertine precipitation, which is what will be shown in section 5.2.1.

There is much more information about the  $\delta^{18}\text{O}$  fractionation and its study has been quite thorough. Several fractionation equations, based on inorganic and biogenic carbonates, have been proposed for the  $\delta^{18}\text{O}$  equilibria between aragonite and water and between calcite and water and the more adequate were selected according to the identified mineralogy of the travertines under study. The FTOP travertines are almost pure aragonite and the equations used

in this work were the ones listed next, including those for biogenic aragonite to check their applicability to inorganic aragonitic travertines (Table 1):

- Grossman and Ku (1986): equation deduced from aragonite foraminifera, gastropods and scaphods in the range of 2.5 to 26 °C.
- Patterson et al. (1993): derived from the study of aragonite fish otoliths in the range of 3.2 to 30.3 °C.
- Thorrold et al. (1997): also derived from aragonite fish otoliths but in the temperature range of 18 to 25 °C.
- White et al. (1999): deduced from marine molluscs in the range of temperatures from 8 to 24 °C.
- Böhm et al. (2000): derived from aragonite sponges in the range of 3 to 28 °C.
- Zhou and Zeng (2003): derived from experiments of aragonite precipitation in the temperature range of 10 to 70 °C.
- Kim et al. (2007): derived from experiments with inorganic synthetic aragonites in the range of 10 to 40 °C. This equation has been corrected for conventional CO<sub>2</sub>-aragonite acid fractionation factor and the equation in Lachniet (2015) has been used.
- Chacko and Deines (2008): calculated the partition function ratios (for aragonite and water) from statistical mechanical calculation and a compilation of vibrational frequency data. The equation is applicable at temperatures between 0 and 130 °C.
- Wang et al. (2013): equation derived from aragonite precipitation from seawater experiments in the temperature range of 25 – 55 °C.
- Kele et al. (2015): proposed from a set of samples constituted by mixtures of calcite and aragonite travertines precipitated between 20 and 95 °C (they also propose other equation including tufas, not shown here, with very similar results).

The FTNP sample consists of a mixing of aragonite and calcite and for the  $\delta^{18}\text{O}$  fractionation evaluation, three equations have been used: the just mentioned equation proposed by Kele et al. (2015) as it corresponds to a mixture of aragonite and calcite, and two of the most used calcite equilibrium equations (Kim and O'Neil, 1997; Coplen, 2007) which cover almost the whole range of values given by the rest of the calcite–water fractionation equations presently available:

- Kim and O'Neil (1997): derived from inorganic calcites synthesised in laboratory in the range of 10 to 40 °C. This equation has been corrected for conventional CO<sub>2</sub>–calcite acid fractionation factor of 1.01025 (Friedman and O'Neil, 1977).
- Coplen (2007): proposed the equation from vein calcite samples from Devils Hole (Nevada, USA).

**Table 1.** Aragonite – water fractionation equations. Temperature (T) is in Kelvin in the equations for the  $\delta^{18}\text{O}_{\text{aragonite-water}}$  but in °C for the  $\delta^{13}\text{C}_{\text{aragonite-water}}$  equations.  $\alpha$  is the fractionation between aragonite and water calculated as  $(1000+\delta^{18}\text{O}_{\text{aragonite}})/(1000 + \delta^{18}\text{O}_{\text{water}})$  or  $(1000+\delta^{13}\text{C}_{\text{aragonite}})/(1000 + \delta^{13}\text{C}_{\text{water}})$  being  $\delta^{18}\text{O}$  values vs SMOW and  $\delta^{13}\text{C}$  values vs PDB.

	Author	Fractionation equation
$\delta^{18}\text{O}_{\text{aragonite-water}}$	Grossman and Ku (1986)	$1000 \ln \alpha = 18.04 \cdot \frac{1000}{T} - 31.12$
	Patterson et al. (1993)	$1000 \ln \alpha = 18.56 \cdot \frac{1000}{T} - 33.49$
	Thorrold et al. (1997)	$1000 \ln \alpha = 18.56 \cdot \frac{1000}{T} - 32.54$
	White et al. (1999)	$1000 \ln \alpha = 16.74 \cdot \frac{1000}{T} - 26.39$
	Böhm et al. (2000)	$1000 \ln \alpha = 18.45 \cdot \frac{1000}{T} - 32.54$
	Zhou and Zheng (2003)	$1000 \ln \alpha = 20.44 \cdot \frac{1000}{T} - 41.48$
	Kim et al. (2007)	$1000 \ln \alpha = 17.88 \cdot \frac{1000}{T} - 30.76$
	Chacko and Deines (2008) <sup>1</sup>	$1000 \ln \alpha = -12.815 + 5.793x - 3.7554 \cdot 10^{-1}x^2 + 3.2966 \cdot 10^{-2}x^3 - 2.2189 \cdot 10^{-3}x^4 + 8.9981 \cdot 10^{-5}x^5 - 1.636 \cdot 10^{-6}x^6$
	Wang et al. (2013)	$1000 \ln \alpha = 22.5 \cdot \frac{1000}{T} - 46.1$
$\delta^{18}\text{O}_{\text{calcite+aragonite-water}}$	Kele et al. (2015)	$1000 \ln \alpha = 20 \cdot \frac{1000}{T} - 36$
$\delta^{18}\text{O}_{\text{calcite-water}}$	Kim and O'Neil (1997)	$1000 \ln \alpha = 18.03 \cdot \frac{1000}{T} - 32.17$
	Coplen (2007)	$1000 \ln \alpha = 17.4 \cdot \frac{1000}{T} - 28.6$

<sup>1</sup> $x = 10^6/T^2$ , where T is Kelvin

## 4. Results

### 4.1. Main characteristics of the thermal waters

Only the most relevant information of the Fitero thermal waters for the present study will be highlighted here. A thorough study of their chemical characteristics (and some modelling results) can be found in another paper from Blasco et al. (2019). Table 2 shows the chemical and isotopic data of the thermal water taken in the main spring (F1) and the analytical data of the water sample taken in the new pipe (FWNP; Figure 3a). The temperature of the thermal water (F1) is 45.5 °C and its pH is near neutral. The water in the new pipe was at 33 °C in the moment of sampling and the pH was higher than in F1, which is coherent with some CO<sub>2</sub> loss. As mentioned before, it was impossible to get a water sample from the old pipe but considering

its location their chemical characteristics would be very similar to the main spring (F1) except for a temperature of 40 °C.

**Table 2.** Chemical and isotopic analyses of the Fitero thermal water that springs in the Becquer spa (F1; whose chemical composition is constant over time) and the chemical analysis of a water sample taken at the exit of a discharging pipe from the spa (FWNP). TDS (calculated using PHREEQC) and dissolved elements are expressed in ppm.

	<b>F1</b>	<b>FWNP</b>
<b>Temperature (°C)</b>	45.50	33
<b>TDS</b>	4820.2	4423
<b>pH</b>	6.86	7.72
<b>HCO<sub>3</sub><sup>-</sup></b>	174.02	125
<b>Cl<sup>-</sup></b>	1610	1505
<b>SO<sub>4</sub><sup>-</sup></b>	1376	1290
<b>Ca</b>	469	441
<b>Mg</b>	92.10	80.8
<b>Na</b>	981	920
<b>K</b>	30.20	30.3
<b>Sr</b>	11.10	10.3
<b>SiO<sub>2</sub></b>	23.75	
<b>Fe</b>	0.13	
<b>δ<sup>18</sup>O in H<sub>2</sub>O (SMOW)</b>	-8.7	
<b>δ<sup>2</sup>H in H<sub>2</sub>O (SMOW)</b>	-63.9	
<b>δ<sup>13</sup>C in DIC (PDB)</b>	-8.42	

The δ<sup>18</sup>O and δ<sup>2</sup>H values in F1 (-8.7 and -63.9, respectively; Table 2) suggest a meteoric origin of the thermal water since they are close to the Global Meteoric Water Line (δ<sup>2</sup>H = 8 δ<sup>18</sup>O + 10; Craig, 1961) and the Spanish Meteoric Water Line calculated from the data of the Spanish Network for the control of the isotopes in the rainfall (δ<sup>2</sup>H = 8 δ<sup>18</sup>O + 9.27; Díaz-Teijeiro et al., 2009). The δ<sup>13</sup>C value in the dissolved inorganic carbon of the thermal water is -8.4‰ (Table 2) and it suggests that, after infiltration through the soils (degradation of C3-type plants results in δ<sup>13</sup>C values of about -23‰; Clark and Fritz, 1997), the thermal water interacts with carbonate rocks in the aquifer (with δ<sup>13</sup>C values around 0‰; Clark and Fritz, 1997; Figure 4).

Some speciation-solubility calculations were carried out with the PHREEQC geochemical code (Parkhurst and Appelo, 2013) and the WATEQ4F thermodynamic database. The main results related to the carbonate system show that calcite and aragonite are in equilibrium or close to equilibrium at spring temperature in F1 (saturation states of 0.14 and 0.01, respectively) and with a high log pCO<sub>2</sub>, -1.58, whilst these minerals are more oversaturated (0.7 and 0.54,



respectively) in the water sample FWNP due to an important CO<sub>2</sub> outgassing during the circulation of the waters through the pipe giving a log pCO<sub>2</sub> of -2.7. The amount of CO<sub>2</sub> outgassing and calcium carbonate precipitation can be calculated by a simple mass balance between the two waters and the results indicate that there are 0.614 mmol/L of CO<sub>2</sub> loss which leads to the precipitation of 0.71 mmol/L of calcium carbonate. Therefore, calcium carbonate was precipitating in the moment of the water sampling in the new pipe, indicating that the CO<sub>2</sub> outgassing is the triggering factor of the carbonate precipitation, promoted by the high pCO<sub>2</sub> and the high temperature of the waters at the spring (CO<sub>2</sub> solubility is lower at higher temperatures, facilitating the degassing to the atmosphere).

This outgassing process must have also taken place in the water circulating through the old pipe to promote the precipitation of the aragonite travertine. The source water was the same thermal spring F1, whose compositional characters show minor variations with time (e.g. Auqué et al., 1989; Blasco et al., 2019). Therefore similar equilibrium conditions with respect to calcite and or aragonite should prevail at the moment of emergence and CO<sub>2</sub> degassing would be necessary to trigger the precipitation of carbonates (otherwise, as the solubility of these minerals increase with the decrease of temperature the waters, initially in equilibrium in the spring, would have suffered the opposite effect in the cooling pool, the undersaturation with respect to the carbonates).

#### 4.2. Main characteristics of the travertines

The travertine samples consist of an alternation of clear and reddish bands (Figure 3b). Each band is also constituted by a thin lamination barely distinguishable at a glance but evident when studying the thin section under the petrographic microscope. This lamination is not related to temporal (or climatic) variations but to the intermittent discharge through the pipes and therefore, they are conditioned by the availability of water, as also described by Rodríguez-Berriguete et al. (2018) in other human induced travertines.

Although both travertines look similar, their mineralogy is quite different. The X – Ray Diffraction analyses of two clear and two reddish bands of sample FTOP (from the old pipe) indicate a proportion of aragonite higher than 98 % with minor amounts of calcite, and this is common to both types of bands. The mineralogical results for sample FTNP (from the new pipe; Figure 3a) indicate a higher proportion of calcite (about 60 %) and much less aragonite (40 %), as an average from one clear and one reddish band.

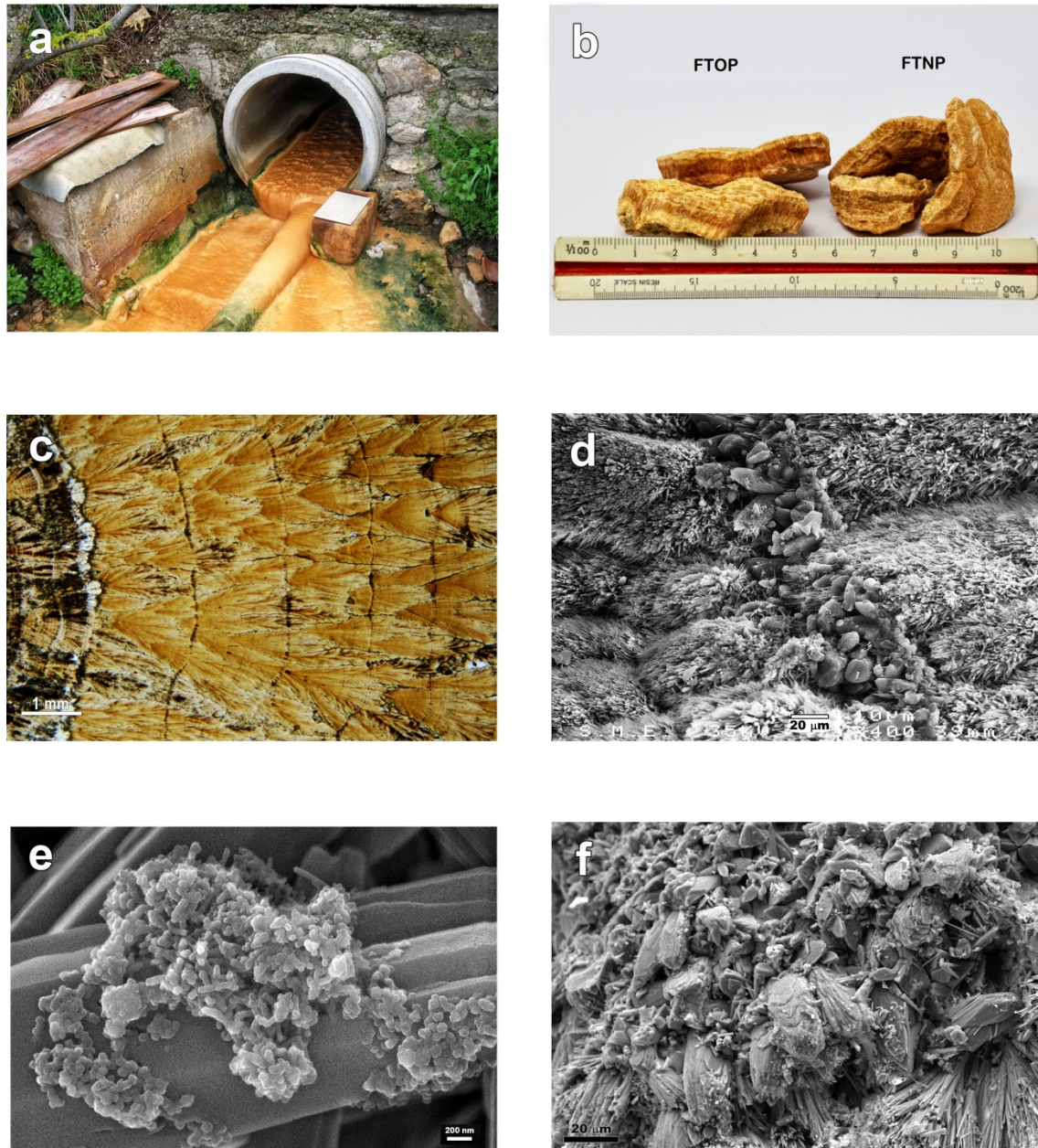


**Figure 3.** Panel a) New pipe at its discharge point on the Cidacos river, where travertine FTNP is precipitating. Panel b) FTOP and FTNP travertine samples where the alternation between clear and reddish bands can be seen. Panel c) Photograph taken with a petrographic microscope where the fibrous-radial texture with fan shaped aggregates can be seen (FTOP). Panel d) FESEM image of the FTOP travertine showing the aragonitic bands (on the right and left of the image) and a calcite interlayer in between. Some disperse calcite crystal in the aragonite can also be appreciated. Panel e) FESEM image of the FTOP travertine with a detail of an aragonite needle with iron oxy-hydroxides growing on it. Panel f) FESEM image of the FTNP travertine where abundant calcite crystals can be identified while aragonite needles are less common.

The detailed mineralogical examination of FTOP allowed identifying additional relevant characteristics of the aragonitic travertines: 1) the petrographic microscope showed a fibrous-radial, fan-shaped texture in the aragonite (Figure 3c) which, in the FESEM, is seen as elongated prisms or needles aggregated forming bushes (Figure 3d); 2) the presence of disperse calcite in all the bands is mainly associated to the thin interlayers between clear and reddish aragonite bands, whilst there is not a preferential distribution of calcite or aragonite in the FTNP travertine (Figures 3d and 3f); 3) lump aggregates of amorphous oxy-hydroxides have been identified on the aragonite needles in the reddish bands (Figure 3e) and they probably are the responsible for the colour of the bands despite their low content (unidentified by XRD and coherent with the low dissolved Fe in waters; Table 2).

Examination of thin sections and detailed FESEM observations show no evidence of microbial activity (e.g. biofilms or extracellular polymeric substances, EPS) in the travertines. These evidences are not usually preserved in old travertines (Jones and Renaut, 1995; Peng and Jones, 2012) but given that the samples studied here are from a present deposit, the lack of them suggests an abiogenic origin (Jones, 2017a).

Isotopic determinations of  $\delta^{18}\text{O}$  and  $\delta^{13}\text{C}$  in the carbonates were made in the travertine sample FTNP (whole sample) and in 6 subsamples of FTOP, in three reddish bands (FTOP-D1, D2, D3), and in three clear bands (FTOP-C1, C2 C3; Table 3). The results show that the  $\delta^{18}\text{O}$  values are similar in all the bands of the aragonite travertine and also in the calcite-aragonite travertine between 17.719 and 17.927 ‰ vs. V-SMOW.

**Table 3.** Isotopic data of travertine samples: the dark bands (FTOP-D) and the clear bands (FTOP-C) of sample FTOP, and the whole sample of travertine FTNP.

	$\delta^{13}\text{C}$ (PDB)	$\delta^{18}\text{O}$ (PDB)	$\delta^{18}\text{O}$ (SMOW)
<b>FTOP-D1</b>	0.536	-12.623	17.896
<b>FTOP-D2</b>	0.544	-12.795	17.719
<b>FTOP-D3</b>	0.364	-12.754	17.761
<b>FTOP-C1</b>	0.859	-12.393	17.927
<b>FTOP-C2</b>	0.803	-12.683	17.834
<b>FTOP-C3</b>	0.794	-12.737	17.778
<b>FTNP</b>	0.87	-12.617	17.854

With respect to the  $\delta^{13}\text{C}$  values (‰ vs V-PDB), they are higher in the clear bands (FTOP-C) and in the sample FTNP, about 0.8 ‰, than in the reddish bands, between 0.36 ‰ and 0.54 ‰ (Table 3). A more detailed description of the alternating clear and reddish bands and their geochemical characterisation will be discussed in the second paper about the trace element contents in the travertine deposits.

## 5. Discussion

There are two main issues to discuss here. The first one refers to the different mineralogical composition of the two studied travertine samples (different amounts of aragonite and calcite) and the second refers to their isotopic composition and their possible use as paleoenvironmental indicators.

### 5.1. Mineralogy

There are several classical studies on the main factors controlling calcite or aragonite precipitation in geological natural samples and in laboratory experiments (Folk, 1994; Fouke et al., 2000; Jones, 2017b; Pentecost, 2005; and references therein). These factors are: temperature, Mg/Ca ratio in the water, dissolved strontium content, CO<sub>2</sub> content and degassing, and the biological influence. Except for the last factor, that will not be discussed here since no evidence of biological effects have been found in the studied travertines, an evaluation of the influence of the other controlling factors is presented next.

Temperature and magnesium concentration have been considered the most important factors controlling the mineralogy of the precipitated carbonates. Generally speaking, aragonite is considered to precipitate at higher temperatures than calcite; for example, Folk (1994) observed that aragonite precipitates if the temperature is higher than 40 °C irrespective of the water composition, and calcite would precipitate if the temperature of the water is lower than 40°C and it is Ca-rich. Fouke et al. (2000), in the same line, indicated that if the temperature is higher than 44 °C only aragonite precipitates, if the temperature is lower than 30 °C only calcite does, and when it is between 30 and 43 °C both mineral phases precipitate together. However, aragonite is not always favoured over calcite at this “critical temperature” of about 40 °C; for example, calcite has been found to precipitate in Egerszalók (Hungary) at a temperature of about 70 °C (Kele et al., 2008) and in North Island (New Zealand), where the water temperature is higher than 90 °C (Jones et al., 1996; see also the review by Jones, 2017b).

Regarding the magnesium concentration in the waters, Fischbeck and Müller (1971) stated that the aragonite precipitation is significant if the Mg/Ca ratio is higher than 2.9; Folk (1994) reported that aragonite would precipitate if the Mg/Ca ratio of the water is higher than 1:1 no matter the water temperature; and AlKhatib and Eisenhauer (2017) indicated that any Mg/Ca ratio higher than 2:1 will assure aragonite precipitation even at temperatures of only 12.5 °C. Furthermore, in some lakes in the Great Plains of North America, the evaporation produces high Mg/Ca ratios that trigger the precipitation of aragonite despite a temperature of the water lower than 30 °C (Last, 1989; Last et al., 1998).

In the case of the sample FTOP, the temperature of the parental water is 40 °C and the composition is assumed to be the same as the thermal water F1, with a very low Mg/Ca ratio of

0.32. According to the previous authors, the water temperature would favour the aragonite precipitation, despite the low Mg/Ca which would allow the precipitation of some minor amounts of calcite. This is exactly what has been observed and, therefore, the thin calcite inter-layers between the aragonite bands seem to represent inter-discharge periods, when the remaining water would probably have a temperature lower than 40 °C. In the case of the sample FTNP, the Mg/Ca ratio in the parental water (FWNP) is 0.27, very similar to the F1 sample, but the temperature of the water discharged through the pipe varies between 40 and 33 °C which would explain the higher proportion of calcite. So, in these travertines temperature seems to be the main control of the mineralogy.

Other controlling factors may play a role, additionally to, or interplayed with, temperature (Jones, 2017b). Some authors argue that the Sr content in the waters favours aragonite precipitation and inhibits calcite growth but others state that the higher Sr concentrations in aragonite, in comparison to calcite, are only due to the partition coefficients, which are higher in aragonite (Sr incorporates easier in aragonite lattice than in calcite). The fact that the two travertine samples FTOP and FTNP have precipitated from a very similar water with similar Sr content (Table 2) and one of them is almost pure aragonite and the other has 60 % of calcite, supports the hypothesis that the dissolved content of Sr is not an important controlling factor of the mineralogical phase, at least in our system.

Finally, regarding the importance of CO<sub>2</sub> content and outgassing rate some authors reported that aragonite precipitation is favoured by high CO<sub>2</sub> contents and degassing rates as it is common in thermal springs (Chafetz et al., 1991; Jones, 2017b; Kitano, 1963). As stated above, CO<sub>2</sub> outgassing is the triggering factor of the carbonate precipitation in the studied travertines, since the spring waters are in equilibrium, or near equilibrium, with respect to aragonite and calcite. However, differences in the rate of CO<sub>2</sub> outgassing may also promote variations in the oversaturation degree and, in turn, in the precipitated carbonate phase (Jones and Peng, 2016; Jones, 2017b). The travertines studied here precipitate inside inclined pipes where an important outgassing rate is expected. But differences may arise by variations in the discharge and/or in the distance of the precipitates from the spring.

In the case of the pure aragonite travertine FTOP, precipitated from waters at nearly constant temperatures (40 °C), the possible variations in the outgassing rate do not seem to induce important mineralogical changes. Only the thin calcite inter-layers between the aragonite bands, which is interpreted as representing inter-discharge periods, could be related to water temperatures lower than 40 °C or periods of lower discharge and lower CO<sub>2</sub> outgassing rate.

The FTNP travertine, located farther away from the source thermal waters than the FTOP deposits, is associated with a wider range of water temperatures (33-40 °C) and with more

variable discharge regimes. In the moment of the sampling of FWNP, the water temperature was 33 °C (Table 2) and the discharge was low. Higher discharges, water temperatures and, most probably, CO<sub>2</sub> outgassing rates, occur in this pipe during the spa activity. Therefore, coupled changes in temperature and CO<sub>2</sub> outgassing rates may also be the cause of the higher proportions of calcite in this deposit, although more detailed studies would be necessary to clarify this hypothesis

## 5.2. Stable isotopes

### 5.2.1. $\delta^{13}\text{C}$

The  $\delta^{13}\text{C}$  values of travertines are considered to reflect the origin of the CO<sub>2</sub> in the source water in the classification scheme of Pentecost (2005) which includes two main travertine types, thermogene and meteogene. Thermogene travertines are those in which the CO<sub>2</sub> has a deep origin (magmatic or from decarbonation processes) and the  $\delta^{13}\text{C}$  values range from -1 to +10 ‰. Travertines are considered as meteogene if the CO<sub>2</sub> has a shallow origin, mainly meteoric, and they can be divided in ambient and superambient (or thermometeogene). The ambient meteogene travertines are formed at ambient temperatures (waters have not suffered a heating process) and they display  $\delta^{13}\text{C}$  values ranging from -12 to -3 ‰. The superambient meteogene travertines precipitate from warm waters (waters heated through deep circulation and emerging as hot springs) and have  $\delta^{13}\text{C}$  values ranging from -12 to +2 ‰. The  $\delta^{13}\text{C}$  data in the studied travertines range from 0.36 to 0.87 ‰ (Table 3) and, therefore, they could be classified as superambient meteogene or thermometeogene travertines.

However, the source of CO<sub>2</sub> can only be properly assessed from the  $\delta^{13}\text{C}$  values in travertines where secondary modifications (e.g. CO<sub>2</sub> outgassing) of the isotopic carrier are minimised (e.g. close to the spring orifice; Kele et al., 2011; Jones and Peng, 2016 and references therein) and this is not exactly the case here. Fitero travertines have precipitated after CO<sub>2</sub> degassing of the thermal waters (see above) and, therefore, their  $\delta^{13}\text{C}$  values would reflect the  $\delta^{13}\text{C}$  in the dissolved CO<sub>2</sub> in the moment of the travertine precipitation. In order to better check the meaning of the values analysed in the travertines, the  $\delta^{13}\text{C}$  in the CO<sub>2</sub> in the precipitation moment and in the spring conditions, previous to the CO<sub>2</sub> outgassing, have been calculated.

As previously done by other authors (e.g. Jones and Peng, 2016; Kele et al., 2011, 2008; Minissale, 2004; Sierralta et al., 2010), the  $\delta^{13}\text{C}$  in the travertine can be used to estimate the  $\delta^{13}\text{C}$  in the dissolved CO<sub>2</sub> in the moment of the travertine precipitation, by using the equation proposed by Panichi and Tongiorgi (1976; Table 4). Applying this equation to all the travertine samples (aragonite and calcite–aragonite), the  $\delta^{13}\text{C}_{\text{CO}_2}$  obtained range from -10 to -9.5 ‰. However, since this equation does not take into account the  $\delta^{13}\text{C}$  dependency on temperature,

the calculations were repeated with the equations proposed by Romanek et al. (1992; Table 4) for the  $\delta^{13}\text{C}$  fractionation between aragonite (or calcite) and  $\text{CO}_2$ .

**Table 4.** Fractionation equations for the  $\delta^{13}\text{C}$  in  $\text{CO}_2$  estimation from  $\delta^{13}\text{C}$  in the carbonate or  $\delta^{13}\text{C}$  in  $\text{HCO}_3$  dissolved.

	Author	Equation
$\text{CaCO}_3\text{-CO}_2$	Panichi and Tongiorgi (1979)	$\delta^{13}\text{C}_{\text{CO}_2} = 1.2 (\delta^{13}\text{C}_{\text{CaCO}_3}) - 10.5$
	Romanek et al. (1992) <sup>1</sup>	$10^3 \ln \alpha^{13}\text{C}_{\text{aragonite-CO}_2} = 13.88 - 0.13T$
	Romanek et al. (1992) <sup>1</sup>	$10^3 \ln \alpha^{13}\text{C}_{\text{calcite-CO}_2} = 11.98 - 0.12T$
$\text{HCO}_3\text{-CO}_2$	Mook et al. (1974) <sup>2</sup>	$10^3 \ln \alpha^{13}\text{C}_{\text{HCO}_3\text{-CO}_2} = 9.522(10^3 T^{-1}) - 24.1$
	Zhang et al. (1995) <sup>1</sup>	$10^3 \ln \alpha^{13}\text{C}_{\text{HCO}_3\text{-CO}_2} = -0.0954T + 10.41$
	Szaran (1997) <sup>1</sup>	$10^3 \ln \alpha^{13}\text{C}_{\text{HCO}_3\text{-CO}_2} = -0.1141T + 10.78$

<sup>1</sup> Temperature (T) is in °C

<sup>2</sup> Temperature (T) is in kelvin

The  $\delta^{13}\text{C}_{\text{CO}_2}$  values obtained for the FTOP samples (aragonite), assuming a precipitation temperature of 40 °C, were from -8.3 to -7.8 ‰. For sample FTNP, the precipitation temperatures considered for the calculation were between 33 and 40 °C (possible range of the circulating waters) and the values obtained were between -7.2 and -6.3 ‰. In summary, considering all the results obtained with the equations proposed by Romanek et al. (1992) the  $\delta^{13}\text{C}$  in the dissolved  $\text{CO}_2$  when the travertine precipitated was in the range of -8.3 to -6.3 ‰.

These values were then compared with the  $\delta^{13}\text{C}$  in the  $\text{CO}_2$  calculated in the emergence spring (water sample F1). This last value was theoretically approximated from the  $\delta^{13}\text{C}$  analysed in the DIC (dissolved inorganic carbon) assuming that the DIC mainly corresponds to  $\text{HCO}_3^-$  (the pH value of the spring water is near 7; Table 2) and using the equations proposed by Mook et al. (1974), Zhang et al. (1995) and Szaran (1997) for the  $\delta^{13}\text{C}$  fractionation between  $\text{HCO}_3$  and  $\text{CO}_2$  (Table 4). A good agreement around -15 ‰ was obtained among all these equations.

Two main conclusions can be extracted from these results:

- First, the  $\delta^{13}\text{C}$  value calculated for the  $\text{CO}_2$  at spring conditions, and the hydrogeological and hydrogeochemical characters of the Fitero geothermal system (Blasco et al, 2019), support the classification of the travertines as thermometeogene, derived from waters heated by a deep circulation but without an “endogenous”  $\delta^{13}\text{C}$  component (Pentecost, 2005). In this scheme, carbon dissolved from the carbonate rocks in the aquifer (with  $\delta^{13}\text{C}$  values usually between -1 and 5‰; Figure 4) would influence the  $\delta^{13}\text{C}$  values of the waters (and travertines) shifting them towards isotopically heavier values than those in the recharge waters (Figure 4).

- Second, the  $\delta^{13}\text{C}$  values calculated for the  $\text{CO}_2$  at spring condition (-15 ‰) are more negative than in the moment of the travertine precipitation (-8.3 to -6.3 ‰). These numbers would be consistent with the aforementioned existence of a  $\text{CO}_2$  outgassing process (resulting in the  $\delta^{13}\text{C}$  enrichment in the  $\text{CO}_2$  of the waters) as the trigger of the travertine precipitation.

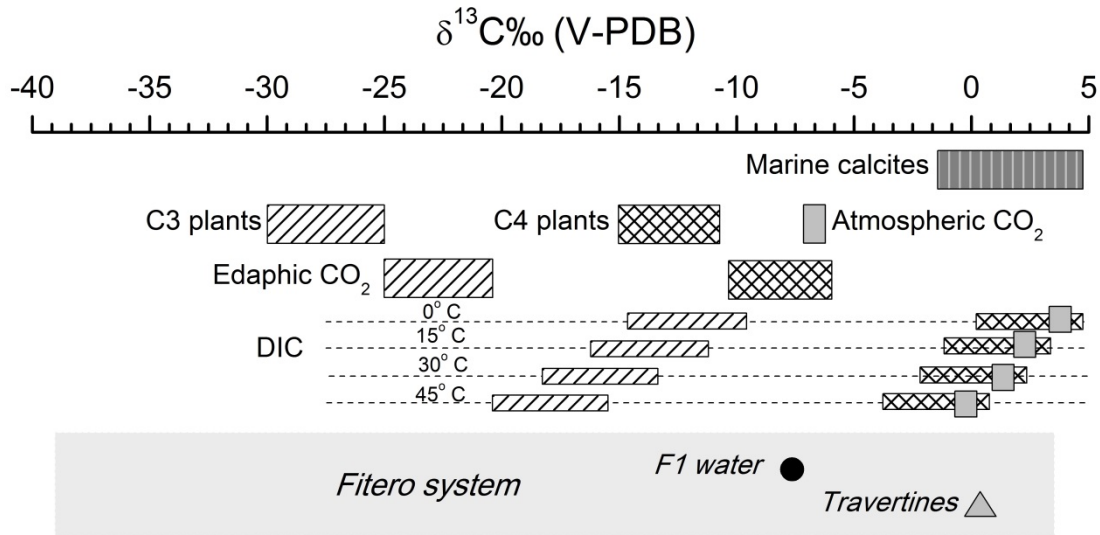


**Figure 4.**  $\delta^{13}\text{C}$  composition of the Fitero thermal water and the travertine precipitated from it (the travertine representation include all the bands of FTOP sample and the FNTP sample, since the values are between 0.9 and 0.3). The isotopic values of the possible  $\delta^{13}\text{C}$  sources are shown in the upper part of the graph. The equations described by Romanek et al. (1992) have been used for the calculation of the isotopic theoretical signature of DIC. Figure modified from Delgado and Reyes (2004) and Reyes et al. (1998).

### 5.2.2. $\delta^{18}\text{O}$

As mentioned above, although with some uncertainties related to the possible equilibrium situations between the solids and their parental waters, the use of  $\delta^{18}\text{O}$  in aragonite (or calcite) for paleoclimatic and paleoenvironmental reconstructions is a very useful tool. There are some examples in natural systems of travertine precipitation under, or close to, equilibrium conditions with respect to some of the fractionation equations (Arenas et al., 2018; Asta et al., 2017; Chafetz et al., 1991; Coplen, 2007; Garnett et al., 2004; Kele et al., 2015; Lachniet et al., 2012; Li et al., 2011, 2012, Osácar et al., 2013, 2016; Wang et al., 2014; Yan et al., 2012). But there are also examples where equilibrium is not maintained during precipitation (Asta et al., 2017; Coplen, 2007; Demény et al., 2010; Fouke et al., 2000; Friedman, 1970; Kele et al., 2015, 2011, 2008, Lojen et al., 2009, 2004; Wang et al., 2014; Yan et al., 2012; Zavdlav et al., 2017).

The study of an active precipitation system, like the one presented here, provides the possibility to compare the temperature results obtained from the application of the  $\delta^{18}\text{O}$  “equilibrium”



fractionation equations and the temperature actually measured in the parental water. This will give a better knowledge of the processes affecting the isotopic equilibrium and will help to interpret the isotopic signature of old travertines.

To do that, several equations (section 3.3) have been applied for  $\delta^{18}\text{O}$  equilibrium between the aragonites from sample FTOP (the 6 subsamples) and the equivalent to their parental water, F1 with 40 °C. For comparative purposes, some of the aragonite and calcite equilibrium equations (section 3.3) have been used for the sample FTNP (constituted by a mixture of calcite and aragonite) and the water F1 (at 40 °C) because, unfortunately, there is not isotopic information from its own parental water FWNP.

All fractionation equations used here have been represented in Figure 5. Panel a shows the equations for aragonite and panel b shows the equations for calcite (or for a mixture of calcite and aragonite). The isotopic values of the studied travertines at their precipitation temperatures are also shown: six open circles for the aragonite travertine in Figure 5a, and a grey rectangle representing the calcite-aragonite travertine and the interval between 33 – 40 °C that covers the temperature variation of the water circulating through the pipe, in Figures 5a and b. As it can be seen, all the travertine samples fall in the “equilibrium window” defined by the area covered by all the fractionation equations, suggesting that they have precipitated under or close to isotope equilibrium (e.g. Lachniet; 2015). However, this overall “equilibrium” situation is translated to a relatively wide range of possible temperatures covered by the whole set of considered equations (Table 5).

Regarding the pure aragonite travertine FTOP, there are two equations that provide discrepant temperatures (Table 5): 1) the one proposed by Zhou and Zheng (2003) which gives a temperature about 30 °C (probably due to the existing controversy about the experimental conditions for its determination; Horita and Clayton, 2007; Kim and O’Neil, 2005; Lécuyer et al., 2012; Wang et al., 2013) and 2) the empirical equation from Kele et al. (2015), which provides a temperature of almost 48 °C, which is higher than the possible parental water (probably due to the fact that the fitting of this equation was strongly influenced by five samples with very high fractionation of unclear origin; Kele et al. 2015). In both cases the results should be used with caution and they would not be taken into account in the discussion below. The temperature obtained using the rest of the equations, regardless if they were calibrated using biogenic or inorganic aragonites, is about 40 °C which is the temperature at which the precipitation actually takes place. These coincident results could be expected as the equations used here are within the uncertainty range defined by Kim et al. (2007) in their calibration ( $\pm 0.46$  ‰, see Figure 5 in Kim et al., 2007).

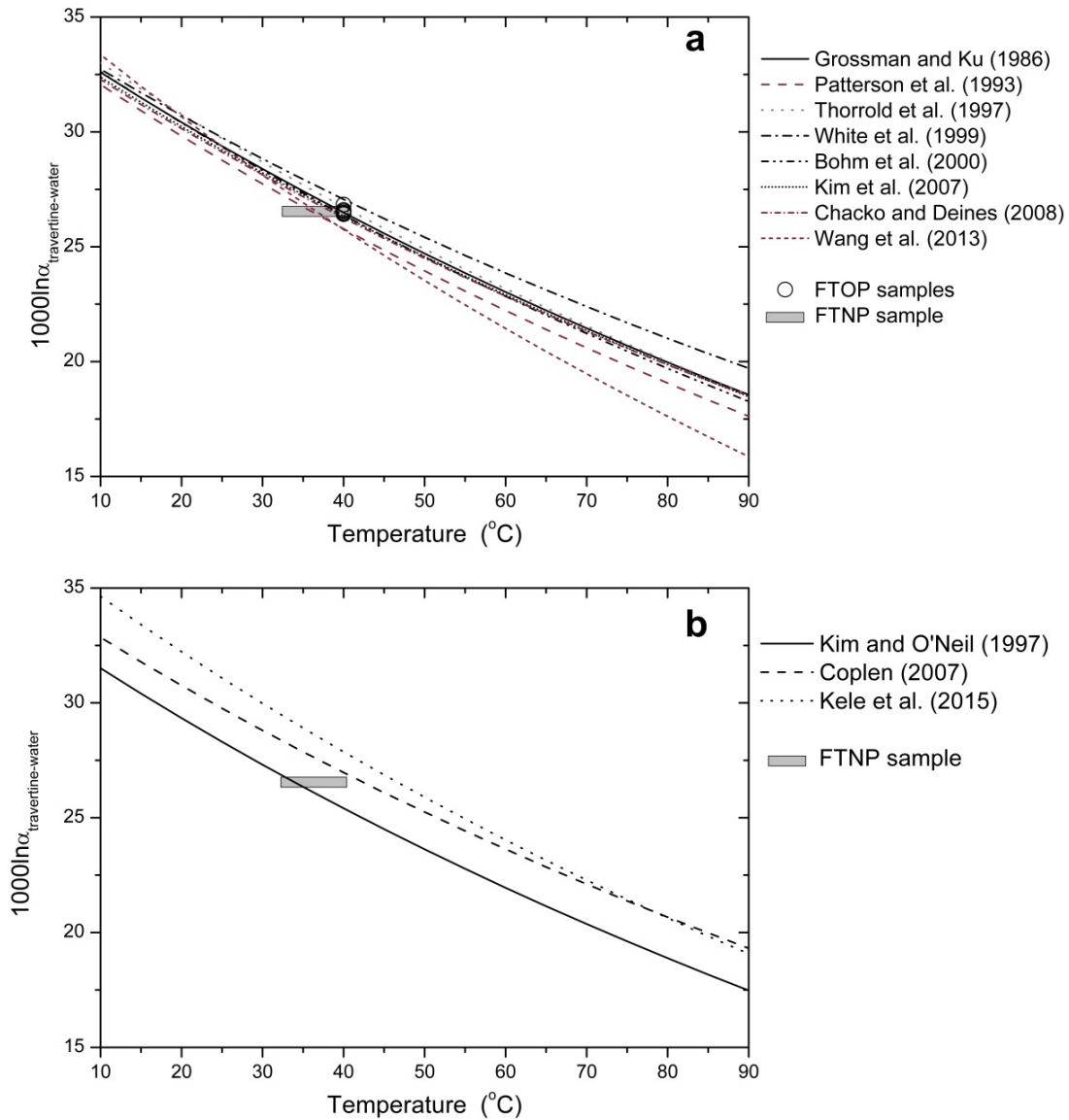


**Figure 5.** Panel a: representation of the  $\delta^{18}\text{O}$  aragonite – water equilibrium lines proposed by different authors and considered in this study. Panel b: The two most used equations for calcite are represented: Kim and O'Neil (1997) and Coplen (2007); the equation from Kele et al. (2015) is also included since it was calculated using a mixture of calcites and aragonites. The samples from travertine FTOP (98 % aragonite) are shown as open circles in panel (a) and the travertine FTNP (60 % calcite) is represented over the possible range of precipitation temperatures (33 – 40  $^{\circ}\text{C}$ ) in panels (a) and (b).

**Table 5.** Temperatures obtained with different oxygen isotopic aragonite – water equilibrium equations. The water isotope values used for these calculations are in all the cases those of water sample F1.

		FTOP-D1	FTOP-D2	FTOP-D3	FTOP-C1	FTOP-C2	FTOP-C3	FTNP
$\delta^{18}\text{O}_{\text{aragonite-water}}$	<b>Grossman and Ku (1986)</b>	40.1	41.0	40.8	39.9	40.4	40.7	40.3
	<b>Patterson et al. (1993)</b>	36.4	37.3	37.0	36.2	36.7	37.0	36.3
	<b>Thorrold et al. (1997)</b>	41.3	42.3	42.1	41.2	41.7	42.0	41.3
	<b>White et al. (1999)</b>	43.5	44.5	44.3	43.3	43.9	44.2	43.5
	<b>Böhm et al. (2000)</b>	39.5	40.4	40.2	39.3	39.8	40.1	39.7
	<b>Zhou and Zheng (2003)</b>	27.6	28.4	28.2	27.5	27.9	28.1	27.6
	<b>Kim et al. (2007)</b>	39.2	40.2	40.0	39.1	39.6	39.9	39.5
	<b>Chacko and Deines (2008)</b>	38.8	39.7	39.5	38.6	39.1	39.4	38.4
	<b>Wang et al. (2013)</b>	36.9	37.6	37.4	36.7	37.1	37.4	37.0
$\delta^{18}\text{O}_{\text{calcite+aragonite-water}}$	<b>Kele et al. (2015)</b>	47.0	47.9	47.7	46.8	47.3	47.6	46.9
$\delta^{18}\text{O}_{\text{calcite-water}}$	<b>Kim and O'Neil (1997)</b>	-	-	-	-	-	-	43
	<b>Coplen (2007)</b>	-	-	-	-	-	-	34.5

The results obtained for the travertine FTNP merit some additional considerations, in terms of comparison with FTOP, as it is constituted by a mixture of calcite (about 60 %) and aragonite (40 %), and the specific mineralogy could be an important factor when studying the  $\delta^{18}\text{O}$  isotopic signature of carbonates.

The relative fractionation factor between calcite and aragonite is still under debate: some authors have experimentally found that the oxygen isotope fractionation is lower between aragonite and water than between calcite and water whereas others have found the opposite (e.g. Kele et al., 2008; Lécuyer et al., 2012; Wang et al., 2013; and references therein). In the case studied here, a relation between the values and the percentages of calcite or aragonite is not observed as the  $\delta^{18}\text{O}$  values are similar in the FTOP and FTNP travertines. Therefore, no differences between the calcite–water and aragonite–water oxygen fractionation are evident, as it has also been observed in other travertines constituted by calcite and aragonite (e.g. Jones and Peng, 2014; Kele et al., 2015).

In the cases like FTNP, it is impossible to evaluate the  $\delta^{18}\text{O}$  fractionation in each mineral phase, intermixed at the microscale, in a separate way (e.g. Jones and Peng, 2016, 2014) and some authors have suggested to use aragonite and calcite calibration equations over the same sample, as if it was pure aragonite or pure calcite, to estimate temperatures/paleotemperatures (e.g. Jones and Peng, 2016).

When the aragonite equations are used for the fractionation of the travertine FTNP and the thermal water F1, the temperature obtained is about 40 °C, which is close to the maximum real temperature in this pipe. It is also the same as the temperature calculated for the aragonite travertine FTOP in the six subsamples (Table 5), which is reasonable since the  $\delta^{18}\text{O}$  value is very similar in all the travertine samples.

For the temperature calculations as if FTNP was pure calcite, using the equations from Coplen (2007) and Kim and O'Neil (1997) the temperatures calculated were 34.5 and 43 °C, respectively. The equation from Kele et al. (2015) gave a temperature of 47 °C, again higher than any possible water temperatures in the pipe, and this result was not considered.

The comparison of the results from these two samples indicate: 1) that the temperature range defined by the calculations from the aragonite travertines, FTOP, is quite narrow (36 – 40 °C) and perfectly coherent with the temperature of the parental water; 2) that the temperature calculated from the calcite-rich travertine, FTNP, using the aragonite fractionation equations, is the same as the previous one, since their isotopic values are also the same; and 3) that the temperature obtained using the calcite equations with the calcite-rich travertine (FTNP) gives a broader range from 34.5 to 43 °C that includes the two previous calculations with the aragonite calibration and also the range of the real waters circulating through the pipe (between 33 and 40 °C).

The  $\delta^{18}\text{O}$  and temperature values of the studied aragonite travertines have been compared with those available in other natural aragonite samples precipitated under different conditions around the world, but always consisting of at least 90 % of aragonite. As it is shown in Figure 6, these data define a clear dependence on temperature that can be expressed as a  $\delta^{18}\text{O}$  fractionation equation for natural aragonites in the temperature range of 23 to 80 °C (T is in Kelvin):

$$1000\ln\alpha = 18.27 (\pm 1.26) \cdot \frac{1000}{T} - 31.47 (\pm 3.85) \quad (1)$$

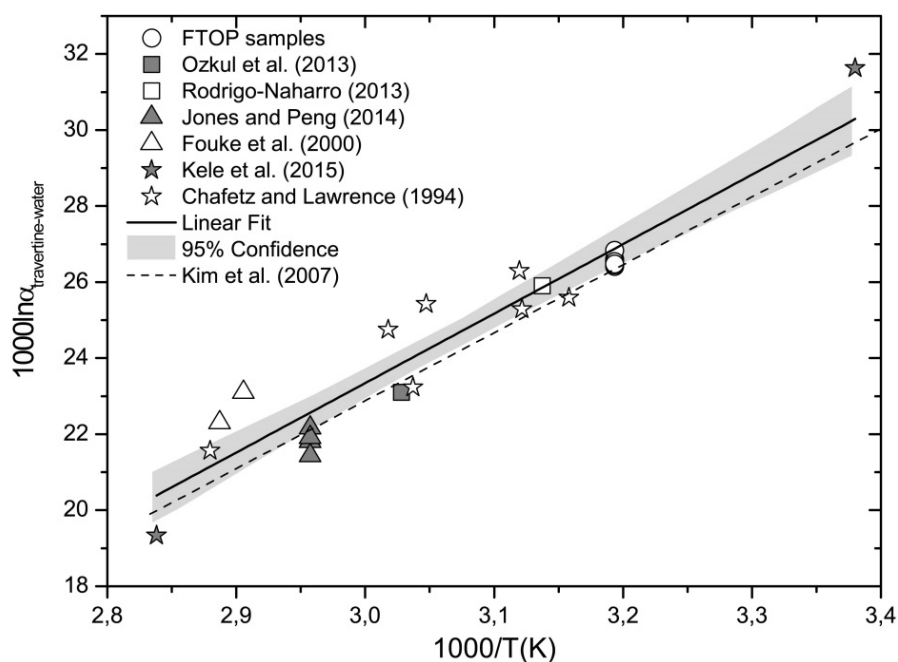


**Figure 6.**  $\delta^{18}\text{O}$  aragonite – water vs.  $1000/T$  (in Kelvin). The natural aragonite samples previously identified as precipitated under an equilibrium situation are represented together with a linear fit. The 95% confidence interval of the fitting is also shown. Finally the Kim et al (2007) aragonite fractionation line is shown for comparison.

This linear fit is represented in Figure 6 together with the Kim et al. (2007) aragonite fractionation equation, which gives the most accurate temperature for the Fitero samples. It is remarkable that, despite the fact that the equation of Kim et al. (2007) was calibrated with synthetic aragonites precipitated under controlled laboratory conditions, it is almost within the 95% of confidence of the fitting using the natural aragonite samples precipitated under different conditions and, most probably, with different precipitation rates. This result suggests that the main control in aragonite fractionation, in the examined samples, is the temperature and that equilibrium situations are not uncommon. The temperatures calculated using the proposed calibration (equation 1) are between 3 and 2.7 °C higher than the ones obtained with the Kim et al. (2007) equations. In any case, the equation proposed here can be used as an additional tool to evaluate the natural aragonite isotope fractionation although it should be improved with new isotope studies on aragonite samples.

### 5.2.3. *Isotope equilibrium/disequilibrium and water temperature*

It is usually considered that isotopic disequilibrium is the dominant condition during calcite and/or aragonite precipitation in travertine deposits due to kinetic effects induced by high  $\text{CO}_2$  outgassing and high precipitation rates (e.g. Kele et al., 2011, 2008; Rodríguez-Berriguete et al., 2018 and references therein). Isotope-based temperature calculations require isotopic

equilibrium and, therefore, disequilibrium situations would critically affect the accuracy of the temperature/paleotemperature calculations.

The fibrous radial texture, the performed geochemical and mass balance calculations and the carbon isotopic compositions discussed in the previous sections, all suggest that disequilibrium conditions, associated to rapid CO<sub>2</sub> degassing and high precipitation rates, would prevail during the precipitation of the studied travertines. However, the δ<sup>18</sup>O values from the carbonates fall in the equilibrium window (Lachniet, 2015) defined by the different δ<sup>18</sup>O aragonite/calcite-water fractionation equations proposed by different authors (Figure 5), and the temperature calculated using those equations fits very well with the measured temperatures (in most cases within ± 3 °C or even better; Table 5).

Similar situations of successful temperature calculations despite the existence of isotopic disequilibrium conditions, have been previously reported in the literature about calcite tufa deposits (e.g. Rodríguez-Berriguete et al., 2018; Wang et al., 2014; Yan et al., 2012) and they have been explained as due to the fact that the precipitated carbonates show an oxygen isotopic signal close to the one in the dissolved HCO<sub>3</sub><sup>-</sup>.

To check this possibility in the studied travertines, and following Kele et al. (2011, 2008), Halas and Wolacewicz (1982) equation ( $1000 \ln \alpha_{\text{HCO}_3\text{-H}_2\text{O}} = 2.92 \cdot 10^6 / T^2 - 2.66$ ) was used to calculate the oxygen isotope fractionation between the dissolved HCO<sub>3</sub><sup>-</sup> and the water at the temperatures of interest (between 33 and 40 °C) in the studied system. The values ranged between 27.11 at 40 °C and 28.49 at 33 °C. These values were compared with the ones measured for the oxygen fractionation between aragonite/calcite and water (as  $1000 \ln \alpha_{\text{carbonate-H}_2\text{O}}$ ) which ranged from 26.42 to 26.63 considering both travertines (FTOP and FTNP).

As it is shown by these results, for the precipitation temperature in the FTOP samples (40 °C, also representing the higher precipitation temperatures in the case of FTNP sample), the travertines show an oxygen isotopic signal close to that of the dissolved HCO<sub>3</sub><sup>-</sup> suggesting an oxygen isotopic equilibrium between dissolved HCO<sub>3</sub><sup>-</sup> and H<sub>2</sub>O and a direct transfer of the HCO<sub>3</sub><sup>-</sup> isotopic signal to the solids without fractionation. As stated by Kele et al. (2011), this absence of isotope fractionation can be promoted by fast CO<sub>2</sub> degassing and rapid carbonate precipitation (in agreement with the initial hypothesis by O'Neil et al., 1969), as it apparently occurs in the Fitero system.

This situation would explain the apparent equilibrium of the travertines with respect to the used δ<sup>18</sup>O aragonite/calcite–water fractionation equations. Furthermore, in agreement with other authors (Rodríguez-Berriguete et al., 2018; Wang et al., 2014; Yan et al., 2012), these results would suggest that some travertines can be used for paleotemperature calculations, even precipitating under disequilibrium conditions.

## 6. Conclusions

A mineralogical and isotopic characterisation of the Fitero aragonite travertines has been presented here. The parental water is the Fitero thermal water, which springs at 45 °C but then is cooled for its use in a spa. Two different travertine samples were studied: 1) one consisting of almost pure aragonite (98%), precipitated in a pipe which discharged water outside the cooling pool at a constant temperature of 40 °C; and 2) other composed of a mixture of 60 % of calcite and 40 % of aragonite taken in the general spa discharging pipe, where the water temperature varies between 33 and 40 °C. The precipitation of calcium carbonate is triggered by a CO<sub>2</sub> outgassing process (as deduced from the performed geochemical calculations and from the  $\delta^{13}\text{C}$  values calculated in the spring water and during the travertines precipitation) leading to the oversaturation of carbonate phases and, in turn, to the travertine precipitation. The main factor controlling aragonite or calcite precipitation in this system is the temperature, although the CO<sub>2</sub> loss can also play a role.

The evaluation of the  $\delta^{18}\text{O}$  values by using different aragonite and calcite  $\delta^{18}\text{O}$  fractionation equations suggests that the precipitation of the Fitero travertines took place close to the isotope equilibrium, obtaining the most precise temperature with the equation proposed by Kim et al. (2007) for the aragonite fractionation. Not representative differences between aragonite–water and calcite–water fractionation have been found since the  $\delta^{18}\text{O}$  values in the aragonite samples and the mixture of calcite and aragonite sample are almost the same.

Given that in natural systems with important CO<sub>2</sub> outgassing rates, as in the case studied here, is unusual that the isotope equilibrium is maintained during precipitation, the possible reasons have been investigated. The most plausible explanation seems to be that the isotope signal of the dissolved HCO<sub>3</sub><sup>-</sup>, in isotope equilibrium with water, is directly transferred to the precipitating carbonate, without fractionation, as result of the quick CO<sub>2</sub> loss and precipitation. Therefore, under these apparent equilibrium situations, accurate temperature results could be expected using the  $\delta^{18}\text{O}$  fractionation equations.

The temperature– $\delta^{18}\text{O}$  values of the aragonite deposits in Fitero have been compared with those in other aragonite travertines from the literature (always with aragonite proportions higher than 90 %). Overall, they define a fractionation equation for natural aragonite in the temperature range of 23 to 80 °C, near the experimental equation of Kim et al. (2007), suggesting the existence of equilibrium, or apparent equilibrium, situations in an important number of systems.

## 7. Acknowledgements

M. Blasco has worked in this study thanks to a scholarship from the Ministry of Science, Innovation and Universities of Spain, for the Training of University Teachers (ref. FPU14/01523). This study forms part of the activities of the Geochemical Modelling Group (University of Zaragoza; Aragón Government). Authors would like to acknowledge the use of “Servicio General de Apoyo a la Investigación-SAI, Universidad de Zaragoza” and the technical assistance of Enrique Oliver from the Earth Sciences Department of the University of Zaragoza. The helpfulness of the Becquer Spa staff during the sampling is also grateful.

## 8. References

- AlKhatib, M., Eisenhauer, A., 2017. Calcium and strontium isotope fractionation during precipitation from aqueous solutions as a function of temperature and reaction rate; II. Aragonite. *Geochim. Cosmochim. Acta* 209, 320–342.
- Andrews, J.E., 2006. Palaeoclimatic records from stable isotopes in riverine tufas: Synthesis and review. *Earth Sci. Rev.* 75, 85–104.
- Arenas, C., Osácar, M.C., Auqué, L.F., Andrews, J.E., Pardo, G., Marca, A., Martín-Bello, L., Pérez-Rivarés, F.J., 2018. Seasonal temperatures from  $\delta^{18}\text{O}$  in recent Spanish tufa stromatolites: Equilibrium redux! *Sedimentology* 65, 1611–1630.
- Asta, M.P., Auqué, L.F., Sanz, F.J., Gimeno, M.J., Acero, P., Blasco, M., García-Alix, A., Gómez, J., Delgado-Huertas, A., Mandado, J., 2017. Travertines associated with the Alhama-Jaraba thermal waters (NE, Spain): Genesis and geochemistry. *Sediment. Geol.* 347, 100–116.
- Auqué, L.F., Fernández, J., Tena Calvo, J.M., 1988. Las aguas termaltes de Fitero (Navarra) y Arnedillo (Rioja). I. Análisis geoquímico de los estados de equilibrio-desequilibrio en las surgencias. *Estud. geológicos* 44, 285–292.
- Auqué, L.F., Fernández, J., Tena Calvo, J.M., Mandado, J., Gimeno, M.J., Tolosa, P., 1989. Análisis de los estados de equilibrio termodinámico en el reservorio de las surgencias termaltes de Tiero (Navarra) y Arnedillo (Rioja). *Rev. la Soc. Geológica España* 2, 125–132.
- Blasco, M., Auqué, L.F., Gimeno, M.J., 2019. Geochemical evolution of thermal waters in carbonate – evaporitic systems: The triggering effect of halite dissolution in the dedolomitisation and albitisation processes. *J. Hydrol.* 570, 623–636.



- Blasco, M., Gimeno, M.J., Auqué, L.F., 2018. Low temperature geothermal systems in carbonate-evaporitic rocks: Mineral equilibria assumptions and geothermometrical calculations. Insights from the Arnedillo thermal waters (Spain). *Sci. Total Environ.* 615, 526–539.
- Böhm, F., Joachimski, M.M., Dullo, W.C., Eisenhauer, A., Lehnert, H., Reitner, J., Wörheide, G., 2000. Oxygen isotope fractionation in marine aragonite of coralline sponges. *Geochim. Cosmochim. Acta* 64, 1695–1703.
- Capezzuoli, E., Gandin, A., Pedley, M., 2014. Decoding tufa and travertine (fresh water carbonates) in the sedimentary record: the state of the art. *Sedimentology* 61, 1–21.
- Chacko, T., Cole, D.R., Horita, J., 2001. Equilibrium Oxygen, Hydrogen and Carbon Isotope Fractionation Factors Applicable to Geologic Systems. *Rev. Mineral. Geochemistry* 43, 1–81.
- Chacko, T., Deines, P., 2008. Theoretical calculation of oxygen isotope fractionation factors in carbonate systems. *Geochim. Cosmochim. Acta* 72, 3642–3660.
- Chafetz, H.S., Lawrence, J.R., 1994. Stable Isotopic Variability within Modern Travertines. *Géographie Phys. Quat.* 48, 257–273.
- Chafetz, H.S., Rush, P.F., Utech, N.M., 1991. Microenvironmental controls on mineralogy and habit of CaCO<sub>3</sub> precipitates: an example from an active travertine system. *Sedimentology* 38, 107–126.
- Clark, I., Fritz, P., 1997. *Environmental Isotopes in Hydrogeology*. CRC Press/Lewis Publishers, Boca -Raton (Florida).
- Coloma, P., 1998. El agua subterránea en La Rioja. *Zubía Monográfico* 10, 63–132.
- Coloma, P., Sánchez, J.A., Jorge, J.C., 1998. Simulación matemática del flujo y transporte de calor del sector oriental de la Cuenca de Cameros. *Zubía Monográfico* 10, 45–61.
- Coloma, P., Sánchez, J.A., Martínez, F.J., 1997a. Sistemas de flujo subterráneo regional en el acuífero carbonatado mesozoico de la Sierra de Cameros. Sector Oriental. *Estud. geológicos* 53, 159–172.
- Coloma, P., Sánchez, J.A., Martínez, F.J., 1996. Procesos geotérmicos causados por la circulación del agua subterránea en el contacto entre la Sierra de Cameros y la Depresión Terciaria del Ebro. *Geogaceta* 20, 749–753.
- Coloma, P., Sánchez, J.A., Martínez, F.J., 1995. El drenaje subterráneo de la cordillera Ibérica en la depresión terciaria del Ebro (sector Riojano). *Geogaceta* 17, 68–71.

- Coloma, P., Sánchez, J.A., Martínez, F.J., Pérez, A., 1997b. El drenaje subterráneo de la Cordillera Ibérica en la Depresión terciaria del Ebro. *Rev. la Soc. Geológica España* 10, 205–218.
- Coplen, T.B., 2007. Calibration of the calcite-water oxygen-isotope geothermometer at Devils Hole, Nevada, a natural laboratory. *Geochim. Cosmochim. Acta* 71, 3948–3957.
- Craig, H., 1961. Isotopic variations in meteoric waters. *Science*. 133, 1702–1703.
- Delgado, A., Reyes, E., 2004. Isótopos estables como indicadores paleoclimáticos y paleohidrológicos en medios continentales. *Semin. la Soc. Española Mineral. Geoquímica Isotópica Apl. al Medioambiente* 1, 37–53.
- Demény, A., Kele, S., Siklósy, Z., 2010. Empirical equations for the temperature dependence of calcite-water oxygen isotope fractionation from 10 to 70 °C. *Rapid Commun. Mass Spectrom.* 24, 3521–3526.
- Díaz-Teijeiro, M.F., Rodríguez-Arévalo, J., Castaño, S., 2009. La Red Española de Vigilancia de Isótopos en la Precipitación (REVIP): distribución isotópica espacial y aportación al conocimiento del ciclo hidrológico. *Ing. Civ.* 155, 87–97.
- Fernández, J., Auqué, L.F., Sánchez Cela, V.S., Guaras, B., 1988. Las aguas termales de Fitero (Navarra) y Arnedillo (Rioja). II. Análisis comparativo de la aplicación de técnicas geotermométricas químicas a aguas relacionadas con reservorios carbonatado-evaporíticos. *Estud. geológicos* 44, 453–469.
- Fischbeck, R., Müller, G., 1971. Monohydrocalcite, hydromagnesite, nesquehonite, dolomite, aragonite and calcite in speleothems of the Frankische Schweiz, Western Germany. *Contrib. to Mineral. Petrol.* 33, 87–92.
- Folk, R.L., 1994. Interaction between bacteria, nanobacteria, and mineral precipitation in hot springs of central Italy. *Géographie Phys. Quat.* 48, 233–246.
- Ford, T.D., Pedley, H.M., 1996. A review of tufa and travertine deposits of the world. *Earth Sci. Rev.* 41, 117–175.
- Fouke, B.W., Farmer, J.D., Des Marais, D.J., Pratt, L., Sturchio, N.C., Burns, P.C., Discipulo, M.K., 2000. Depositional facies and aqueous-solid geochemistry of travertine-depositing hot springs (Angel Terrace, Mammoth Hot Springs, Yellowstone National Park, U.S.A.). *J. Sediment. Res.* 70, 565–585.
- Friedman, I., 1970. Some investigations of the deposition of travertine from Hot Springs-I. The isotopic chemistry of a travertine-depositing spring. *Geochim. Cosmochim. Acta* 34, 1303–1315.

- Friedman, I., O'Neil, J.R., 1977. Compilation of stable isotope fractionation factors of geochemical interest, in: Fleischer, M. (Ed.), Data on Geochemistry, USGS Professional Paper 440-KK. United States Government Printing Office, Washington, p. 109.
- Gabitov, R.I., 2013. Growth-rate induced disequilibrium of oxygen isotopes in aragonite : An in situ study. *Chem. Geol.* 351, 268–275.
- Garnett, E.R., Andrews, J.E., Preece, R.C., Dennis, P.F., 2004. Climatic change recorded by stable isotopes and trace elements in a British Holocene tufa. *J. Quat. Sci.* 19, 251–262.
- Gil, A., Villalaín, J.J., Barbero, L., González, G., Mata, P., Casas, A.M., 2002. Aplicación de Técnicas geoquímicas, geofísicas y mineralógicas al estudio de la Cuenca de Cameros. Implicaciones geométricas y evolutivas. *Zubía Monográfico* 14, 65–98.
- Goy, A., Gómez, J.J., Yébenes, A., 1976. El Jurásico de la Rama Castellana de la Cordillera Ibérica (Mitad norte) I. Unidades litoestratigráficas. *Estud. geológicos* 32, 391–423.
- Grossman, E.L., Ku, T., 1986. Oxygen and carbon isotope fractionation in biogenic aragonite: temperature effects. *Chem. Geol.* 59, 59–74.
- Halas, S., Wolacewicz, W., 1982. The experimental study of oxygen isotope exchange reaction between dissolved bicarbonate and water. *J. Chem. Phys.* 76, 5470–5472.
- Horita, J., Clayton, R.N., 2007. Comment on the studies of oxygen isotope fractionation between calcium carbonates and water at low temperatures by Zhou and Zheng (2003; 2005). *Geochim. Cosmochim. Acta* 71, 3131–3135.
- Jones, B., 2017a. Review of aragonite and calcite crystal morphogenesis in thermal spring systems. *Sediment. Geol.* 354, 9–23.
- Jones, B., 2017b. Review of calcium carbonate polymorph precipitation in spring systems. *Sediment. Geol.* 353, 64–75.
- Jones, B., Peng, X., 2016. Mineralogical, crystallographic, and isotopic constraints on the precipitation of aragonite and calcite at Shiqiang and other hot springs in Yunnan Province, China. *Sediment. Geol.* 345, 103–125.
- Jones, B., Peng, X., 2014. Hot spring deposits on a cliff face: A case study from Jifei, Yunnan Province, China. *Sediment. Geol.* 302, 1–28.
- Jones, B., Renaut, R.W., 2010. Calcareous spring deposits in continental settings, in: Alonso-Zarza, A.M., Tanner, L.H. (Eds.), *Developments in Sedimentology: Carbonates in Continental Settings: Facies, Environments and Processes*. Elsevier, Amsterdam, pp. 177–224.

- Jones, B., Renaut, R.W., 1995. Noncrystallographic cendrites from hot-spring deposits at Lake Bogoria, Kenya. *J. Sediment. Res.* A65, 154–169.
- Jones, B., Renaut, R.W., Rosen, M.R., 1996. High-temperature (>90°C) calcite precipitation at Waikite Hot Springs, North Island, New Zealand. *J. Geol. Soc. London.* 153, 481–496.
- Kele, S., Breitenbach, S.F., Capezzuoli, E., Meckler, A.N., Ziegler, M., Millan, I.M., Kluge, T., Deák, J., Hanselmann, K., John, C.M., Yan, H., Liu, Z., Bernasconi, S.M., 2015. Temperature dependence of oxygen- and clumped isotope fractionation in carbonates: A study of travertines and tufas in the 6–95°C temperature range. *Geochim. Cosmochim. Acta* 168, 172–192.
- Kele, S., Demény, A., Siklósy, Z., Németh, T., Tóth, M., Kovács, M.B., 2008. Chemical and stable isotope composition of recent hot-water travertines and associated thermal waters, from Egerszalók, Hungary: Depositional facies and non-equilibrium fractionation. *Sediment. Geol.* 211, 53–72.
- Kele, S., Özkul, M., Fórizs, I., Gökgöz, A., Baykara, M.O., Alçiçek, M.C., Németh, T., 2011. Stable isotope geochemical study of Pamukkale travertines: New evidences of low-temperature non-equilibrium calcite-water fractionation. *Sediment. Geol.* 238, 191–212.
- Kim, S.-T., O’Neil, J.R., Hillaire-marcel, C., Mucci, A., Kim, S., Neil, J.R.O., Hillaire-marcel, C., Mucci, A., 2007. Oxygen isotope fractionation between synthetic aragonite and water. Influence of temperature and Mg<sup>2+</sup> concentrations. *Geochim. Cosmochim. Acta* 71, 4704–4715.
- Kim, S.T., O’Neil, J.R., 2005. Comment on “An experimental study of oxygen isotope fractionation between inorganically precipitated aragonite and water at low temperatures” by G.-T. Zhou and Y.-F. Zheng. *Geochim. Cosmochim. Acta* 69, 3195–3197.
- Kim, S.T., O’Neil, J.R., 1997. Equilibrium and nonequilibrium oxygen isotope effects in synthetic carbonates. *Geochim. Cosmochim. Acta* 61, 3461–3475.
- Kitano, Y., 1963. Geochemistry of calcareous deposits found in hot springs. *J. Earth Sci.* 11, 68–100.
- Lachniet, M.S., 2015. Are aragonite stalagmites reliable paleoclimate proxies? Tests for oxygen isotope time-series replication and equilibrium. *GSA Bull.* 1521–1533.
- Lachniet, M.S., Bernal, J.P., Asmerom, Y., Polyak, V., Piperno, D., 2012. A 2400-yr Mesoamerican rainfall history links climate and cultural change in Mexico: *Geology* 40, 259–262.

- Last, W.M., 1989. Continental brines and evaporites of the northern Great Plains of Canada. *Sediment. Geol.* 64, 207–221.
- Last, W.M., Vance, R.E., Wilson, S., Smol, J. P., 1998. A multi-proxy limnologic record of rapid early-Holocene hydrologic change on the northern Great Plains, southwestern Saskatchewan, Canada. *The Holocene* 8, 503–520.
- Lécuyer, C., Hutzler, A., Amiot, R., Daux, V., Grosheny, D., Otero, O., Martineau, F., Fourel, F., Balter, V., Reynard, B., 2012. Carbon and oxygen isotope fractionations between aragonite and calcite of shells from modern molluscs. *Chem. Geol.* 332–333, 92–101.
- Li, H.C., Lee, Z.H., Wan, N.J., Shen, C.C., Li, T.Y., Yuan, D.X., Chen, Y.H., 2011. The  $\delta^{18}\text{O}$  and  $\delta^{13}\text{C}$  records in an aragonite stalagmite from Furong Cave, Chongqing, China: A-2000-year record of monsoonal climate. *J. Asian Earth Sci.* 40, 1121–1130.
- Li, T.Y., Shen, C.C., Li, H.C., Li, J.Y., Chiang, H.W., Song, S.R., Yuan, D.X., Lin, C.D.J., Gao, P., Zhou, L., Wang, J.L., Ye, M.Y., Tang, L.L., Xie, S.Y., 2012. Oxygen and carbon isotopic systematics of aragonite speleothems and water in Furong Cave, Chongqing, China. *Geochim. Cosmochim. Acta* 75, 4140–4156.
- Liu, Z., Li, H., You, C., Wan, N., Sun, H., 2006. Thickness and stable isotopic characteristics of modern seasonal climate-controlled sub-annual travertine laminae in a travertinedepositing stream at Baishuitai, SW China: implications for paleoclimate reconstruction. *Environ. Geol.* 51, 257–265.
- Liu, Z., Sun, H., Baoying, L., Xiangling, L., Wenbing, Y., Cheng, Z., 2010. Wet-dry seasonal variations of hydrochemistry and carbonate precipitation rates in a travertinedepositing canal at Baishuitai, Yunnan, SW China: Implications for the formation of biannual laminae in travertine and for climatic reconstruction. *Chem. Geol.* 273, 258–266.
- Lojen, S., Dolenc, T., Vokal, B., Cukrov, N., Mihelčić, G., Papesch, W., 2004. C and O stable isotope variability in recent freshwater carbonates (River Krka, Croatia). *Sedimentology* 51, 361–375.
- Lojen, S., Trkov, A., Ščančar, J., Vázquez-Navarro, J.A., Cukrov, N., 2009. Continuous 60-year stable isotopic and earth-alkali element records in a modern laminated tufa (Jaruga, river Krka, Croatia): implications for climate reconstruction. *Chem. Geol.* 258, 242–250.
- Mas, J.R., Alonso, A., Guimera, J., 1993. Evolución tectonosedimentaria de una cuenca extensional intraplaca: la cuenca finijurásica-eocretácica de los Cameros (La Rioja-Soria). *Rev. la Soc. Geológica España* 6, 129–144.
- McCrea, J.M., 1950. On the isotopic chemistry of carbonates and a paleotemperature scale. *J. Chem. Phys.* 18, 849–857.

- Minissale, A., 2004. Origin, transport and discharge of CO<sub>2</sub> in central Italy. *Earth-Science Rev.* 66, 89–141.
- Mook, W.G., Bommerson, J.C., Staverman, W.H., 1974. Carbon isotope fractionation between dissolved bicarbonate and gaseous carbon dioxide. *Earth Planet. Sci. Lett.* 22, 169–176.
- O'Neil, J.R., Clayton, R.N., Mayeda, T.K., 1969. Oxygen isotope fractionation in divalent metal carbonates. *J. Chem. Phys.* 51, 5547–5558.
- Osácar, C., Arenas, C., Auqué, L.F., Sancho, C., Pardo, G., Vázquez-Urbez, M., 2016. Discerning the interactions between environmental parameters reflected in  $\delta^{13}\text{C}$  and  $\delta^{18}\text{O}$  of recent fluvial tufas: lessons from a Mediterranean climate region. *Sediment. Geol.* 345, 126–144.
- Osácar, C., Arenas, C., Vázquez-Urbez, M., Sancho, C., Auqué, L.F., Pardo, G., 2013. Environmental factors controlling the  $\delta^{13}\text{C}$  and  $\delta^{18}\text{O}$  variations of recent fluvial tufas: a 12-year record from the monasterio de piedra natural park (NE Iberian Peninsula). *Sediment. Geol.* 83, 309–322.
- Özkul, M., Kele, S., Gökğöz, A., Shen, C.C., Jones, B., Baykara, M.O., Föziz, I., Németh, T., Chang, Y.W., Alçiçek, M.C., 2013. Comparison of the Quaternary travertine sites in the Denizli extensional basin based on their depositional and geochemical data. *Sediment. Geol.* 294, 179–204.
- Panichi, C., Tongiorgi, E., 1976. Carbon isotopic composition of CO<sub>2</sub> from springs, fumaroles, mofettes and travertines of central and southern Italy: a preliminary prospection method of geothermal areas., in: *Proceedings 2<sup>nd</sup> U.N. Symposium on the Development and Use of Geothermal Energy*, San Francisco. pp. 815–825.
- Parkhurst, D.L., Appelo, C.A.J., 2013. Description of Input and Examples for PHREEQC Version 3. A Computer Program for Speciation, Batch Reaction, One Dimensional Transport, and Inverse Geochemical Calculations, in: *U.S. Geological Survey (Ed.), Techniques and Methods, Book 6, Chap. A43*. U.S. Geological Survey, Denver, Colorado.
- Patterson, W.P., Smith, G.R., Lohmann, K.C., Kyger, C.L., 1993. Continental Paleothermometry And Seasonality Using The Isotopic Composition Of Aragonitic Otoliths Of Freshwater Fishes, in: *Swart, P.K., Lohmann, K.C., McKenzie, J., Savin, S. (Eds.), Climate Change in Continental Isotopic Records*. American Geophysical Union, pp. 191–202.
- Pedley, M., 2009. Tufas and travertines of the Mediterranean region: a testing ground for freshwater carbonate concepts and developments. *Sedimentology* 56, 221–246.

- Peng, X., Jones, B., 2012. Rapid precipitation of silica (opal-A) disguises evidence of biogenicity in high-temperature geothermal deposits: case study from Dagunguo hot spring, China. *Sediment. Geol.* 257–258, 45–62.
- Pentecost, A., 2005. *Travertine*. Springer Science & Business Media.
- Reyes, E., Pérez del Villar, L., Delgado, A., Cortecchi, G., Núñez, R., Pelayo, M., Cózar, J., 1998. Carbonatation processes at the El Berrocal analogue granitic systema (Spain): mineralogical and isotopic study. *Chem. Geol.* 150, 293–315.
- Rietveld, H.M., 1969. A profile refinement method for nuclear and magnetic structures. *J. Appl. Crystallogr.* 2, 65–71.
- Rodrigo-Naharro, J., Delgado, A., Herrero, M.J., Granados, A., Pérez del Villar, L., 2013. Current Travertines Precipitation from CO<sub>2</sub>-rich Groundwaters as an Alert of CO<sub>2</sub> Leakages from a Natural CO<sub>2</sub> Storage at Gañuelas-Mazarrón Tertiary Basin (Murcia, Spain). CIEMAT, Madrid.
- Rodríguez-Berriguete, Á., Alonso-Zarza, A.M., Martín-García, R., Cabrera, M. del C., 2018. Sedimentology and geochemistry of a human-induced tufa deposit: Implications for palaeoclimatic research. *Sedimentology* 65, 2253–2277.
- Romanek, C.S., Grossman, E.L., Morse, J.W., 1992. Carbon isotopic fractionation in synthetic aragonite and calcite: Effects of temperature and precipitation rate. *Geochim. Cosmochim. Acta* 56, 419–430.
- Sánchez, J.A., Coloma, P., 1998. Hidrogeología de los manantiales termales de Arnedillo. *Zubía Monográfico* 10, 11–25.
- Scheele, N., Hoefs, J., 1992. Carbon isotope fractionation between calcite, graphite and CO<sub>2</sub>: An experimental study. *Contrib. to Mineral. Petrol.* 112, 35–45.
- Sierralta, M., Kele, S., Melcher, F., Hambach, U., Reinders, J., van Geldern, R., Frechen, M., 2010. Uranium-series dating of travertine from Süttő: implications for reconstruction of environmental change in Hungary. *Quat. Int.* 222, 178–193.
- Szaran, J., 1997. Achievement of carbon isotope equilibrium in the system HCO<sub>3</sub><sup>-</sup> (solution)-CO<sub>2</sub> (gas). *Chem. Geol.* 142, 79–86.
- Thorrold, S.R., Campana, S.E., Jones, C.M., Swart, P.K., 1997. Factors determining δ<sup>13</sup>C and δ<sup>18</sup>O fractionation in aragonitic otoliths of marine fish. *Pergamon Geochim. Cosmochim. Acta* 61, 2909–2919.
- Turner, J.V., 1982. Kinetic fractionation of carbon-13 during calcium carbonate precipitation. *Geochim. Cosmochim. Acta* 46, 1183–1191.

- Wang, H., Yan, Y., Liu, Z., 2014. Contrasts in variations of the carbon and oxygen isotopic composition of travertines formed in pools and a ramp stream at Huanglong Ravine, China: implications for paleoclimatic interpretations. *Geochim. Cosmochim. Acta* 125, 34–48.
- Wang, Z., Gaetani, G., Liu, C., Cohen, A., 2013. Oxygen isotope fractionation between aragonite and seawater: Developing a novel kinetic oxygen isotope fractionation model. *Geochim. Cosmochim. Acta* 117, 232–251.
- White, R.M.P., Dennis, P.F., Atkinson, T.C., 1999. Experimental calibration and field investigation of the oxygen isotopic fractionation between biogenic aragonite and water. *Rapid Commun. Mass Spectrom.* 13, 1242–1247.
- Yan, H., Sun, H., Liu, Z., 2012. Equilibrium vs. kinetic fractionation of oxygen isotopes in two low-temperature travertine-depositing systems with differing hydrodynamic conditions at Baishuitai, Yunnan, SW China. *Geochim. Cosmochim. Acta* 95, 63–78.
- Zavdlav, S., Rozic, B., Dolenc, M., Lojen, S., 2017. Stable isotopic and elemental characteristics of recent tufa from a karstic Krka River (south-east Slovenia): useful environmental proxies? *Sedimentology* 64, 808–831.
- Zhang, J., Quay, P.D., Wilbur, D.O., 1995. Carbon isotope fractionation during gas-water exchange and dissolution of CO<sub>2</sub>. *Geochim. Cosmochim. Acta* 59, 107–114.
- Zheng, Y.F., 2011. On the theoretical calculations of oxygen isotope fractionation factors for carbonate-water systems. *Geochem. J.* 45, 341–354.
- Zheng, Y.F., 1999. Oxygen isotope fractionation in carbonate and sulfate minerals. *Geochem. J.* 33, 109–126.
- Zhou, G.-T., Zheng, Y.-F., 2003. An experimental study of oxygen isotope fractionation between inorganically precipitated aragonite and water at low temperatures. *Geochim. Cosmochim. Acta* 67, 387–399.



# 5. JOINT DISCUSSION AND CONCLUSIONS

---

## 5.1 Geothermometrical approach

The main objective of this research was to identify the best methodological approach to establish the reservoir temperature in low-temperature carbonate systems. The main difficulties arising in this type of systems, when compared with others of higher temperatures or hosted in crystalline rocks, have been extensively discussed along the presented papers and they are summarised as follows:

- The minerals present in the aquifer are more limited. In carbonate aquifers these are mainly carbonates, evaporites, quartz and some aluminosilicates although in some cases disperse detrital material can be present.
- The thermodynamic properties of some of these minerals are not well established or their application and interpretation can present some difficulties:
  - Saturation states of carbonate phases are affected by CO<sub>2</sub> outgassing processes and changes in the pH of the waters.
  - Dolomite is highly affected by uncertainties associated to the order/disorder degree (e.g. Carpenter, 1980; Helgeson et al., 1978; Hyeong and Capuano, 2001; Reeder, 2000).
  - Aluminosilicates are also affected by uncertainties due to the crystallinity degree or to the compositional variations (e.g. Merino and Ramson, 1982; Nordstrom et al., 1990; Palandri and Reed, 2001).

- The low temperature of the waters makes the reactions slower and, therefore, difficult to attain the mineral equilibria in the deep reservoir.

Considering these limitations and the fact that the geothermometrical approach will be conditioned by the minerals present in the aquifer, we have proposed a methodological protocol that is detailed below.

The easiest case is when along with carbonates some detrital rocks are present in the reservoir allowing the waters to attain the equilibrium with respect to phases such as albite or K-feldspar. The methodology to follow does not differ too much to the one traditionally used in other systems: the classical cationic geothermometers can be used (e.g. Na-K) and phases like albite and K-feldspar can be considered in the geothermometrical modelling. This situation was found in the studies of the Tiermas and Arnedillo thermal waters.

Quartz (or chalcedony) is a very useful phase in geothermometrical calculations. It is quite common in geothermal systems (D'Amore and Arnórsson, 2000) and it is likely that waters have attained equilibrium with respect it; Moreover, the thermodynamical data are well defined and, therefore, the results can be reliable. Therefore, the use of the silica geothermometers and the consideration of quartz (or chalcedony) equilibria in the geothermometrical modelling should be especially considered. In all the systems studied here the silica phase in equilibrium with the waters is quartz.

Anhydrite is another very reliable phase in geothermometrical calculations as its thermodynamic data are also well characterised. The combination of the equilibrium quartz (or chalcedony) – anhydrite was previously proposed as very reliable (Kharaka and Mariner, 1989; Pastorelli et al., 1999), because their saturation states are not affected by pH variations during the ascent of thermal waters and they are completely independent of possible uncertainties. This quartz – anhydrite geothermometer has been very useful to establish the reservoir temperature in the systems where waters are in equilibrium with anhydrite, that is, Tiermas and Fitero-Arnedillo.

Other common mineral phases present in these systems are the aluminosilicates. As mentioned before, they have a very large compositional and crystallinity variability that makes their use very uncertain. Therefore the recommendation is to perform a sensitivity analyses to the thermodynamic data of these phases, comparing different phases and different thermodynamic databases in order to minimise the possible uncertainties.

Although all the previous minerals can be very useful for temperature estimation, the most important phases in these systems are carbonates: calcite and dolomite. These phases should be always considered because it is almost sure that the waters are in equilibrium with them in the reservoir and they become of vital importance when the previous situations (detrital material in the reservoir or anhydrite equilibrium) are not satisfied. This has been the case of the Alhama-Jaraba system, where the geothermometrical calculations relied only on carbonates, quartz and aluminosilicates. The problem is that these phases, especially dolomite, are not free from uncertainties. Some recommendations are indicated below.

First of all, as carbonate phases, the saturation states of calcite and dolomite are strongly affected by the CO<sub>2</sub> loss, a common process during the ascent of the waters to surface. This situation has been found in the Tiermas and the Fitero-Arnedillo systems. The methodology to deal with this problem was recommended by Palandri and Reed (2001) or Pang and Reed (1998) and consists of the reconstruction of the conditions in the deep reservoir by the addition of the necessary amount of CO<sub>2</sub> to the waters to obtain an equilibrium temperature for these phases (mainly considering calcite since it is not affected by thermodynamic uncertainties) similar to the temperature for rest of phases considered in the geothermometrical modelling.

Although calcite is almost unaffected by thermodynamic uncertainties, dolomite data are very much affected by the order degree, ranging from a completely ordered to a completely disordered dolomite. These dolomite uncertainties can be responsible for the bad results from the Ca-Mg chemical geothermometer (Chiodini et al., 1995). Despite being specifically calibrated for low temperature systems hosted in carbonate rocks, it does not always provide an accurate result since that would depend on the similarity between the dolomite used in the calibration of the geothermometer and the one present in the system under study. To evaluate the dolomite thermodynamic uncertainties the methodology proposed here consists of representing the  $\text{Log}(a\text{Ca}^{2+}/\text{Mg}^{2+})$  of several dolomites with different order degrees versus the temperature (Figure 12) and compare the values with the  $(a\text{Ca}^{2+}/\text{Mg}^{2+})$  of the studied waters assuming the temperature previously established with the previous techniques. In this way, the order degree of the dolomite present in the reservoir can be approximated. However, we have gone a step forward and the next suggestion is to actually calculate the order degree of the dolomite present in the system under study.

For this calculation, the equilibrium calcite-dolomite is assumed to have been attained in the reservoir at certain temperature (previously deduced with the assistance of other geothermometrical techniques).  $\text{Log}K$  for the dissolution reaction  $\text{CaMg}(\text{CO}_3)_2 + 2\text{H}^+ = \text{Ca}^{2+} + \text{Mg}^{2+} + 2\text{HCO}_3^-$  is calculated at that temperature, and that allows the calculation of the Gibbs free energy of the reaction (eq. 5). Then, from eq. (6), knowing the Gibbs free energy of the

reaction and the Gibbs free energy of formation of the species ( $\text{Ca}^{2+}$ ,  $\text{Mg}^{2+}$  and  $\text{HCO}_3^-$ ), we can obtain the Gibbs free energy of dolomite formation ( $\Delta G_f$ ):

$$\log K = \frac{-\Delta G_R}{2.303RT} \quad (5)$$

$$\Delta G_R = \sum \Delta G_{f,products} - \sum \Delta G_{f,reactants} \quad (6)$$

where R is the constant of the ideal gases and T the temperature in K.

Finally from the  $\Delta G_f$  value of the ordered and disordered dolomites<sup>2</sup> (at the temperature of interest) the proportion of order and disorder dolomite can be determined by using the following equation (Anderson and Crerar, 1993):

$$\Delta G_f = X_{ord} \cdot \Delta G_{f,ord} + X_{dis} \cdot \Delta G_{f,dis} + RT(X_{ord} \cdot \ln X_{ord} + X_{dis} \cdot \ln X_{dis}) \quad (7)$$

where  $X_{ord}$  is the molar ratio of the ordered dolomite and  $X_{dis}$  the molar ratio of the disordered dolomite.

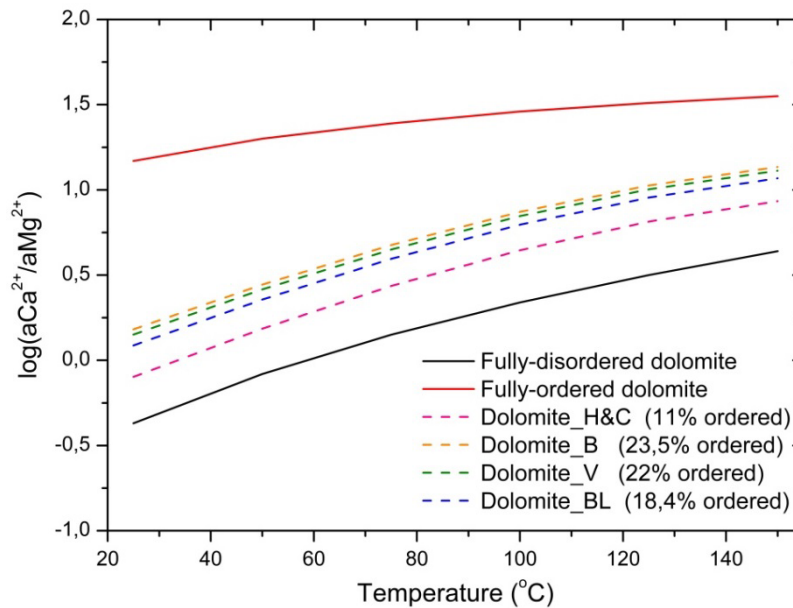


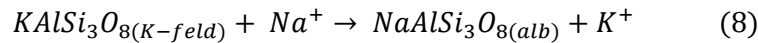
**Figure 12.** Log  $a\text{Ca}^{2+}/a\text{Mg}^{2+}$  vs. temperature plot for the calcite–dolomite equilibrium using different dolomites, from 25 to 150 °C. The equilibria with respect to calcite and fully-disordered dolomite and with respect to calcite and fully-ordered dolomite have been calculated with the thermodynamic data included in the LLNL database. Dolomite\_H&C (Hyeong and Capuano, 2001) is a dolomite from with an order degree of 11%. Dolomite\_B (Busby et al., 1991) is the dolomite from the Carboniferous Madison with an order degree of 23.5%. Dolomite\_V (Vespasiano et al., 2014) is from Triassic rocks affected by a low-grade metamorphism in Calabria (Italy) with an order of 22%. Finally, Dolomite\_BL (Blasco et al., 2018) is the dolomite in the Arnedillo reservoir, with an order degree of 18.4%.

<sup>2</sup> The values of  $\Delta G_f$  of the different species needed to calculate the  $\Delta G_f$  of the dolomite in the aquifer and the values of  $\Delta G_{f,ord}$  and  $\Delta G_{f,dis}$  at the temperature of interest, can be easily obtained from <http://geopig3.la.asu.edu:8080/GEOPIG/pigopt1.html>

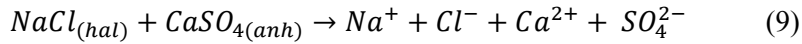
## 5.2 The influence of halite in the reservoir

One of the most interesting results of this thesis is the confirmation that the presence of halite in the deep reservoir is a determinant factor conditioning the chemical characteristics of the waters and their evolution in rock-buffered systems. This has been demonstrated in the Tiermas and the Fitero-Arnedillo thermal systems.

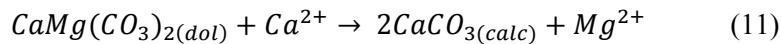
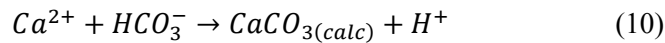
Although the concentration of major elements (Ca, Mg, SO<sub>4</sub>, K, Na) in the reservoir are controlled by equilibrium situations (equilibrium with calcite, dolomite, anhydrite, albite and K-feldspar), halite dissolution causes an increase of those concentrations while silica contents remain almost unaffected. Halite dissolution is the triggering factor of important processes that influence the final characteristics of the waters and the aquifer. It produces a direct increase on dissolved Na which causes the K-feldspar dissolution and the albite precipitation (albitisation process; eq. (8)):



Another effect of the dissolution of halite is the dissolution of anhydrite as its solubility increases with salinity.



As shown in eq. (10) anhydrite dissolution produces an increase of dissolved calcium in waters, generating the oversaturation and precipitation of calcite (eq. 10) and, at the same time, dolomite dissolution (dedolomitisation process; eq. 11):



The fundament of these reactions as a consequence of the salinity increase (halite dissolution) is known as salting-in and salting-out effects (Langmuir, 1997). Due to these effects the solubility of minerals that dissolve forming ionic species increase with increasing ionic strength (salinity) explaining the anhydrite dissolution and the dedolomitisation (salting-in effect). At the same time, the solubility of minerals that dissolve forming molecular species, such as quartz (H<sub>4</sub>SiO<sub>4</sub><sup>0</sup>), decrease with increasing ionic strength, explaining why quartz has been found to precipitate with halite dissolution (salting-out effect). In detail this is explained by the activity definition (eq. 12) where  $a_i$  is the activity,  $\gamma_i$  the activity coefficient and  $m_i$  the concentration:

$$a_i = \gamma_i \cdot m_i \quad (12)$$

Since  $\gamma_i$  of ionic species decrease with the ionic strength, the concentration of ions must increase and, therefore, the solubility of the mineral becomes greater. Conversely, the  $\gamma_i$  of molecular species increase with the ionic strength and therefore the concentration of the species decrease and also the solubility of the mineral.

The processes identified in these aquifers are also likely to occur in other environments with a similar rock assemblage and therefore an extension of the study was done investigating how different factors (salinity, pH and temperature) can affect them. The results indicated that the intensity of the processes is higher as the salinity of the water increases. The pH influence has been found negligible in the range of 6 to 8 (the one that was evaluated since it is the most common pH in natural environments). The range of temperature evaluated was from 25 to 200 °C and the results indicated that the albitisation process was more intense with the increase of temperature, while the opposite was found for the dissolution of anhydrite and the dedolomitisation, both are more intense with the decrease of temperature.

## **5.3 Fitero travertines**

### **5.3.1 Mineralogy**

The carbonate precipitate study has been mainly focus on the characterisation of the Fitero travertine, with more than 98 % of aragonite and only minor amounts of calcite. The aragonite sample (FTOP) consists of an alternation of clear and reddish bands, precipitated at the end of a pipe through which the water was always at 40 °C (this pipe was clogged and removed). The mineralogy of both types of bands is almost the same but in the FESEM study was identified that the reddish colour of some bands are due to the growing of aggregates of iron oxy-hydroxides in that bands, which it is also coherent with the higher Fe contents in them (Figure 13a). Moreover, it was identified that calcite is mainly forming thin interlayers between aragonite bands (Figure 13b). An additional sample (FTNP), taken in a current pipe, which discharges water from the spa with temperatures ranging between 33 and 40 °C, has also been considered for comparative purposes. This appearance of this sample is similar but with calcite proportions of 60 % and 40 % of aragonite.

Several factors are usually considered as controlling factors of the precipitating calcium carbonate phase (i.e. calcite or aragonite): temperature, Mg/Ca ratio, CO<sub>2</sub> contents or degassing rate, pH, organic matter or some elemental contents such as Sr, Fe, Ba or SO<sub>4</sub> (e.g. Jones, 2017; Pentecost, 2005). In the Fitero travertines the factor controlling the calcite or aragonite temperature has been identified to be the temperature. The main water temperature discharged

through this pipe where FTOP sample (almost pure aragonite) precipitated was 40 °C which favours aragonite precipitation (for example, Folk (1994) indicates that if the temperature is higher than 40 °C aragonite precipitates). Calcite interlayers between aragonite bands should have precipitated in the inter-discharge periods, when some water remains in the pipe and cool down. In the case of the pipe where FTNP sample (calcite-aragonite mixture), the water circulation at temperatures ranging between 33 and 40 °C (generally lower than 40 °C) explains the higher calcite proportions.

The rest of factors do not play a decisive role in the precipitation of calcite or aragonite, although the CO<sub>2</sub> outgassing could also give place to differences in the mineralogical phase and, moreover, it is the triggering factor of the precipitation, leading to the oversaturation of calcium carbonate phases.

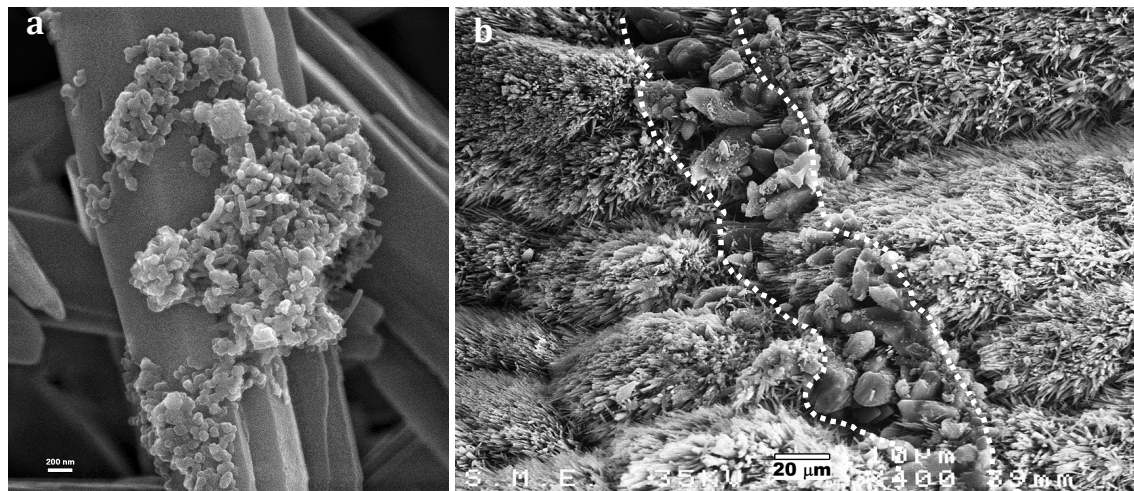


**Figure 13.** FESEM images of one of the Fitero travertines (FTOP). In panel a, a detail of iron oxyhydroxides aggregates growing in an aragonite needle. In panel b, two aragonite bands and a thin interlayer of calcite between them.

### 5.3.2 Isotope signature

The  $\delta^{13}\text{C}$  contents of the travertines has allowed to classified them as meteogene, according to Pentecost (2005), These type is divided at the same time in ambient and superambient (also known as thermometeogene). According to the classification of this author, the Fitero travertines are classified as superambient meteogene travertines, in which the CO<sub>2</sub> has a shallow origin, mainly meteoric, and the deep circulation of waters give place to hot discharges.

Moreover, the  $\delta^{13}\text{C}$  values of the travertines have been used to calculate the  $\delta^{13}\text{C}$  in the dissolved CO<sub>2</sub> during travertine precipitation using the equations proposed by Romanek et al. (1992). Additionally, considering the  $\delta^{13}\text{C}$  in the HCO<sub>3</sub><sup>-</sup> of the spring water, it can be estimated the  $\delta^{13}\text{C}$  in the dissolved CO<sub>2</sub> just in the spring using the equations proposed by Mook et al.

(1974), Zhang et al. (1995) and Szaran (1997). In the spring this value is more negative than during the precipitation which confirms the existence of an important outgassing process as triggering of the calcium carbonate precipitation.

The  $\delta^{18}\text{O}$  values in the travertine, and its parental water, has been used to test several  $\delta^{18}\text{O}$  fractionation equations. Their application in an active system gives the opportunity to compare the temperature results to the actual temperature of the waters, which can provide valuable information to be applied in the interpretation of the isotope data in ancient travertines.

Although several  $\delta^{18}\text{O}$  fractionation equations for aragonite (and also for calcite) have been proposed, the main problem in their application is that it is still uncertain if some of those equations represent a real equilibrium situation. However, they allow evaluating if the precipitation took place, at least, close to the isotope equilibrium. In the Figure 14 the range defined by the used  $\delta^{18}\text{O}$  aragonite-water equilibrium equations (the named as “equilibrium window” by Lachniet (2015) are represented, along with the FTOP sample (6 subsamples corresponding to the different bands) and the FTNP sample. The results obtained with the different equations are in a quite narrow range (36 – 40 °C), for both FTOP and FTNP sample. The equation that provided the most similar temperature to the real water temperature (40 °C) was the one from Kim. et al. (2007).

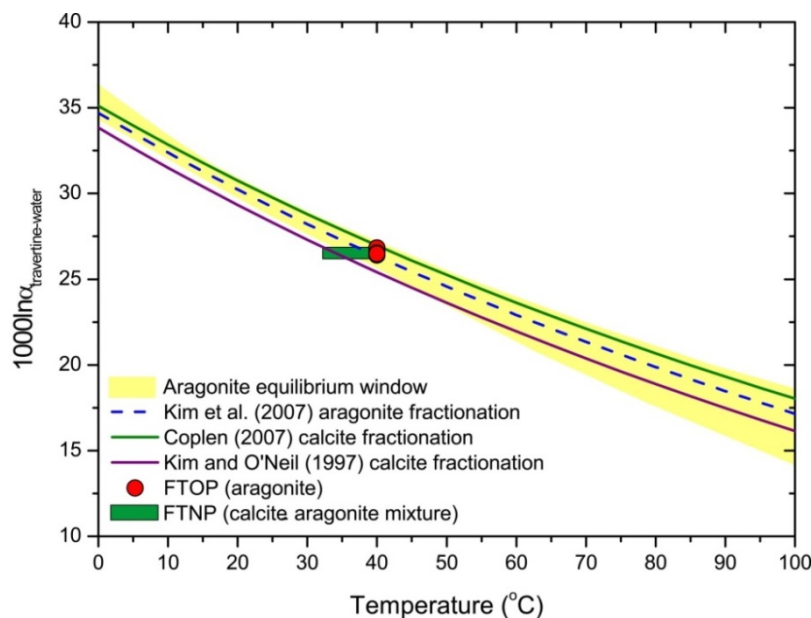


**Figure 14.**  $\delta^{18}\text{O}$  aragonite – water vs temperature plot. The aragonite equilibrium window defined by all the equations used in this study is shadowed in yellow. The Kim et al. (2007) equation for aragonite-water equilibrium is shown as a dashed line, since it is the one that provides the results closest to 40 °C. Additionally, the two calcite equilibrium equations considered in the study are also represented as continuous line. The Fitero aragonite samples (FTOP) are shown as red circles and the calcite–aragonite mixture of FTNP as a rectangle covering the possible temperature range of precipitation (33 – 40 °C).



In the case of the FTNP, which consist of a mixture of aragonite and calcite, the calculation has been repeated using some  $\delta^{18}\text{O}$  calcite-water equilibrium equations, as proposed by Jones and Peng (2016) for the cases in which a mixture of both calcium carbonate phases exists, and the results are in a boarder range, 34 to 43 °C.

Although some authors indicate the existence of differences between the aragonite-water oxygen fractionation and the calcite-water fractionation (e.g. Kele et al., 2008; Wang et al., 2013) in this study the  $\delta^{18}\text{O}$  values are almost the same no matter the calcite proportion, as also previously found by others (e.g. Kele et al., 2015).

These travertines apparently have precipitated close to an equilibrium situation since the temperatures obtained with several fractionation equations are similar to the actual water temperature. However, in natural systems, with high  $\text{CO}_2$  outgassing as deduced for the studied system, it is usually considered that a disequilibrium situation will exists due to kinetic isotope effects (Kele et al., 2011, 2008; Rodríguez-Berriguete et al., 2018). Other authors have also obtained accurate temperature calculations despite an isotope disequilibrium (Rodríguez-Berriguete et al., 2018; Wang et al., 2014; Yan et al., 2012) explaining that as due to the isotope signature of the carbonate is very close to the signal in the dissolved  $\text{HCO}_3^-$ . This explanation has been checked to be valid also in this system where the aragonite/calcite-water fractionation is very similar to the  $\text{HCO}_3^-$ -water fractionation calculated using the equation from Halas and Wolacewicz (1982). The explanation is that when the  $\text{HCO}_3^-$  and water isotope equilibrium exists, due to the fast  $\text{CO}_2$  and precipitation the isotope signature in the  $\text{HCO}_3^-$  can be directly transferred to the solid without fractionation (Kele et al., 2011). Therefore, it seems that the  $\delta^{18}\text{O}$  data can be used for paleotemperature calculations even in some cases of disequilibrium situations.

Finally, considering additional aragonite data from other sites in the world where precipitation also seems to took place close to a  $\delta^{18}\text{O}$  equilibrium situation, and displaying a clear temperature dependence, a fractionation equation for natural aragonites in the range 23 to 80 °C has been proposed (eq. 13; where T is in K; Figure 15):

$$1000\ln\alpha = 18.27 (\pm 1.26) \cdot \frac{1000}{T} - 31.47 (\pm 3.85) \quad (13)$$

This equation is quite similar to the experimental Kim et al. (2007) equation (Figure 15). This seems to indicate that the main control in aragonite fractionation, at least in the considered samples, is the temperature and, moreover, suggests that equilibrium situations are not uncommon. Therefore the proposed equation does not attempt to solve the problem about the uncertainties regarding the real equilibrium line, it is proposed as an additional tool for the isotope signature evaluation of natural aragonites.

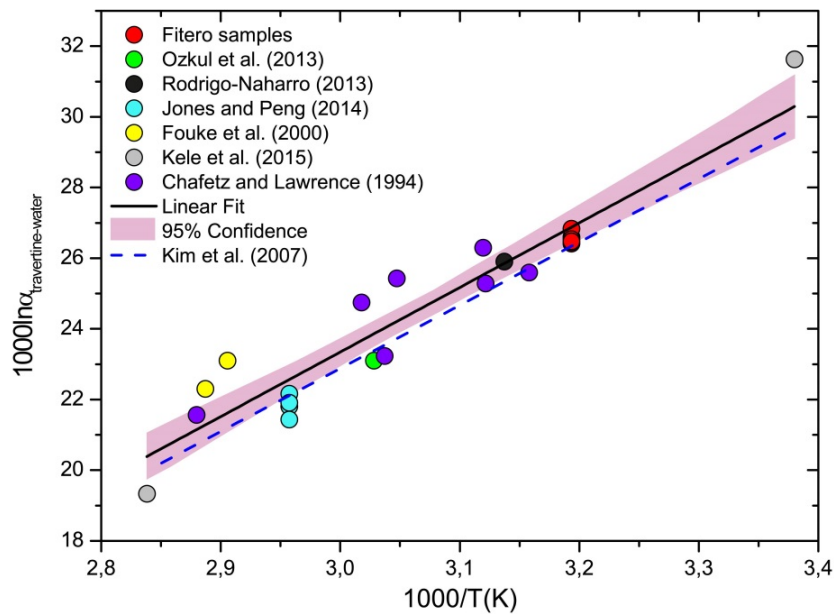


**Figure 15.**  $\delta^{18}\text{O}$  aragonite – water vs  $1000/T$  plot. The different natural aragonite samples considered for the linear fitting are represented. The fitting and the 95 % confidence band is also shown along with the Kim et al. (2007) equation. It is remarkable that the 95% confidence range of the fitting include almost completely the fractionation equation of Kim. et al. (2007) which was calibrated using synthetic aragonites precipitated in laboratory experiments under controlled conditions in the temperature range of 10 to 40 °C.

## 5.4 Applications to $\text{CO}_2$ geological storages

Apart from the purely scientific interest of the characterisation of geothermal systems and the information that these studies can provide for future geothermal energy exploitations, an additional interest is the information that they provide as a starting point for the study and understanding of  $\text{CO}_2$  geological storages in deep saline aquifers. Some of the characteristics of these aquifers, such as temperature, salinity or depth are similar to the systems studied here and, therefore, the processes are expected to be similar (e.g. Auqué et al., 2009; Güleç and Hilton, 2016).

Prior to the construction of a geological storage, an in-depth study of the area is needed to assess the feasibility of the injection and the long-term safety, and therefore, an evaluation of the  $\text{CO}_2$  behaviour once injected in the aquifer will be necessary (Trémosa et al., 2014). One of the first steps, along with the geological characterisation of the area, will be the hydrogeochemical characterisation of the aquifer in order to establish the mineral equilibria existing and depth and the main processes controlling the chemical characteristics of the waters. Given that the characteristics of the potential  $\text{CO}_2$  storage sites in saline aquifers are similar to those of the systems studied here, similar problems may arise and the methodology proposed for their characterisation will be directly applicable. Moreover, as dolomite is an important mineral

phase to take into account in the evaluation of the possible mass transfers due to the CO<sub>2</sub> injection, it can be especially interesting to know its solubility (log K). This log K can be estimated if the order of the dolomite present in the system is calculated as suggested in this thesis (5.1 section) and then equations 8, 7 and 6 can be applied at the temperature or temperatures of interest.

The study performed here about the influence of halite dissolution and the evaluation of the different processes associated to it, can also be used in the evaluation of the performance of a CO<sub>2</sub> storage in saline aquifers. The injection of supercritical CO<sub>2</sub> will displace the saline water present in the aquifer. Then a small fraction of CO<sub>2</sub> will dissolve into the brine and some water will evaporate becoming more saline and enriched in salts (André et al., 2007; Muller et al., 2009). This increase in salinity could trigger the anhydrite dissolution, the dedolomitisation and the albitisation processes and their consideration is crucial since they can produce important modifications in the porosity and permeability of the storage making difficult the CO<sub>2</sub> injection and modifying the storage capacities.

## 5.5 Future research lines

After the evaluation of these low-temperature carbonate geothermal systems the next goal will be to extend the study to other carbonate systems with similar temperatures but with naturally CO<sub>2</sub>-rich waters. Due to their CO<sub>2</sub> contents, these water are more acidic and aggressive making the mineral equilibria attainment more difficult in the deep reservoir (Arnórsson, 2014; Fouillac, 1983). The methodology proposed in this thesis dissertation needs to be tested in these CO<sub>2</sub>-rich systems and modified if necessary. The study on CO<sub>2</sub>-rich water will be extended to other low temperature systems hosted in different rocks, such as granites, since the characterisation of these waters will provide valuable information about the behaviour of the waters in the CO<sub>2</sub> geological storages (e.g. Choi et al., 2014; Gal et al., 2012).

More studies will be done on the Fitero travertines taking the great opportunity of analysing almost pure aragonite. The future works will focus in the evaluation of distribution coefficients as they provide relevant information about the mobilisation and retention of potentially contaminant elements. This information can also be especially important in the context of the CO<sub>2</sub> geological storages as the CO<sub>2</sub> injection will promote the acidification of waters and the enhancement of dissolution and mobilisation (and also the possible ulterior retention in carbonates) of major, minor and trace elements, some of which are contaminant and a risk for health (Olsson et al., 2014; Lions et al., 2014; Marcon and Kaszuba, 2015; Qafoku et al., 2017). The understanding of the potential element retention in carbonate phases is also of great interest

in the safety assessment of radioactive wastes storages (e.g. Curti, 1999; Drake et al., 2018) and for the remediation strategies in contaminated sites (e.g. Sutton, 2009).

## 5.6 Final conclusions

- The study of different low temperature geothermal systems hosted in carbonate rocks has allowed establishing a methodology for their geothermometrical characterisation, especially interesting when waters have not attained the equilibrium with respect to phases such as anhydrite, albite or K-feldspar. This methodology includes the sensitivity analyses to the aluminosilicate thermodynamic data and the evaluation of the order degree of dolomite.
- Halite dissolution is an important controlling factor of the water evolution, triggering anhydrite dissolution, dedolomitisation and albitisation processes.
- The intensity of these processes increases with salinity and they are almost unaffected by the pH. The temperature increase produces and increases in the albitisation processes but a decrease in the intensity of anhydrite dissolution and dedolomitisation.
- The methodology proposed here for the characterisation of these thermal systems and the processes identified in them can be useful for the characterisation of potential CO<sub>2</sub> storage sites in deep saline aquifers.
- The precipitation of the Fitero travertines is triggered by an important CO<sub>2</sub> outgassing and the main factor controlling calcite or aragonite precipitation seems to be temperature.
- The  $\delta^{13}\text{C}$  values of the precipitates allow classifying them as superambient meteogene (or thermometeogene).
- The  $\delta^{18}\text{O}$  stable isotope data of the Fitero travertines suggest an apparent equilibrium situation during precipitation despite the high CO<sub>2</sub> outgassing identified. This can be explained as due to a direct transfer of the dissolved HCO<sub>3</sub><sup>-</sup> isotope signature to the precipitated carbonate (without fractionation) favoured fast precipitation, resulting in a good temperature estimation despite a real disequilibrium.
- A  $\delta^{18}\text{O}$  fractionation equation for natural aragonites in the range 23 to 80 °C has been proposed considering additional aragonite samples.

## 5.7 Conclusiones finales

- El estudio de diferentes sistemas geotermales alojados en rocas carbonatadas ha permitido establecer una metodología para su caracterización geotermométrica, especialmente útil cuando las aguas no han alcanzado el equilibrio con fases como la anhidrita, la albita o el feldespato potásico. Esta metodología consiste principalmente en realizar un análisis de sensibilidad a los datos termodinámicos de los aluminosilicatos y una evaluación del grado de orden de la dolomita.
- Se ha identificado que la disolución de halita es un factor muy importante en el control de la evolución de las aguas en el acuífero, dando lugar a la disolución de anhidrita y a los procesos de dedolomitización y albitización.
- La intensidad de estos procesos aumenta con la salinidad de las aguas, pero casi no se ven afectados por el pH. En el caso de la temperatura, mientras que la disolución de anhidrita y la dedolomitización son mayores a temperaturas menores, la albitización es más importante según aumenta la temperatura.
- La metodología de caracterización de sistemas termales propuesta y los procesos identificados pueden ser útiles para la caracterización y evaluación de potenciales almacenes de CO<sub>2</sub> en acuíferos salinos profundos.
- La precipitación de los travertinos en Fitero está desencadenada por la pérdida de CO<sub>2</sub> de las aguas y el principal factor que determina la precipitación de calcita o aragonito parece ser la temperatura.
- A partir de los valores de  $\delta^{13}\text{C}$  de los precipitados, estos se han podido clasificar como metegénicos superambientales.
- Los datos  $\delta^{18}\text{O}$  de estos travertinos sugieren que la precipitación tiene lugar cercana a una situación de equilibrio a pesar de haber identificado una importante pérdida de CO<sub>2</sub>. Esto se puede explicar por una transferencia directa del valor isotópico del HCO<sub>3</sub><sup>-</sup> disuelto al carbonato que precipita (sin fraccionamiento) favorecida por la rápida precipitación).
- Considerando muestras adicionales de aragonito se ha propuesto una ecuación para el fraccionamiento de  $\delta^{18}\text{O}$  en aragonitos naturales en el rango de temperaturas entre 23 y 80 °C.



# REFERENCES

---

*The different papers included in the Results section have their own reference section. Therefore, here only the references in the rest of sections are listed.*

- Anderson, G.M., Crerar, D.A., 1993. Thermodynamics in Geochemistry. The Equilibrium Model. Oxford University Press, Oxford.
- André, L., Audigane, P., Azaroual, M., Menjoz, A., 2007. Numerical modeling of fluid-rock chemical interactions at the supercritical CO<sub>2</sub>-liquid interface during CO<sub>2</sub> injection into a carbonate reservoir, the Dogger aquifer (Paris Basin, France). Energy Convers. Manag. 48, 1782–1797.
- Andrews, J.E., 2006. Palaeoclimatic records from stable isotopes in riverine tufas: Synthesis and review. Earth Sci. Rev. 75, 85–104.
- Apollaro, C., Dotsika, E., Marini, L., Barca, D., Bloise, A., de Rosa, R., Doveri, M., Lelli, M., Muto, F., 2012. Chemical and isotopic characterization of the thermomineral water of Terme Sibarite springs (Northern Calabria, Italy). Geochem. J. 46, 117–129.
- Appelo, C.A.J., Postma, D., 2005. Geochemistry, Groundwater and Pollution, 2<sup>nd</sup> ed. A.A. Balkema, Rotterdam.
- Armijo, F., 2006. Balnearios y manantiales del prineo aragonés a través de los viajeros. Balena 1, 111–125.
- Arnórsson, S., 2014. Carbon dioxide waters and chemical geothermometer interpretation, in: Proceedings 5<sup>th</sup> African Rift Geothermal Conference. Arusha, Tanzania, Tanzania, pp. 1–9.

- Arnórsson, S., Gunnlaugsson, E., Svavarsson, H., 1983. The chemistry of geothermal waters in Iceland. III. Chemical geothermometry in geothermal investigations. *Geochim. Cosmochim. Acta* 47, 567–577.
- Asta, M.P., Auqué, L.F., Sanz, F.J., Gimeno, M.J., Acero, P., Blasco, M., García-Alix, A., Gómez, J., Delgado-Huertas, A., Mandado, J., 2017. Travertines associated with the Alhama-Jaraba thermal waters (NE, Spain): Genesis and geochemistry. *Sediment. Geol.* 347, 100–116.
- Asta, M.P., Gimeno, M.J., Auqué, L.F., Gómez, J., Acero, P., Lapuente, P., 2010. Secondary processes determining the pH of alkaline waters in crystalline rock systems. *Chem. Geol.* 273, 41–52.
- Auqué, L.F., Acero, P., Gimeno, M.J., Gómez, J.B., Asta, M.P., 2009. Hydrogeochemical modeling of a thermal system and lessons learned for CO<sub>2</sub> geologic storage. *Chem. Geol.* 268, 324–336.
- Auqué, L.F., Mandado, J., López, P.L., Lapuente, P.L., Gimeno, M.J., 1997. Los sistemas geotermales del Pirineo Central. II. Resultados de la aplicación de técnicas geotermométricas. *Estud. geológicos* 53, 45–54.
- Ayora, C., Taberner, C., Pierre, C., Pueyo, J.J., 1995. Modeling the sulfur and oxygen isotopic composition of sulfates through a halite-potash sequence: Implications for the hydrological evolution of the Upper Eocene Southpyrenean. *Geochim. Cosmochim. Acta* 59, 1799–1808.
- Bachu, S., 2000. Sequestration of CO<sub>2</sub> in geological media: criteria and approach for site selection in response to climate change. *Energy Convers. Manag.* 41, 953–970.
- Back, W., Hanshaw, B.B., Plummer, L.N., Rahn, P.H., Rightmire, C.T., Rubin, M., 1983. Process and rate of dedolomitization: mass transfer and <sup>14</sup>C dating in a regional carbonate aquifer. *Geol. Soc. Am. Bull.* 94, 1415–1429.
- Ball, J.W., Nordstrom, D., 2001. User's manual for WATEQ4F with revised thermodynamic database and test cases for calculating speciation of major, trace and redox elements in natural waters, in: U.S. Geological Survey (Ed.), *Water-Resources Investigation Report*. U.S. Geological Survey, Menlo Park (California), pp. 91–183.
- Bauluz, B., González, J.M., Yuste, A., Mayayo, M.J., 2008. Evolución diagenética de las turbiditas del Grupo Hecho (Eoceno) en la Cuenca de Jaca (España). *Macla* 9, 47–48.
- Bethke, C.M., 2008. *Geochemical and Biogeochemical Reaction Modeling*, 2<sup>nd</sup> ed. Cambridge University Press, New York.



- Blasco, M., Auqué, L.F., Gimeno, M.J., 2016. Caracterización geoquímica del proceso de mezcla de aguas termales y no termales en los manantiales de Jaraba (Aragón, España). *Geotemas* 16, 531–534.
- Blasco, M., Gimeno, M.J., Auqué, L.F., 2018. Low temperature geothermal systems in carbonate-evaporitic rocks: Mineral equilibria assumptions and geothermometrical calculations. Insights from the Arnedillo thermal waters (Spain). *Sci. Total Environ.* 615, 526–539.
- Blasco, M., Gimeno, M.J., Auqué, L.F., 2017. Comparison of different thermodynamic databases used in a geothermometrical modelling calculation. *Procedia Earth Planet. Sci.* 17, 120–123.
- Böhm, F., Joachimski, M.M., Dullo, W.C., Eisenhauer, A., Lehnert, H., Reitner, J., Wörheide, G., 2000. Oxygen isotope fractionation in marine aragonite of coralline sponges. *Geochim. Cosmochim. Acta* 64, 1695–1703.
- Boschetti, T., Cortecchi, G., Toscani, L., Iacumin, P., 2011. Sulfur and oxygen isotope compositions of Upper Triassic sulfates from northern Apennines (Italy): paleogeographic and hydrogeochemical implications. *Geol. Acta* 9, 129–147.
- Brenninkmeijer, C.A.M., Kraft, P., Mook, W.G., 1983. Oxygen isotope fractionation between CO<sub>2</sub> and H<sub>2</sub>O. *Isot. Geosci.* 1, 181–190.
- Buil, B., Gómez, P., Turrero, M.J., Garralón, A., Lago, M., Arranz, E., de la Cruz, B., 2006. Factors that control the geochemical evolution of hydrothermal systems of alkaline water in granites in Central Pyrenees (Spain). *J. Iber. Geol.* 32, 283–302.
- Busby, J.F., Plummer, L.N., Lee, R.W., Hanshaw, B.B., 1991. Geochemical Evolution of Water in the Madison Aquifer in Parts of Montana, South Dakota, and Wyoming, in: U.S. Geological Survey Professional Paper 1273-F. United States Government Printing Office, Washington, p. 89.
- Capezzuoli, E., Gandin, A., Pedley, M., 2014. Decoding tufa and travertine (fresh water carbonates) in the sedimentary record: the state of the art. *Sedimentology* 61, 1–21.
- Carpenter, A.B., 1980. The chemistry of dolomite formation I: the stability of dolomite, in: Zenger, D.H., Dunham, J.B., Ethington, R.L. (Eds.), *Concepts and Models of Dolomitization*. Society of Economic Paleontologists and Mineralogists Spec. Publ. 28, pp. 111–121.

- Chacko, T., Cole, D.R., Horita, J., 2001. Equilibrium Oxygen, Hydrogen and Carbon Isotope Fractionation Factors Applicable to Geologic Systems. *Rev. Mineral. Geochemistry* 43, 1–81.
- Chacko, T., Deines, P., 2008. Theoretical calculation of oxygen isotope fractionation factors in carbonate systems. *Geochim. Cosmochim. Acta* 72, 3642–3660.
- Chafetz, H.S., Lawrence, J.R., 1994. Stable Isotopic Variability within Modern Travertines. *Géographie Phys. Quat.* 48, 257–273.
- Chiba, H., Kusakabe, M., Hirano, S.I., Matsuo, S., Somiya, A., 1981. Oxygen isotope fractionation factors between anhydrite and water from 100 to 550 °C. *Earth Planet. Sci. Lett.* 53, 55–62.
- Chiodini, G., Cioni, R., Guidi, M., Marini, L., 1991. Chemical geothermometry and geobarometry in hydrothermal aqueous solutions: a theoretical investigation based on a mineral-solution equilibrium model. *Geochim. Cosmochim. Acta* 55, 2709–2727.
- Chiodini, G., Frondini, F., Marini, L., 1995. Theoretical geothermometers and pCO<sub>2</sub> indicators for aqueous solutions coming from hydrothermal systems of medium-low temperature hosted in carbonate-evaporite rocks. Application to the thermal springs of the Etruscan Swell. Italy. *Appl. Geochemistry* 10, 337–346.
- Choi, B.Y., Yun, S.T., Kim, K.H., Choi, H.S., Chae, G.T., Lee, P.K., 2014. Geochemical modeling of CO<sub>2</sub>-water-rock interactions for two different hydrochemical types of CO<sub>2</sub>-rich springs in Kangwon District, Korea. *J. Geochemical Explor.* 144, 49–62.
- Choi, B.Y., Yun, S.T., Mayer, B., Hong, S.Y., Kim, K.H., Jo, H.Y., 2012. Hydrogeochemical processes in clastic sedimentary rocks, South Korea: a natural analogue study of the role of dedolomitization in geologic carbon storage. *Chem. Geol.* 306–307, 103–113.
- Choi, H.S., Koh, Y.K., Bae, D.K., Park, S.S., Hutcheon, I., Yun, S.T., 2005. Estimation of deep-reservoir temperature of CO<sub>2</sub>-rich springs in Kangwon district, South Korea. *J. Volcanol. Geotherm. Res.* 141, 77–89.
- Chopping, C., Kaszuba, J.P., 2012. Supercritical carbon dioxide–brine–rock interactions in the Madison Limestone of Southwest Wyoming: an experimental investigation of a sulfur-rich natural carbon dioxide reservoir. *Chem. Geol.* 322–323, 223–236.
- Coloma, P., 1998. El agua subterránea en La Rioja. *Zubía Monográfico* 10, 63–132.

- Coloma, P., Sánchez, J.A., Martínez, F.J., 1997. Sistemas de flujo subterráneo regional en el acuífero carbonatado mesozoico de la Sierra de Cameros. Sector Oriental. *Estud. geológicos* 53, 159–172.
- Coloma, P., Sánchez, J.A., Martínez, F.J., 1995. El drenaje subterráneo de la cordillera Ibérica en la depresión terciaria del Ebro (sector Riojano). *Geogaceta* 17, 68–71.
- Coplen, T.B., 2007. Calibration of the calcite-water oxygen-isotope geothermometer at Devils Hole, Nevada, a natural laboratory. *Geochim. Cosmochim. Acta* 71, 3948–3957.
- Curti, E., 1999. Coprecipitation of radionuclides with calcite: estimation of partition coefficients based on a review of laboratory investigations and geochemical data. *Appl. Geochemistry* 14, 433–445.
- D'Amore, F., Arnórsson, S., 2000. Geothermometry, in: Arnórsson S. (Ed.), *Isotopic and Chemical Techniques in Geothermal Exploration, Development and Use*. International Atomic Agency, Vienna.
- D'Amore, F., Fancelli, R., Caboi, R., 1987. Observations of the application of chemical geothermometers to some hydrothermal systems in Sardinia. *Geothermics* 16, 271–282.
- De Toledo, F.O., Arqued, V., 1990. Estudio de los recursos hidráulicos subterráneos de los acuíferos relacionados con la provincia de Zaragoza. *Unidad Hidrogeológica* 43, Sierra del Solorio. MOPU, 09.803.183/0411.
- Deines, P., Langui, D., Harmon, R.S., 1974. Stable carbon isotope ratios and the existence of a gas phase in the evolution of carbonate ground water. *Geochim. Cosmochim. Acta* 38, 1147–1168.
- Drake, H., Mathurin, F.A., Zack, T., Schäfer, T., Roberts, N.M.W., Whitehouse, M., Karlsson, A., Broman, C., Åström, M.E., 2018. Incorporation of Metals into Calcite in a Deep Anoxic Granite Aquifer. *Environ. Sci. Technol.* 52, 493–502.
- Echevarria, R.N., Xiu, T., 2014. Energy related CO<sub>2</sub> emissions and the progress on CCS projects: A review. *Renew. Sustain. Energy Rev.* 31, 368–385.
- Elío, J., Ortega, M.F., Nissi, B., Mazadiego, L.F., Vaselli, O., Caballero, J., Grandia, F., 2015. CO<sub>2</sub> and Rn degassing from the natural analog of Campo de Calatrava (Spain): Implications for monitoring of CO<sub>2</sub> storage sites. *Int. J. Greenh. Gas Control* 32, 1–14.
- Faci, E. (Ed.), 1997. *Cartografía Geológica de Navarra*. E, 1:25000. Hoja 175-I: Tiermas. Gobierno de Navarra. Departamento de Obras Públicas, Transportes y Comunicaciones, Navarra.

- Fernández, J., Auqué, L.F., Sánchez Cela, V.S., Guaras, B., 1988. Las aguas termales de Fitero (Navarra) y Arnedillo (Rioja). II. Análisis comparativo de la aplicación de técnicas geotermométricas químicas a aguas relacionadas con reservorios carbonatado-evaporíticos. *Estud. geológicos* 44, 453–469.
- Flaathen, T.K., Gislason, S.R., Oelkers, E.H., Sveinbjörnsdóttir, Á.E., 2009. Chemical evolution of the Mt. Hekla, Iceland, groundwaters: A natural analogue for CO<sub>2</sub> sequestration in basaltic rocks. *Appl. Geochemistry* 24, 463–474.
- Folk, R.L., 1994. Interaction between bacteria, nanobacteria, and mineral precipitation in hot springs of central Italy. *Géographie Phys. Quat.* 48, 233–246.
- Ford, T.D., Pedley, H.M., 1996. A review of tufa and travertine deposits of the world. *Earth Sci. Rev.* 41, 117–175.
- Fouillac, C., 1983. Chemical geothermometry in CO<sub>2</sub>-rich thermal waters. Example of the French Massif Central. *Geothermics* 12, 149–160.
- Fouillac, C., Michard, G., 1981. Sodium/lithium ratio in water applied to geothermometry of geothermal reservoirs. *Geothermics* 10, 55–70.
- Fouke, B.W., Farmer, J.D., Des Marais, D.J., Pratt, L., Sturchio, N.C., Burns, P.C., Discipulo, M.K., 2000. Depositional facies and aqueous-solid geochemistry of travertine-depositing hot springs (Angel Terrace, Mammoth Hot Springs, Yellowstone National Park, U.S.A.). *J. Sediment. Res.* 70, 565–585.
- Fournier, R.O., 1991. Water geothermometers applied to geothermal energy, in: D'Amore, F. (Ed.), *Application of Geochemistry in Geothermal Reservoir Development*. UNITAR, Rome, Italy, Italy, pp. 37–69.
- Fournier, R.O., 1981. Application of water geochemistry to geothermal exploration and reservoir engineering, in: Rybach, L., Muffler, L.J.P. (Eds.), *Geothermal Systems: Principles and Case Histories*. John Willey & Sons Ltd., New York, pp. 109–141.
- Fournier, R.O., 1979. A revised equation for the Na-K geothermometer. *Geotherm. Resour. Counc. Trans.* 3, 221–224.
- Fournier, R.O., 1977. Chemical geothermometers and mixing models for geothermal systems. *Geothermics* 5, 41–50.
- Fournier, R.O., Potter, R.W., 1982. An equation correlating the solubility of quartz in water from 25 to 900 °C at pressures up to 10000 bars. *Geochim. Cosmochim. Acta* 46, 1975–1978.

- Fournier, R.O., Truesdell, A.H., 1973. An empirical Na–K–Ca geothermometer for natural waters. *Geochim. Cosmochim. Acta* 37, 1255–1275.
- Friedman, I., O'Neil, J.R., 1977. Compilation of stable isotope fractionation factors of geochemical interest, in: Fleischer, M. (Ed.), *Data on Geochemistry*, USGS Professional Paper 440-KK. United States Government Printing Office, Washington, p. 109.
- Gal, F., Brach, M., Braibant, G., Bény, C., Michel, K., 2012. What can be learned from natural analogue studies in view of CO<sub>2</sub> leakage issues in Carbon Capture and Storage applications? Geochemical case study of Sainte-Marguerite area (French Massif Central). *Int. J. Greenh. Gas Control* 10, 470–485.
- Garnett, E.R., Andrews, J.E., Preece, R.C., Dennis, P.F., 2004. Climatic change recorded by stable isotopes and trace elements in a British Holocene tufa. *J. Quat. Sci.* 19, 251–262.
- Garrels, R.M., Mackenzie, F.T., 1967. Origin of the chemical composition of some springs and lakes. *Equilib. Concepts Nat. Waters, Adv. Chem. Ser.* 67, 222–242.
- Garrels, R.M., Thompson, M.E., 1962. A chemical model for seawater at 25 °C and one atmosphere total pressure. *Am. J. Sci.* 260, 57–66.
- Giggenbach, W.F., 1988. Geothermal solute equilibria. Derivation of Na-K-Mg-Ca geoindicators. *Geochim. Cosmochim. Acta* 52, 2749–2765.
- Giggenbach, W.F., Gonfiantini, R., Jangi, B.L., Truesdell, A.H., 1983. Isotopic and chemical composition of Parbati valley geothermal discharges, N.W. Himalaya. India. *Geothermics* 12, 199–222.
- Gil, A., Villalaín, J.J., Barbero, L., González, G., Mata, P., Casas, A.M., 2002. Aplicación de Técnicas geoquímicas, geofísicas y mineralógicas al estudio de la Cuenca de Cameros. Implicaciones geométricas y evolutivas. *Zubía Monográfico* 14, 65–98.
- Gimeno, M.J., Peña, J., 1994. Principios básicos de la modelización geoquímica directa e inversa. *Estud. geológicos* 50, 359–367.
- Gökgöz, A., Tarkan, G., 2006. Mineral equilibria and geothermometry of the Dalaman–Köycegiz thermal springs, southern Turkey. *Appl. Geochemistry* 21, 253–268.
- Gómez, J.J., Goy, A., 1979. Las unidades litoestratigráficas del Jurásico medio y superior, en facies carbonatadas del Sector Levantino de la Cordillera Ibérica. *Estud. geológicos* 35, 569–598.
- González, J.F., 1867. *Crónica de la provincia de Zaragoza*. Editores Ruvio y Compañía, Madrid.

- Goy, A., Gómez, J.J., Yébenes, A., 1976. El Jurásico de la Rama Castellana de la Cordillera Ibérica (Mitad norte) I. Unidades litoestratigráficas. *Estud. geológicos* 32, 391–423.
- Grossman, E.L., Ku, T., 1986. Oxygen and carbon isotope fractionation in biogenic aragonite: temperature effects. *Chem. Geol.* 59, 59–74.
- Güleç, N., Hilton, D.R., 2016. Turkish geothermal fields as natural analogues of CO<sub>2</sub> storage sites: Gas geochemistry and implications for CO<sub>2</sub> trapping mechanisms. *Geothermics* 64, 96–110.
- Halas, S., Pluta, I., 2000. Empirical calibration of isotope thermometer  $\delta^{18}\text{O}(\text{SO}_4^{2-})-\delta^{18}\text{O}(\text{H}_2\text{O})$  for low temperature brines, in: V Isotope Workshop. European Society for Isotope Research, Kraków, Poland, pp. 68–71.
- Halas, S., Wolacewicz, W., 1982. The experimental study of oxygen isotope exchange reaction between dissolved bicarbonate and water. *J. Chem. Phys.* 76, 5470–5472.
- Hanshaw, B.B., Back, W., 1985. Deciphering hydrological systems by means of geochemical processes. *Hydrological Sci. J.* 30, 257–271.
- Helgeson, H.C., 1968. Evaluation of irreversible reactions in geochemical processes involving minerals and aqueous solutions, I. Thermodynamic relations. *Geochim. Cosmochim. Acta* 32, 853–877.
- Helgeson, H.C., Delany, J.M., Nesbitt, H.W., Bird, D.K., 1978. Summary and critique of the thermodynamic properties of rock forming minerals. *Am. J. Sci.* 278A, 229 pp.
- Herzog, H.J., Drake, E.M., Adams, E.E., 1997. CO<sub>2</sub> capture, reuse, and storage technologies for mitigating global climate change. Final Report, DOE No. DE-AF22-96PC01257,. Massachusetts Institute of Technology, Cambridge.
- Hyeong, K., Capuano, R., 2001. Ca/Mg of brines in Miocene/Oligocene clastic sediments of the Texas Gulf Coast: Buffering by calcite/disordered dolomite equilibria. *Geochim. Cosmochim. Acta* 65, 3065–3080.
- IGME, 2010. ALGECO2 Project: elección y caracterización de áreas y estructuras geológicas favorables para el almacenamiento geológico de CO<sub>2</sub> en España. URL <http://info.igme.es/algeco2/> (accessed 5.24.17).
- IGME, 1991. Mapa Geológico de España. E. 1:50000. Hoja 436: Alhama de Aragón.
- IGME, 1980. Informe hidrogeológico del subsistema acuífero Sierra del Solorio (Sistema acuífero 57).

- IGME, 1973. Mapa Geológico de España. E. 1:50000. Hoja 175: Sigües. Instituto Geológico y Minero de España (IGME), Madrid.
- ITGE-DGA, 1994. Estudio de las aguas minero-medicinales, minero-industriales, termales y de bebida envasada en la Comunidad Autónoma de Aragón. Instituto Geológico y Minero de España (IGME), Madrid.
- Johnson, J., Anderson, G., Parkhurst, D., 2000. Database “thermo.com.V8.R6.230,” Rev. 1.11. Livermore, California.
- Jones, B., 2017. Review of calcium carbonate polymorph precipitation in spring systems. *Sediment. Geol.* 353, 64–75.
- Jones, B., Peng, X., 2016. Mineralogical, crystallographic, and isotopic constraints on the precipitation of aragonite and calcite at Shiqiang and other hot springs in Yunnan Province, China. *Sediment. Geol.* 345, 103–125.
- Jones, B., Peng, X., 2014. Hot spring deposits on a cliff face: A case study from Jifei, Yunnan Province, China. *Sediment. Geol.* 302, 1–28.
- Jones, B., Renaut, R.W., 2010. Calcareous spring deposits in continental settings, in: Alonso-Zarza, A.M., Tanner, L.H. (Eds.), *Developments in Sedimentology: Carbonates in Continental Settings: Facies, Environments and Processes*. Elsevier, Amsterdam, pp. 177–224.
- Karimi, H., Moore, F., 2008. The source and heating mechanism for the Ahram, Mirahmad and Garu thermal springs, Zagros Mountains, Iran. *Geothermics* 37, 84–100.
- Kele, S., Breitenbach, S.F., Capezzuoli, E., Meckler, A.N., Ziegler, M., Millan, I.M., Kluge, T., Deák, J., Hanselmann, K., John, C.M., Yan, H., Liu, Z., Bernasconi, S.M., 2015. Temperature dependence of oxygen and clumped isotope fractionation in carbonates: A study of travertines and tufas in the 6-9 °C temperature range. *Geochim. Cosmochim. Acta* 168, 172–192.
- Kele, S., Demény, A., Siklósy, Z., Németh, T., Tóth, M., Kovács, M.B., 2008. Chemical and stable isotope composition of recent hot-water travertines and associated thermal waters, from Egerszalók, Hungary: Depositional facies and non-equilibrium fractionation. *Sediment. Geol.* 211, 53–72.
- Kele, S., Özkul, M., Fórizs, I., Gökgöz, A., Baykara, M.O., Alçiçek, M.C., Németh, T., 2011. Stable isotope geochemical study of Pamukkale travertines: New evidences of low-temperature non-equilibrium calcite-water fractionation. *Sediment. Geol.* 238, 191–212.

- Kharaka, Y.K., Mariner, R.H., 1989. Chemical geothermometers and their application to formation waters from sedimentary basins, in: Naeser, N.D., McCollon, T.H. (Eds.), *Thermal History of Sedimentary Basins*. Springer, Berlin, pp. 99–117.
- Kim, S.T., O'Neil, J.R., Hillaire-marcel, C., Mucci, A., Kim, S., Neil, J.R.O., Hillaire-Marcel, C., Mucci, A., 2007. Oxygen isotope fractionation between synthetic aragonite and water. Influence of temperature and  $Mg^{2+}$  concentrations. *Geochim. Cosmochim. Acta* 71, 4704–4715.
- Kim, S.T., O'Neil, J.R., 1997. Equilibrium and nonequilibrium oxygen isotope effects in synthetic carbonates. *Geochim. Cosmochim. Acta* 61, 3461–3475.
- Lachniet, M.S., 2015. Are aragonite stalagmites reliable paleoclimate proxies? Tests for oxygen isotope time-series replication and equilibrium. *GSA Bull.* 1521–1533.
- Langmuir, D., 1997. *Aqueous environmental geochemistry*. Prentice Hall, Upper Saddle River, New Jersey, New Jersey.
- Larrasoña, J.C., Pueyo, E.I., del Valle, J., Millán, H., Pocoví, A., Dinarés, J., 1996. Datos magnetotectónicos del Eoceno de la Cuenca de Jaca–Pamplona: resultados iniciales. *Geogaceta* 30, 1058–1061.
- Lee, K.C., 1996. Classification of geothermal resources - An engineering approach, in: *Twenty-First Workshop on Geothermal Reservoir Engineering*. Stanford, California, California, pp. 85–92.
- Levet, S., Toutain, J.P., Munoz, M., Berger, G., Negrel, P., Jendrzewski, N., Agrinier, P., Sortino, F., 2002. Geochemistry of the Bagnères de Bigorre thermal waters from the North Pyrenean Zone sedimentary environment (France). *Geofluids* 2, 1–16.
- Lions, J., Devau, N., de Lary, L., Dupraz, S., Parmentier, M., Gombert, P., Dictor, M., 2014. Potential impacts of leakage from CO<sub>2</sub> geological storage on geochemical processes controlling fresh groundwater quality: A review. *Int. J. Greenh. Gas Control* 22, 165–175.
- Liu, Z., Li, H., You, C., Wan, N., Sun, H., 2006. Thickness and stable isotopic characteristics of modern seasonal climate-controlled sub-annual travertine laminas in a travertinedepositing stream at Baishuitai, SW China: implications for paleoclimate reconstruction. *Environ. Geol.* 51, 257–265.
- Liu, Z., Sun, H., Baoying, L., Xiangling, L., Wenbing, Y., Cheng, Z., 2010. Wet-dry seasonal variations of hydrochemistry and carbonate precipitation rates in a travertinedepositing canal at Baishuitai, Yunnan, SW China: Implications for the formation of biannual laminae in travertine and for climatic reconstruction. *Chem. Geol.* 273, 258–266.



- Lloyd, R.M., 1968. Oxygen isotope behaviour in the sulfate-water system. *J. Geophys. Res.* 73, 6099–6110.
- López-Chicano, M., Cerón, J.C., Vallejos, A., Pulido-Bosch, A., 2001. Geochemistry of thermal springs, Alhama de Granada (southern Spain). *Appl. Geochemistry* 16, 1153–1163.
- Lu, H.Y., Lin, C.K., Lin, W., Liou, T.S., Chen, W.F., Chang, P.Y., 2011. A natural analogue for CO<sub>2</sub> mineral sequestration in Miocene basalt in the Kuanhsi-Chutung area, Northwestern Taiwan. *Int. J. Greenh. Gas Control* 5, 1329–1338.
- Marcon, V., Kaszuba, J.P., 2015. Carbon dioxide-brine-rock interactions in a carbonate reservoir capped by shale. Experimental insights regarding the evolution of trace metals. *Geochim. Cosmochim. Acta* 168, 22–42.
- Mariner, R.H., Evans, W.C., Young, H.W., 2006. Comparison of circulation times of thermal waters discharging from the Idaho batholith based on geothermometer temperatures, helium concentrations, and <sup>14</sup>C measurements. *Geothermics* 35, 3–25.
- Marini, L., 2004. Geochemical techniques for the exploration and exploitation of geothermal energy. *Laboratorio di Geochimica, Università degli Studi di Genova, Genova.*
- Marini, L., Chidioni, G., Cioni, R., 1986. New geothermometers for carbonate-evaporite geothermal reservoirs. *Geothermics* 15, 77–86.
- Martín, C., 2016. Inmersión en las aguas termales del sur de Aragón. *Sociedad de Amigos del Museo Nacional de Ciencias Naturales.*
- Mas, J.R., Alonso, A., Guimera, J., 1993. Evolución tectonosedimentaria de una cuenca extensional intraplaca: la cuenca finijurásica-eocretácica de los Cameros (La Rioja-Soria). *Rev. la Soc. Geológica España* 6, 129–144.
- McCrea, J.M., 1950. On the isotopic chemistry of carbonates and a paleotemperature scale. *J. Chem. Phys.* 18, 849–857.
- Merino, E., Ramson, B., 1982. Free energies of formation of illite solid solutions and their compositional dependence. *Clays Clay Miner.* 30, 29–39.
- Metz, B., Davidson, O., Coninck, H., Loos, M., Meyer, L. (Eds.), 2005. IPCC Special Report on Carbon Dioxide Capture and Storage. Prepared by Working Group III of the Intergovernmental Panel on Climate Change. Cambridge University Press, Cambridge, United Kingdom and New York, USA, United Kingdom and New York, USA.
- Michard, G., 1979. Geothermomètres chimiques. *Bur. Rech. Géologiques Minières (2<sup>nd</sup> Ser.), Sect. III 2*, 183–189.

- Michard, G., Bastide, J.P., 1988. Géochimie de la nappe du Dogger du Bassin de Paris. *J. Volcanol. Geotherm. Res.* 35, 151–163.
- Michard, G., Fouillac, C., 1980. Contrôle de la composition chimique des eaux thermals sulfurées sodiques du Sud de la France, in: Tardy, Y. (Ed.), *Geochimie Des Interactions Entre Les Eaux Le Minéraux et Les Roches*. Elements, Tarbes, pp. 147–166.
- Michard, G., Roekens, E., 1983. Modelling of the chemical composition of alkaline hot waters. *Geothermics* 12, 161–169.
- Michard, G., Sanjuan, B., Criaud, A., Fouillac, C., Pentcheva, E.N., Petrov, P.S., Alexieva, R., 1986. Equilibria and geothermometry in hot alkaline waters from granites of S.W. Bulgaria. *Geochem. J.* 20, 159–171.
- Minissale, A.A., Duchi, V., 1988. Geothermometry on fluids circulating in a carbonate reservoir in north-central Italy. *J. Volcanol. Geotherm. Res.* 35, 237–252.
- Mizutani, Y., Rafter, T.A., 1969. Oxygen isotopic composition of sulphates, part. 3. Oxygen isotopic fractionation in the bisulfate ion-water system. *New Zel. J. Sci.* 22, 169–176.
- Mohammadi, Z., Bagheri, R., Jahanshahi, R., 2010. Hydrogeochemistry and geothermometry of Changan thermal springs, Zagros region, Iran. *Geothermics* 39, 242–249.
- Mook, W.G., Bommerson, J.C., Staverman, W.H., 1974. Carbon isotope fractionation between dissolved bicarbonate and gaseous carbon dioxide. *Earth Planet. Sci. Lett.* 22, 169–176.
- Moore, J., Adams, M., Allis, R., Lutz, S., Rauzi, S., 2005. Mineralogical and geochemical consequences of the long-term presence of CO<sub>2</sub> in natural reservoirs: an example from the Springerville - St. Johns Field, Arizona, and New Mexico, U.S.A. *Chem. Geol.* 217, 365–385.
- Muller, N., Qi, R., Mackie, E., Pruess, K., Blunt, M.J., 2009. CO<sub>2</sub> injection impairment due to halite precipitation. *Energy Procedia* 1, 3507–3514.
- Mutlu, H., Güleç, N., 1998. Hydrogeochemical outline of thermal waters and geothermometry applications in Anatolia (Turkey). *J. Volcanol. Geotherm. Res.* 85, 495–515.
- Nemeth, K., 1963. Photometric determination of sulphate in soil extracts. *Z. PflErnahr. Dung.* 103, 193–196.
- Nicholson, K., 1993. *Geothermal Fluids. Chemistry and Exploration Techniques*. Springer-Verlag, Berlin.
- Nordstrom, D.K., Ball, J.W., Donahoe, R.J., Whittemore, D., 1989. Groundwater chemistry and water-rock interactions at Stripa. *Geochim. Cosmochim. Acta* 53, 1727–1740.

- Nordstrom, D.K., Plummer, L.N., Langmuir, L., Busenberg, E., May, H.M., Jones, B.F., Parkhurst, D.L., 1990. Revised chemical equilibrium data for major water-mineral reactions and their limitation, in: Melchior, D.C., Basset, R.L. (Eds.), *Chemical Modeling of Aqueous Systems II. Symposium Series 416*. American Chemical Society, Washington.
- O'Neil, J.R., Adami, L.H., 1969. The oxygen isotope partition function ratio of water and the structure of liquid water. *J. Phys. Chem.* 73, 1553–1558.
- Olcoz, S., 2017. *Los Baños Romanos de Fitero. Apuntes para el estudio de la historia de los Baños de Fitero*. Fundación Navarra Cultural.
- Osácar, C., Arenas, C., Auqué, L.F., Sancho, C., Pardo, G., Vázquez-Urbez, M., 2016. Discerning the interactions between environmental parameters reflected in  $\delta^{13}\text{C}$  and  $\delta^{18}\text{O}$  of recent fluvial tufas: lessons from a Mediterranean climate region. *Sediment. Geol.* 345, 126–144.
- Osácar, C., Arenas, C., Vázquez-Urbez, M., Sancho, C., Auqué, L.F., Pardo, G., 2013. Environmental factors controlling the  $\delta^{13}\text{C}$  and  $\delta^{18}\text{O}$  variations of recent fluvial tufas: a 12-year record from the monasterio de piedra natural park (NE Iberian Peninsula). *Sediment. Geol.* 83, 309–322.
- Özkul, M., Kele, S., Gökgöz, A., Shen, C.C., Jones, B., Baykara, M.O., Fórizs, I., Németh, T., Chang, Y.W., Alçiçek, M.C., 2013. Comparison of the Quaternary travertine sites in the Denizli extensional basin based on their depositional and geochemical data. *Sediment. Geol.* 294, 179–204.
- Palandri, J.L., Reed, M.H., 2001. Reconstruction of in situ composition of sedimentary formation waters. *Geochim. Cosmochim. Acta* 65, 1741–1767.
- Pang, Z., Reed, M.H., 1998. Theoretical chemical thermometry on geothermal waters: Problems and methods. *Geochim. Cosmochim. Acta* 62.
- Parkhurst, D.L., Appelo, C.A.J., 2013. Description of Input and Examples for PHREEQC Version 3. A Computer Program for Speciation, Batch Reaction, One Dimensional Transport, and Inverse Geochemical Calculations, in: U.S. Geological Survey (Ed.), *Techniques and Methods, Book 6, Chap. A43*. U.S. Geological Survey, Denver, Colorado.
- Pastorelli, S., Marini, L., Hunziker, J.C., 1999. Water chemistry and isotope composition of the Acquarossa thermal system, Ticino, Switzerland. *Geothermics* 28, 75–93.
- Patterson, W.P., Smith, G.R., Lohmann, K.C., Kyger, C.L., 1993. Continental Paleothermometry And Seasonality Using The Isotopic Composition Of Aragonitic

- Otoliths Of Freshwater Fishes, in: Swart, P.K., Lohmann, K.C., McKenzie, J., Savin, S. (Eds.), *Climate Change in Continental Isotopic Records*. American Geophysical Union, pp. 191–202.
- Pauwels, H., Gaus, I., le Nindre, Y.M., Pearce, J., Czernichowski-Lauriol, I., 2007. Chemistry of fluids from a natural analogue for a geological CO<sub>2</sub> storage site (Montmiral, France): lessons for CO<sub>2</sub>–water–rock interaction assessment and monitoring. *Appl. Geochemistry* 22, 2817–2833.
- Pedley, M., 2009. Tufas and travertines of the Mediterranean region: a testing ground for freshwater carbonate concepts and developments. *Sedimentology* 56, 221–246.
- Pentecost, A., 2005. *Travertine*. Springer Science & Business Media.
- Pingitore, N.E., Iglesias, A., Lytle, F., Wellington, G.M., 2002. X-Ray absorption spectroscopy of uranium at low ppm levels in coral skeletal aragonite. *Microchem. J.* 71, 261–266.
- Plummer, L.N., 1992. Geochemical modeling of water-rock interaction: Past, present and future, in: Kharaka, Y.K., Maest, A.S. (Eds.), *Water-Rock Interaction. I. Low Temperature Environments*. pp. 22–33.
- Plummer, L.N., 1984. Geochemical modeling: a comparison of forward and inverse methods, in: Hitchon, B., Wallick, E.I. (Eds.), *Practical Applications of Ground Water Geochemistry. Proceedings of First Canadian/American Conference on Hydrogeology*. Banff, Alberta, Canada, Alberta, Canada.
- Plummer, L.N., 1977. Defining reactions and mass transfer in part of the Floridan aquifer. *Water Resour. Res.* 13, 801–812.
- Plummer, L.N., Back, W., 1980. The mass balance approach: application to interpreting the chemical evolution of hydrologic systems. *Am. J. Sci.* 280, 130–142.
- Plummer, L.N., Busby, J.F., Lee, R.W., Hanshaw, B.B., 1990. Geochemical modelling of the Madison aquifer in parts of Montana, Wyoming, and South-Dakota. *Water Resour. Res.* 26, 1981–2014.
- Plummer, L.N., Parkhurst, D.L., Thorstenson, D.C., 1983. Development of reaction models for ground-water systems. *Geochim. Cosmochim. Acta* 47, 665–686.
- Pueyo, E.L., Calvin, P., Casas, A.M., Olivia-Ucria, B., Klimowitz, J., Garcia-Lobón, J.L., Rubio, F.M., Ibarra, P.I., Martínez-Duran, P., Rey-Moral, M.C., Pérez, I., Martín, J.M., 2012. A research plan for a large potential CO<sub>2</sub> reservoir in the Southern Pyrenees. *Geotemas* 13, 1970–1973.

- Puigdefàbregas, C., 1975. La sedimentación molásica en la cuenca de Jaca. *Pirineos* 104, 1–188.
- Qafoku, N.P., Lawter, A.R., Bacon, A.H., Zhent, L., Kyle, J., Brown, C.F., 2017. Review for the impacts of leaking CO<sub>2</sub> gas and brine on groundwater quality. *Earth Sci. Rev.* 169, 69–84.
- Reed, M., Spycher, N., 1984. Calculation of pH and mineral equilibria in hydrothermal waters with application to geothermometry and studies of boiling and dilution. *Geochim. Cosmochim. Acta* 48, 1479–1492.
- Reeder, R.J., 2000. Constraints on cation order in calcium-rich sedimentary dolomite. *Aquat. Geochemistry* 6, 213–226.
- Rietveld, H.M., 1969. A profile refinement method for nuclear and magnetic structures. *J. Appl. Crystallogr.* 2, 65–71.
- Rodrigo-Naharro, J., Delgado, A., Herrero, M.J., Granados, A., Pérez del Villar, L., 2013. Current Travertines Precipitation from CO<sub>2</sub>-rich Groundwaters as an Alert of CO<sub>2</sub> Leakages from a Natural CO<sub>2</sub> Storage at Gañuelas-Mazarrón Tertiary Basin (Murcia, Spain). CIEMAT, Madrid.
- Rodríguez-Berriguete, Á., Alonso-Zarza, A.M., Martín-García, R., Cabrera, M. del C., 2018. Sedimentology and geochemistry of a human-induced tufa deposit: Implications for palaeoclimatic research. *Sedimentology* 65, 2253–2277.
- Román-Mas, A., Lee, R.W., 1987. Geochemical evolution of waters within the North Coast limestone aquifers of Puerto Rico: a conceptualization based on a flow path in the Barceloneta area, in: U.S. Geological Survey Water-Resources Investigations Report 86-4080. U.S. Geological Survey, San Juan, Puerto Rico, p. 28.
- Romanek, C.S., Grossman, E.L., Morse, J.W., 1992. Carbon isotopic fractionation in synthetic aragonite and calcite: Effects of temperature and precipitation rate. *Geochim. Cosmochim. Acta* 56, 419–430.
- Sánchez, J.A., 2000. Las aguas termales en Aragón: Estudio hidrogeotérmico. Consejo de Protección de la Naturaleza de Aragón, Zaragoza.
- Sánchez, J.A., Coloma, P., 1998. Hidrogeología de los manantiales termales de Arnedillo. *Zubía Monográfico* 10, 11–25.
- Sánchez, J.A., Coloma, P., Pérez-García, A., 2004. Evaluation of geothermal flow at the springs in Aragón (Spain), and its relation to geologic structure. *Hydrogeol. J.* 12, 601–609.

- Sánchez, J.A., Coloma, P., Pérez-García, A., De Leiva, A., 2000. Evaluación del flujo geotérmico en manantiales de Aragón. *Geogaceta* 27, 155–158.
- Sánchez, J.A., Coloma, P., Pérez, A., 1999. Sedimentary processes related to the groundwater flows from the Mesozoic Carbonate Aquifer of the Iberian Chain in the Tertiary Ebro Basin, northeast Spain. *Sediment. Geol.* 129, 201–213.
- Sánchez, J., Sanz, L., Ocaña, L., 2011. Evaluación del potencial de energía geotérmica. Madrid.
- Saura, E., Teixell, A., 2006. Inversion of small basins: effects on structural variations at the leading edge of the Axial Zone antiformal stack (Southern Pyrenees, Spain). *J. Struct. Geol.* 28, 1909–1920.
- Scheele, N., Hoefs, J., 1992. Carbon isotope fractionation between calcite, graphite and CO<sub>2</sub>: An experimental study. *Contrib. to Mineral. Petrol.* 112, 35–45.
- Seal, R.R.I., Alpers, C.N., Rye, R.O., 2000. Stable isotope systematics of sulfate minerals, in: Alpers, C.N., Jambor, J.L., Nordstrom, D. (Eds.), *Sulfate Minerals - Crystallography: Geochemistry and Environmental Significance*. Mineral Society of America, Chantilly (Virginia), pp. 541–602.
- Sonney, R., Vuataz, F.D., 2010. Validation of chemical and isotopic geothermometers from low temperature deep fluids of Northern Switzerland, in: *Proceedings World Geothermal Congress 2010*. Bali, Indonesia, Indonesia, pp. 25–29.
- Stefánsson, A., Arnórsson, S., 2000. Feldspar saturation state in natural waters. *Geochim. Cosmochim. Acta* 64, 2567–2584.
- Sutton, M., 2009. Review of Distribution Coefficients for Radionuclides in Carbonate Minerals.
- Szaran, J., 1997. Achievement of carbon isotope equilibrium in the system HCO<sub>3</sub><sup>-</sup>(solution)-CO<sub>2</sub>(gas). *Chem. Geol.* 142, 79–86.
- Tena, J.M., Auqué, L.F., Gimeno, M.J., Mandado, J., 1995. Evolución fisicoquímica y geotermometría del sistema hidrotermal de Alhama-Jaraba. Institución Fernando el Católico.
- Thorrold, S.R., Campana, S.E., Jones, C.M., Swart~, P.K., 1997. Factors determining δ<sup>13</sup>C and δ<sup>18</sup>O fractionation in aragonitic otoliths of marine fish. *Pergamon Geochim. Cosmochim. Acta* 61, 2909–2919.
- Tischer, G., 1965. Über die Wealden-Ablagerung und die Tektonik der östlichen Sierra de los Cameros in den nordwestlichen Iberischen Ketten (Spanien). *Beihefte zum Geol. Jahrb.* 44, 123–164.

- Trémosa, J., Castillo, C., Vong, C.Q., Kervévan, C., Lassin, A., Audigane, P., 2014. Long-term assessment of geochemical reactivity of CO<sub>2</sub> storage in highly saline aquifers: Application to ketzin, in salah and snøhvit storage sites. *Int. J. Greenh. Gas Control* 20, 2–26.
- Truesdell, A.H., 1976. Geochemical Techniques in Exploration. Summary of Section III, in: *Proceedings of the Second United Nations Symposium on the Development Y Use of Geothermal Resources*. San Francisco (California), pp. iii–xxix.
- Truesdell, A.H., 1974. Oxygen isotope activities and concentrations in aqueous salt solutions at elevated temperatures: Consequences for isotope geochemistry. *Earth Planet. Sci. Lett.* 33, 387–396.
- Turner, J.V., 1982. Kinetic fractionation of carbon-13 during calcium carbonate precipitation. *Geochim. Cosmochim. Acta* 46, 1183–1191.
- Verma, S.P., Santoyo, E., 1997. New improved equations for Na/K, Na/Li and SiO<sub>2</sub> geothermometers by outlier detection and rejection. *J. Volcanol. Geotherm. Res.* 79, 9–24.
- Vespasiano, G., Apollaro, C., Muto, F., Dotsika, E., de Rosa, R., Marini, L., 2014. Chemical and isotopic characteristics of the warm and cold waters of the Luigiane Spa near Guardia Piemontese (Calabria, Italy) in a complex faulted geological framework. *Appl. Geochemistry* 41, 73–88.
- Wang, H., Yan, Y., Liu, Z., 2014. Contrasts in variations of the carbon and oxygen isotopic composition of travertines formed in pools and a ramp stream at Huanglong Ravine, China: implications for paleoclimatic interpretations. *Geochim. Cosmochim. Acta* 125, 34–48.
- Wang, J., Jin, M., Jia, B., Kang, F., 2015. Hydrochemical characteristics and geothermometry applications of thermal groundwater in northern Jinan, Shandong, China. *Geothermics* 57, 185–195.
- Wang, Z., Gaetani, G., Liu, C., Cohen, A., 2013. Oxygen isotope fractionation between aragonite and seawater: Developing a novel kinetic oxygen isotope fractionation model. *Geochim. Cosmochim. Acta* 117, 232–251.
- Watson, M.N., Zwingmann, N., Lemon, N.M., 2004. The Ladbroke Grove–Katnook carbon dioxide natural laboratory: a recent CO<sub>2</sub> accumulation in a lithic sandstone reservoir. *Energy* 29, 1457–1466.
- White, R.M.P., Dennis, P.F., Atkinson, T.C., 1999. Experimental calibration and field investigation of the oxygen isotopic fractionation between biogenic aragonite and water. *Rapid Commun. Mass Spectrom.* 13, 1242–1247.

- Williams, C.F., Reed, M.J., Anderson, A.F., 2011. Updating the Classification of Geothermal Resources. 36<sup>th</sup> Work. Geotherm. Reserv. Eng.
- Yan, H., Sun, H., Liu, Z., 2012. Equilibrium vs. kinetic fractionation of oxygen isotopes in two low-temperature travertine-depositing systems with differing hydrodynamic conditions at Baishuitai, Yunnan, SW China. *Geochim. Cosmochim. Acta* 95, 63–78.
- Zeebe, R.E., 2010. A new value for the stable oxygen isotope fractionation between dissolved sulfate ion and water. *Geochim. Cosmochim. Acta* 74, 818–828.
- Zhang, J., Quay, P.D., Wilbur, D.O., 1995. Carbon isotope fractionation during gas-water exchange and dissolution of CO<sub>2</sub>. *Geochim. Cosmochim. Acta* 59, 107–114.
- Zheng, Y.F., 1999. Oxygen isotope fractionation in carbonate and sulfate minerals. *Geochem. J.* 33, 109–126.
- Zhu, C., Anderson, G., 2002. *Environmental Applications of Geochemical Modeling*. Cambridge University Press.



# **SUPPLEMENTARY MATERIAL**

---



Available online at [www.sciencedirect.com](http://www.sciencedirect.com)**ScienceDirect**

Procedia Earth and Planetary Science 17 (2017) 120 – 123

---



---

**Procedia**  
 Earth and Planetary Science
 

---



---

15th Water-Rock Interaction International Symposium, WRI-15

## Comparison of different thermodynamic databases used in a geothermometrical modelling calculation

Mónica Blasco<sup>a,1</sup>, Maria J. Gimeno<sup>a</sup>, Luis F. Auqué<sup>a</sup><sup>a</sup>Earth Sciences Department, University of Zaragoza. C/Pedro Cerbuna, 12, Zaragoza 50009, Spain

---

### Abstract

Different thermodynamic databases usually have common thermodynamic data for some minerals or aqueous species, but in many cases they present important differences. Four different thermodynamic databases (WATEQ4F, LLNL, DATA0.YMP.R5 and SOLTHERM) have been used in a geothermometrical modelling problem and they are compared in this work. The main differences found in the thermodynamic data are related to the order, degree, crystallinity and composition of the considered aluminosilicate phases and the effects of these properties in the experimental, or theoretical, data used for the fitting of the equilibrium constant at different temperatures.

© 2017 The Authors. Published by Elsevier B.V. This is an open access article under the CC BY-NC-ND license

(<http://creativecommons.org/licenses/by-nc-nd/4.0/>).

Peer-review under responsibility of the organizing committee of WRI-15

**Keywords:** Thermodynamic database; geothermometrical modelling; thermal water; geothermal system

---

### 1. Introduction

The geothermometrical modelling is a useful technique to study and characterise a thermal system. It allows estimating the reservoir temperature of the waters from the study of the evolution of the saturation states of different mineral phases when an increase of the temperature of the waters is simulated.

This kind of determination is carried out by using geochemical modelling codes such as PHREEQC<sup>1</sup> or GeoT<sup>2</sup> among others, which are provided with different databases that contain the thermodynamic data for minerals, gases and aqueous species. The fact that these databases can present significant differences in their data, which would affect the temperature prediction<sup>3</sup>, makes the selection of the most adequate one according to the characteristics of the studied waters and minerals in contact to, a necessary task.

The aim of this study is to present the differences found when performing the geothermometrical modelling of a

---

\* Corresponding author. Tel.: +34-976-761071; fax: +34-976-761106.

*E-mail address:* [monicabc@unizar.es](mailto:monicabc@unizar.es)

thermal water by using four of the most commonly used thermodynamic databases in this type of calculations, and explain the main reason for that. The water sample selected for this study belongs to a low temperature carbonate evaporitic system (Arnedillo thermal system), located in La Rioja, Spain. The water is of chloride – sodium type with a spring temperature of 45.3 °C and TDS value of 7352 ppm.

## 2. Materials and methods

### 2.1. Geothermometrical modelling

The geothermometrical modelling is a kind of reaction path calculation which allows estimating the temperature of the thermal water in the reservoir from the chemical analysis of a water<sup>4</sup>. In order to do this, it is necessary to assume that thermal waters have not changed their composition while ascending. Then, a temperature increase is simulated and the final temperature is found when the set of minerals, previously selected as present in the reservoir, converge towards equilibrium simultaneously.

### 2.2. Databases

The four thermodynamic databases compared in this work are: WATEQ4F<sup>5</sup> and LLNL<sup>6</sup> databases, which have been used with the PHREEQC code<sup>1</sup>, and DATA0.YMP.R5<sup>7</sup> and SOLTHERM<sup>8</sup> used with the code GeoT<sup>2</sup>.

The WATEQ4F database has been developed by the U.S. Geological Survey and it contains most of the major and trace species, mineral and gas phases in natural water systems. It was developed to be used in a temperature range of 0 to 100 °C, and care should be taken when outside this range<sup>5</sup>. In any case, it can be used for the study of a wide range of natural waters, including waters from low enthalpy geothermal systems. Among the four databases compared in this work, WATEQ4F is the only one that uses, mainly, the Van't Hoff equation for the calculation of the equilibrium constants at different temperatures. Some exceptions are the cases of calcite, anhydrite or quartz, for which the calculation is through a polynomial K(T) expression fitted to experimental data. That is the main procedure for the other three databases used in this work.

The LLNL includes reliable data for a vast number of minerals and aqueous species in a temperature range of 0 to 300 °C<sup>6</sup>. The DATA0.YMP.R5 is one of the versions performed for the Yucca Mountain Project and it has also been prepared to be used for a temperature range of 0 – 300 °C<sup>7</sup>. Finally, the SOLTHERM database is derived from the databases of Holland and Powell<sup>9</sup> and the SLOP.98<sup>10</sup>. It was developed to be applied in a temperature range from 25 to 300 °C<sup>8</sup>. For the activity coefficient calculations all databases rely on different extensions of the Debye-Hückel equation (Davis, B-dot, etc.). The ionic strength of the studied waters is 0.13 molal and, therefore, the different equations are not expected to promote important differences in the calculations<sup>4</sup>.

Most of the data contained in these databases present important differences regarding 1) the solubility constant and composition of certain minerals and 2) the aqueous species dissociation constants<sup>3</sup>. Furthermore, these databases do not contain data for the same minerals and, therefore, only common or equivalent minerals included in the four databases have been selected for comparison in the geothermometrical modelling performed in this work. The selected minerals are anhydrite, quartz, calcite, dolomite (disordered dolomite), albite (low temperature albite in all cases except from the WATEQ4F database, which only contains one type of albite), K-feldspar (maximum microcline in DATA0.YMP.R5, microcline in SOLTHERM, and adularia in WATEQ4F since it does not contain other K-feldspar), and some aluminosilicates like laumontite, pyrophyllite, kaolinite and illite.

## 3. Results

The modelling results obtained with the four different databases are presented in Table 1 and Figure 1 (as the evolution of the SI values,  $\log IAP/K(T)$ , for the selected minerals). There are not significant differences in the results obtained for anhydrite (differences of 7 °C), and slightly larger for quartz (up to 14 °C). However, the differences found in results obtained for the rest of the minerals are more important. The results for calcite vary in a range of 17 °C. For dolomite three of the results vary in a range of 8 °C whilst with the WATEQ4F database this mineral is always undersaturated. Something similar happens for albite and K-feldspar, they are undersaturated

when the WATEQ4F database is used, while using the other databases these minerals are in equilibrium in a range of 24 and 20 °C, being DATA0.YMP.R5 and LLNL in a better agreement and SOLTHERM giving the highest value obtained. The major differences have been found in the case of laumontite, with differences of 106 °C, kaolinite with 38 °C, illite with 40°C, and pyrophyllite, always oversaturated if the calculations are done with the WATEQ4F database, and showing differences of 24 °C when using the other three databases.

Table 1. Temperatures (°C), predicted by geothermometrical modelling, by using the different database, at which the different mineral phases considered reach the equilibrium with waters.

	WATEQ4F	LLNL	DATA0.YMP	SOLTHERM
Anhydrite	88	81	82	82
Quartz	97	90	83	96
Calcite	85	79	96	92
Dolomite	- <sup>a</sup>	98	102	106
Albite	- <sup>a</sup>	79	72	96
K-feldspar	- <sup>a</sup>	80	75	95
Laumontite	58	77	164	89
Pyrophyllite	- <sup>b</sup>	89	85	109
Kaolinite	88	103	102	126
Illite	56	96	95	69

Notes: <sup>a</sup> always undersaturated; <sup>b</sup> always oversaturated.

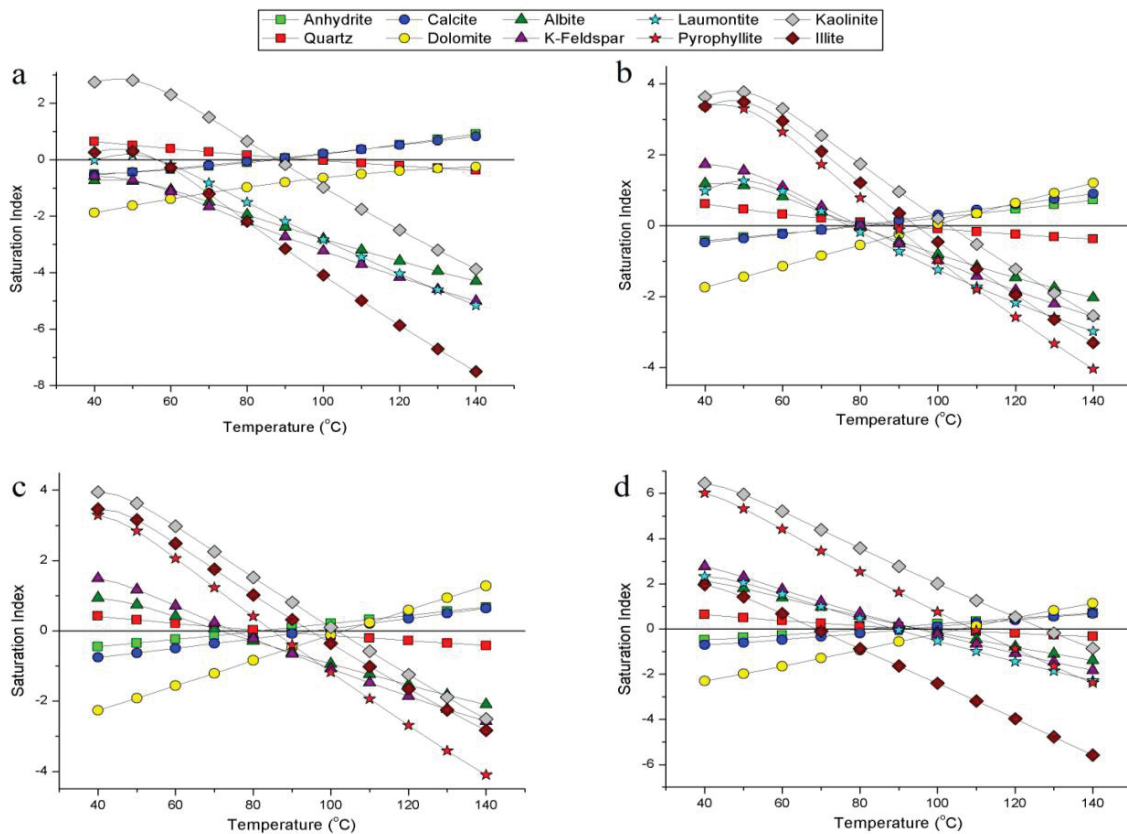


Figure 1. Graphical representation against temperature of the saturation indices of the different minerals considered in the study. (a) Results obtained with WATEQ4F database; note that pyrophyllite does not appear in the representation since it is always oversaturated with a Saturation Index close 10. (b) Results with LLNL database. (c) Results with DATA0.YMP.R5 database; note that laumontite does not appear since it is oversaturated in the considered temperature range, it reaches equilibrium at 164 °C. (d) Results with SOLTHERM database.

#### 4. Discussion and conclusions

The main differences in the results obtained when using the four thermodynamic databases have been found for the aluminosilicates. This is due to the fact that the solubility of those phases (and its variation with temperature) presents important uncertainties related to the compositional variability and/or the degree of crystallinity<sup>11</sup>. That is, depending on the similarity between the characteristics of the phase considered in the different databases and the phase involved in the study, the results will be more or less accurate.

The differences found in the results obtained for the rest of the considered phases seem to be related to the experimental data used for them and the mathematical fitting to those data. An additional cause of differences is the fact that the WATEQ4F database uses the Van't Hoff equation to calculate the equilibrium constant at different temperatures for some phases. However, the saturation states of calcite, anhydrite and quartz are not calculated using the Van't Hoff equation, but a polynomial K(T) expression from experimental data which are fitted in the temperature range of 0 – 90°C<sup>12</sup>, 25 – 56 °C<sup>13</sup> and 70 – 250 °C<sup>14</sup>, respectively.

In the case of dolomite, in which the disordered phase has been selected in all cases, the differences found seem to be due to differences in the polynomial expression used for the calculation of the equilibrium constant at different temperatures. Nonetheless, the largest difference has been found when using the WATEQ4F database, which is the only one that calculates the saturation state of this phase with the Van't Hoff equation.

In any case, despite the differences found, the results obtained with the different databases would allow establishing a temperature in the reservoir of about 90 °C (obviously excluding some of the results obtained with some aluminosilicates phases). Two additional conclusions are that there is not a thermodynamic database more reliable than other for this type of systems, and that it is necessary to be careful when selecting the aluminosilicate phases to consider in the modelling due to their high uncertainties.

#### Acknowledgements

Mónica Blasco has worked on this study thanks to a scholarship from the Ministry of Education, Culture and Sports of Spain, for the Training of University Teachers (ref. FPU14/01523). This study forms parts of the activities of the Geochemical Modelling Group (Aragón Government).

#### References

1. Parkhurst DL, Appelo CAJ. Description of Input and Examples for PHREEQC Version 3. A Computer Program for Speciation, Batch-Reaction, One-Dimensional Transport, and Inverse Geochemical Calculations. In U.S. Geological Survey, editor. *Techniques and Methods*, book 6, chap. A43; 2013.
2. Spycher N, Sonnenthal E, Kennedy BM. Integrating Multicomponent Chemical Geothermometry with Parameter Estimation Computations for Geothermal Exploration. *GRC Transactions* 2011; **35**: 663-666.
3. Spycher N, Peiffer L, Sonnenthal EL, Saldi G, Reed MH, Kennedy BM. Integrated multicomponent solute geothermometry. *Geothermics* 2014; **51**: 113-123.
4. Bethke CM. *Geochemical and biogeochemical reaction modeling*. 2<sup>nd</sup> ed. Cambridge: Cambridge University Press; 2008.
5. Ball JW, Nordstrom D. User's manual for WATEQ4F with revised thermodynamic database and test cases for calculation speciation of major, trace and redox elements in natural waters. In US Geological Survey, editor. *Water-Resources Investigation Report*. Menlo Park, California; April 2001..
6. Johnson J, Anderson F, Parkhurst DL. *Database thermo.com.V8.R6.230, Rev 1.11*. Lawrence Livermore National Laboratory, Livermore, California; 2000.
7. Wolery TJ, Jove-Colon CF, Jareck, RL. *Qualification of Thermodynamic Data for Geochemical Modeling of Mineral-Water Interactions in Dilute Systems. ANL-WIS-GS-000003 Rev 01*. Sandia National Laboratories: Las Vegas, Nevada, ACC: DOC.20070619.0007; 2007.
8. Reed M, Palandri J. SOLTHERM.H06, a database of equilibrium constants for minerals and aqueous species. *Available from the authors*; 2006.
9. Holland TJB, Powell R. An internally consistent thermodynamic dataset for phases of petrological interest. *J Met Geol* 1998; **16**: 309-343.
10. Plyasunova N, Plyasunov A, Shock E. Database of thermodynamic properties for aqueous organic compounds. *Inter J Thermophysics* 2004; **25**: 351-360.
11. Helgeson HC, Delany JM, Nesbitt HW, Bird DK. Summary and critique of the thermodynamic properties of rock forming minerals. *Amer J Sci* 1978; **278** (A): 1-292.
12. Plummer LN, Busenberg E. The solubilities of calcite, aragonite and vaterite in CO<sub>2</sub>-H<sub>2</sub>O solutions between 0 and 90°C and an evaluation of the aqueous model for the system CaCO<sub>3</sub>-CO<sub>2</sub>-H<sub>2</sub>O. *Geochim et Cosmochim Acta* 1982; **46**: 1011-1040.
13. Langmuir D, Melchior D. The geochemistry of Ca, Sr, Ba and Ra sulfates in some deep brines from the Palo Duro Basin, Texas. *Geochim et Cosmochim Acta* 1985; **49**: 2423-2432.
14. Fournier R. The behavior of silica in hydrothermal solutions. In Berger BR, Bethke, editors. *Geology and Geochemistry of Epithermal System; Reviews in Economic Geology* 1985; **2**: 45-61.

# APPENDICES

---





## **APPENDIX 1**

### **IMPACT FACTOR, SUBJECT CATEGORY AND CONTRIBUTIONS**

#### **PAPER 1**

##### **Citation:**

Blasco, M., Auqué, L. F., Gimeno, M. J., Acero, P., Asta, M. P. (2017). Geochemistry, geothermometry and influence of the concentration of mobile elements in the chemical characteristics of carbonate-evaporitic thermal systems. The case of the Tiermas geothermal system (Spain). *Chemical Geology*, 466, 696–709. DOI: 10.1016/j.chemgeo.2017.07.013

##### **Journal metrics:**

- Impact Factor (2017): 3.57
- Quartile and Category (2017): Q1 (19/85), Geochemistry and geophysics.

##### **Contributions of the PhD candidate:**

Mónica Blasco designed and organised the study, performed the bibliographic review, the data treatment and interpretation of the results and wrote the paper, with the assistance of the co-authors.

## PAPER 2

### Citation:

Blasco, M., Gimeno, M. J., Auqué, L. F. (2018). Low temperature geothermal systems in carbonate-evaporitic rocks: Mineral equilibria assumptions and geothermometrical calculations. Insights from the Arnedillo thermal waters (Spain). *Science of The Total Environment*, 615, 526–539. DOI: 10.1016/j.scitotenv.2017.09.269

### Journal metrics:

- Impact Factor (2017): 4.61
- Quartile and Category (2017): Q1 (27/241), Environmental Sciences.

### Contributions of the PhD candidate:

Mónica Blasco designed and organised the study, collaborated in the sampling campaign, performed the bibliographic review, the data treatment and interpretation of the results and wrote the paper, with the assistance of the co-authors.

### PAPER 3

#### Citation

Blasco, M., Auqué, L. F. , Gimeno, M. J. (2019). Geochemical evolution of thermal waters in carbonate – evaporitic systems: the triggering effect of halite dissolution in the dedolomitisation and albitisation processes. *Journal of Hydrology*, 570, 623-636. DOI: 10.1016/j.jhydrol.2019.01.013

#### Journal metrics:

- Impact Factor (2017): 3.727
- Quartile and Category (2017): Q1 (7/128), Engineering Civil; Q1 (7/90), Water Resources; Q1 (27/189), Geosciences.

#### Contributions of the PhD candidate:

Mónica Blasco designed and organised the study, collaborated in the sampling campaign, performed the bibliographic review, the data treatment and interpretation of the results and wrote the paper, with the assistance of the co-authors.

## PAPER 4

### Citation

Blasco, M., Auqué, L. F., Gimeno, M. J., Acero, P., Gómez J., Asta, M. P. (2019). Mineral equilibria and thermodynamic uncertainties in the geothermometrical characterisation of carbonate geothermal systems of low temperature. The case of the Alhama-Jaraba system (Spain). *Geothermics*, 78, 170-182. DOI: 10.1016/j.geothermics.2018.11.004

### Journal metrics

- Impact Factor (2017): 2.693
- Quartile and Category (2017): Q2 (57/189), Geosciences; Q2 (47/97), Energy & Fuels.

### Contributions of the PhD candidate:

Mónica Blasco collaborated in the design of the study, performed the bibliographic review, the data treatment and interpretation of the results and wrote the paper, with the assistance of the co-authors.

PAPER 5 (under review)

Citation

Blasco, M., Auqué, L. F. , Gimeno, M. J., Asta, M.P., Mandado, J. (2019). Element partition and stable isotope equilibrium evaluation in recent aragonite travertine associated to the Fitero thermal waters (Spain).

Journal metrics:

- Impact Factor (2017): 2.575
- Quartile and category: Q1 (9/47), Geology.

Contributions of the PhD candidate:

Mónica Blasco designed and organised the study, collaborated in the water sampling campaign, performed the bibliographic review, the data treatment and interpretation of the results and wrote the paper, with the assistance of the co-authors.



## **APPENDIX 2**

### **RESIGNATION OF THE CO-AUTHORS TO USE THE PAPERS IN OTHER PHD DISSERTATIONS**

All the co-authors of the different papers presented in this thesis dissertation hold a PhD Degree and, therefore, their resignation to present the papers in other PhD dissertation is not necessary (Acuerdo de 20/12/2013 del Consejo de Gobierno de la Universidad de Zaragoza relativo al Reglamento sobre Tesis Doctorales).











